

# MRI analysis and neurodevelopmental outcome in preterm infants

door  
**Britt van Kooij**

© ® van Kooij, B.J.M, 2011

All rights reserved. No part of this book may be reproduced or transmitted, in any form or by any means, without the written permission of the author.  
ISBN 978-90-393-5665-4

**Design & Layout**  
**Printing**  
**Contact auteur**

Richard Bekkers i.s.m. Buro Rauwekost  
Gildeprint Enschede  
[brittvankooij@gmail.com](mailto:brittvankooij@gmail.com)

# MRI analysis and neurodevelopmental outcome in preterm infants

MRI analyse en psychomotore ontwikkeling van prematuur geboren kinderen  
(met een samenvatting in het Nederlands)

## Proefschrift

ter verkrijging van de graad van doctor aan de Universiteit Utrecht op gezag van de rector magnificus, prof.dr. G.J. van der Zwaan, ingevolge het besluit van het college voor promoties in het openbaar te verdedigen op woensdag 9 november 2011 des middags te 2.30 uur

*door*

**Britt Joan Maria van Kooij**  
geboren op 20 mei 1983 te Oosterhout

Promotoren: Prof.dr. L.S. de Vries  
Prof.dr.ir. M.A. Viergever

Co-promotoren: Dr. F. Groenendaal  
Dr. M.J.N.L. Benders

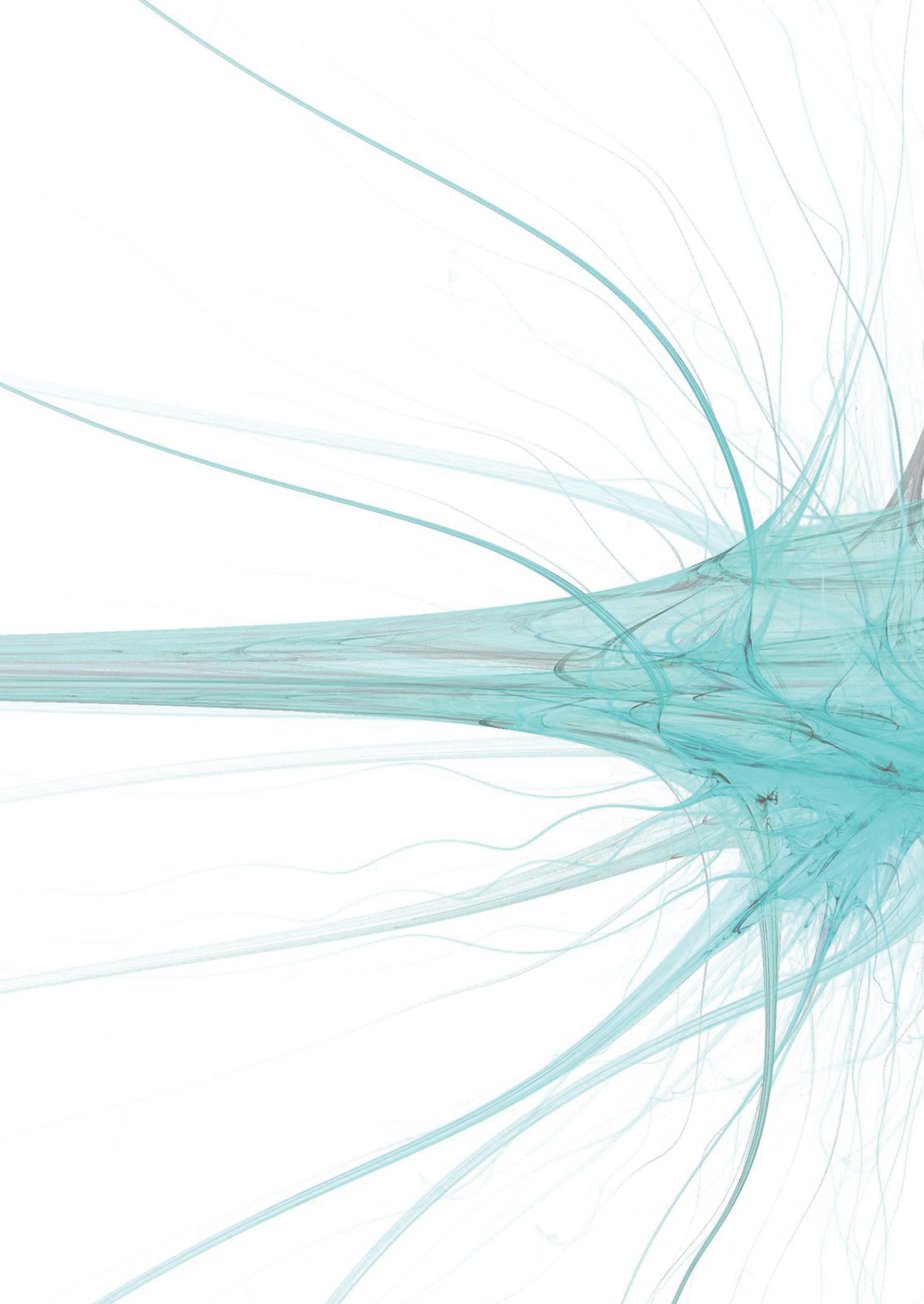
## CONTENTS

List of abbreviations	<i>p8</i>
<b>Chapter 1</b>	White matter injury and neurodevelopmental outcome in preterm infants Aim of the study and outline of the thesis <i>p10</i>
<b>PART 1</b>	<b>Implementation of MRI postprocessing techniques</b> <i>p26</i>
<b>Chapter 2</b>	Automatic neonatal brain segmentation of eight cerebral tissue classes <i>p28</i>
<b>Chapter 3</b>	Quantitative fiber tracking in corpus callosum and internal capsule reveals microstructural abnormalities in preterm infants at term equivalent age. <i>p44</i>
<b>PART 2</b>	<b>MRI postprocessing techniques and neurodevelopment</b> <i>p62</i>
<b>Chapter 4</b>	Brain volumes at term equivalent age: biomarker for neurodevelopmental outcome in preterm infants <i>p64</i>
<b>Chapter 5</b>	Cerebellar volume and proton MR spectroscopy at term and neurodevelopment at two years of age in preterm infants <i>p82</i>
<b>Chapter 6</b>	Neonatal tract-based spatial statistics findings and outcome in preterm infants <i>p100</i>
<b>Chapter 7</b>	Fiber tracking at term displays gender differences regarding cognitive and motor outcome at two years of age in preterm infants <i>p118</i>
<b>Chapter 8</b>	Anatomy of the circle of Willis and blood flow in the brain-feeding vasculature in prematurely born infants <i>p136</i>
<b>PART 3</b>	<b>Summary, discussion and future directions</b> <i>p150</i>
<b>Chapter 9</b>	Summary, general discussion and future directions <i>p152</i>
<b>Chapter 10</b>	Samenvatting in het Nederlands <i>p162</i>
List of co-authors / List of publications	<i>p172</i>
Dankwoord	<i>p176</i>
Curriculum Vitae	<i>p182</i>

### List of abbreviations

ACA	anterior cerebral artery
AD	axial diffusivity
ADC	apparent diffusion coefficient
BA	basilar artery
BG	basal ganglia/thalamus
BS	brainstem
BSITD-III	Bayley Scales of Infant- and Toddler Development-III
BT	brain tissue volume
BW	birth weight
BWz	birth weight Z-score
CB	cerebellum
CBF	cerebral blood flow
CC	corpus callosum
CeGM	central gray matter
Cho	choline
CI	case linear anisotropy index
CoGM	cortical gray matter
CSF	cerebrospinal fluid in the extra-cerebral space
cPVL	cystic periventricular leukomalacia
CV	cerebellar volume
DEHSI	diffuse excessive high signal intensity
DTI	Diffusion Tensor Imaging
FA	fractional anisotropy
FSL	FMRIB's software library
FT	fiber tracking
GA	gestational age
Glx	glutamate/glutamine/ $\gamma$ -aminobutyric acid
GM	gray matter
GMH	germinal matrix haemorrhage
HC	head circumference
<sup>1</sup> H-MRS	proton magnetic resonance spectroscopy
ICA	internal carotid artery
ICV	intracranial volume
IVH	intraventricular haemorrhages
Lac	lactate
MCA	middle cerebral artery
MD	mean diffusivity
ml	myo-inositol
MRA	magnetic resonance angiography
MRI	magnetic resonance imaging
MWM	myelinated white matter
NAA	N-acetylaspartate
PC-MRA	phase-contrast magnetic resonance angiography
PCA	posterior cerebral artery
PCoA	posterior communicating artery
PHVD	post-haemorrhagic ventricular dilatation
PLIC	posterior limb of the internal capsule
PMA	postmenstrual age

PVL	periventricular leukomalacia
PWMI	periventricular white matter injury
RD	radial diffusivity
ROI	region of Interest
TBSS	tract-based spatial statistics
TBV	total brain volume
TE	echo time
TEA	term-equivalent age
TFCE	threshold-free cluster enhancement
TMWM	total myelinated white matter
TOF-MRA	time-of-flight magnetic resonance angiography
TR	repetition time
UWM	unmyelinated white matter
VENT	cerebrospinal fluid in the ventricles
VLBW	very low birth weight
WM	white matter
WMI	white matter injury



The background of the page features a complex, abstract design. It consists of numerous thin, flowing lines in various shades of teal and grey. These lines originate from the left side and spread out towards the right, creating a sense of movement and depth. The lines vary in opacity, with some being more prominent and others fading into the background. The overall effect is a modern, artistic representation of neural pathways or data flow.

# CHAPTER ONE

## White matter injury and neurodevelopmental outcome in preterm infants

B.J.M van Kooij

## INTRODUCTION

In 2003-2007, the Perinatal Registry of the Netherlands (PRN) reported around 1700-1800 live born infants born below 32 weeks' gestation per year, of whom 460-480 were born at a gestational age (GA) between 24 and 27 weeks. Important risk factors for preterm birth are foetal or maternal infection, maternal demographic characteristics, e.g. age and marital status, multiple pregnancy and preeclampsia.<sup>1</sup> While the mortality rate of preterm infants is decreasing, they remain at risk for neurological disabilities later in life, especially those born below 30 weeks' gestation.<sup>2</sup> Preterm infants are prone to brain injury, especially to the white matter (WM) and subsequent neurodevelopmental impairments. In the Wilhelmina Children's Hospital, the incidence of cerebral palsy in infants born below 35 weeks' gestation has dropped from around 6% to 2.2%.<sup>3</sup> Additionally, in a cohort of Dutch adolescents born below 32 weeks, 38.4% had mild neuromotor problems and 3.2% severe problems.<sup>4</sup> Mild cognitive impairments were seen in 14.8% of the adolescents and only 4.3% suffered from moderate cognitive deficits.<sup>4</sup> It is important to detect brain pathology at an early stage to improve parental counseling and to identify those neonates susceptible to neurological disabilities who could benefit from 'developmental support' programs.<sup>5,6</sup> Motor deficits have been well defined and are associated with several patterns of brain injury detected by cranial ultrasound and magnetic resonance imaging (MRI) before or around term-equivalent age (TEA).<sup>7,8</sup> To predict cognitive outcome at an early point in time is still less straightforward. Cranial ultrasound is a cheap and easy bedside tool and can routinely be performed to detect obvious brain lesions in the preterm infant, such as germinal matrix-intraventricular haemorrhage (GMH-IVH) or cystic periventricular leukomalacia (cPVL).<sup>9-14</sup> MRI of the brain performed around TEA, or even soon after birth, is a potential tool to detect (more subtle) brain lesions.<sup>7,15-17</sup> Conventional T1- and T2-weighted images provide detailed information about the anatomy of the preterm brain and detect apparent lesions, especially in the WM, which is known to be especially susceptible for injury.<sup>18</sup> Brain lesions apparent on conventional MRI have been shown to be related to neurodevelopmental outcome.<sup>7,8,15</sup> However, neurological impairments have been reported in preterm infants without obvious abnormalities on conventional MRI.<sup>19</sup> In the last decade more advanced MRI techniques have been developed to assess brain development and injury in more detail. Different neonatal brain segmentation methods were developed to evaluate (regional) brain volumes, brain growth and cortical folding and to assess the relationship with neurodevelopment.<sup>8,20-22</sup> Other MRI techniques are based on the diffusion of water molecules. Using diffusion weighted (DWI) or diffusion tensor imaging (DTI), it is possible to assess the microstructural development of WM, including the connectivity of the axons, fiber bundle integrity and myelination of WM.<sup>8,23-25</sup> WM maturation is accompanied by an increase in fractional anisotropy (FA) and a decrease in apparent diffusion coefficient (ADC).<sup>26</sup> In this chapter, first the most common pathologies of the premature brain are discussed and next the different advanced MRI techniques to detect these lesions. At the end of this chapter, the contents of this thesis are outlined based on the previously described issues.

## White matter injury in preterm infants

### *Intraventricular haemorrhage*

In spite of improved perinatal care, germinal matrix haemorrhage (GMH)-IVH is still a common neonatal morbidity with an incidence of approximately 15-25% in infants born between 28-31 weeks up to 30-40% in infants born between 25-27 weeks' gestation.<sup>15;18;27</sup> The origin of an GMH-IVH in preterm infants is most often the periventricular matrix zone located between the caudate nucleus and the thalamus.<sup>28</sup> Grunnet *et al.* hypothesized that because of the larger diameter of the vessels in the germinal plate compared to cortical vessels, these immature vessels are under a higher pressure, which could explain their susceptibility for rupture.<sup>29</sup> Volpe described three major groups of causes of a GMH-IVH: intravascular, such as fluctuation in cerebral blood flow and platelet disturbances; vascular factors, e.g. vulnerability of the matrix capillaries to hypoxia-ischemia; and extravascular factors, such as deficient vascular support and fibrinolytic activity. Spontaneous vaginal preterm delivery, intrapartum asphyxia and lower GA, have been revealed as risk factors for the development of a GMH-IVH.<sup>27;28</sup> A GMH-IVH is associated with reduced cortical and cerebellar volume and/or development.<sup>30-32</sup> Different studies illustrated reduced motor and cognitive skills in children with an IVH in the neonatal period compared to children without an IVH<sup>10;33;34</sup>, even after a GMH or IVH grade II.<sup>35</sup> The severity of the haemorrhage was associated with neurological impairments (15-25% in GMH-IVH grade II and 50-75% in IVH III/IV). The main determinant of a poor outcome, however, is the presence of associated injury to WM.<sup>18</sup> Post-haemorrhagic ventricular dilatation (PHVD) is a complication of IVH seen in 5-15% of the neonates with a GMH-IVH grade II up to 65-85% in preterm infants with an IVH III/IV. The pathogenesis is not fully understood, but it is generally assumed that the reabsorption of cerebrospinal fluid (CSF) is impaired by particulate blood clots or obliterative arachnoiditis in the posterior fossa.<sup>18</sup> Cherian *et al.* used a rat model to assess the pathogenesis of PHVD. Their findings suggested that besides an impaired reabsorption of CSF, acute ventricular enlargement and raised intracranial pressure played a role in the development of PHVD.<sup>36</sup> It has been shown that PHVD in very preterm infants is related to a poor (cognitive) outcome, especially in those requiring intervention.<sup>37;38</sup>

### *Periventricular white matter injury*

Periventricular WM injury (PWMI) contains a spectrum of WM injury that varies from diffuse WM abnormalities (diffuse PWMI) to focal necrosis in WM. The latter is often referred to as cystic periventricular leukomalacia (cPVL).<sup>39</sup> Diffuse PWMI is characterised by astrogliosis, microgliosis and a decrease in premyelinating oligodendrocytes diffusely apparent in WM. As a response, there appears to be an upregulation of oligodendroglial progenitors. These cells seem to miss the capacity to differentiate to mature myelin-producing cells, which leads to hypomyelination with ventriculomegaly. cPVL refers to localised, sometimes macroscopic necrosis in WM with loss of cellular elements, which can evolve into multiple cysts. PWMI is commonly seen in prematurely born infants and imaging studies indicated that at least 50% of very low birth weight (VLBW) infants showed signs consistent with diffuse PWMI; however, cPVL is less common (<5% of VLBW

infants).<sup>40</sup> Periventricular WM of the preterm infant is very vulnerable to injury because of several maturation-dependent factors. Two factors play a crucial role in the pathogenesis of PWMI: ischemia and infection. Cerebral WM is prone to injury following ischemia due to the presence of vascular end zones and border zones and because of an immature cerebral blood flow autoregulation. The mechanism by which infection may initiate WM injury is not fully understood, but it is known that microglia play a central role. In response to inflammation, microglia will be activated and subsequently secrete products, such as cytokines, which are harmful for WM. Excitotoxicity and free radicals are two other mechanisms in the pathogenesis of PWMI.<sup>18;39</sup> Neurodevelopmental outcome of infants with cPVL was associated with the extent and site of the cysts: cysts which were restricted to frontal WM were associated with cognitive impairments, whereas cysts in parieto-occipital WM were more likely to lead to subsequent development of cerebral palsy.<sup>41;42</sup> Diffuse PWMI at TEA was related to both cognitive and motor delay at two years corrected age and was influenced by WM loss and ventricular dilatation.<sup>8</sup>

#### *Diffuse excessive high signal intensity*

A normal characteristic of developing WM is an increased signal intensity on a T2-weighted MR image in the area around the frontal horns, forming a 'cap' shape, and around the posterior horns of the lateral ventricles, forming an arrowhead shape. It is hypothesized that these areas represent the different WM layers or 'cross-roads' and the increased signal intensity is supposed to decrease with increasing GA.<sup>43</sup> In contrast, 'diffuse excessive high signal intensity' or DEHSI on conventional T2-weighted images was described in WM of the premature brain<sup>43</sup> and it was seen in about 70-80% of preterm infants at TEA.<sup>15;44</sup> The underlying pathology remains unclear; however, it was suggested that DEHSI is a sign of WM injury rather than a normal feature of (delayed) WM development.<sup>45-47</sup> Recently, it has been shown that the visual appearance of DEHSI is highly subjective, which limits clinical application.<sup>48</sup> Additionally, the relation between DEHSI and diffusion parameters displayed contrasting results. Counsell *et al.* found elevated radial and axial diffusivity in preterm infants with DEHSI at TEA (n=29) compared to both preterm infants without DEHSI (n=9) and to term born controls (n=8).<sup>49</sup> However Hart *et al.* were not able to show a difference in apparent diffusion coefficient (ADC), a measure for mean diffusivity, between preterm infants with DEHSI without other overt abnormalities and preterm infants with a normal MRI at TEA.<sup>50</sup> The clinical importance of DEHSI is still rather uncertain. One study in a small group of preterm infants with only signs of DEHSI at TEA revealed a lower developmental quotient of the Griffiths Mental Development Scales at a median age of two years corrected as compared with preterm infants with a normal MRI at TEA.<sup>15</sup> Long-term consequences of DEHSI have not yet been reported.

#### *Punctate white matter lesions*

WM injury in the preterm brain is not always as widespread as DEHSI or diffuse PWMI. Miller *et al.* described the presence of more focal, small punctate lesions in WM.<sup>7</sup> Lesions with an increased signal intensity on T1-weighted images, but without a decreased

signal intensity on T2-weighted images were presumably referring to gliosis, whereas lesions with an increased signal intensity on T1-weighted images and a decreased signal intensity on T2-weighted images were most likely sites of haemorrhage. Susceptibility weighted imaging may help to distinguish between haemorrhage and another origin of the lesion, such as gliosis after a small infarction. In conformity with PWMI, WM of the preterm brain is most vulnerable to punctate lesions in a certain time frame, not including the extremely preterm brain.<sup>15</sup> In agreement with Debillon *et al.*<sup>11</sup>, our own experience is that punctate lesions diagnosed on conventional MRI soon after birth can be missed on cranial ultrasound, although the presence of inhomogeneous echogenicity does suggest the presence of the punctuate lesions. Since punctate lesions decrease in number over time, their presence in the preterm brain could be overlooked on an MRI only performed at TEA.<sup>41</sup> Ramenghi *et al.* demonstrated that punctate WM lesions were related to reduced total maturation score as derived from delayed and reduced cortical folding.<sup>51</sup> Data regarding clinical implications are rather scarce and contradictory. One study demonstrated altered WM microstructure at TEA in the fibers of the corticospinal tract in preterm infants showing punctate lesions on MRI as compared with gender and GA matched preterm controls without punctate lesions.<sup>52</sup> A Mental Developmental Index score <70 on the Bayley Scales of Infant Development-II and/or functional motor deficits at 12-18 months corrected age were displayed in children with more than three areas of abnormal T1 signal intensity at TEA or when more than 5% of the hemisphere was involved<sup>7</sup>. No differences in developmental quotient of the Griffiths Mental Development Scales were seen at two years corrected age between preterm infants with and without punctate lesions at TEA.<sup>15</sup>

## **MRI techniques and analysis methods**

### *Conventional MRI*

Conventional MRI is commonly performed to assess brain anatomy and development in preterm infants. Different patterns of apparent lesions have been described in relation to neurodevelopmental outcome.<sup>8</sup> Conventional MRI does not always detect subtle abnormalities and an abnormal outcome has been demonstrated in preterm infants with normal MRI findings.<sup>19</sup> Common conventional MRI findings in preterm infants are DEHSI, increased subarachnoid space, thinning of the corpus callosum and ventriculomegaly.<sup>15</sup>

During the last decade advanced MR imaging techniques and analysis methods have been designed to assess brain development and pathology in more detail. These techniques and analysis methods and additionally the implementation in this thesis are discussed below. Next, the delineation of the different research questions are outlined.

### *Brain segmentation methods*

Conventional MRI is increasingly applied to measure brain volumes in the neonatal period. Segmentation of the neonatal brain at TEA is challenging because of the low contrast between the different brain tissues. Besides, the maturation processes around TEA and consequently different proportions of myelinated and unmyelinated WM leads to rapid changes in signal intensities. Over the last decade, several methods have been

developed for the segmentation of gray matter (GM), unmyelinated (UWM) and myelinated white matter (MWM) and volume of the cerebrospinal fluid (CSF).<sup>22;53-61</sup> The method described by Warfield *et al.* was mostly used in studies assessing brain volumes of preterm infants at TEA.<sup>62</sup> This algorithm contained different steps to segment cortical (CoGM) and central GM (CeGM), UWM, MWM and total CSF. Sample voxels of each tissue class were manually selected to estimate the distribution of MRI signal intensities associated with each tissue class. Next, a template of normal brain anatomy was aligned with the image data. The anatomical template provided a set of features describing anatomical localization. A segmentation was computed with k-Nearest Neighbor classification based on signal intensity and localization features. By using this method, reduced CoGM and UWM volumes have been reported in preterm infants at TEA as compared with term born controls.<sup>20;63</sup> Lower CoGM volumes and an increase in total CSF volume at TEA were found in infants with moderate/severe disabilities at one year of age. Furthermore, in children and adolescents reduced volumes of CoGM, CeGM, cerebral WM and cerebellum, and an increase in total CSF were associated with neurodevelopmental impairment.<sup>64-66</sup> Additionally, the role of cerebellar development in preterm infants is increasingly recognized to be associated with neurodevelopmental outcome.<sup>67-69</sup>

Brain volumes of preterm infants at TEA in relation to neurodevelopmental outcome have not been studied extensively and not previously in The Netherlands. The population in our region is relatively affluent and benefits from adequate perinatal health care. It is as yet unknown whether brain volumes at TEA are related to neurodevelopment at two years corrected age in a relatively healthy cohort of preterm infants.

#### *Diffusion weighted imaging and diffusion tensor imaging*

In diffusion weighted imaging (DWI), the contrast is based on the Brownian motion of water molecules, which is influenced by various factors, e.g. cell membranes, cell organelles and the degree of myelination.<sup>70</sup> Low ADC values indicate that random motion is restricted, as e.g. in the case of stroke. ADC values are higher in infants than in adults, due to the higher water content.<sup>71</sup> In preterm infants with DEHSI, higher ADC values were found as compared with preterm infants without DEHSI.<sup>45;46</sup>

Diffusion tensor imaging (DTI) can be used to assess brain connectivity.<sup>72</sup> DTI describes the diffusion of water molecules in tissues and is assumed to reflect the direction of the underlying microstructure.<sup>73;74</sup> WM maturation is accompanied by an increase in FA and a decrease in ADC.<sup>26</sup> Besides FA, the diffusion parallel (axial diffusion: diffusion eigenvalue:  $\lambda_1$ ) and perpendicular (radial diffusion: diffusion eigenvalues  $(\lambda_2 + \lambda_3)/2$ ) to the WM tracts can provide supplementary information regarding WM microstructure. DTI studies showed that radial and axial diffusivity in WM were elevated in children with DEHSI as compared with preterm neonates without DEHSI and term born controls.<sup>49</sup> Several studies displayed lower FA and higher ADC values in e.g. posterior limb of the internal capsule (PLIC) or corpus callosum before abnormalities were seen on conventional MRI. These alterations were related to neurodevelopmental outcome.<sup>47;75-78</sup>

Visual analysis of WM lesions seen on T1- and T2-weighted imaging is rather subjective and subtle lesions can be easily missed. It was hypothesized that diffusion parameters could be used to quantify changes in WM microstructure and could provide information regarding the underlying pathology. Diffusion parameters are assumed to reflect WM maturation and organization, which likely relate to neurodevelopment.<sup>71</sup> Diffusion parameters at TEA have not been studied extensively in relation to neurodevelopmental outcome in preterm infants. Accordingly, the role of diffusion imaging as a biomarker for neurodevelopment is unclear.

#### *Proton magnetic resonance spectroscopy*

Proton magnetic resonance spectroscopy (<sup>1</sup>H-MRS) can be used to assess brain integrity and maturation with age.<sup>79,80</sup> In full-term infants with perinatal asphyxia, <sup>1</sup>H-MRS of the cerebrum, especially the N-acetylaspartate/choline (NAA/Cho) ratio, has been shown to predict neuromotor development.<sup>81</sup> Cerebellar <sup>1</sup>H-MRS revealed a two-fold increase of the NAA/Cho ratio in the preterm infant after birth and at term age, and between term age and adulthood.<sup>82</sup> As previously described, several studies support the hypothesis that the cerebellum plays an important role in neurodevelopment in preterm infants.<sup>67-69</sup>

To the best of our knowledge, no studies have been performed previously to assess the relation between changes in cerebellar <sup>1</sup>H-MRS and neurodevelopment in preterm infants. We hypothesized that a reduced NAA/Cho ratio in the cerebellum was associated with an adverse outcome at two years.

#### *Imaging of the vascular system: 2D phase-contrast magnetic resonance angiography and time-of-flight MRA*

Three-dimensional time-of-flight magnetic resonance angiography (TOF-MRA) and two-dimensional phase-contrast MRA (PC-MRA), both non-invasive imaging techniques, may allow a combined anatomical evaluation of the vasculature with a functional evaluation of the blood flow in the brain feeding arteries, respectively. Recently, it has been reported that preterm infants showed a decreased tortuosity in all proximal segments of the cerebral vasculature at TEA compared to full term infants, which indicates that preterm delivery alters the development of the cerebral blood vessels.<sup>83</sup> For normal brain function and development an adequate blood flow to the brain is required and alterations in cerebral blood flow play an important role in the pathogenesis of brain injury in neonates.<sup>84;85</sup> In adults, the anatomical configuration of the circle of Willis was closely related to blood flow in the brain feeding arteries.<sup>86</sup> Post-mortem evaluation of the anatomy of the circle of Willis demonstrated that the anatomy alters in relation to the development of the brain.<sup>87</sup> To date, no prevalence of the various major variations of the circle of Willis have been reported in preterm infants at TEA using non-invasive MR imaging techniques. Additionally, it is unknown whether variations in the anterior or posterior part of the circle of Willis influence cerebral blood flow.

## AIM OF THE STUDY AND OUTLINE OF THE THESIS

The aim of this thesis is to quantify MRI findings at TEA in preterm infants. Additionally (advanced) MR techniques are implemented and it is assessed whether they can be used in the prediction of neurodevelopmental outcome at two years corrected age. We conducted a prospective cohort study of preterm infants born before 31 weeks' gestation. All infants reached TEA between January 2007 and July 2008 and an MRI scan of the brain was performed at a mean postmenstrual age (PMA) of  $41.7 \pm 1.1$  weeks (range 39-45 weeks). Besides conventional T1- and T2-weighted imaging, several more advanced imaging sequences were included in the MR protocol. At two years corrected age cognition, fine motor and gross motor function were assessed using the Bayley Scales of Infant and Toddler Development-III (BSITD-III).<sup>88</sup> All children were tested by a single developmental specialist who was blinded to the MRI findings.

In **Chapter 2** an in-home developed neonatal brain segmentation method is presented to measure eight different brain structures, i.e. MWM, UWM, CoGM, CeGM, ventricles, cerebrospinal fluid in the extra-cerebral space, cerebellum and brain stem. This method is based on k-Nearest Neighbor classification and categorizes voxels of the axial T2- and T1-weighted images based on their signal intensities in both images and on their x-, y- and z-coordinates. The main differences with previously presented neonatal brain segmentation methods are that this method is automatic and thereby user-independent. Furthermore, it is possible to distinguish cerebrospinal fluid in the ventricles from that in the extra-cerebral space, and to segment the cerebellum as a separate structure.

In **Chapter 3** an in-home developed tool to analyse DTI data is administered to perform fiber tracking in the corpus callosum and the left and right PLIC. It is assessed whether quantitative fiber tracking parameters can provide additional information regarding WM injury compared with conventional MRI. In addition, the effect of GA, birth weight, head circumference, gender and the PMA at time of scanning on these parameters is analysed.

In **Chapter 4** our segmentation method presented in *Chapter 2* is used to assess brain tissue volumes of preterm infants at TEA in relation to characteristics of the infant at time of scanning. Furthermore, it is assessed whether cerebral brain tissue volumes at TEA can be used as biomarker for neurodevelopmental outcome at two years corrected age.

In **Chapter 5** the role of cerebellar parameters at TEA is analysed in the development of neurological impairments. The cerebellar volume is calculated with the segmentation method described in *Chapter 2*. The influence of cerebellar lesions on the volume is assessed. It is evaluated whether cerebellar volume corrected for PMA is associated with neurodevelopment at two years corrected age. In a subgroup of our study cohort, <sup>1</sup>H-MRS was performed in the cerebellum. It is assessed whether cerebellar metabolites measured with <sup>1</sup>H-MRS at TEA are related to neurodevelopmental outcome at two years corrected age.

In **Chapter 6** DTI data are evaluated using tract-based spatial statistics (TBSS).<sup>89</sup> This automatic technique can be applied for voxelwise statistical analysis of the major WM tracts across subjects. TBSS is used to determine whether FA values, axial and

radial diffusivity in the major WM tracts of preterm infants at TEA are associated with neurodevelopmental outcome at two years corrected age.

In **Chapter 7** fiber tracking of the fiber passing through the PLIC and corpus callosum is performed. The method presented in *Chapter 3* is used to determine whether volume, length, FA, axial and radial diffusivity and ADC in the corpus callosum bundle and the PLIC bundles at TEA in preterm infants are associated with cognitive and motor outcome at two years corrected age.

In **Chapter 8** flow measurements in the left and right internal carotid arteries and the basilar artery obtained in preterm infants at TEA with 2D PC-MRA are illustrated. The anatomy of the circle of Willis is determined using TOF-MRA. In particular, the presence or absence of a dominant A1 segment of the anterior cerebral artery or a fetal-type posterior cerebral artery is established. Furthermore, it is evaluated whether anatomical variations in the circle of Willis have an effect on blood flow through the internal carotid and basilar arteries.

## Reference List

- (1) Goldenberg RL, Culhane JF, Iams JD, Romero R. Epidemiology and causes of preterm birth. *Lancet* 2008; 371(9606):75-84.
- (2) Saigal S, Doyle LW. An overview of mortality and sequelae of preterm birth from infancy to adulthood. *Lancet* 2008; 371(9608):261-269.
- (3) van Haastert IC, Groenendaal F, Uiterwaal CS, Termote JU, Heide-Jalving M, Eijssermans MJ *et al.* Decreasing Incidence and Severity of Cerebral Palsy in Prematurely Born Children. *J Pediatr* 2011.
- (4) Hille ET, Weisglas-Kuperus N, van Goudoever JB, Jacobusse GW, Ens-Dokkum MH, de Groot L *et al.* Functional outcomes and participation in young adulthood for very preterm and very low birth weight infants: the Dutch Project on Preterm and Small for Gestational Age Infants at 19 years of age. *Pediatrics* 2007; 120(3):e587-e595.
- (5) Koldewijn K, van Wassenauer A, Wolf MJ, Meijssen D, Houtzager B, Beelen A *et al.* A neurobehavioral intervention and assessment program in very low birth weight infants: outcome at 24 months. *J Pediatr* 2010; 156(3):359-365.
- (6) Spittle AJ, Anderson PJ, Lee KJ, Ferretti C, Eeles A, Orton J *et al.* Preventive care at home for very preterm infants improves infant and caregiver outcomes at 2 years. *Pediatrics* 2010; 126(1):e171-e178.
- (7) Miller SP, Ferriero DM, Leonard C, Piecuch R, Glidden DV, Partridge JC *et al.* Early brain injury in premature newborns detected with magnetic resonance imaging is associated with adverse early neurodevelopmental outcome. *J Pediatr* 2005; 147(5):609-616.
- (8) Woodward LJ, Anderson PJ, Austin NC, Howard K, Inder TE. Neonatal MRI to predict neurodevelopmental outcomes in preterm infants. *N Engl J Med* 2006; 355(7):685-694.
- (9) de Vries LS, Eken P, Dubowitz LM. The spectrum of leukomalacia using cranial ultrasound. *Behav Brain Res* 1992; 49(1):1-6.
- (10) Vohr B, Allan WC, Scott DT, Katz KH, Schneider KC, Makuch RW *et al.* Early-onset intraventricular hemorrhage in preterm neonates: incidence of neurodevelopmental handicap. *Semin Perinatol* 1999; 23(3):212-217.
- (11) Debillon T, N'Guyen S, Muet A, Quere MP, Moussaly F, Roze JC. Limitations of ultrasonography for diagnosing white matter damage in preterm infants. *Arch Dis Child Fetal Neonatal Ed* 2003; 88(4):F275-F279.
- (12) Inder TE, Anderson NJ, Spencer C, Wells S, Volpe JJ. White matter injury in the premature infant: a comparison between serial cranial sonographic and MR findings at term. *AJNR Am J Neuroradiol* 2003; 24(5):805-809.
- (13) Maalouf EF, Duggan PJ, Counsell SJ, Rutherford MA, Cowan F, Azzopardi D *et al.* Comparison of findings on cranial ultrasound and magnetic resonance imaging in preterm infants. *Pediatrics* 2001; 107(4):719-727.
- (14) Miller SP, Cozzio CC, Goldstein RB, Ferriero DM, Partridge JC, Vigneron DB *et al.* Comparing the diagnosis of white matter injury in premature newborns with serial MR imaging and transfontanel ultrasonography findings. *AJNR Am J Neuroradiol* 2003; 24(8):1661-1669.
- (15) Dyet LE, Kennea N, Counsell SJ, Maalouf EF, Ajayi-Obe M, Duggan PJ *et al.* Natural history of brain lesions in extremely preterm infants studied with serial magnetic resonance imaging from birth and neurodevelopmental assessment. *Pediatrics* 2006; 118(2):536-548.

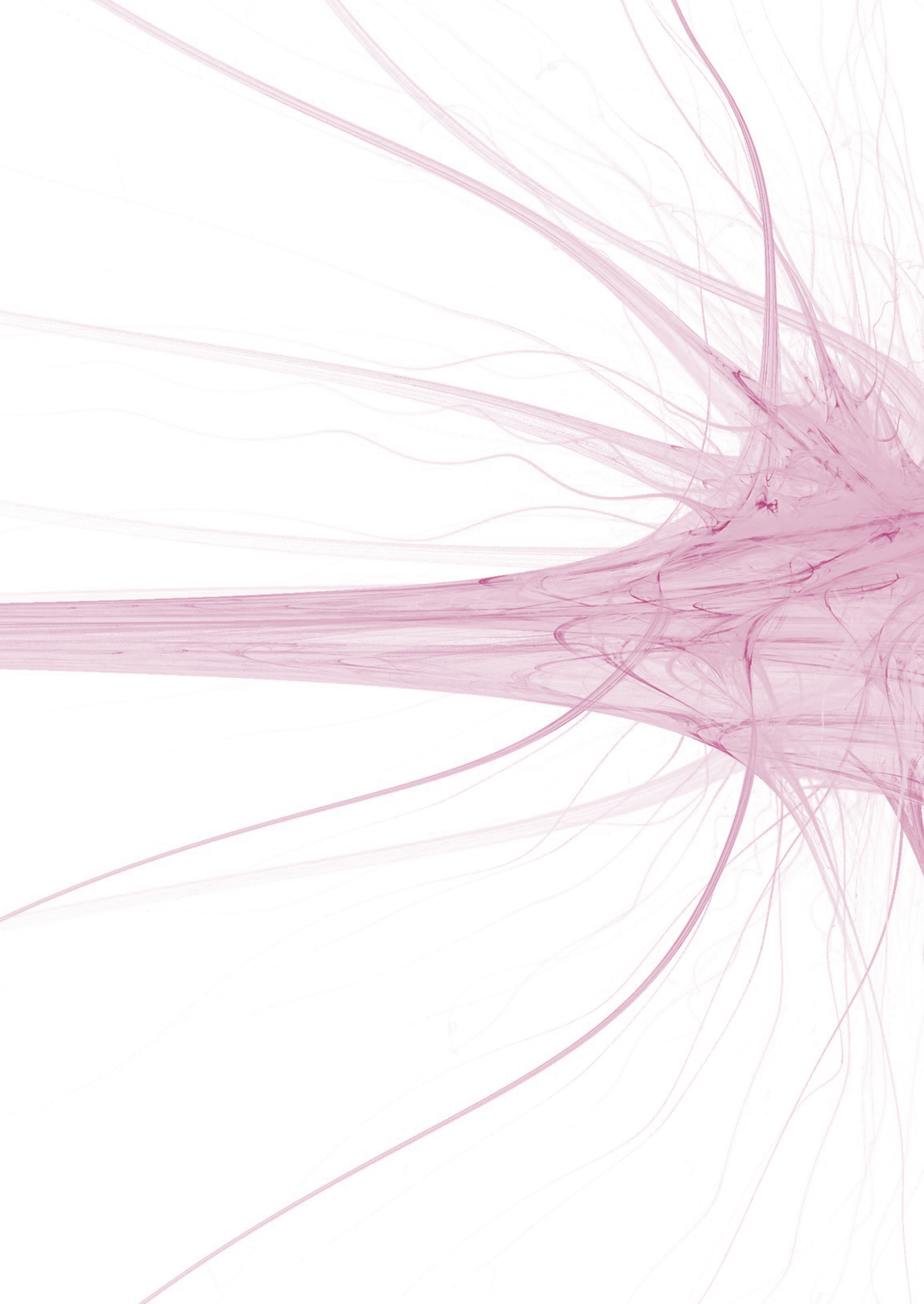
- (16) Horsch S, Hallberg B, Leifsdottir K, Skiold B, Nagy Z, Mosskin M *et al.* Brain abnormalities in extremely low gestational age infants: a Swedish population based MRI study. *Acta Paediatr* 2007; 96(7):979-984.
- (17) Inder TE, Wells SJ, Mogridge NB, Spencer C, Volpe JJ. Defining the nature of the cerebral abnormalities in the premature infant: a qualitative magnetic resonance imaging study. *J Pediatr* 2003; 143(2):171-179.
- (18) Volpe JJ. *Neurology of the newborn*. 5th ed. Philadelphia: Saunders; 2008.
- (19) Mirmiran M, Barnes PD, Keller K, Constantinou JC, Fleisher BE, Hintz SR *et al.* Neonatal brain magnetic resonance imaging before discharge is better than serial cranial ultrasound in predicting cerebral palsy in very low birth weight preterm infants. *Pediatrics* 2004; 114(4):992-998.
- (20) Inder TE, Warfield SK, Wang H, Huppi PS, Volpe JJ. Abnormal cerebral structure is present at term in premature infants. *Pediatrics* 2005; 115(2):286-294.
- (21) Peterson BS, Anderson AW, Ehrenkranz R, Staib LH, Tageldin M, Colson E *et al.* Regional brain volumes and their later neurodevelopmental correlates in term and preterm infants. *Pediatrics* 2003; 111(5 Pt 1):939-948.
- (22) Prastawa M, Gilmore JH, Lin W, Gerig G. Automatic segmentation of MR images of the developing newborn brain. *Med Image Anal* 2005; 9(5):457-466.
- (23) Anjari M, Srinivasan L, Allsop JM, Hajnal JV, Rutherford MA, Edwards AD *et al.* Diffusion tensor imaging with tract-based spatial statistics reveals local white matter abnormalities in preterm infants. *Neuroimage* 2007; 35(3):1021-1027.
- (24) Counsell SJ, Edwards AD, Chew AT, Anjari M, Dyet LE, Srinivasan L *et al.* Specific relations between neurodevelopmental abilities and white matter microstructure in children born preterm. *Brain* 2008; 131(Pt 12):3201-3208.
- (25) Miller SP, Vigneron DB, Henry RG, Bohland MA, Ceppi-Cozzio C, Hoffman C *et al.* Serial quantitative diffusion tensor MRI of the premature brain: development in newborns with and without injury. *J Magn Reson Imaging* 2002; 16(6):621-632.
- (26) Ment LR, Hirtz D, Huppi PS. Imaging biomarkers of outcome in the developing preterm brain. *Lancet Neurol* 2009; 8(11):1042-1055.
- (27) Larroque B, Marret S, Ancel PY, Arnaud C, Marpeau L, Supernant K *et al.* White matter damage and intraventricular hemorrhage in very preterm infants: the EPIPAGE study. *J Pediatr* 2003; 143(4):477-483.
- (28) Vohr B, Ment LR. Intraventricular hemorrhage in the preterm infant. *Early Hum Dev* 1996; 44(1):1-16.
- (29) Grunnet ML. Morphometry of blood vessels in the cortex and germinal plate of premature neonates. *Pediatr Neurol* 1989; 5(1):12-16.
- (30) Vasileiadis GT, Gelman N, Han VK, Williams LA, Mann R, Bureau Y *et al.* Uncomplicated intraventricular hemorrhage is followed by reduced cortical volume at near-term age. *Pediatrics* 2004; 114(3):e367-e372.
- (31) Tam EW, Ferriero DM, Xu D, Berman JI, Vigneron DB, Barkovich AJ *et al.* Cerebellar development in the preterm neonate: effect of supratentorial brain injury. *Pediatr Res* 2009; 66(1):102-106.
- (32) Srinivasan L, Allsop J, Counsell SJ, Boardman JP, Edwards AD, Rutherford M. Smaller cerebellar volumes in very preterm infants at term-equivalent age are associated with the presence of supratentorial lesions. *AJNR Am J Neuroradiol* 2006; 27(3):573-579.
- (33) Erikson C, Allert C, Carlberg EB, Katz-Salamon M. Stability of longitudinal motor development in very low birthweight infants from 5 months to 5.5 years. *Acta Paediatr* 2003; 92(2):197-203.

- (34) Gaddlin PO, Finnstrom O, Wang C, Leijon I. A fifteen-year follow-up of neurological conditions in VLBW children without overt disability: relation to gender, neonatal risk factors, and end stage MRI findings. *Early Hum Dev* 2008; 84(5):343-349.
- (35) Patra K, Wilson-Costello D, Taylor HG, Mercuri-Minich N, Hack M. Grades I-II intraventricular hemorrhage in extremely low birth weight infants: effects on neurodevelopment. *J Pediatr* 2006; 149(2):169-173.
- (36) Cherian SS, Love S, Silver IA, Porter HJ, Whitelaw AG, Thoresen M. Posthemorrhagic ventricular dilation in the neonate: development and characterization of a rat model. *J Neuropathol Exp Neurol* 2003; 62(3):292-303.
- (37) de Vries LS, Liem KD, van Dijk K, Smit BJ, Sie L, Rademaker KJ *et al.* Early versus late treatment of posthaemorrhagic ventricular dilatation: results of a retrospective study from five neonatal intensive care units in The Netherlands. *Acta Paediatr* 2002; 91(2):212-217.
- (38) Brouwer A, Groenendaal F, van Haastert IL, Rademaker K, Hanlo P, de Vries L. Neurodevelopmental outcome of preterm infants with severe intraventricular hemorrhage and therapy for post-hemorrhagic ventricular dilatation. *J Pediatr* 2008; 152(5):648-654.
- (39) Back SA. Perinatal white matter injury: the changing spectrum of pathology and emerging insights into pathogenetic mechanisms. *Ment Retard Dev Disabil Res Rev* 2006; 12(2):129-140.
- (40) Volpe JJ. Brain injury in premature infants: a complex amalgam of destructive and developmental disturbances. *Lancet Neurol* 2009; 8(1):110-124.
- (41) Rutherford MA, Supramaniam V, Ederies A, Chew A, Bassi L, Groppo M *et al.* Magnetic resonance imaging of white matter diseases of prematurity. *Neuroradiology* 2010; 52(6):505-521.
- (42) van Haastert IC, de Vries LS, Eijsermans MJ, Jongmans MJ, Helders PJ, Gorter JW. Gross motor functional abilities in preterm-born children with cerebral palsy due to periventricular leukomalacia. *Dev Med Child Neurol* 2008; 50(9):684-689.
- (43) Maalouf EF, Duggan PJ, Rutherford MA, Counsell SJ, Fletcher AM, Battin M *et al.* Magnetic resonance imaging of the brain in a cohort of extremely preterm infants. *J Pediatr* 1999; 135(3):351-357.
- (44) Hagmann CF, De Vita E, Bainbridge A, Gunny R, Kapetanakis AB, Chong WK *et al.* T2 at MR imaging is an objective quantitative measure of cerebral white matter signal intensity abnormality in preterm infants at term-equivalent age. *Radiology* 2009; 252(1):209-217.
- (45) Cheong JL, Thompson DK, Wang HX, Hunt RW, Anderson PJ, Inder TE *et al.* Abnormal White Matter Signal on MR Imaging Is Related to Abnormal Tissue Microstructure. *AJNR Am J Neuroradiol* 2009.
- (46) Counsell SJ, Allsop JM, Harrison MC, Larkman DJ, Kennea NL, Kapellou O *et al.* Diffusion-weighted imaging of the brain in preterm infants with focal and diffuse white matter abnormality. *Pediatrics* 2003; 112(1 Pt 1):1-7.
- (47) Rose J, Butler EE, Lamont LE, Barnes PD, Atlas SW, Stevenson DK. Neonatal brain structure on MRI and diffusion tensor imaging, sex, and neurodevelopment in very-low-birthweight preterm children. *Dev Med Child Neurol* 2009; 51(7):526-535.
- (48) Hart AR, Smith MF, Rigby AS, Wallis LI, Whitby EH. Appearances of diffuse excessive high signal intensity (DEHSI) on MR imaging following preterm birth. *Pediatr Radiol* 2010; 40(8):1390-1396.
- (49) Counsell SJ, Shen Y, Boardman JP, Larkman DJ, Kapellou O, Ward P *et al.* Axial and radial diffusivity in preterm infants who have diffuse white matter changes on magnetic resonance imaging at term-equivalent age. *Pediatrics* 2006; 117(2):376-386.

- (50) Hart AR, Whitby EH, Clark SJ, Paley MN, Smith MF. Diffusion-weighted imaging of cerebral white matter and the cerebellum following preterm birth. *Dev Med Child Neurol* 2010; 52(7):652-659.
- (51) Ramenghi LA, Fumagalli M, Righini A, Bassi L, Groppo M, Parazzini C *et al*. Magnetic resonance imaging assessment of brain maturation in preterm neonates with punctate white matter lesions. *Neuroradiology* 2007; 49(2):161-167.
- (52) Bassi L, Chew A, Merchant N, Ball G, Ramenghi L, Boardman J *et al*. Diffusion tensor imaging in preterm infants with punctate white matter lesions. *Pediatr Res* 2011.
- (53) Anbeek P, Vincken KL, Groenendaal F, Koeman A, van Osch MJ, van der Grond J. Probabilistic brain tissue segmentation in neonatal magnetic resonance imaging. *Pediatr Res* 2008; 63(2):158-163.
- (54) Kazemi K, Moghaddam HA, Grebe R, Gondry-Jouet C, Wallois F. Design and construction of a brain phantom to simulate neonatal MR images. *Comput Med Imaging Graph* 2010.
- (55) Nishida M, Makris N, Kennedy DN, Vangel M, Fischl B, Krishnamoorthy KS *et al*. Detailed semiautomated MRI based morphometry of the neonatal brain: preliminary results. *Neuroimage* 2006; 32(3):1041-1049.
- (56) Shi F, Shen D, Yap PT, Fan Y, Cheng JZ, An H *et al*. CENTS: Cortical enhanced neonatal tissue segmentation. *Hum Brain Mapp* 2011; 32(3):382-396.
- (57) Song Z, Awate SP, Licht DJ, Gee JC. Clinical neonatal brain MRI segmentation using adaptive nonparametric data models and intensity-based Markov priors. *Med Image Comput Comput Assist Interv* 2007; 10(Pt 1):883-890.
- (58) Wang L, Shi F, Gilmore JH, Lin W, Shen D. Automatic Segmentation of Neonatal Images Using Convex Optimization and Coupled Level Set Method. *Lect Notes Comput Sci* 2010; 6326:1-10.
- (59) Weisenfeld NI, Mewes AU, Warfield SK. Highly accurate segmentation of brain tissue and subcortical gray matter from newborn MRI. *Med Image Comput Comput Assist Interv* 2006; 9(Pt 1):199-206.
- (60) Xue H, Srinivasan L, Jiang S, Rutherford M, Edwards AD, Rueckert D *et al*. Automatic segmentation and reconstruction of the cortex from neonatal MRI. *Neuroimage* 2007; 38(3):461-477.
- (61) Yu X, Zhang Y, Lasky RE, Datta S, Parikh NA, Narayana PA. Comprehensive brain MRI segmentation in high risk preterm newborns. *PLoS One* 2010; 5(11):e13874.
- (62) Warfield SK, Kaus M, Jolesz FA, Kikinis R. Adaptive, template moderated, spatially varying statistical classification. *Med Image Anal* 2000; 4(1):43-55.
- (63) Mewes AU, Huppi PS, Als H, Rybicki FJ, Inder TE, McAnulty GB *et al*. Regional brain development in serial magnetic resonance imaging of low-risk preterm infants. *Pediatrics* 2006; 118(1):23-33.
- (64) Martinussen M, Flanders DW, Fischl B, Busa E, Lohaugen GC, Skranes J *et al*. Segmental brain volumes and cognitive and perceptual correlates in 15-year-old adolescents with low birth weight. *J Pediatr* 2009; 155(6):848-853.
- (65) Nosarti C, Giouroukou E, Healy E, Rifkin L, Walshe M, Reichenberg A *et al*. Grey and white matter distribution in very preterm adolescents mediates neurodevelopmental outcome. *Brain* 2008; 131(Pt 1):205-217.
- (66) Peterson BS, Vohr B, Staib LH, Cannistraci CJ, Dolberg A, Schneider KC *et al*. Regional brain volume abnormalities and long-term cognitive outcome in preterm infants. *JAMA* 2000; 284(15):1939-1947.
- (67) Allin M, Matsumoto H, Santhouse AM, Nosarti C, AlAsady MH, Stewart AL *et al*. Cognitive and motor function and the size of the cerebellum in adolescents born very pre-term. *Brain* 2001; 124(Pt 1):60-66.

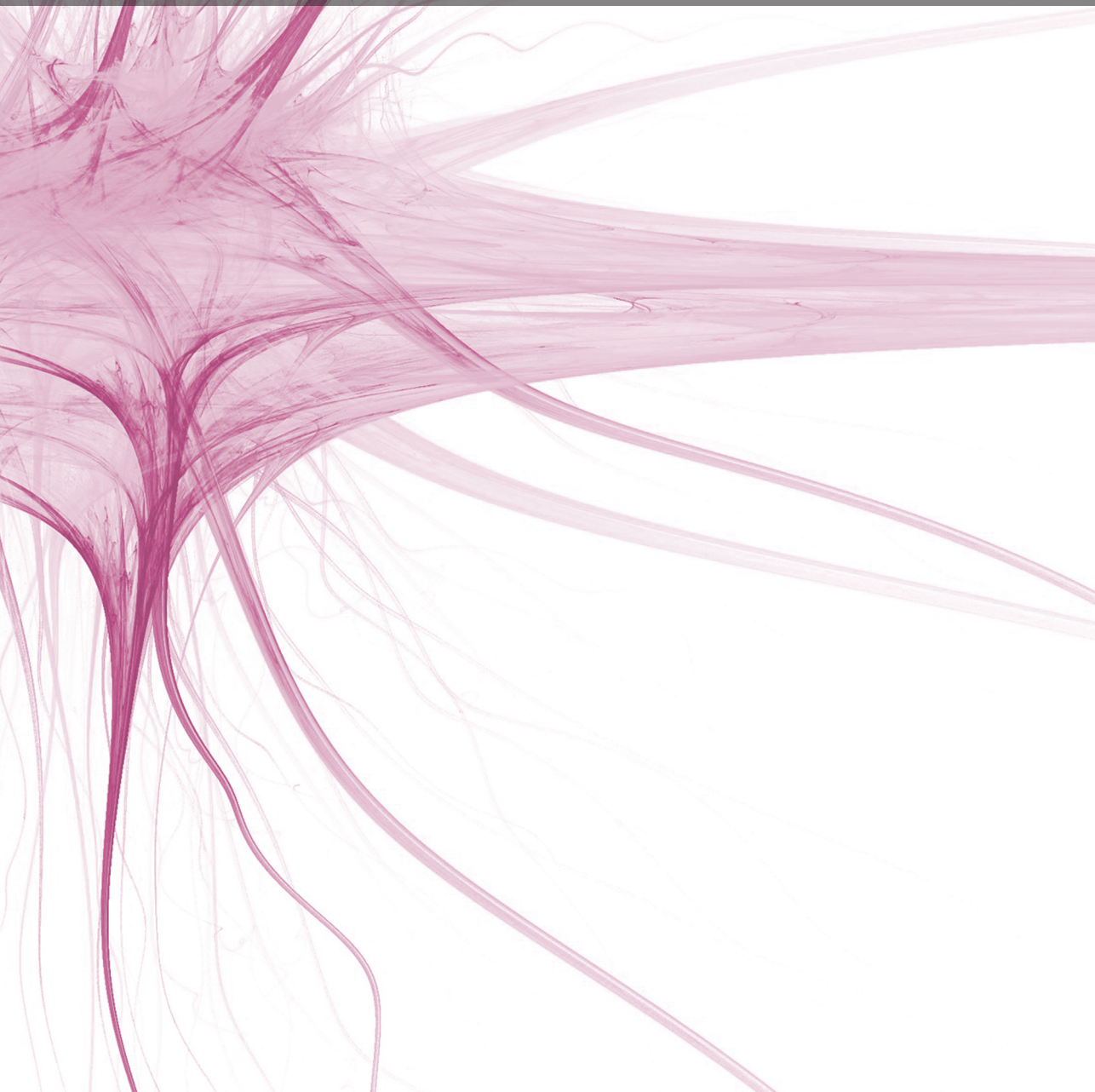
- (68) Messerschmidt A, Fuiko R, Prayer D, Brugger PC, Boltshauser E, Zoder G *et al.* Disrupted cerebellar development in preterm infants is associated with impaired neurodevelopmental outcome. *Eur J Pediatr* 2008; 167(10):1141-1147.
- (69) Shah DK, Anderson PJ, Carlin JB, Pavlovic M, Howard K, Thompson DK *et al.* Reduction in cerebellar volumes in preterm infants: relationship to white matter injury and neurodevelopment at two years of age. *Pediatr Res* 2006; 60(1):97-102.
- (70) Le Bihan D, Breton E, Lallemand D, Grenier P, Cabanis E, Laval-Jeantet M. MR imaging of intravoxel incoherent motions: application to diffusion and perfusion in neurologic disorders. *Radiology* 1986; 161(2):401-407.
- (71) Morriss MC, Zimmerman RA, Bilaniuk LT, Hunter JV, Haselgrove JC. Changes in brain water diffusion during childhood. *Neuroradiology* 1999; 41(12):929-934.
- (72) Huppi PS, Dubois J. Diffusion tensor imaging of brain development. *Semin Fetal Neonatal Med* 2006; 11(6):489-497.
- (73) Basser PJ, Mattiello J, LeBihan D. MR diffusion tensor spectroscopy and imaging. *Biophys J* 1994; 66(1):259-267.
- (74) Mori S, van Zijl PC. Fiber tracking: principles and strategies - a technical review. *NMR Biomed* 2002; 15(7-8):468-480.
- (75) Arzoumanian Y, Mirmiran M, Barnes PD, Woolley K, Ariagno RL, Moseley ME *et al.* Diffusion tensor brain imaging findings at term-equivalent age may predict neurologic abnormalities in low birth weight preterm infants. *AJNR Am J Neuroradiol* 2003; 24(8):1646-1653.
- (76) Drobyshevsky A, Bregman J, Storey P, Meyer J, Prasad PV, Derrick M *et al.* Serial diffusion tensor imaging detects white matter changes that correlate with motor outcome in premature infants. *Dev Neurosci* 2007; 29(4-5):289-301.
- (77) Krishnan ML, Dyet LE, Boardman JP, Kapellou O, Allsop JM, Cowan F *et al.* Relationship between white matter apparent diffusion coefficients in preterm infants at term-equivalent age and developmental outcome at 2 years. *Pediatrics* 2007; 120(3):e604-e609.
- (78) Mathur AM, Neil JJ, Inder TE. Understanding brain injury and neurodevelopmental disabilities in the preterm infant: the evolving role of advanced magnetic resonance imaging. *Semin Perinatol* 2010; 34(1):57-66.
- (79) Dezortova M, Hajek M. (1)H MR spectroscopy in pediatrics. *Eur J Radiol* 2008; 67(2):240-249.
- (80) Roelants-van Rijn AM, van der GJ, Stigter RH, de Vries LS, Groenendaal F. Cerebral structure and metabolism and long-term outcome in small-for-gestational-age preterm neonates. *Pediatr Res* 2004; 56(2):285-290.
- (81) Roelants-van Rijn AM, van der GJ, de Vries LS, Groenendaal F. Value of (1)H-MRS using different echo times in neonates with cerebral hypoxia-ischemia. *Pediatr Res* 2001; 49(3):356-362.
- (82) Huppi PS, Posse S, Lazeyras F, Burri R, Bossi E, Herschkowitz N. Magnetic resonance in preterm and term newborns: 1H-spectroscopy in developing human brain. *Pediatr Res* 1991; 30(6):574-578.
- (83) Malamateniou C, Counsell SJ, Allsop JM, Fitzpatrick JA, Srinivasan L, Cowan FM *et al.* The effect of preterm birth on neonatal cerebral vasculature studied with magnetic resonance angiography at 3 Tesla. *Neuroimage* 2006; 32(3):1050-1059.
- (84) Back SA, Riddle A, McClure MM. Maturation-dependent vulnerability of perinatal white matter in premature birth. *Stroke* 2007; 38(2 Suppl):724-730.
- (85) Volpe JJ. Brain injury in the premature infant--from pathogenesis to prevention. *Brain Dev* 1997; 19(8):519-534.

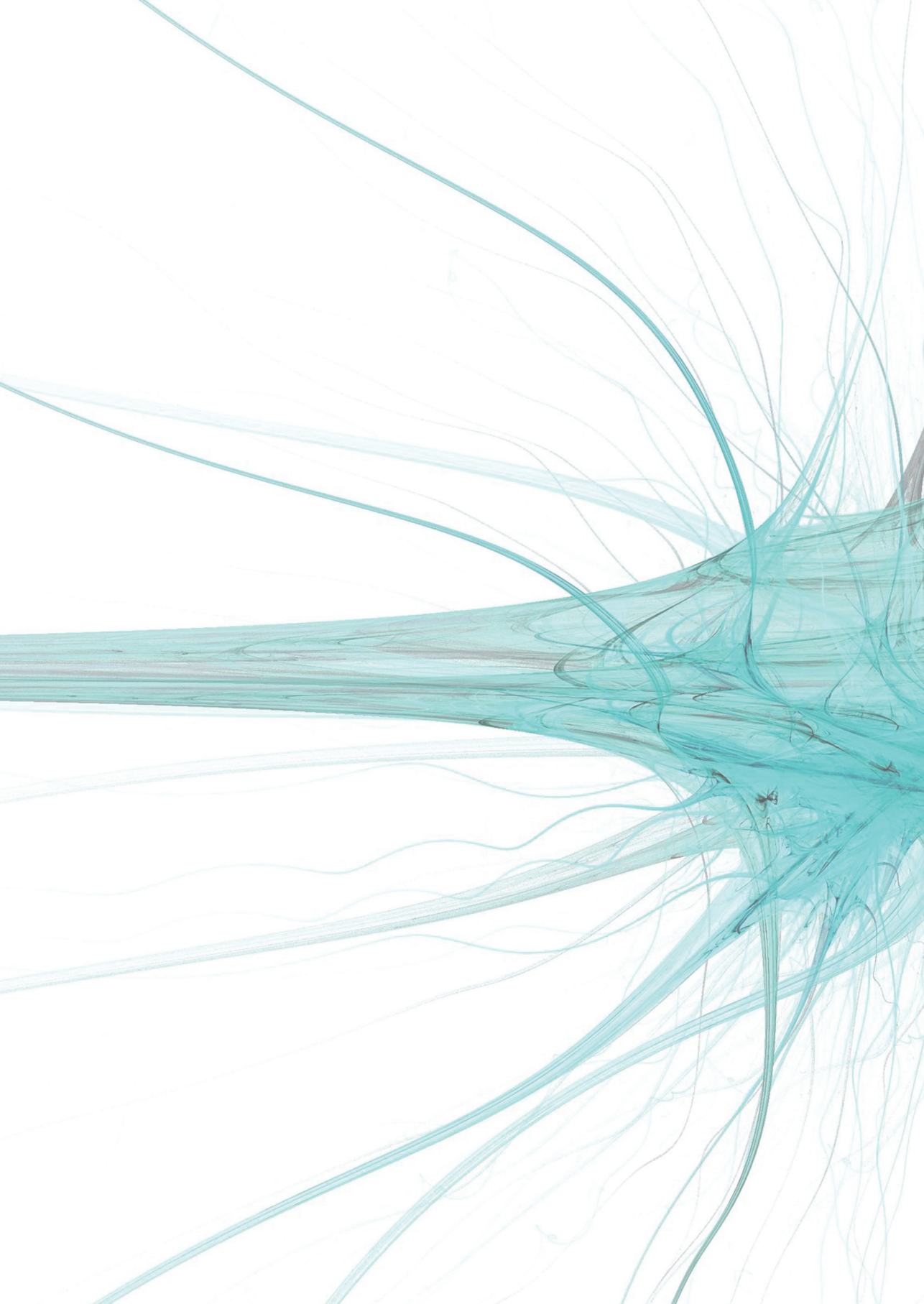
- (86) Hendrikse J, van Raamt AF, van der Graaf Y, Mali WP, van der Grond J. Distribution of cerebral blood flow in the circle of Willis. *Radiology* 2005; 235(1):184-189.
- (87) Van Overbeeke JJ, Hillen B, Tulleken CA. A comparative study of the circle of Willis in fetal and adult life. The configuration of the posterior bifurcation of the posterior communicating artery. *J Anat* 1991; 176:45-54.
- (88) Bayley N. Bayley Scales of Infant and Toddler Development, Third edition. San Antonio, USA: Harcourt Assessment; 2006.
- (89) Smith SM, Jenkinson M, Johansen-Berg H, Rueckert D, Nichols TE, Mackay CE *et al*. Tract-based spatial statistics: voxelwise analysis of multi-subject diffusion data. *Neuroimage* 2006; 31(4):1487-1505.



# PART ONE

## Implementation of MRI postprocessing techniques







## CHAPTER TWO

# Automatic segmentation of eight tissue classes in neonatal brain MRI

Petronella Anbeek, Britt J.M. van Kooij, Karina J. Kersbergen, Linda S. de Vries, Floris  
Groenendaal, Ivana Išgum, Max A. Viergever, Manon J.N.L. Benders

*In preparation*

**ABSTRACT**

**Purpose** - We propose an automatic method for probabilistic brain segmentation in neonatal MRI in eight tissue classes: cortical and central grey matter, unmyelinated and myelinated white matter, cerebrospinal fluid in the ventricles and in the extracerebral space, brainstem and cerebellum.

**Materials and Methods** - Axial T1- and T2-weighted MR images were acquired at term-equivalent age for a preterm cohort of 108 neonates. A method for automatic probabilistic segmentation of the images into the eight tissue classes was developed, based on k-Nearest Neighbor classification, using the T1 and T2 signal intensities and the spatial positions of the image voxels. The method was trained and evaluated using leave-one-out experiments on seven images, for which a reference standard had been set by manual segmentation of the eight tissue classes. Subsequently, the method was applied to the remaining 101 scans, and the resulting segmentations were evaluated visually by two experts. In this way, volumes of the eight segmented tissue classes could be estimated for each patient.

**Results** - The probabilistic segmentation method produced volumes that compared favorably with the reference standard. The Dice similarity coefficients ranged from 0.78 to 0.93. Application of the method to the preterm at term-equivalent age cohort yielded accurate segmentations of the eight tissue classes and reliable estimates of the corresponding volumes.

**Conclusion** - The proposed method provides accurate automatic segmentation of neonatal brain MR images into eight different brain tissue classes. This method separately segments cerebellum and brain stem and is the first method that distinguishes cerebrospinal fluid in the ventricles from cerebrospinal fluid in the extracerebral space.

## INTRODUCTION

Cerebral volumetric segmentation and voxel-based morphometry have recently been applied to MR images of newborn infants, and have shown to be of great additional value in studying brain development at early stages.<sup>1-3</sup> In neonates, different risk factors for altered brain volumes have been identified, such as preterm birth, chronic lung disease and intra-uterine growth restriction.<sup>4-6</sup> Several studies have illustrated the correlation between brain volumes and neurodevelopmental outcome in children and adolescents, who were born prematurely.<sup>2,7,8</sup> However, data regarding brain volumes at term-equivalent age (TEA) and long-term neurodevelopmental outcome are rather limited.<sup>9</sup>

Many adult segmentation methods use signal intensity for voxel classification, which relies on the contrast between different tissues and an adequate signal-to-noise ratio. In neonatal brain images the tissue contrast is less as compared with adults because the majority of white matter is unmyelinated and has higher water content. In addition, the scan time in neonatal brain imaging is limited because of possible motion of the infants, which reduces the signal-to-noise ratio.<sup>4</sup>

In the last decade, several semi-automatic<sup>10-12</sup> or automatic<sup>13-17</sup> neonatal brain segmentation algorithms have been described. To study subtle differences in volumes of brain tissues in large cohorts, an automatic method is preferable, since manual segmentations are time-consuming and subjective. The neonatal brain develops relatively quickly in the first year after birth. To assess brain development and maturation in newborns, it is necessary to identify different tissue classes. Some segmentation methods distinguished unmyelinated (UWM) from myelinated white matter (MWM)<sup>14;15;17</sup>, and/or central (CeGM) from cortical gray matter (CoGM).<sup>10;11;13;14;17</sup> While the cerebellum (CB) was shown to be important in the neurodevelopment in preterm infants<sup>18</sup>, only two methods have segmented CB separately.<sup>11;14</sup> Furthermore, the ventricles were segmented as individual structure by Nishida *et al.*; however, they excluded the cerebrospinal fluid in the extracerebral space.<sup>10</sup>

We propose an automatic probabilistic brain segmentation method to segment eight neonatal brain structures, viz. UWM, MWM, CeGM, CoGM, cerebrospinal fluid both in the extracerebral space (referred to as 'CSF') and in the ventricles (VENT), brainstem (BS) and CB. This method is an expansion of our previously presented method.<sup>13</sup> The present method was developed because we hypothesized that neonatal brain volume can be used as a biomarker for neurodevelopmental outcome at two years.<sup>9</sup> The results regarding brain volumes in relation to neurodevelopmental outcome in the preterm cohort will be described separately.

## MATERIALS AND METHODS

### Patients and MR images

This prospective study was approved by the Medical Ethics Committee of our institute and written informed parental consent was obtained for all infants.

MRI of the brain was performed in 108 preterm infants around TEA, who belonged to a preterm cohort with a gestational age below 31 weeks and reached TEA in 2007-2008 (mean gestation age  $28.5 \pm 1.7$ ; mean postmenstrual age at time of scanning  $41.7 \pm 1.0$ ).<sup>19</sup> Axial 3D T1-weighted (TR=9.4 ms; TE= 4.6 ms; scan time=3.44 min, FOV=180x180; scan matrix=512x512; no slice gap; slice thickness=2.0 mm; number of slices=50) and axial T2-weighted images (TR=6293 ms; TE=120 ms; scan time=5.40 min; FOV=180x180; scan matrix=512x512; no slice gap; slice thickness=2.0 mm; number of slices=50) were acquired.

### Method

In the first seven infants with normal MRI finding, all 50 slices of the T2-weighted images were manually segmented by one researcher. For MWM, the T1-weighted images were used to improve the segmentations. Each brain voxel was assigned to one of the eight tissue classes: CoGM, CeGM, UWM, MWM, CSF, VENT, BS and CB. These manual segmentations were verified independently by three neonatologists with at least five years of experience in reading neonatal MRI scans, corrected according to their findings and reevaluated in a consensus meeting. The manual segmentations were considered as reference standard for training and validation of the segmentation method.

Before automatic segmentation, a shading correction was performed to the T1- and T2-weighted MR images to compensate for acquisition inhomogeneity effects.<sup>20</sup> Furthermore, differences due to head movement during image acquisition were corrected by affine intra-patient registration of the T1- and T2-weighted images. An average brain was constructed by registering the T2-weighted images of all 108 patients in the preterm cohort. In this average image, a mask ('average brain mask') demarking the intracranial volume was drawn manually.

A supervised classification method, k-Nearest Neighbor classification, was used for the assignment of samples (image voxels) to a class (tissue type).<sup>21</sup> Two types of voxel features were used for classification: signal intensity on T1- and T2-weighted images and spatial information (x-, y- and z-coordinates). Only voxels inside the average brain mask were classified. To enable comparison across patients, the spatial features were extracted in the coordinate system of the average brain. To this end, the T2-weighted scan of each patient was elastically registered to the average brain. The two (T1, T2) MR signal intensities of a voxel together with its three spatial coordinates resulted in a 5-dimensional feature space. Since different features have different ranges, a rescaling of the feature space was performed by variance scaling: subtraction of the feature values by their mean and division by the standard deviation. This resulted in a mean of 0 and variance of 1 for every feature. Pilot experiments showed that setting the number of neighbors' k in the classifier to 50 gave best results. Owing to the large number of samples, only 20% of the image voxels

were randomly selected for inclusion in the training set, to reduce computation time and computer memory usage.

Instead of assigning a voxel to one tissue class, we determined the probability that the voxel belonged to a particular tissue type, which resulted in probability maps for each tissue type. Each voxel was assigned a probability (value between 0 and 1) for each tissue class that was defined as the fraction of voxels of this tissue class among the 50 neighbors.

## Experiments and Evaluation

For evaluation, automatic segmentation of the images of the seven patients for whom a manual reference had been established was performed by the “leave-one-out”-method: each patient was classified based on the learning set composed from the images of the other six patients.

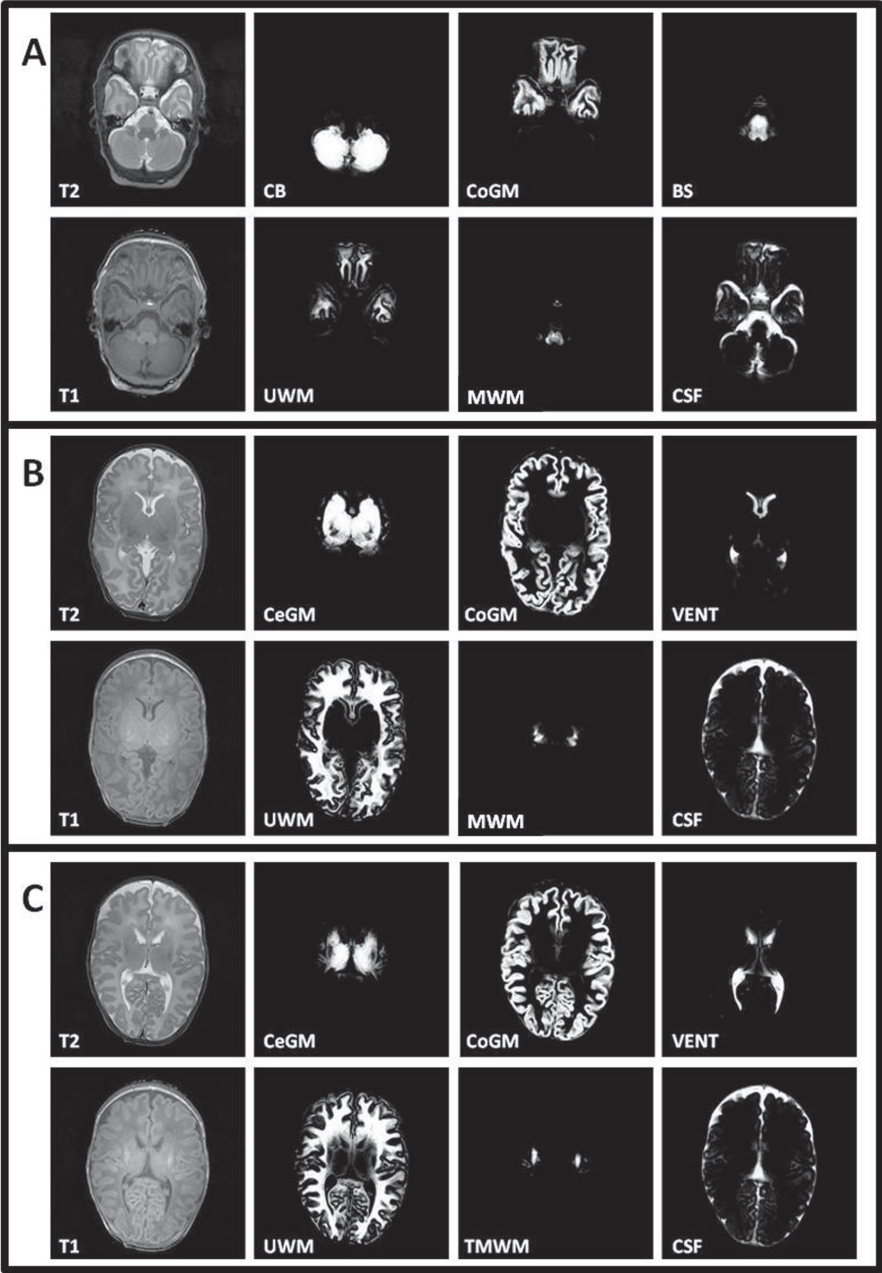
The obtained probability maps had to be transformed to binary segmentations so as to enable a comparison with the manual reference segmentations. This was accomplished in two different ways: (1) by applying optimal thresholds on the tissues in the probability maps, and (2) by majority segmentation. In approach (1), ROC-curves were calculated by applying different thresholds to the probability maps to segment each tissue. The optimal threshold value for a tissue class was the point on the curve where the accuracy was maximal. In approach (2), each voxel was assigned to the tissue class with the highest probability. These two binary segmentations were compared with the reference standard, where the number of true positive (TP), true negative (TN), false positive (FP) and false negative (FN) voxels were determined. The Dice similarity coefficient (DSC)<sup>22</sup> was calculated from these numbers by:

$$DSC = \frac{2 \times TP}{2 \times TP + FP + FN}$$

In addition, the sensitivity (  $\frac{TP}{TP + FN}$  ), and specificity (  $\frac{TN}{TN + FP}$  ) were calculated.

Volumes of the different brain tissues were calculated in three different ways: 1) directly from the probability maps; 2) from the binary optimal threshold segmentations, and 3) from the binary majority segmentations. For all three calculated segmentation volumes, the average volume per tissue class was compared with the average volume of the reference standard (average: over the seven patient images).

**Figure 1A, B and C: Probabilistic segmentations at different levels of the brain illustrating the eight brain tissue classes.**



Abbreviations: T2, T2-weighted image; CB, cerebellum; CoGM, cortical gray matter; BS, brainstem; T1, T1-weighted image; UWM, unmyelinated white matter; MWM, myelinated white matter; CSF, cerebrospinal fluid in the extracerebral space; CeGM, central gray matter; VENT, ventricles

## RESULTS

Figures 1A, 1B and 1C show probabilistic segmentations at three levels in the brain in one infant. For each brain tissue class the DSC as a function of the threshold (range 0-1) is presented in Figure 2. ROC-curves for segmentation of the eight brain tissue classes with different thresholds running from 0 to 1 are shown in Figure 3.

Table 1 presents the accuracy, i.e. DSC, sensitivity and specificity, for the binary segmentations obtained by the optimal threshold approach and by majority segmentation. For all tissue classes, optimal threshold segmentation provided accurate and reliable segmentations compared to the reference standard with DSCs between 0.78 (CSF) and 0.93 (CB), except for MWM (0.57).

**Table 1: Average accuracy (over seven patients with manual reference segmentations) of binary brain tissue segmentations**

Tissue type	Majority class segmentation			Optimal threshold segmentation			
	DSC	Sensitivity	Specificity	DSC	Sensitivity	Specificity	Threshold
<b>Cerebellum</b>	0.886	0.944	0.990	0.926	0.921	0.996	0.44
<b>MWM</b>	0.494	0.418	0.999	0.570	0.659	0.998	0.30
<b>CeGM</b>	0.909	0.918	0.995	0.910	0.906	0.996	0.46
<b>Ventricles</b>	0.823	0.828	0.997	0.824	0.829	0.997	0.42
<b>UWM</b>	0.852	0.870	0.923	0.861	0.858	0.939	0.47
<b>Brainstem</b>	0.833	0.833	0.998	0.846	0.879	0.998	0.35
<b>CoGM</b>	0.815	0.870	0.894	0.835	0.869	0.915	0.43
<b>CSF</b>	0.705	0.727	0.930	0.777	0.754	0.961	0.31

*Abbreviations: DSC, Dice similarity coefficient; MWM, myelinated white matter; CeGM, central grey matter; ventricles, cerebrospinal fluid in the ventricles; UWM, unmyelinated white matter; CoGM, cortical grey matter; CSF, cerebrospinal fluid in the extracerebral space*

Table 2 lists the average volumes of the different tissues and the reference standard volumes over the seven patients. A paired-samples t-test was performed to compare the means of the volumes, and Bonferroni correction for multiple comparisons was performed for all tissues. The volumes calculated by majority segmentation differ significantly from the reference values for CB and CoGM. No significant differences with the reference standard were observed for tissue volumes obtained with optimal threshold binary segmentation or with probabilistic volume segmentation.

**Table 2: Average volumes (in cc) of brain tissues as calculated by three different approaches**

Tissue type	Reference standard	Optimal threshold	Probability map	Majority
Cerebellum	28.855	28.581	28.871	32.574*
Myelinated white matter	1.821	2.389	1.991	1.259
Central gray matter	22.782	22.545	22.745	23.260
Ventricles	8.398	8.489	8.676	8.503
Unmyelinated white matter	166.140	165.208	171.018	172.992
Brainstem	6.404	6.903	6.098	6.406
Cortical gray matter	153.494	166.001	152.602	174.410*
Cerebrospinal fluid	93.142	87.828	82.162	99.038

Abbreviations: Reference standard, mean volume of the manual segmentations over the seven patients; Optimal threshold, mean volume of the binary segmentations after applying the optimal thresholds on the probability maps; Probability map, mean volumes calculated by summing the tissue probabilities of each voxel multiplied by the voxel volume; Majority, mean volume of the binary segmentations after the majority rule (each voxel was assigned to the tissue class with the highest probability); MWM, myelinated white matter; CeGM, central grey matter; ventricles, cerebrospinal fluid in the ventricles; UWM, unmyelinated white matter; CoGM, cortical grey matter; CSF, cerebrospinal fluid in the extracerebral space

\*:  $p$ -value < 0.01 paired samples  $t$ -test, with bonferroni correction

The proposed segmentation method was subsequently applied to the remaining 101 preterm infants of the cohort. Visual inspection of the results for all eight tissue classes revealed that the tissues were segmented correctly and consistently across 99 out of 101 infants, except for the segmentation of the MWM. In two infants, significant misclassification was observed due to brain injury, i.e. a large cerebellar hemorrhage, and a large temporal cyst following a temporal hemorrhage. Infants with mild motion artifacts on their original T1- and/or T2-weighted scans demonstrated adequate segmentation results. The results of the segmentations of the 101 preterm infants demonstrated that the method was not influenced by the large variations in head shape and size of the ventricles and the subarachnoid space, which frequently occur in preterm infants. The tissue volumes of the 101 infants calculated by probability segmentation and by optimal threshold binary segmentation showed no statistically significant differences. The analyses of these volumes with respect to neurodevelopmental outcome in preterm infants will be reported separately.

**Figure 2: Dice similarity coefficients (y-axis) for segmentations of eight brain tissues with thresholds running from 0 to 1 (x-axis)**

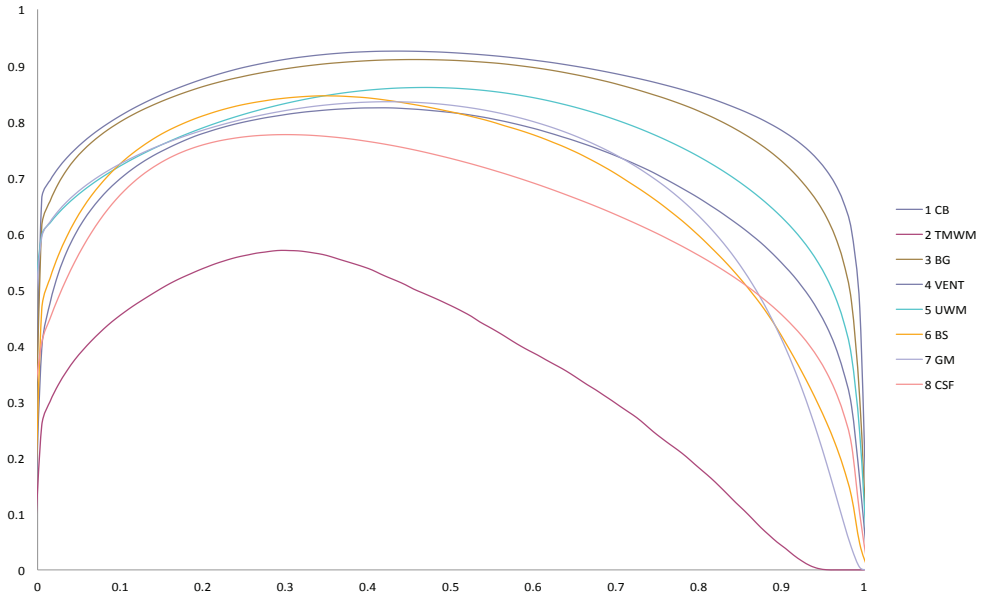
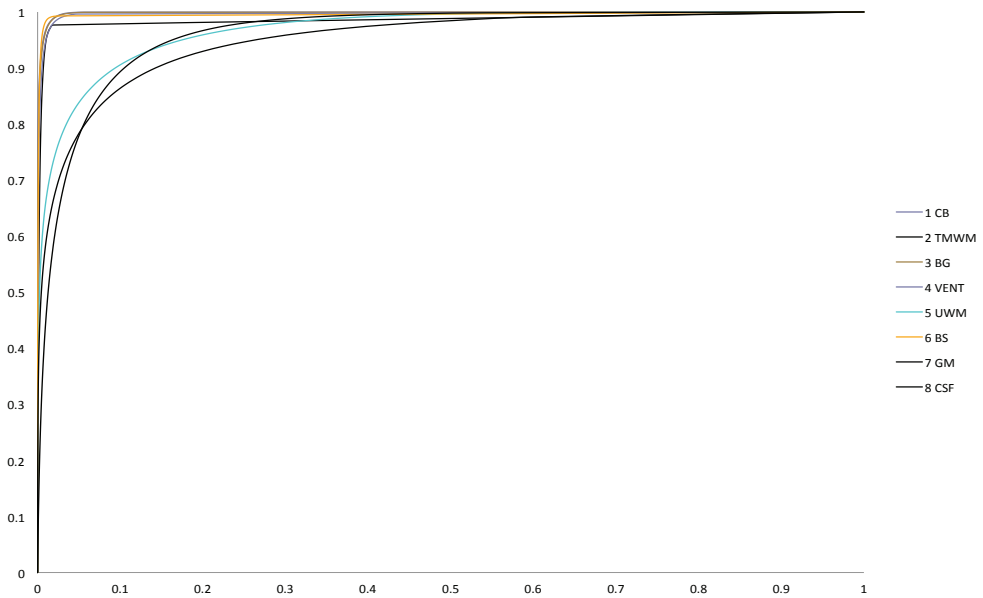


**Figure 3: ROC curves for segmentations of the eight brain tissues**



## DISCUSSION

This study has presented an automatic, probabilistic brain segmentation method to calculate volumes of eight brain tissue classes, i.e. CoGM, CeGM, UWM, MWM, CSF, VENT, BS and CB, in neonates.

The method was based on our previously reported method.<sup>13</sup> An average brain was introduced to align all patients before the segmentation step. The entire segmentation process took about 20 minutes per infant; no manual intervention was required. The binary segmentation with the optimal thresholds showed higher DSC values than the binary majority segmentation. A disadvantage of the optimal threshold binary segmentation approach is that it does not produce complementary segmentations of the eight tissues. Therefore, some voxels may not be classified or double classified. The probabilistic segmentation approach gave comparable results and does provide complementary segmentations of all brain tissues. Accordingly, we consider probabilistic segmentation the method of choice for further segmentation studies.

The DSCs demonstrated that the automatic segmentations provided accurate brain tissue volumes with DSCs between 0.78 and 0.93, except for MWM (DSC 0.57). The segmentation of MWM in the preterm brain around TEA is a difficult task. The maturation of the preterm brain is an ongoing process showing different degrees of myelination and it is very difficult, if at all possible, to define the exact ending of MWM and the beginning of CeGM in a learning set. Additionally, the volume of MWM in the preterm infant at TEA is relatively small, which implies that a small difference in segmented volume compared with the true volume resulted in a large proportional deviation as illustrated by a lower DSC. It is questionable whether T1- and T2-weighted scans are satisfactory for the segmentation of MWM. Since the study of MWM is related to the analysis of fiber tracts in the developing brain, it may be a better to determine MWM using diffusion tensor imaging.

Warfield *et al.* were the first who reported a semi-automatic neonatal brain segmentation method.<sup>12</sup> This method is often used in studies assessing brain volumes of preterm infants at TEA.<sup>6;9</sup> The method has been extended recently to automatic segmentation.<sup>17</sup> The validation of the latter method was performed on a single mid-coronal slice. The mean DSC for this slice ranged from 0.72 (MWM) to 0.92 (UWM and total CSF). To the best of our knowledge, this new automatic method has not been reported in clinical studies yet.

Prastawa *et al.* used a probabilistic brain atlas that provided prior probabilities for only WM, GM and CSF in the developing newborn brain.<sup>15</sup> The atlas was generated by taking the average of three semi-automatic segmentations. This method was validated on one 2D coronal slice in four datasets, with DSCs in the range of 0.5-0.8.

Yu *et al.* described a method that combined manual and semi-automatic segmentation.<sup>11</sup> Five subcortical GM structures, BS, CB, corpus callosum and the hippocampi were segmented manually. Voxels of cortical GM, WM and CSF were classified based on their signal intensity on proton-density and T2-weighted images. This process took about two hours per infant; the operators who performed the manual segmentations were extensively trained. Ten MRI scans were randomly chosen for validation. Cortical GM

and WM and total CSF were manually segmented and used as reference standard. The segmentation yielded DSCs between 0.84 and 0.88.

Recently, Gui *et al.* presented a promising automatic neonatal brain segmentation that calculated the volumes of both hemispheres, CB and BS separately in addition to CoGM, CeGM, MWM, UWM and total CSF.<sup>14</sup> They used MRI scans of 25 newborns with a GA between 38-44 weeks. The brain was separated in two hemispheres, which is an improvement over other methods. The different structures were segmented by using voxel location and intensity information and by employing region growing and anatomical conditions on voxel neighborhood. However, the validation was performed on only one mid-coronal slice of four different subjects. The mean DSCs were rather well, around 0.90 for all structures, except for MWM showing a DSC of 0.75.

The reference standard described in previously presented methods ranged from a single or few manually segmented slices<sup>14-17</sup> to an entire manually segmented brain<sup>10;11;13</sup>. In the present study, we validated all eight structures based on all 50 slices of seven infants.

None of the previous methods distinguished VENT from CSF. We consider this distinction important in preterm infants, since it could be an indicator of underlying pathology, e.g. brain atrophy or, in case of solitary ventricular dilatation, an intraventricular hemorrhage. An increase in total CSF volume with additional brain pathology at TEA has been associated with an impaired outcome in preterm infants.<sup>9;23</sup>

Besides our present segmentation method, only the methods described by Yu *et al.* and Gui *et al.* provided cerebellar volumes.<sup>11;14</sup> The CB has shown to be important in the development of the preterm infant.<sup>18</sup> Segmentation of the CB is a difficult issue, since this structure shows inhomogeneous signal intensities on both T1- and T2-weighted scans, varying from values similar to UWM to intensities of GM. The use of spatial information in the proposed method solved the problem to a certain extent. However, separation of occipital CoGM and cerebellum remained difficult. A similar issue was the segmentation of CoGM and CeGM, which have similar signal intensities and can only be distinguished by location and shape. Misclassifications were observed as oversegmentation of CB or CeGM with respect to CoGM. Nevertheless, the DSCs of CoGM and CeGM segmentations produced by our method were high, which could be related to a relatively low volume of misclassified voxels.

A classification error was seen in UWM areas where the signal intensity approached that of CSF. A diffuse, high signal intensity in UWM is a common finding in preterm infants at TEA.<sup>24;25</sup> In those infants, UWM was misclassified as CSF. This issue was also described by Yu *et al.*<sup>11</sup> They performed a manual correction as the final step in their segmentation process. We suggest that the severity of the misclassification may be useful as an indication of pathological WM tissue. Further study is necessary to gain more insight into this issue.

Another misclassification error was observed at the border between CSF and CoGM. Owing to partial volume effects, the signal intensities of these border voxels were similar to UWM. The method used by Yu *et al.* corrected voxels belonging to CSF that were misclassified as WM.<sup>11</sup> Gui *et al.* utilized anatomical conditions on voxel neighborhood to

correct misclassification as UWM at the interface between CoGM and CSF, which is an interesting approach.<sup>14</sup>

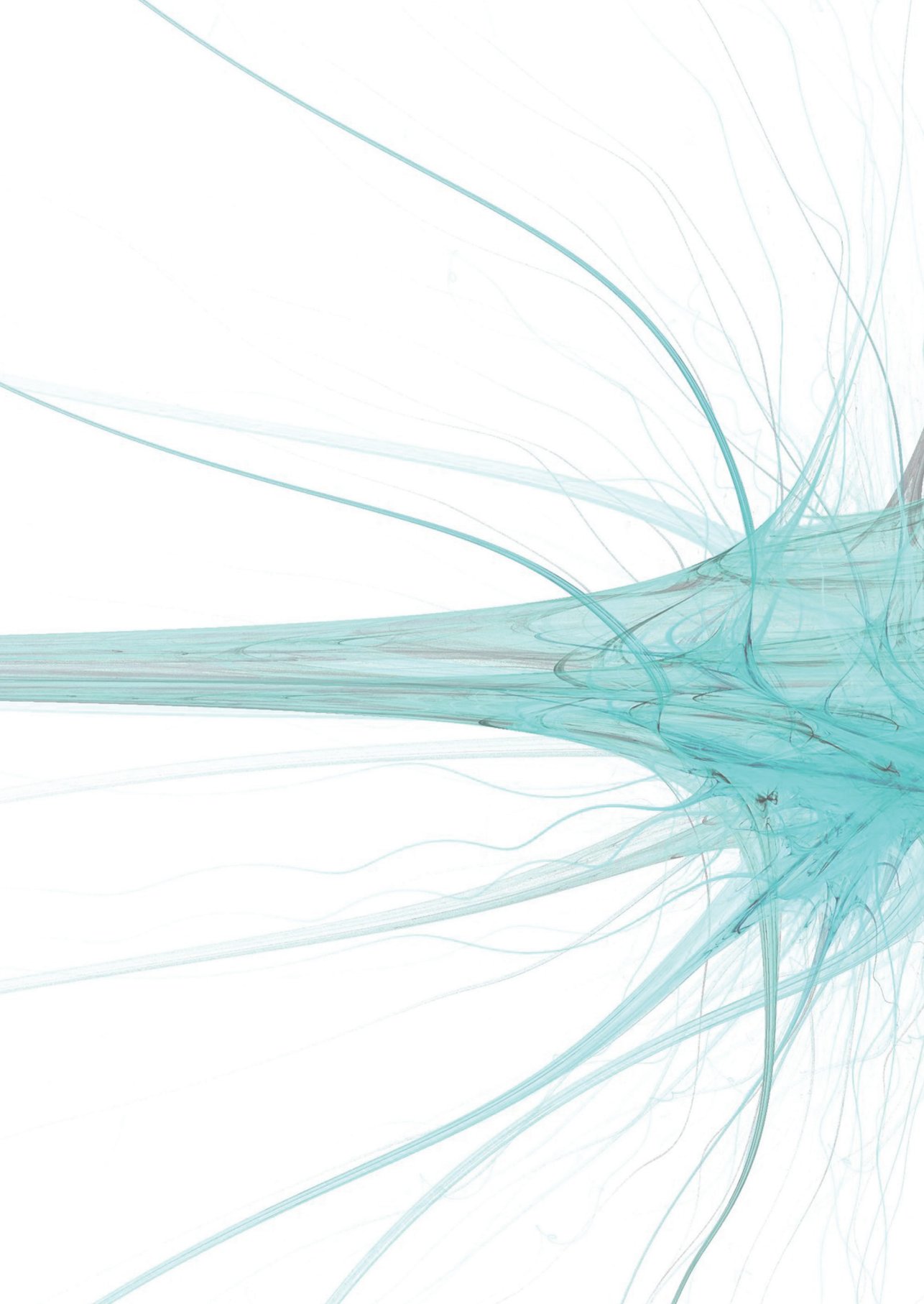
To conclude, we proposed an automatic, probabilistic brain segmentation method to calculate brain volumes in eight different tissue classes accurately for neonates, based on T1- and T2-weighted MR images. Besides CoGM, CeGM, UWM and MWM, it segments CB and BS separately. Furthermore, it is the first method that distinguishes CSF from VENT, which is clinical useful to distinguish ventriculomegaly caused by atrophy or posthemorrhagic ventricle dilatation. The first clinical implementation in 108 infants yielded accurate segmentation of the eight tissue classes and reliable estimates of the corresponding volumes.

## Reference List

- (1) Ment LR, Hirtz D, Huppi PS. Imaging biomarkers of outcome in the developing preterm brain. *Lancet Neurol* 2009; 8(11):1042-1055.
- (2) Peterson BS, Anderson AW, Ehrenkranz R, Staib LH, Tageldin M, Colson E *et al.* Regional brain volumes and their later neurodevelopmental correlates in term and preterm infants. *Pediatrics* 2003; 111(5 Pt 1):939-948.
- (3) Zacharia A, Zimine S, Lovblad KO, Warfield S, Thoeny H, Ozdoba C *et al.* Early assessment of brain maturation by MR imaging segmentation in neonates and premature infants. *AJNR Am J Neuroradiol* 2006; 27(5):972-977.
- (4) Mewes AU, Huppi PS, Als H, Rybicki FJ, Inder TE, McAnulty GB *et al.* Regional brain development in serial magnetic resonance imaging of low-risk preterm infants. *Pediatrics* 2006; 118(1):23-33.
- (5) Thompson DK, Warfield SK, Carlin JB, Pavlovic M, Wang HX, Bear M *et al.* Perinatal risk factors altering regional brain structure in the preterm infant. *Brain* 2007; 130(Pt 3):667-677.
- (6) Tolsa CB, Zimine S, Warfield SK, Freschi M, Sancho RA, Lazeyras F *et al.* Early alteration of structural and functional brain development in premature infants born with intrauterine growth restriction. *Pediatr Res* 2004; 56(1):132-138.
- (7) Martinussen M, Flanders DW, Fischl B, Busa E, Lohaugen GC, Skranes J *et al.* Segmental brain volumes and cognitive and perceptual correlates in 15-year-old adolescents with low birth weight. *J Pediatr* 2009; 155(6):848-853.
- (8) Nosarti C, Giouroukou E, Healy E, Rifkin L, Walshe M, Reichenberg A *et al.* Grey and white matter distribution in very preterm adolescents mediates neurodevelopmental outcome. *Brain* 2008; 131(Pt 1):205-217.
- (9) Inder TE, Warfield SK, Wang H, Huppi PS, Volpe JJ. Abnormal cerebral structure is present at term in premature infants. *Pediatrics* 2005; 115(2):286-294.
- (10) Nishida M, Makris N, Kennedy DN, Vangel M, Fischl B, Krishnamoorthy KS *et al.* Detailed semiautomated MRI based morphometry of the neonatal brain: preliminary results. *Neuroimage* 2006; 32(3):1041-1049.
- (11) Yu X, Zhang Y, Lasky RE, Datta S, Parikh NA, Narayana PA. Comprehensive brain MRI segmentation in high risk preterm newborns. *PLoS One* 2010; 5(11):e13874.
- (12) Warfield SK, Kaus M, Jolesz FA, Kikinis R. Adaptive, template moderated, spatially varying statistical classification. *Med Image Anal* 2000; 4(1):43-55.
- (13) Anbeek P, Vincken KL, Groenendaal F, Koeman A, van Osch MJ, van der Grond J. Probabilistic brain tissue segmentation in neonatal magnetic resonance imaging. *Pediatr Res* 2008; 63(2):158-163.
- (14) Gui L, Lisowski R, Faundez T, Huppi P, Lazeyras F, Kocher M. Automatic segmentation of newborn brain MRI using mathematical morphology. *IEEE* . 2011.
- (15) Prastawa M, Gilmore JH, Lin W, Gerig G. Automatic segmentation of MR images of the developing newborn brain. *Med Image Anal* 2005; 9(5):457-466.
- (16) Xue H, Srinivasan L, Jiang S, Rutherford M, Edwards AD, Rueckert D *et al.* Automatic segmentation and reconstruction of the cortex from neonatal MRI. *Neuroimage* 2007; 38(3):461-477.
- (17) Weisenfeld NI, Warfield SK. Automatic segmentation of newborn brain MRI. *Neuroimage* 2009; 47(2):564-572.

- (18) Allin M, Matsumoto H, Santhouse AM, Nosarti C, AlAsady MH, Stewart AL *et al.* Cognitive and motor function and the size of the cerebellum in adolescents born very pre-term. *Brain* 2001; 124(Pt 1):60-66.
- (19) van Kooij BJ, Hendrikse J, Benders MJ, de Vries LS, Groenendaal F. Anatomy of the Circle of Willis and Blood Flow in the Brain-Feeding Vasculature in Prematurely Born Infants. *Neonatology* 2009; 97(3):235-241.
- (20) Likar B, Maintz JB, Viergever MA, Pernus F. Retrospective shading correction based on entropy minimization. *J Microsc* 2000; 197(Pt 3):285-295.
- (21) Duda R, Hart P. Pattern classification. John Wiley & Sons.Inc, New York, USA; 2001. 174-195.
- (22) Dice LR. Measures of the amount of ecologic association between species. *Schizophrenia Bulletin* 1945; 17:483-489.
- (23) Maunu J, Lehtonen L, Lapinleimu H, Matomaki J, Munck P, Rikalainen H *et al.* Ventricular dilatation in relation to outcome at 2 years of age in very preterm infants: a prospective Finnish cohort study. *Dev Med Child Neurol* 2011; 53(1):48-54.
- (24) Dyet LE, Kennea N, Counsell SJ, Maalouf EF, Ajayi-Obe M, Duggan PJ *et al.* Natural history of brain lesions in extremely preterm infants studied with serial magnetic resonance imaging from birth and neurodevelopmental assessment. *Pediatrics* 2006; 118(2):536-548.
- (25) Hagmann CF, De Vita E, Bainbridge A, Gunny R, Kapetanakis AB, Chong WK *et al.* T2 at MR imaging is an objective quantitative measure of cerebral white matter signal intensity abnormality in preterm infants at term-equivalent age. *Radiology* 2009; 252(1):209-217.







## CHAPTER THREE

# Quantitative fiber tracking in corpus callosum and internal capsule reveals microstructural abnormalities in preterm infants at term equivalent age

Carola van Pul, Britt J.M. van Kooij, Linda S. de Vries, Manon J.N.L. Benders,  
Anna Vilanova, Floris Groenendaal

*American Journal of Neuroradiology, in press*

## ABSTRACT

**Background and purpose** - Abnormalities like signal abnormalities in the posterior limb of the internal capsule (PLIC) and thinning of the corpus callosum (CC) are often seen in preterms and associated with a worse outcome. Diffusion Tensor Imaging (DTI) is able to detect small abnormalities in the white matter and therefore we used fiber tracking to select these bundles of interest (CC and PLIC). We hypothesize that there will be a relation between DTI-parameters and white matter injury (WMI).

**Methods** - One-hundred-twenty preterm infants born <31 weeks with 3.0T Diffusion Tensor Imaging at term-equivalent age entered this prospective study, approved by the Medical Ethical Committee. Parental informed consent was obtained. Quantitative information, i.e. volume, length, anisotropy and mean diffusivity (MD), were obtained of fiber bundles passing through PLIC and CC. In SPSS, General Linear Model was used to assess the effects of factor (gender) and variables (gestation age, birth weight, head circumference, postmenstrual age and WMI) on fiber tracking (FT)-segmented parameters.

**Results** - Seventy-two CC and 85 PLIC fiber bundles were assessed. For CC, with increasing WMI, decreasing anisotropy ( $p=0.038$ ), bundle volume ( $p<0.001$ ) and length ( $p=0.001$ ) were observed, whereas MD increased ( $p=0.001$ ). For PLIC, MD increased with increasing WMI ( $p=0.002$ ). The post-menstrual age was an important covariate for most FT-segmented parameters. Higher anisotropy and larger bundle length were observed in left PLIC compared to right ( $p=0.003$ ;  $p=0.018$ ).

**Conclusion** - Quantitative fiber tracking is useful in CC and left and right PLIC bundles in preterm infants at term-equivalent age to detect WMI and provides additional insight into underlying changes in white matter microstructure compared to conventional MRI.

## INTRODUCTION

Premature birth <30 weeks is associated with a high risk of neurodevelopmental impairments, including cognitive and motor disabilities.<sup>1,2,3</sup> The underlying neuropathology for cognitive disabilities is largely unknown, although it has been suggested that disturbances in the white matter (WM) maturation play a role.<sup>4,5</sup> In teenagers, the effects of preterm birth are associated with thinning of the corpus callosum (CC), widening of the ventricles, reduced volumes of the WM and microstructural changes in the posterior limb of the internal capsule (PLIC) and the CC.<sup>6-9</sup>

Magnetic resonance imaging (MRI) is commonly performed in preterm infants around term-equivalent age (TEA) to detect brain injury. Different scoring systems have been developed to quantify MRI findings.<sup>4,10</sup> Although these scoring systems related to outcome, they did not provide information about the pathology on a microstructural level. WM maturation may best be followed with diffusion tensor imaging (DTI) since this technique uses both information on the diffusion properties of water molecules that are restricted in a tissue and information on the preference in the direction of diffusion (anisotropy). DTI has been shown to be sensitive to microstructural WM changes, like myelination<sup>11,12</sup>. Most information concerning DTI changes in relation to brain maturation is available from studies assessing selected regions of interest (ROIs) in the WM.<sup>11</sup> It has been shown that the anisotropy in preterm infants is decreased at TEA in certain brain regions (among which the CC and the frontal WM) compared to term born controls.<sup>13</sup>

Instead of measuring local effects in selected ROIs, fiber tracking (FT) can be applied to measure changes in bundles of WM. FT is a 3D visualization technique that reconstructs the underlying linear structure defined by the diffusion tensor<sup>14</sup>. Quantification of WM tracts in infants has been performed previously<sup>15-23</sup> and is based on calculating an average of a certain DTI parameter over the complete bundle. DTI parameters quantifying the corticospinal tract are affected in preterm infants with WM injury (WMI) with differences in axial and radial diffusivity indicating structural differences in the white matter structure.<sup>22</sup> Only one study recently investigated the genu and splenium of the CC in premature infants at TEA using FT.<sup>23</sup> The CC is of interest since reduced callosal volumes have been shown to correlate with motor function and cognitive impairment.<sup>24,25</sup>

The aim of our study was to investigate whether diffusion tensor parameters abstracted using fiber tracking to select complete CC and PLIC-bundles displays abnormalities known as white matter injury in the premature at term equivalent age. The WMI score<sup>2</sup> (as measured with conventional MR imaging) was used as a reference index. We hypothesized that WMI will be well detected with DTI and give information on the microstructure. We investigated furthermore how the DTI parameters were affected by gestational age (GA), birth weight (BW), head circumference (HC), gender and the postmenstrual age (PMA) at time of scanning.

## METHODS

### Study group

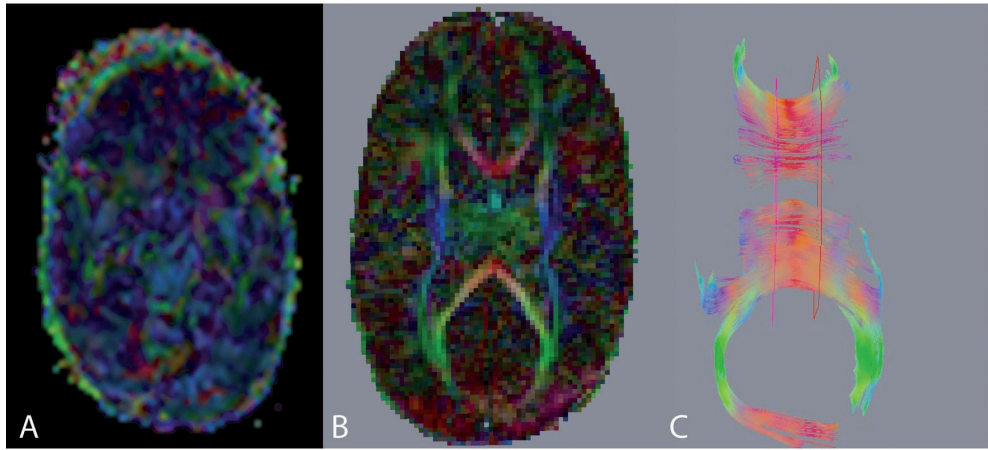
Preterm infants with a GA below 31 weeks and who reached TEA between January 2007 and July 2008 were part of a prospective cohort study. This study was approved by the Institute's Medical Ethical Committee. Informed parental consent was obtained for all neonates. Infants were included if a 3T MRI scan was obtained at TEA with a high-resolution DTI. Neonates were excluded if they showed signs of chromosomal or syndromal abnormalities with known effects on brain development or neuromotor development, or when they had an infection of the central nervous system. The infants were sedated with 50-60mg/kg chloralhydrate orally fifteen minutes prior to the MRI and hearing protection was used. Heart rate, transcutaneous oxygen saturation and respiratory rate were monitored during scanning. A neonatologist was present throughout the MRI examination.

### MRI protocol

The MRI was performed on a 3.0T scanner (Achieva, Philips Medical Systems, Best) using an 8-channel SENSE-head-coil and contained a sagittal T1-weighted scan with echo time (TE)/repetition time (TR)=15/886ms and scan voxel size 0.78x0.98x3.0mm (reconstruction voxel size 0.39x0.39x3.0mm), axial 3D T1-weighted series with TE/TR=4.6/9.4 and scan voxel size 0.94x0.94x2.0mm (reconstruction 0.35x0.35x2.0mm) and axial T2-weighted series with TE/TR=120/6293 and scan voxel size 0.54x0.61x2.0mm (reconstruction 0.35x0.35x2.0mm). DTI was based on an axial single-shot-EPI sequence with sense-factor 3 (TE/TR=48/7745; duration 4:32 minutes), 2 b-values (0-800s/mm<sup>2</sup>) in 32 directions. Fifty slices were acquired with scan voxel size 1.41x1.44x2.0mm (reconstruction 1.41x1.41x2.0mm). Correction for Eddy currents and rigid motion was performed using registration software of the Philips workstation. Following registration, DICOM images were converted to a format compatible to the fiber-tracking program.<sup>26</sup>

### White matter score (WM-score)

MRIs were assessed by two neonatologists with >10 years expertise in reading MRI<sup>27,28</sup> and blinded to the neurodevelopmental outcome. In case of disagreement, a third reader was consulted to achieve consensus. WM signal intensity, size of the subarachnoid space, presence of cysts, size of the ventricles and shape of the CC were scored as (1) normal, (2) mildly abnormal or (3) moderately/severely abnormal (adjusted from Woodward *et al.*<sup>2</sup>). The WM-score is the sum of these subscores (range 5-15) and was applied as indicator for WMI (normal: 5-6; mildly abnormal: 7-9; moderately abnormal: 10-12; severely abnormal: 13-15). The size of the CC was measured on the sagittal T1-weighted MR Image by one independent researcher at the location of 0.5 cm from the natural incurvation near the level of the genu and the splenium and perpendicular to the contour and to the middle of the CC. The CC was scored as: (1) normal if both measurements were > 2.4mm; (2) mildly abnormal (focal thinning of the CC) if at least one measurement was between 1.8-2.3 mm and both measurements were > 1.7mm; and (3) moderately abnormal

**Figure 1**

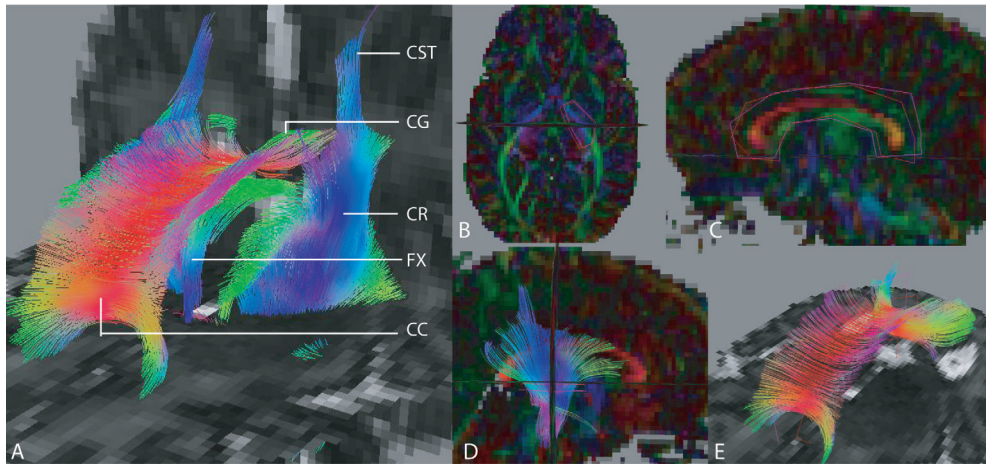
Examples of artifacts leading to exclusion of dataset: A. DTI image artifact due to motion artifacts, the colormap displayed a completely wrong color. B. DTI artifact due to Sense-artifact, the colormap displayed a large red area posterior. C. artifactual fibers: errors in fiber tracking, resulting in fibers in areas with artifacts.

(general thinning) if both measurements  $\leq 1.7\text{mm}$ . For an additional analysis, we have divided our study group into three groups: normal CC, focal thinning of the CC and generalised thinning of the CC.

### Fiber tracking

The quality of the DTI data was assessed and infants with fractional anisotropy (FA)-based colormaps displaying large artifacts (e.g. wrong colors in colormap by motion artifacts (Figure 1A), or sense artifacts (Figure 1B) were excluded from further analysis. FT was conducted in DTI-tool<sup>26,18</sup>, based on deterministic tracking, using “case linear anisotropy” ( $CI = (\lambda_1 - \lambda_2) / (\lambda_1 + \lambda_2 + \lambda_3)$ )  $CI < 0.12$  and maximum angle  $\alpha > 10^\circ$  as stopping criteria. CI is less prone to continue tracing in planar anisotropy areas than FA<sup>18</sup>.

FT was performed with seeding in every voxel in the brain (Figure 2A). By using filtering ROIs, drawn manually on axial slices of the FA-color-map, separate fiber structures were visualized.<sup>18</sup> The PLIC-bundle (Figure 2D) was defined by those fibers passing through two filtering ROIs in the PLIC area, with the first ROI positioned at the anatomic level of the foramen of Monro, the second on the adjacent slice above this landmark. The ROIs were drawn roughly surrounding the bundle, but taking care that fibers from the anterior limb of the internal capsule were not included (Figure 2B). This procedure was followed for left and right hemisphere separately. By using two roughly drawn ROIs instead of one ROI, only fibers in feet-head direction were selected and the method was less influenced by the exact drawing of the ROIs. We placed the ROIs on adjacent slices because we want to “segment” at least all information in the PLIC in all children. Since WMI frequently occurs in the white matter areas surrounding the ventricles, we may not draw the second ROI on a level too high, otherwise we would not be able to trace any fibers.

**Figure 2**

Abbreviations: CST, Corticospinal tract; CR, Corona Radiata; FX, fornix; CG, cingulum; CC, corpus callosum. PLIC, Posterior limb of the internal capsule.

3D fiber tracking superimposed on 2D Apparent Diffusion Coefficient (ADC) maps.

- A. Whole brain Fiber Tracking results, in a preterm infant at term equivalent age. View from front left.
- B. Definition of PLIC ROIs. View from top (on axial plane). ROIs superimposed on FA-weighted colormap.
- C. Definition of CC ROIs. View from left (on sagittal plane). ROIs superimposed on FA-weighted colormap.
- D. PLIC fiber bundle. View from right (on sagittal plane). ROIs superimposed on FA-weighted colormap.
- E. CC fiber bundle. View from front left. (on sagittal plane). ROIs superimposed on FA-weighted colormap.

To generate the CC-bundle (Figure 2E), two ROIs in sagittal slices around the midplane of the CC were used as filtering ROIs (Figure 2C). For the CC, the slices on which the ROIs were positioned were 3 slices (4.2mm) apart. Experimentally it was determined that less than three slices apart gave too much erroneous traced fibers. All ROIs were placed by one researcher to minimize interobserver variability.

Next, the quality of the generated fiber bundle was assessed by two authors separately (FT-experience >7 and >3 years): if the volume of artifactual fibers was visually estimated to be more than 10% of the total bundle volume, the bundle was excluded from further analysis (Figure 1C). The visual estimation was performed by rotating the volume of fibers in 3D and estimating the extend of the artifact. If no consensus was obtained, a third reader was consulted.

Quantification of the generated fiber bundles was done by taking DTI but also volumetric information from the voxels that are included in the CC and PLIC fiber bundles, as segmented by our FT method. In the next part, we will denote the quantification of these parameters by “FT-segmented parameters” since it includes not only DTI values but also bundle volume and length as segmented using fiber tracking. The bundle volume (mm<sup>3</sup>)

was defined as the volume of all pixels through which one or more fibers passed. The average bundle length (mm) was the average length of all fibers included in the bundle. The mean diffusivity ( $MD=(\lambda_1+\lambda_2+\lambda_3)/3$ ) ( $m^2/s$ ), axial ( $\lambda_1$ ) and radial diffusivity ( $=(\lambda_2+\lambda_3)/2$ ), FA and CI of all voxels through which one or more fibers passed were calculated.

### Statistical analysis

SPSS (version 13.0, SPSS Inc., Chicago, USA) was utilized for statistical analysis. To assess the relation between FT-segmented parameters and WM-score, a multivariate General Linear Model was used with factor (gender) and covariates (GA, PMA, HC, WM-score and BW) to determine which covariate contributed significantly to the model. The relation between FT-parameter and WM-score was further evaluated using linear regression. Differences in FT-segmented parameters between WMI-groups and between WM-aspects (e.g. thinning of CC) were assessed using an independent-samples T-Test. Furthermore, differences in FT-segmented parameters between left and right PLIC-bundle were tested using a paired-samples T-Test. A  $p$ -value  $< 0.05$  was considered statistically significant.

## RESULTS

### Study group

Of the 120 patients who entered this study, 31 patients had to be excluded because of large artifacts. Of the included 89 patients (48 boys, 41 girls), the mean GA was  $28.5 \pm 1.7$  weeks, mean BW  $1121 \pm 338$  grams, mean PMA at time of scanning  $41.7 \pm 1.1$  weeks (range 39.6-44.7) and mean weight at scan of  $3262 \pm 604$  grams. In consensus, further exclusion of PLIC-bundle tracts of four infants (leaving 85) and CC-bundles of 17 infants (leaving 72) was deemed necessary because of artifactual fibers taking more than 10% of the volume of the fiber bundle.

### White matter score

The scoring results of the five aspects of WM are shown in Table 1. Eleven infants had no WM abnormalities, and most infants (74%) had a mildly abnormal WM-score. Severe abnormalities, indicated by a WM-score  $> 12$ , were not observed in this population. In 20% of the infants, a normal WM signal intensity was observed, most patients had a mildly abnormal signal intensity in the WM (69%), the abnormality was always diffuse and bilateral. Other common findings were a mildly enlarged subarachnoid space, always bilateral, and mildly enlarged ventricles. Having moderate-severe enlargement of both items was rare. For the CC, the most common finding was focal thinning (58%). One neonate showed a small subcortical cyst frontally and one child had a cyst due to a haemorrhage in the temporal lobe. During the neonatal period, 7 infants were diagnosed to have a moderate or severe intraventricular haemorrhage on sequential cranial ultrasound examinations, showing residual blood in the lateral ventricles on MRI.

**Table 1: Scoring results for WM in infants, based on Woodward *et al.*<sup>2</sup>**

WM aspect	Normal (score 1)	Mildly abnormal (score 2)	Moderate/severe (score 3)
WM signal intensity, n (%)	18 (20)	61 (69)	10 (11)
Subarachnoid space, n (%)	45 (51)	40 (45)	4 (4)
Presence of cysts, n (%)	87 (98)	2 (2)	0 (0)
Size of Ventricles, n (%)	40 (45)	45 (51)	4 (4)
Thickness of CC, n (%)	24 (27)	52 (58)	13 (15)
Total WM-score, n (%)	11 (12)	66 (74)	12 (14)

Abbreviations: WM, White Matter; n, number; CC, corpus callosum. For each aspect of the WM-score, the number of patients in our study obtaining this score is denoted. None of the infants had severe WM abnormalities.

**Fiber tracking and patient specific factors**

Using a General Linear Model, the dependency of the FT-segmented parameters on patient specific factors and covariates was evaluated (Table 2). The *p*-value indicates whether the FT-parameter depends significantly on the factor/covariate, taking into account the relation with the other factors/covariates.

All evaluated FT-segmented parameters in the CC bundle correlated significantly with the total WM-score. The GA at birth was a significant contributor to the model for the CC-bundle volume and length. The PMA at time of scan had a significant influence on the radial diffusivity and consequently also on FA and CI. The HC was an important covariate for bundle volume, length and CI, however not for the other FT-segmented parameters. Gender and BW (not shown) were only important for CC-bundle volume and CC-bundle length.

For the left PLIC-bundle, the relation with WM-score was only observed for MD, axial and radial diffusivity. Diffusivity also depended on GA at birth and PMA. FA and CI depended mainly on the PMA due to the contribution of the radial diffusivity.

For the right PLIC-bundle, only GA, PMA and WM-score were important for the models of the FT-segmented parameters. However, the influence was much less compared to the Left PLIC-bundle.

**Fiber tracking and WM-score**

In Figure 3, FT-segmented parameters are shown as a function of WM-score. The CC-bundle volume and length were larger for infants with normal or mildly abnormal WM (low WM-score values), than for infants with moderately abnormal WM. Furthermore, anisotropy CI decreased and MD increased with increasing WM-score. For the PLIC-bundles, only the MD showed a significant correlation with WM-score, and the increase of the MD with increasing WM-score was smaller for the PLIC-bundles than for the CC-bundle.

**Table 2: Relations between FT-segmented parameters and patient specific factors**

covariate/factor ->	GA	PMA	HC	WM-score	Gender
dependent variable	<i>p-value</i>	<i>p-value</i>	<i>p-value</i>	<i>p-value</i>	<i>p-value</i>
CC-bundle volume	0.001**	-	0.000**	0.000**	-
CC FA	-	0.004**	0.052	0.038*	-
CC CI	-	0.004**	0.002**	0.001**	-
CC MD	-	0.035*	-	0.001**	-
CC axial diffusivity	-	-	-	0.010*	-
CC radial diffusivity	-	0.007**	-	0.003**	-
CC-bundle length	0.000**	-	0.006**	0.001**	0.010*
PLIC L bundle volume	-	0.014*	-	-	-
PLIC L FA	0.007**	0.001**	-	-	-
PLIC L CI	-	0.001**	-	-	-
PLIC L MD	0.006**	0.003**	-	0.002**	-
PLIC L axial diffusivity	0.010**	0.019*	-	0.001**	-
PLIC L radial diffusivity	0.006**	0.001**	-	0.004**	-
PLIC L bundle length	-	-	-	-	-
PLIC R bundle volume	0.006**	0.008**	-	-	-
PLIC R FA	-	0.005**	-	-	-
PLIC R CI	-	-	-	-	-
PLIC R MD	-	0.008**	-	0.032*	-
PLIC R axial diffusivity	-	0.017*	-	0.008**	-
PLIC R radial diffusivity	-	0.008**	-	-	-
PLIC R bundle length	0.023*	-	0.022*	-	-

Abbreviations: GA, Gestational Age; PMA, Postmenstrual Age; HC, Head Circumference; WM-score, White Matter score, CC, Corpus callosum; FA, Fractional Anisotropy; CI, case linear anisotropy index; MD, Mean diffusivity; PLIC, Posterior Limb of the Internal Capsule with L indicating Left and R indicating Right. The relations were investigated using a general linear model. For each FT-segmented parameter (rows), the *p-value* is shown for the influence of the patient factors and covariates (columns) when  $p < 0.01$  (marked \*\*) or  $p < 0.05$  (marked \*). No value indicates no significant influence. Birth weight had no significant role in the model and was therefore not displayed in this Table.

Looking in more detail to the diffusivity, the axial diffusivity showed a significant correlation with WM for all evaluated bundles; however the radial diffusivity only displayed a correlation for the CC and left PLIC-bundles, but not for the right PLIC-bundle.

A larger variation in the “size characteristics” volume and length was observed for all bundles, compared to the voxel averaged characteristics like FA, CI and MD. In addition, the variation was larger for the CC than for the PLIC-bundles.

### FT-segmented parameters and aspect of the WM-score

Differences in FT-segmented parameters were analyzed between infants with a normal shape of the CC (score 1), focal thinning (score 2) or with generalized thinning of the CC (score 3) and the results are shown in Figure 4. Compared to the group with normal CC, significantly reduced values for CC-bundle volume were observed in the group with focal and generalized thinning of the CC ( $p=0.022$  and  $p=0.001$ , respectively). In addition, CI was decreased ( $p<0.001$ ) and MD increased ( $p=0.005$ ) in the CC-bundle in the group with generalized thinned CC. A trend towards decreased length was observed with increasing CC score, though not significant ( $p=0.054$ ). The differences in the MD in the CC-bundle between the group with a normal shape and focal thinning of the CC ( $p=0.032$ ) was mainly due to a significant increase in radial diffusivity ( $p=0.027$ ) and not in axial diffusivity, whereas a significant increase in both axial ( $p=0.028$ ) and radial diffusivity ( $p=0.027$ ) was observed in the group with a generalized thinning of the CC.

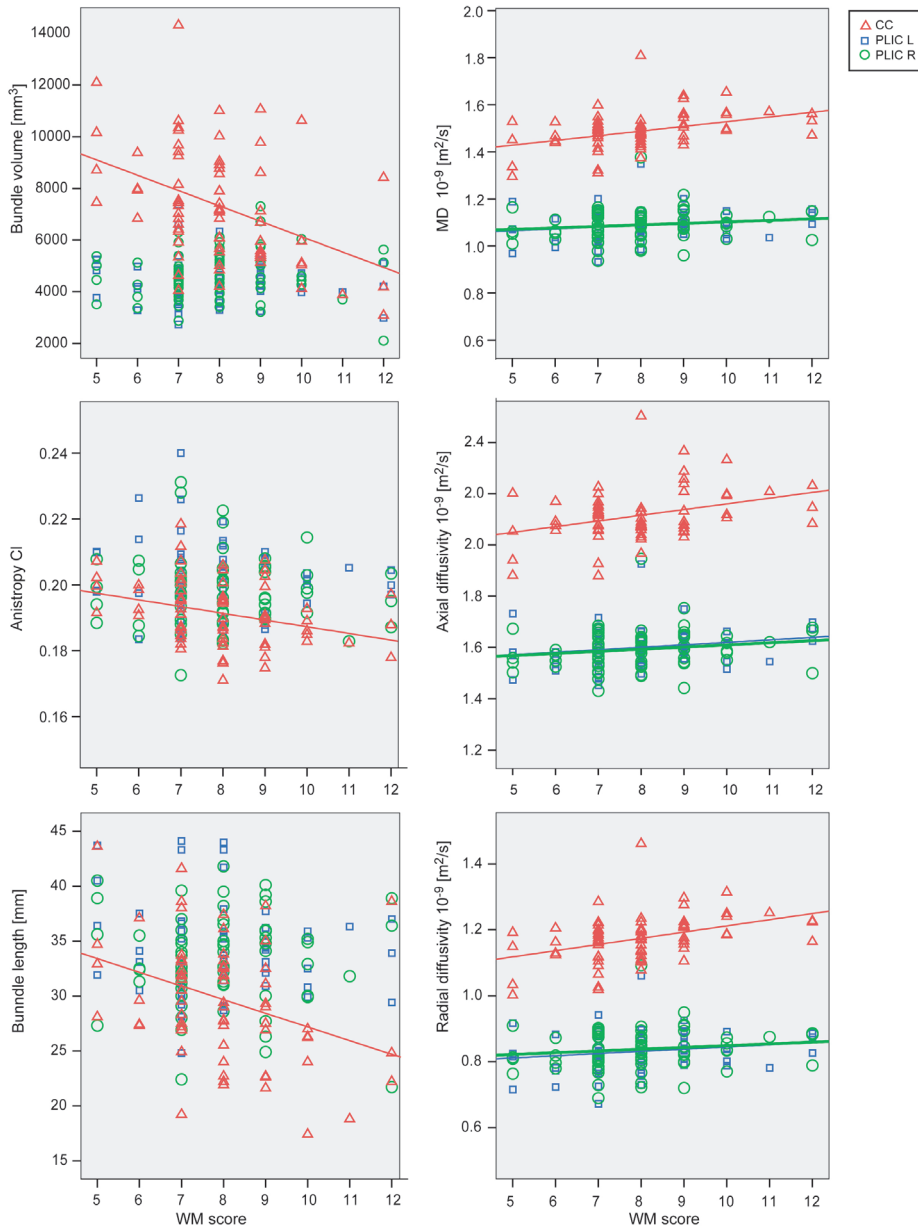
In 85 infants, both left and right PLIC-bundle were eligible for analysis. A significantly higher FA and CI ( $p=0.002$  and  $p=0.003$ , respectively) and larger average length (length=34.2mm) was observed in the left PLIC-bundle compared to the right PLIC-bundle (length=33.2mm,  $p=0.018$ ).

### DISCUSSION

Fiber tracking was performed to quantify CC-bundle and PLIC-bundles in preterm infants at TEA, in order to detect WMI. The CC-bundle is of interest since thinning of the CC is commonly seen in preterm infants and associated with a worse outcome.<sup>6,9</sup> Not only CC-bundle volume and length were smaller for infants with WMI, also lower anisotropy was observed in combination with an increased MD, suggesting less hindered diffusion. The decrease in anisotropy was mainly driven by an increased radial diffusivity in the group with focal CC-thinning, whereas both axial and radial diffusivities were increased for the group with generalized thinning. Our findings were in agreement with ROI-based DTI-studies, showing in the CC decreased FA and increased ADC<sup>29</sup> and radial diffusivity<sup>30</sup> in infants with WMI. It was suggested that changes in radial diffusion reflect myelin and premyelin effects, whereas changes in axial diffusivity are likely related to changes in axon integrity.<sup>22,31</sup> Therefore we hypothesized that changes in the group with focal thinning of the CC were mainly due to a slowdown in (pre)myelin maturation, whereas the group with generalized thinning displayed larger injury, potentially including axonal injury. This correlation of FT-segmented parameters in the CC-bundle with WMI was not observed by Bruine et al<sup>23</sup>, however they evaluated splenium and genu of the CC separately, and not an average of the CC-bundle as we did.

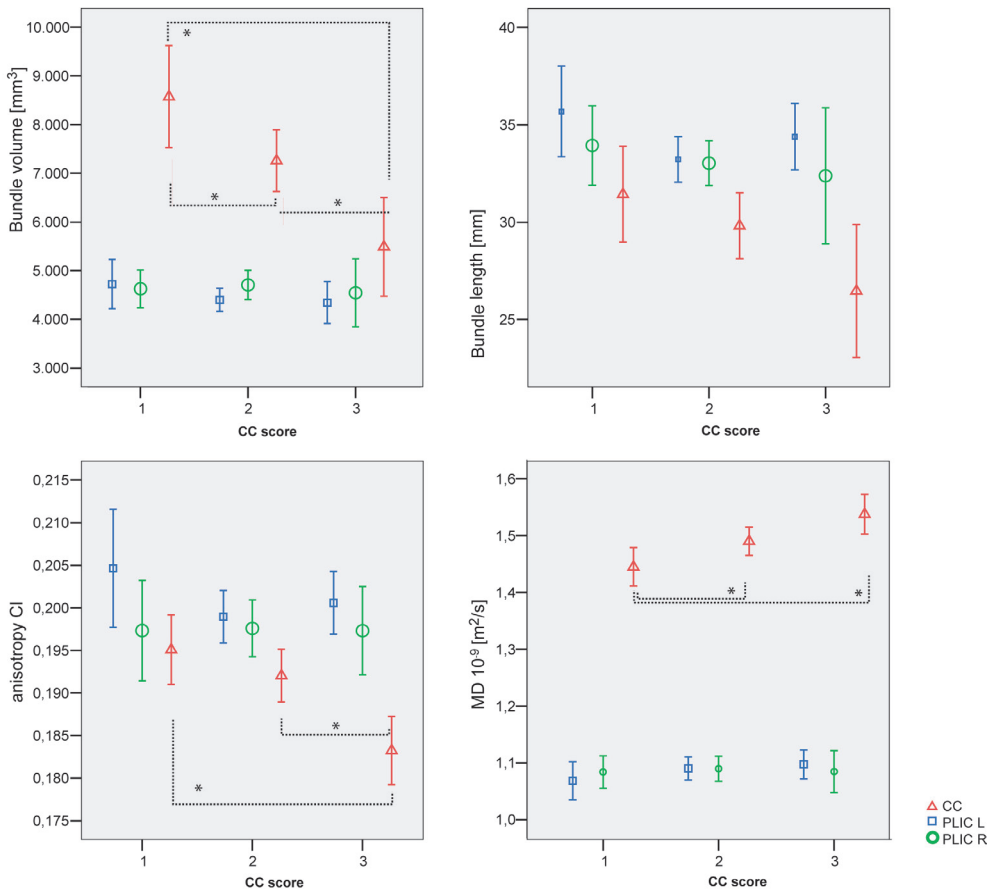
For the left PLIC-bundle, both axial and radial diffusivity increased significantly with WMI. This is in contrast to findings by Adams *et al.*<sup>22</sup>, showing lower FA in the corticospinal tract due to changes in radial and not in axial diffusivity. The difference might be explained by the fact that part of the corticospinal tract is included in the much larger PLIC-bundle in our study.

**Figure 3**



Bundle volume, anisotropy index CI, length, average MD, axial diffusivity and radial diffusivity are shown as a function of WM-score. For CC (red triangles); PLIC L (blue squares) and PLIC R (green circles). The trendlines are only displayed in the graphs if the correlation was significant. For the CC, 72 bundles were evaluated and displayed in this graph, for the PLIC 85 bundles.

Figure 4



Average values for bundle volume, anisotropy CI, bundle length, average MD, for the groups with CC score 1 (normal corpus callosum), 2 (mild thinning of the corpus callosum), and 3 (severe thinning of the corpus callosum). For CC (red triangles); PLIC L (blue squares) and PLIC R (green open circles). In total, 72 CC fiber bundles were evaluated, with  $n=19$  in group 1,  $n=40$  in group 2 and  $n=11$  in group 3 for the CC. Displayed are the mean and the error bar displays the standard average of the mean. The \* denotes a significant difference ( $p<0.05$ ).

Comparing left and right PLIC-bundles, the longer bundle length and higher anisotropy in the left PLIC-bundle could reflect a better maturation compared to the right PLIC. Higher FA values in the left PLIC-bundle have been observed in older children<sup>21</sup> and in neonates larger WM volumes in the left hemisphere have been found.<sup>32</sup>

Radial diffusivity decreased and anisotropy (FA, CI) increased with increasing PMA, in agreement with literature.<sup>11,22,33,34</sup> Furthermore, CC-bundle volume and length were lower and MD in the left PLIC-bundle higher for infants born at a lower GA. Since there was no relation between GA at birth and PMA at scan-time, this finding may suggest

an effect of GA on brain maturation. Similar findings were observed in adolescents born prematurely<sup>8</sup>, showing a positive association between WM volume and GA, though a relation with GA was not observed in recent studies in preterm infants.<sup>22,23</sup>

The main limitation of our study is in the large number of artifacts in the DTI acquisition. DTI is more prone to artifacts than conventional MRI scans. In this study, 26% of the patients had to be excluded due to motion and/or sense artifacts. The DTI sequence was at the end of the MR protocol and although the infants were sedated and hearing protection was applied, it could not be prevented that some of the infants woke up during the DTI scan. Severe motion artifacts in the DTI images resulted in errors in fiber tracking, in particular when using a line propagation technique as applied in this study.<sup>14</sup> To minimize the influence of errors in the quantification of the tracts, we excluded all bundles for which we agreed in consensus that the artifactual fibers contributed for more than 10% to the volume of the fibers.

The distribution of white matter injury in the artifacts group was similar to the finally included group and therefore no bias was introduced by excluding the patients with artifacts in the DTI data. The artifacts are not due to the white matter injury. Furthermore, the visual interpretation whether the erroneous traced fibers are >10% of the total bundle volume is user-biased, however two users observed and by rotating the fiber structure in 3D, the visual estimation of the size of the artifact compared to the size of the fiber bundle was possible. In case of disagreement, a third observer was consulted.

Our study shows the strength but also the weaknesses of using the complete bundle for evaluation, instead of ROI-based DTI<sup>29,30,34</sup> or a part of the bundle<sup>22,23</sup>. The strength is that a complete structure is evaluated, and not only a local effect, making the method less sensitive to ROI-positioning errors. On the other hand, small effects may be missed because they are lost in the variances in the large bundle.

A limitation of our study was the use of manually drawn ROIs for bundle selection, though our fiber tracking is seeded in all voxels in the brain. The reproducibility of our method was analyzed and by using the protocolized ROI-definition, generated bundles were visually similar and also quantitatively comparable. However, problems with FT still occurred in areas of crossing fibers, since deterministic tracking does not trace well in these areas<sup>14</sup>, which is inherent to the use of only the diffusion tensor and not high angular information. Therefore tracking was stopped in areas of crossing fibers, where CI is below the stopping value. We realize that the choice of stopping criteria influences bundle volume and length, however we emphasize that within our study, differences in bundle FT-segmented parameters between groups can be compared, since the same stopping criteria were used.

Compared to conventional MRI, quantitative fiber tracking gives microstructural information, which may give insight into understanding the pathology with subsequent poor outcome. In our study, most infants appeared to have mildly abnormal WM-scores, a larger percentage than observed by Woodward et al,<sup>2</sup> whose scoring system we adapted. This could be partly due to the use of 3.0T instead of 1.5T MR, resulting in changes in T1 and T2 values, which could influence the interpretation of the WM signal intensity.

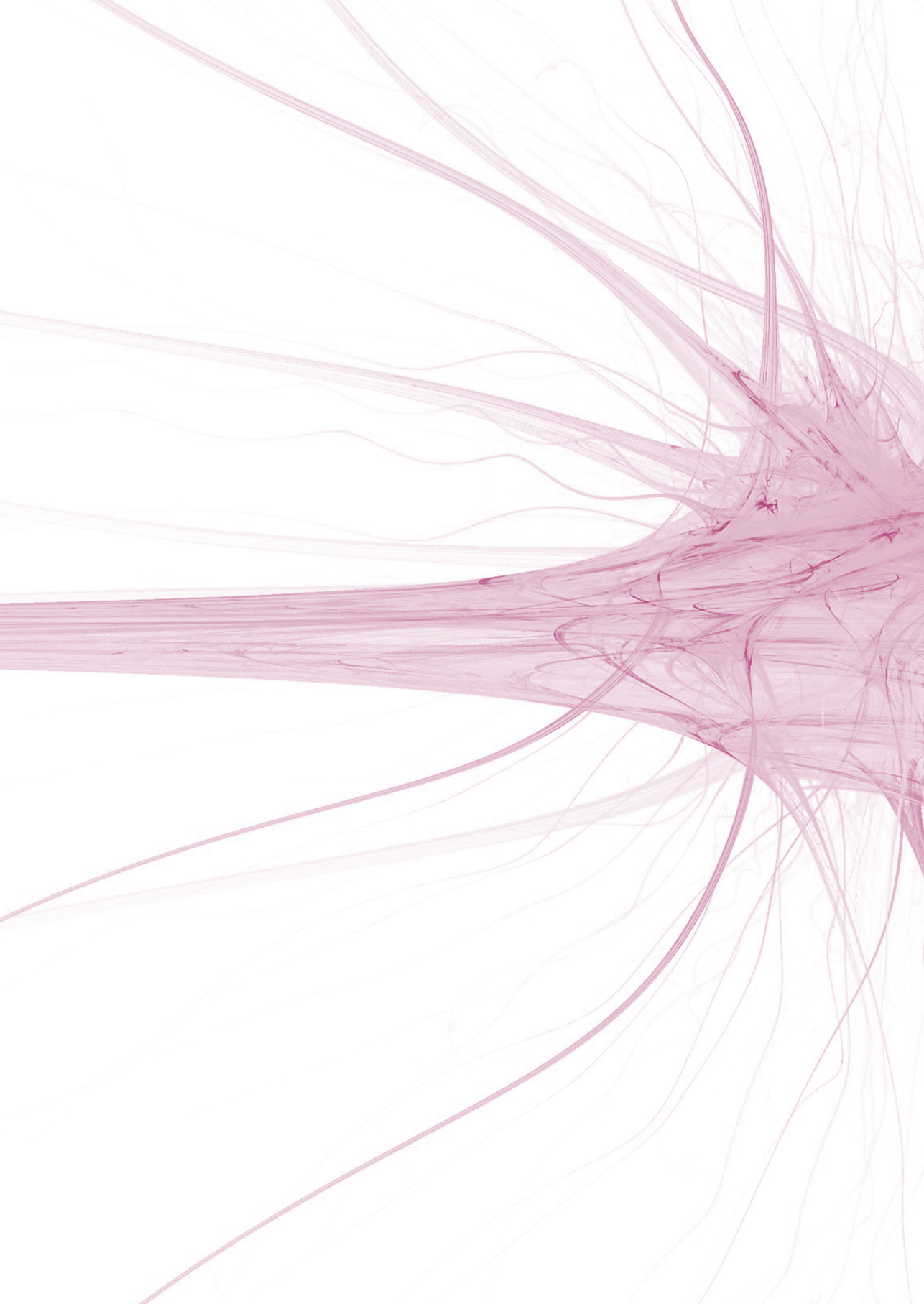
To conclude, we have performed FT to quantify the CC-bundle and PLIC-bundles in preterm infants at TEA. The anisotropy in the CC-bundle was decreased and diffusivity increased with WMI, with increased radial diffusivity in infants with focal CC-thinning, and both axial and radial diffusivities were increased in infants with generalized thinning of the CC, suggesting a difference in underlying white matter pathology. Brain maturation is affected by premature birth (GA-relation). A relation of the PLIC with WMI was also shown but it was less pronounced, suggesting that the CC is more prone to WMI in the maturing brain than the PLIC. Fiber tracking additionally gives information of changes in bundle length and volume, which also decreased with WMI.

## Reference List

- (1) Bhutta AT, Cleves MA, Casey PH, *et al.* Cognitive and behavioral outcomes of school-aged children who were born preterm: a meta-analysis. *JAMA* 2002;288:728-37.
- (2) Woodward LJ, Anderson PJ, Austin NC, *et al.* Neonatal MRI to predict neurodevelopmental outcomes in preterm infants. *N Engl J Med* 2006;355:685-94.
- (3) Latal B. Prediction of neurodevelopmental outcome after preterm birth. *Pediatr Neurol* 2009;40:413-9.
- (4) Counsell SJ, Boardman JP. Differential brain growth in the infant born preterm: current knowledge and future developments from brain imaging. *Semin Fetal Neonatal Med* 2005;10:403-10.
- (5) Dudink J, Kerr JL, Paterson K, *et al.* Connecting the developing preterm brain. *Early Hum Dev* 2008;84:777-82.
- (6) Stewart AL, Rifkin L, Amess PN, *et al.* Brain structure and neurocognitive and behavioural function in adolescents who were born very preterm. *Lancet* 1999;353:1653-7.
- (7) Nagy Z, Westerberg H, Skare S, *et al.* Preterm children have disturbances of white matter at 11 years of age as shown by diffusion tensor imaging. *Pediatr Res* 2003;54:672-79.
- (8) Nagy Z, Ashburner J, Andersson J, *et al.* Structural correlates of preterm birth in the adolescent brain. *Pediatrics* 2009;124:e964-72.
- (9) Skranes J, Vangberg TR, Kulseng S, *et al.* Clinical findings and white matter abnormalities seen on diffusion tensor imaging in adolescents with very low birth weight. *Brain* 2007;130:654-66.
- (10) Childs AM, Ramenghi LA, Cornette L, *et al.* Cerebral maturation in premature infants: quantitative assessment using MR imaging. *AJNR Am J Neuroradiol* 2001;22:1577-82.
- (11) Neil J, Miller J, Mukherjee P, *et al.* Diffusion tensor imaging of normal and injured developing human brain - a technical review. *NMR Biomed* 2002;15:543-52.
- (12) Hüppi PS, Dubois J. Diffusion tensor imaging of brain development. *Semin Fetal Neonatal Med* 2006;11:489-97.
- (13) Hüppi PS, Maier SE, Peled S, *et al.* Microstructural development of human newborn cerebral white matter assessed in vivo by diffusion tensor magnetic resonance imaging. *Pediatr Res* 1998;44:584-590.
- (14) Mori S, van Zijl PC. Fiber tracking: principles and strategies. *NMR Biomed* 2002;15:468-80.
- (15) Partridge SC, Mukherjee P, Berman JL, *et al.* Tractography-based quantitation of diffusion tensor imaging parameters in white matter tracts of preterm newborns. *J Magn Reson Imaging* 2005;22:467-74.

- (16) Berman JI, Mukherjee P, Partridge SC, *et al.* Quantitative diffusion tensor MRI fiber tractography of sensorimotor white matter development in premature infants. *Neuroimage* 2005;27:862-71.
- (17) Berman JI, Glass HC, Miller SP, *et al.* Quantitative fiber tracking analysis of the optic radiation correlated with visual performance in premature newborns. *AJNR Am J Neuroradiol* 2009;30:120-4.
- (18) van Pul C, Buijs J, Vilanova A, *et al.* Infants with perinatal hypoxic ischemia: feasibility of fiber tracking at birth and 3 months. *Radiology* 2006;240:203-14.
- (19) Dubois J, Hertz-Pannier L, Dehaene-Lambertz G, *et al.* Assessment of the early organization and maturation of infants' cerebral white matter fiber bundles: a feasibility study using quantitative diffusion tensor imaging and tractography. *Neuroimage* 2006;30:1121-32.
- (20) Dubois J, Dehaene-Lambertz G, Perrin M, Mangin *et al.* Asynchrony of the early maturation of white matter bundles in healthy infants: quantitative landmarks revealed noninvasively by diffusion tensor imaging. *Hum Brain Mapp* 2008;29:14-27.
- (21) Dubois J, Hertz-Pannier L, Cachia A, *et al.* Structural asymmetries in the infant language and sensori-motor networks. *Cereb Cortex* 2009;19:414-23.
- (22) Adams E, Chau V, Poskitt KJ, *et al.* Tractography-based quantitation of corticospinal tract development in premature newborns. *J Pediatr* 2010;156:882-8.
- (23) de Bruijne FT, van Wezel-Meijler G, Leijser LM, *et al.* Tractography of developing white matter of the internal capsule and corpus callosum in very preterm infants. *Eur Radiol* 2011;21:538-47.
- (24) Rademaker KJ, Lam JN, Van Haastert IC, *et al.* Larger corpus callosum size with better motor performance in prematurely born children. *Semin Perinatol* 2004;28:279-87.
- (25) Caldú X, Narberhaus A, Junqué C, *et al.* Corpus callosum size and neuropsychologic impairment in adolescents who were born preterm. *J Child Neurol* 2006;21:406-10.
- (26) Vilanova A, Berenschot G, Pul van C. DTI Visualization with streamsurfaces and evenly-spaced volume seeding. *Eurographics/IEEE TCVG VisSym* 2004:173-182.
- (27) de Vries LS, Groenendaal F. Neuroimaging in the preterm infant. *Ment Retard Dev Disabil Res Rev* 2002;8:273-80..
- (28) de Vries LS, Groenendaal F. Patterns of neonatal hypoxic-ischaemic brain injury. *Neuroradiology* 2010;52:555-66.
- (29) Skiöld B, Horsch S, Hallberg B, *et al.* White matter changes in extremely preterm infants, a population-based diffusion tensor imaging study. *Acta Paediatr* 2010;99:842-9.
- (30) Counsell SJ, Shen Y, Boardman JP, *et al.* Axial and radial diffusivity in preterm infants who have diffuse white matter changes on magnetic resonance imaging at term-equivalent age. *Pediatrics* 2006;117:376-86.

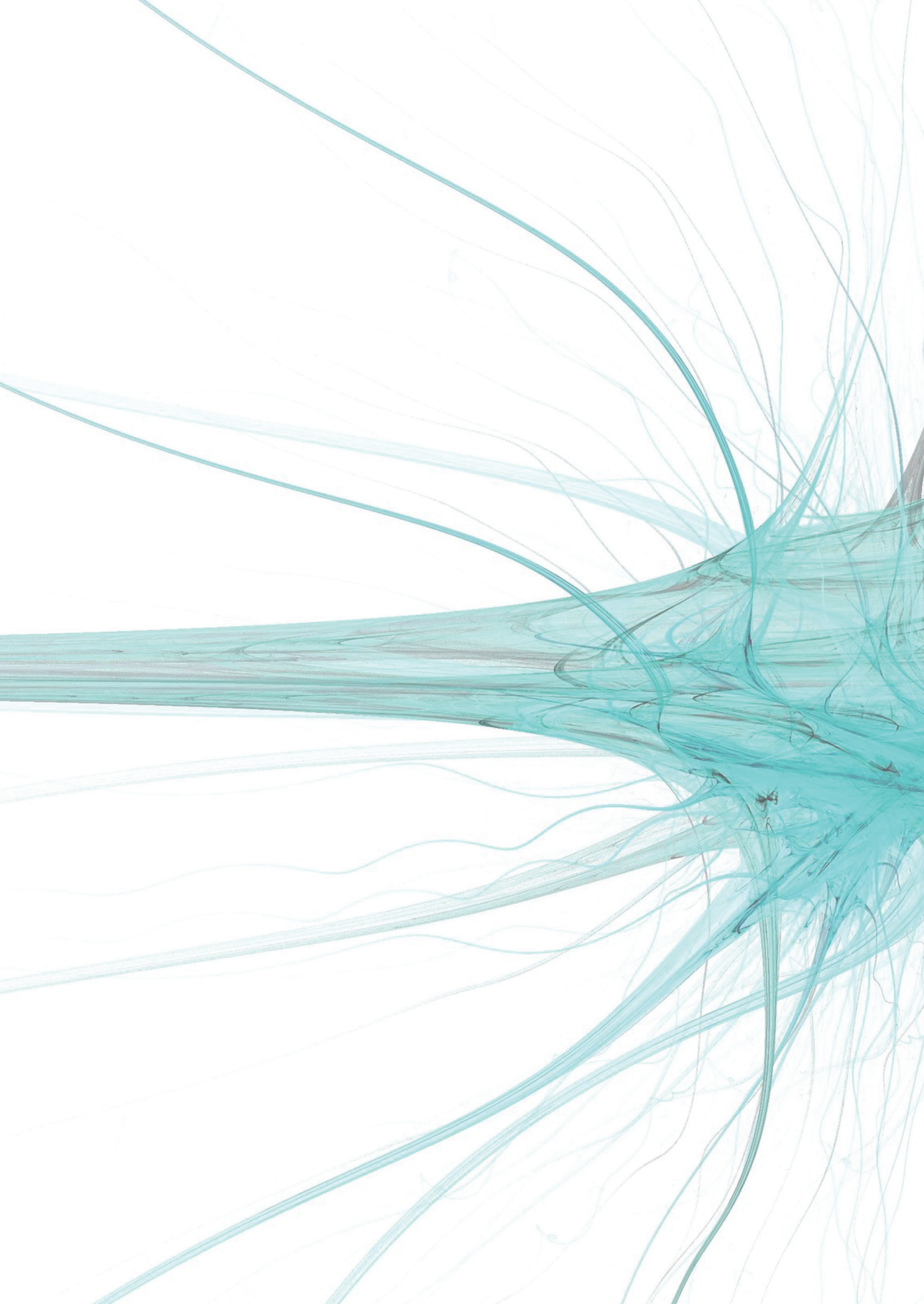
- (31) Song SK, Sun SW, Ramsbottom MJ, *et al.* Dysmyelination revealed through MRI as increased radial (but unchanged axial) diffusion of water. *Neuroimage* 2002;17:1429-36.
- (32) Gilmore JH, Lin W, Corouge I, *et al.* Early postnatal development of CC and corticospinal white matter assessed with quantitative tractography. *AJNR Am J Neuroradiol* 2007;28:1789-95.
- (33) Gilmore JH, Lin W, Prastawa MW, *et al.* Regional gray matter growth, sexual dimorphism, and cerebral asymmetry in the neonatal brain. *J Neurosci* 2007;27:1255-60.
- (34) Mathur AM, Neil JJ, Inder TE. Understanding brain injury and neurodevelopmental disabilities in the preterm infant: the evolving role of advanced magnetic resonance imaging. *Semin Perinatol* 2010;34:57-66.



# **PART TWO**

## **MRI postprocessing techniques and neurodevelopment**







## CHAPTER FOUR

### **Brain volume at term equivalent age: biomarker for neurodevelopmental outcome in preterm infants**

Britt J.M van Kooij, Petronella Anbeek, Ingrid C. van Haastert, Rutger A.J. Nievelstein,  
Floris Groenendaal, Linda S. de Vries, Max A. Viergever, Manon J.N.L. Benders

*Submitted*

**ABSTRACT**

**Background** - In preterm infants, reduced brain volumes between childhood and adolescence have been related to neurodevelopment. We assessed whether brain tissue volumes at term-equivalent age (TEA) in preterm infants can be used as a biomarker for neurodevelopment at two years corrected age.

**Methods** - In this prospective study, unmyelinated white matter (UWM), cortical gray matter (CoGM), central gray matter, cerebrospinal fluid in the ventricles and in the extracerebral space, brainstem and cerebellar volumes were measured at TEA in preterm infants ( $n=108$ , mean $\pm$ SD gestational age:  $28.5\pm1.7$  weeks) using an in-home developed automatic brain segmentation method. Volumes were adjusted for total brain size and postmenstrual age (PMA). The volumes were related to cognitive and motor scores on the Bayley Scales of Infant and Toddler Development-III.

**Results** - Only ventricular volume was negatively associated with cognition and fine and gross motor scores. A decrease in UWM and an increase in CoGM volumes in reference to brain size were observed between 39 and 43 weeks PMA.

**Conclusion** - After correction for PMA and total brain size, ventricular volume at TEA was associated with neurodevelopment at two years' corrected age in preterm infants. UWM and CoGM volumes showed rapid changes in reference to brain size around TEA.

## INTRODUCTION

Preterm infants are at risk to develop neurodevelopmental disabilities.<sup>1,2</sup> The nature of subtle brain abnormalities related to cognitive impairments is still poorly understood. Several studies have revealed a relation between moderate-severe white matter (WM) injury on conventional magnetic resonance imaging (MRI) and adverse neurodevelopmental outcome.<sup>3-5</sup> In the last decade, different (semi-)automatic neonatal brain segmentation methods have been developed to evaluate brain development.<sup>6-8</sup> Reduced brain volumes have been found in preterm infants at term-equivalent age (TEA) compared to term born controls.<sup>9</sup> Several studies demonstrated that reduced brain volume persisted during late childhood and early adolescence. Reduced global or regional volumes of the cortical and central gray matter CoGM and CeGM, respectively), unmyelinated WM (UWM) and cerebellum (CB) and an increase in cerebrospinal fluid mediated neurodevelopmental sequelae.<sup>10-12</sup>

Brain volumes of preterm infants at TEA in relation to long-term neurodevelopmental outcome have not been studied extensively. Inder et al. illustrated that infants with moderate to severe neurodevelopmental impairments at one year of age exhibited a significant reduction of absolute CoGM and CeG volume in combination with increased total cerebrospinal fluid volume at TEA.<sup>13</sup> Reduced volumes at TEA of the hippocampus or occipital brain region were related to an inferior memory function or deficits in the control of the oculomotor function respectively.<sup>14,15</sup>

For the present study, we adapted our automatic neonatal brain segmentation method previously described by Anbeek et al.<sup>6</sup> We were able to distinguish myelinated from UWM and cerebrospinal fluid in the ventricles (VENT) from cerebrospinal fluid in the extracerebral space (CSF). With the adapted segmentation method, the cerebellar volume can be calculated separately.

In the present study, we assessed whether brain tissue volumes at TEA could be used as biomarker for neurodevelopmental outcome at two years corrected age in preterm infants.

## METHODS

### Patients

Neonates admitted to our hospital were recruited for a large prospective preterm cohort study if they were born at a gestational age (GA) <31 weeks and reached TEA between January 2007 and August 2008. Congenital abnormalities and infection of the central nervous system were exclusion criteria. Of the 175 neonates who met the inclusion criteria, 22 infants (13%) died in the neonatal period, informed parental consent was not obtained for 14 neonates and in 15 infants the MRI scan could not be performed on a 3.0 Tesla system due to technical problems, which resulted in 124 neonates that were eligible for this study. This prospective study was approved by the Medical Ethical Committee of the University Medical Centre Utrecht and performed in the Wilhelmina Children's Hospital in Utrecht, The Netherlands. Written informed parental consent was obtained for all neonates.

## MRI

All MR investigations were performed on a 3.0 Tesla MR system (Philips Healthcare, Best, The Netherlands) using a sense head coil. The infants were sedated with 50-60 mg/kg chloralhydrate by gastric tube 15 minutes prior to the examination. During MR examination, the infants were placed in a vacuum fixation pillow to reduce movement and hearing protection was administered while heart rate, transcutaneous oxygen saturation and respiration rate were monitored. A neonatologist was present throughout the whole examination.

The protocol involved conventional sagittal T1-weighted (repetition time (TR)=886 ms; echo time (TE)=15 ms; slice thickness, 3.0 mm), axial 3D T1-weighted (TR=9.4 ms; TE=4.6 ms; slice thickness, 2.0 mm, no gap) and axial T2-weighted imaging (TR=6293 ms; TE=120 ms; slice thickness, 2.0 mm, no gap). The axial T1- and T2-weighted images were used for segmentation of the different brain structures.

MRIs were evaluated independently by two experienced neonatologists (LSdV and MJNLB) and a radiologist (RAJN), who were blinded to the neurodevelopmental outcome. In case of disagreement, a fourth reader (FG) was consulted to achieve consensus. WM signal intensity, size of the subarachnoid space, presence of cysts, size of the ventricles and shape of the corpus callosum (CC) were scored as (1) normal, (2) mildly abnormal or (3) moderately/severely abnormal (adjusted from Woodward et al.<sup>16</sup>). The overall WM score was the sum of the five subscores (range 5-15). The ventricles were mildly abnormal if the largest diameter was between 8-10 mm and moderately/severely abnormal in case of a largest diameter above 10 mm. The CC was measured by one independent researcher at the location of 0.5 cm from the natural incurvation near the level of the genu and the splenium, and perpendicular to the contour and the middle of the CC. Mildly abnormal (= focal thinning) was defined if at least one measurement was between 1.8-2.3 mm and moderately / severely abnormal (= generalized thinning) if both measurements were  $\leq 1.7$  mm.

## Brain segmentation

We extended our user-independent, fully automatic neonatal brain segmentation method to be able to segment eight different brain structures (Anbeek et al.<sup>9</sup>): CoGM, CeGM, VENT, CSF, myelinated white matter (MWM), UWM, brainstem (BS) and CB. Voxels were classified by the k-Nearest Neighbor classification system and based on their signal intensities on the T1- and T2- weighted images and their x-, y- and z-coordinates. For each voxel the probability was calculated, which was defined as the chance that the voxel belonged to one of the eight tissue types. The various volumes were determined by adding up the probabilities of all voxels for each tissue type multiplied by the voxel volume. More technical details regarding this neonatal brain segmentation method will be reported separately. Validation of the method was performed on seven representative infants. All slices were manually segmented into the eight tissue classes; the result was used as 'gold standard'. The Dice similarity indices (Dice SI) were between 0.78 - 0.93 except for the MWM (Dice SI 0.57). The accuracy of all segmentations was visually confirmed by two observers (BJMvK and MJNLB).

This neonatal brain segmentation method distinguishes cerebrospinal fluid in the ventricles (defined as 'VENT') from that in the extracerebral space (defined as 'CSF'). We evaluated different measures for brain size: 1) intracranial volume (ICV): the sum of the volumes of all eight different brain structures, i.e. brain tissue with ventricles and CSF 2) total brain volume (TBV): the sum of the volume of all brain tissues and the volume of the ventricles, without the CSF and 3) brain tissue volume (BT): the sum of all brain tissues, without the volume of the ventricles and CSF.

Of the 124 scans, 113 were eligible for further analysis: six infants were scanned in the coronal plane instead of the axial plane, two infants could not be segmented due to motion artifacts, in one infant the brain was not totally imaged and two infants were excluded because they were scanned at a postmenstrual age >44 weeks. The MRI of one infant displayed misclassification of voxels in the region of the occipital lobe because of a large bilateral cerebellar hemorrhage and another infant presented with the same problem in the temporal lobe caused by a temporal hemorrhage. In the latter two cases, manual editing was required; these were the only cases in which segmentations needed to be edited.

### Neurological assessment

The neurodevelopmental outcome was assessed by use of the Bayley Scales of Infant and Toddler Development-III (BSITD-III) at a mean corrected age of  $24.2 \pm 0.6$  months.<sup>17</sup> All children were tested by a single developmental specialist (ICvH) who was blinded to the MRI findings. Due to the limited time children of that age are able to concentrate during one session, only the cognitive and motor (fine and gross motor) subtest of the BSITD-III were administered. Both subtests scaled scores as composite scores were calculated corrected for prematurity (mean  $\pm$  SD in a normative population:  $10 \pm 3$  and  $100 \pm 15$ , respectively). Five children were lost to follow-up, therefore 108 children were finally included in this study.

### Data analyses

SPSS software version 15.0 (SPSS INC, Chicago, Illinois) was used for all analyses. The volumes of the different brain structures were analyzed in relation to infants' parameters at time of the scan. Subsequently, it was assessed if brain structure volumes at TEA could be used as biomarker for neurodevelopment at two years corrected age. The neonatal parameters GA, birth weight Z-score (BWz), gender, WM score and intraventricular hemorrhage (IVH) were considered to be possible confounders as was maternal education. IVH was categorized in normal/mild IVH (no IVH or germinal matrix hemorrhage/IVH grade II) and moderate/severe IVH (IVH III/IV). Maternal education was classified as low, middle and high, according to the CBS (Statistics Netherlands, The Hague, The Netherlands; <http://www.cbs.nl/en-GB/menu/home/default.htm>). Results were analyzed for absolute volumes and volumes corrected for both PMA and brain size (i.e. ICV, TBV or BT) to take size and age of the infant into account. The results for cerebellar volumes in relation to neurodevelopmental outcome will be reported separately. A p-value of <0.05 was considered statistically significant.

**Table 1: neonatal characteristics of the neonates included in this study**

	Total (n=108)
<b>Gestational age, mean ± SD (weeks)</b>	28.5 ± 1.7
<b>Birth weight, mean ± SD (gram)</b>	1134 ± 327
<b>Male, no (%)</b>	58 (53.7)
<b>Birthset: Singleton / Twins, no (%)</b>	80 (74.1) / 28 (25.9)
<b>PPROM, no (%)</b>	23 (21.3)
<b>Full course of antenatal steroids, no (%)</b>	84 (77.8)
<b>Race, no (%)</b>	
Caucasian	84 (77.8)
Other	18 (16.7)
Mixed	6 (5.6)
<b>Apgar at 5 min, median (range)</b>	9 (1-10)
<b>Late onset sepsis positive blood culture, no (%)</b>	49 (45.4)
<b>Days of ventilation, median (range)</b>	5 (0-40)
<b>Intraventricular haemorrhage (IVH), no (%)</b>	
No IVH	73 (67.6)
IVH I	8 (7.4)
IVH II	17 (15.7)
IVH III	8 (7.4)
IVH IV	2 (1.9)
<b>Educational level mother, no (%)*</b>	
Low	26 (24.1)
Middle	45 (41.7)
High	35 (32.4)
<b>Postmenstrual age, mean ± SD (weeks; range)</b>	41.7 ± 1.0 (39.7-43.6)

Abbreviations: SD, standard deviation; no, number; PPRM, preterm prolonged rupture of membranes; sufficient antenatal steroids, two doses of steroids administered 24 hours before labour; Postmenstrual age, postmenstrual age at the time of the scan

\*Maternal education of two infants are missing

## RESULTS

Neonatal details are presented in Table 1. There were no differences in GA, BW, PMA at time of the scan, gender, severity of an IVH and WM score, between the children who were included in this study and those who were excluded because brain tissue volumes were not obtained or who were lost to follow-up. During the neonatal period, 35 infants were diagnosed to have an IVH on sequential cranial ultrasound examinations (Table 1). Eight of them developed post-haemorrhagic ventricular dilatation requiring treatment.

Since normalization of brain structure volumes to ICV, TBV or BT yielded similar results, only the results after correction for ICV are presented below where appropriate.

**Table 2: Brain volumes: growth/week for the total cohort and volumes for boys and girls separately**

	Growth / week*	Boys		Girls		p-value
	n = 108	n = 58	% ICV	n = 50	% ICV	
<b>CB</b>	2.0	30.0 ± 4.7	5.9	28.5 ± 3.5	5.9	Ns
<b>CeGM</b>	1.1	23.7 ± 2.3	4.6	22.6 ± 2.2	4.7	0.014
<b>VENT</b>	0.5	10.6 ± 4.8	2.1	10.6 ± 4.8	2.2	Ns
<b>UWM</b>	5.8	174.4 ± 24.8	34.2	161.1 ± 19.0	33.6	0.003
<b>BS</b>	0.2	6.3 ± 0.6	1.2	6.0 ± 0.5	1.2	0.024
<b>GM</b>	12.5	166.5 ± 20.9	32.7	156.4 ± 22.2	32.6	0.017
<b>CSF</b>	5.8	96.3 ± 16.3	19.9	91.8 ± 18.0	19.1	Ns
<b>ICV</b>	27.9	510.3 ± 50.4	100	479.5 ± 46.6	100	0.001
<b>TBV</b>	22.2	414.0 ± 41.7	81.1	387.7 ± 33.9	80.9	0.001
<b>BT</b>	21.6	403.4 ± 40.7	79.1	377.2 ± 32.4	78.7	0.001

\*Growth per week in ml between PMA 40-43 weeks. The mean volume ± standard deviation for the different brain structures are presented in the columns 'boys' and 'girls'. The p-values were calculated for the difference in volume between boys and girls;

Abbreviations: % ICV, relative percentage in reference to intracranial volume; n, number; CB, cerebellum; BG, basal ganglia/thalamus; VENT, ventricles; UWM unmyelinated white matter; BS, brainstem; GM, cortical gray matter; CSF, cerebrospinal fluid in the extracerebral space; ICV, intracranial volume; TBV, total brain volume; BT, brain tissue volume

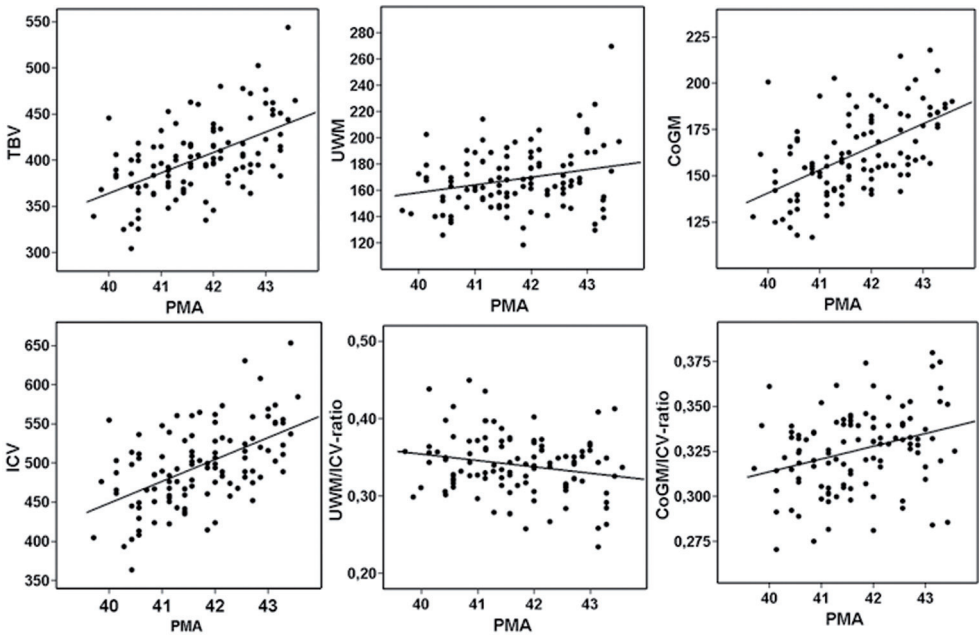
**Infants' characteristics at time of scanning and brain tissue volumes**

Boys and girls displayed no differences in GA, BWz, WM score and PMA at time of scanning. Table 2 shows the results for the brain volumes for boys and girls separately. Boys had larger absolute volumes than girls for all brain structures except for the volume of the CB, VENT and CSF. After correction for ICV, the relative brain volumes were no longer statistically different.

Absolute brain structure volumes demonstrated a statistically significant positive relation with PMA at time of scanning, except for the volume of the ventricles (Figure 1). After correction for ICV, the relation between PMA and UWM, BS and CoGM remained significant. However, the UWM/ICV-ratio was now negatively associated with PMA, which indicated that the fraction UWM of the ICV decreased between 39 and 43 weeks PMA.

All brain structure volumes demonstrated a significant relation with body weight at time of scanning. After correction for ICV, these associations did not remain statistically significant except for the BS/ICV ratio.

**Figure 1: Brain tissue volumes in relation to postmenstrual age at time of scanning**



Abbreviations: PMA, postmenstrual age; TBV, total brain volume = intracranial volume without cerebrospinal fluid in the extracerebral space; UWM, volume of the unmyelinated white matter; CoGM, volume of the cortical gray matter; ICV, intracranial volume; UWM/ICV-ratio, volume of the unmyelinated white matter in reference to the intracranial volume; CoGM/ICV-ratio, volume of the cortical gray matter in reference to the intracranial volume

## White matter score and brain volumes

In this cohort, 11 infants (10.2%) showed a normal MRI scan, 84 infants (77.8%) mildly abnormal WM, and 13 infants (12.0%) moderately abnormal WM.<sup>16</sup> The visual score of the size of the ventricles and subarachnoid space into normal, mildly or moderately/severely enlargement corresponded with the volumes of the ventricles and extracerebral CSF, respectively. (Figure 2) The UWM/ICV/PMA-ratio was negatively associated with the visual scores of the size of the ventricles ( $p=0.012$ ; UWM/ICV/PMA-ratio\*100: 0.84, 0.80 and 0.75, respectively) and with the VENT/ICV/PMA-ratio ( $R^2=0.07$ ,  $p=0.005$ ). The visual score of the subarachnoid space was associated with a gradual decrease in UWM ( $p<0.001$ ; UWM/ICV/PMA-ratio\*100: 0.87, 0.77 and 0.69, respectively) and the UWM/ICV/PMA-ratio demonstrated a negative relation with the CSF/ICV/PMA-ratio ( $R^2=0.51$ ,  $p<0.001$ ). Additionally, in infants with a normal shape, focal thinning or generalized thinning of the CC, a gradual decrease in UWM volume was revealed ( $p=0.034$ ; UWM/ICV/PMA-ratio\*100: 0.86, 0.81 and 0.78, respectively) and an increase was seen in CSF ( $p=0.009$ ; CSF/ICV/PMA-ratio\*100: 0.43, 0.46 and 0.48, respectively). (Figure 2)

**Figure 2: Items of the white matter score based on conventional MRI versus brain volumes**

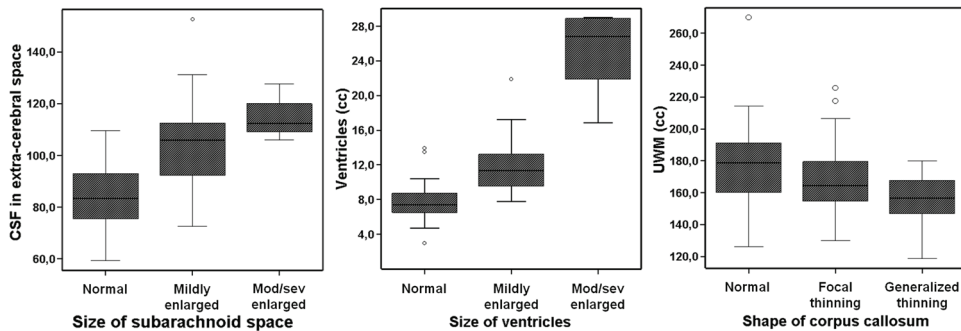


Figure a: mean volumes of the extra-cerebral CSF for infants with normal, mildly or moderately/severely enlargement of the subarachnoid space scored on conventional MRI:  $84.0 \pm 12.7$  cc,  $103.1 \pm 15.3$  cc and  $115.3 \pm 11.1$  cc, respectively;  $p<0.0010$ ; Figure b: mean ventricular volumes for infants with normal, mildly or moderately/severely enlarged ventricles scored on conventional MRI:  $7.6 \pm 1.9$  cc,  $11.8 \pm 2.8$  cc and  $25.1 \pm 4.9$  cc, respectively;  $p<0.001$ ; Figure c: mean UWM volumes for infants with normal shape, focal thinning or generalized thinning of the corpus callosum scored on conventional MRI:  $177.9 \pm 28.6$  cc,  $167.7 \pm 21.0$  cc,  $156.0 \pm 16.4$  cc;  $p=0.010$

**Table 3: Cognitive and motor outcome on the BSITD-III at two years corrected age**

	Median	Range	Infants with score $\leq$ -1SD
<b>Cognition:</b>			
Scaled score corrected age	11	4-19	n = 10 (9.3%)
Composite score corrected age	105	70-145	n = 10 (9.3%)
Composite score chronological age	95	70-130	n =24 (22.2%)
<b>Fine motor:</b> Scaled score corrected age			
	13	5-19	n = 3 (2.8%)
<b>Gross motor:</b> Scaled score corrected age			
	9	6-15	n = 9 (8.3%)
<b>Total motor:</b>			
Composite score corrected age	107	73-142	n = 3 (2.8%)
Composite score chronological age	97	70-133	n = 10 (9.3%)

*Abbreviations: Corrected age, score corrected for prematurity; Chronological age, score uncorrected for prematurity*

*Scaled score: mean  $\pm$  standard deviation in the normative population 10  $\pm$  3; Composite score: mean  $\pm$  standard deviation in the normative population 100  $\pm$ 15*

**Neurodevelopmental outcome and brain volumes**

Table 3 shows the results for the cognitive, fine motor, gross motor and total motor scores on the BSITD-III. There were no children who developed cerebral palsy or had other major motor deficits at two years corrected age.

The results regarding the relationship between the brain structure volumes and cognition, fine motor and gross motor performance with a  $p$ -value<0.1 are shown in table 4 and discussed in more detail below.

The absolute volumes of the CeGM and UWM were positively and VENT negatively associated with cognition. The VENT/ICV/PMA-ratio and the CoGM/ICV/PMA-ratio were negatively related to the cognitive scores. After correction for the neonatal parameters and maternal education, the association between cognition and ventricular volume remained statistically significant.

The absolute volume of the VENT was negatively and of the UWM positively related to fine motor performance. The VENT/ICV/PMA-ratio and the CoGM/ICV/PMA-ratio were negatively related to the fine motor scores. After correction for the neonatal parameters and maternal education, these associations were no longer statistically significant.

The absolute volumes of the VENT and extracerebral CSF were negatively and UWM volume positively associated with gross motor scores. The VENT/ICV/PMA-ratio, CoGM/ICV/PMA-ratio and the CSF/ICV/PMA-ratio were negatively related to the fine motor scores and the UWM/ICV/PMA-ratio was positively associated with gross motor performance. After correction for the neonatal parameters and for maternal education, these associations were no longer statistically significant.

**Table 4: Brain volumes in relation to neurodevelopmental outcome**

	Univariate			Multivariate		
	$\beta$	95% CI	<i>p</i>	$\beta$	95% CI	<i>p</i>
<b>Cognition</b>						
- CeGM	0.21	0.01 – 0.41	0.042	0.27	0.05 – 0.48	0.017
- VENT	-0.13	-0.23 – -0.04	0.008	-0.12	-0.24 – -0.01	0.061
- UMW	0.02	-0.00 – 0.04	0.076	0.02	-0.00 – 0.04	0.073
- VENT-ratio	-30.65	-51.39 – -9.92	0.004	-31.26	-56.66 – -5.85	0.016
- CoGM-ratio	-13.51	-22.42 – -4.61	0.003	-9.57	-19.20 – 0.05	0.051
<b>Fine motor</b>						
- VENT	-0.15	-0.25 – -0.05	0.005	-0.10	-0.23 – 0.04	0.171
- UWM	0.03	0.01 – 0.05	0.018	0.01	-0.23 – 0.04	0.318
- VENT-ratio	-35.01	-57.71 – -12.31	0.003	-23.04	-51.69 – 5.61	0.114
- CoGM-ratio	-10.34	-20.33 – -0.35	0.043	-0.27	-11.15 – 10.61	0.961
<b>Gross motor</b>						
- VENT	-0.10	-0.17 – -0.03	0.008	-0.06	-0.15 – 0.03	0.191
- UWM	0.02	0.00 – 0.03	0.028	0.00	-0.01 – 0.02	0.593
- CSF	-0.02	-0.04 – 0.00	0.074	-0.01	-0.03 – 0.01	0.260
VENT-ratio	-22.25	-37.98 – -6.57	0.006	-11.89	-31.01 – 7.22	0.220
UWM-ratio	4.41	0.90 – 7.92	0.014	1.87	-1.74 – 5.48	0.306
CoGM-ratio	-9.54	-16.30 – -2.77	0.006	-3.18	-10.37 – 4.02	0.383
CSF-ratio	-6.38	-12.35 – -0.41	0.036	-2.43	-8.42 – 3.56	0.422

In the multivariate regression analyses, gestational age, birth weight Z-score, gender, white matter score, intraventricular hemorrhage and maternal education were included.

Abbreviations:  $\beta$ , regression coefficient; 95% CI, 95% confidence interval; *p*, *p*-value; VENT, absolute ventricular volume; UWM, absolute unmyelinated white matter volume; VENT-ratio, ventricular volume/ intracranial volume (ICV) / postmenstrual age at time of scanning (PMA)-ratio\*100; CoGM-ratio, cortical grey matter/ICV/PMA-ratio\*100; UWM-ratio, UWM/ICV/PMA-ratio\*100; CSF, absolute extra-cerebral cerebrospinal fluid volume; CSF-ratio, CSF/ICV/PMA-ratio\*100

Exclusion of the eight infants with PHVD requiring treatment yielded similar results for cognition and gross motor scores. However, only an association between the absolute UWM volume and fine motor score was found, which did not remain valid after correction for the neonatal parameters and for maternal education.

## DISCUSSION

It was assessed whether brain tissue volumes at TEA could be used as biomarkers for neurodevelopmental outcome at two years corrected age in preterm infants. Ventricular volume at TEA was the most important in relation to neurodevelopment. Our automatic neonatal brain segmentation method distinguishes between cerebrospinal fluid in the ventricles and CSF in the extracerebral space. This gives the opportunity to consider these CSF fractions separately. Moreover, it may provide additional information regarding the underlying pathology of ventricular dilatation as a sequel of a hemorrhage or due to brain atrophy.

We found a correlation for ventricles and outcome independent of WM injury. Maunu *et al.* demonstrated a relation between ventricular volume at term and neurodevelopmental outcome at two years corrected age only in preterm infants with associated brain pathology and not in infants with isolated ventricular enlargement.<sup>18</sup> In the present study, WM score was included in the analyses as an indicator for WM injury. We analysed both the absolute brain structure volumes and volumes after correction for both PMA and normalization to brain size in relation to outcome. In this cohort, these different approaches yielded similar results. We suggest to correct brain tissue volumes for total brain size using the ICV. However, it is strongly recommended also to take absolute volumes into account in analyses of brain development around TEA. Brain volumes at TEA were used as ‘readout’ for the events in the neonatal period and we assessed if these volumes could be used as biomarkers for neurodevelopmental outcome. Further studies will be needed to determine the role of different potential risk factors for altered brain volumes.

We did not find a significant correlation between UMW, CoGM and CeGM and neurodevelopmental impairments, which is in contrast with previous studies.<sup>13;19</sup> This could be due to studying a relatively healthy population. Furthermore, in these studies only differences in volume were seen in infants with neurological impairments, which may have been caused by underlying pathology, compared to children with a normal development. Lind *et al.* did not distinguish between cerebral UWM and CoGM, the scan weight was significantly different between the two groups and no information was presented regarding PMA. Only a relation between absolute cerebellar volume and outcome was shown in all infants.<sup>19</sup> In the present cohort, we demonstrated a positive correlation between cerebellar volume and cognition. The role of cerebellar volume and MR spectroscopy in preterm infants in relation to neurodevelopmental outcome will be reported in detail separately.

Brain structure volumes were noted to be related to gender, PMA and scan weight. After normalization to ICV, TBV or BT, the confounding effect of gender and body weight at time of the scan disappeared. However, some brain structure volumes in reference to brain size remained statistically significant related to PMA, possibly indicating a maturation effect. Infants in this study were scanned between 39.7 and 43.6 weeks PMA. In this time frame an increase was seen in relative CoGM and a decline in relative UWM volume, probably due to faster growth of other tissues. These findings are in agreement with previously reported studies assessing brain volumes in preterm infants at TEA.<sup>20;21</sup>

An unexpected finding in the present study was the relation between lower scores on the BSITD-III and higher CoGM/brain size ratios. Studies assessing brain volumes at TEA in relation to neurodevelopment in preterm infants are rather scarce. Contrary to our findings, lower absolute CoGM volumes were found in preterm infants with moderate/severe disabilities at one year of age<sup>13</sup> and were associated with attention-interaction capacity at term age in infants with intrauterine growth restriction.<sup>22</sup> The segmentation method used in both studies included part of the cerebellar volume in the CoGM volume, hence a reduced cerebellar volume could have been measured as a smaller CoGM volume. Decreased cerebellar volumes are correlated with neurological impairments.<sup>23-25</sup> Tzarouchi *et al.* illustrated larger regional CoGM volumes in preterm infants with PVL analyzed at a mean age of 27 months compared to controls, possibly explained by brain plasticity as a response to injury.<sup>26</sup> However, a reduction in cortical layer V neurons was recently demonstrated in infants with PVL compared to controls, nevertheless the overall cortical thickness was not statistically significant different between the two groups.<sup>27</sup> Regional volumetric analysis in preterm infants assessed between childhood and adolescents demonstrated both areas of increased and decreased UWM and CoGM volumes compared to term born controls.<sup>11;28</sup> Visual assessment of the border between CoGM and UWM of children with larger CoGM volumes in our study, showed a gradual transition of the signal intensity of CoGM to UWM on both T2-weighted and T1-weighted images instead of a clear border. The subplate zone, located between the cortical plate and the intermediate zone, serves as a reservoir for neurons that form temporary neuronal circuits, especially for waiting thalamocortical afferents. Subplate neurons project into the developing cortical plate and play a major role in guiding thalamocortical pathfinding.<sup>29-31</sup> These neurons are prone to injury following hypoxia-ischemia in preterm infants.<sup>32</sup> It was hypothesized that dysfunctioning of the subplate neurons could result in incomplete migration of neuroblasts into the cortex and an incomplete apoptotic process of subplate neurons, especially in infants with WM injury. In the present study, infants displayed larger CoGM/ICV/PMA-ratio when more WM injury was apparent on conventional MRI. Differences in cell patterning are likely to influence MRI signal intensities and the subsequent, algorithm-dependent classification of voxels in this area, resulting in different brain volumes.

This study has several limitations that need to be addressed. The mean volume for MWM was  $2.5 \pm 1.4$  ml, but with a very wide range. Validation analysis demonstrated that MWM was less accurately segmented compared to the gold standard (data not shown) and therefore it was decided not to include MWM volumes in the analysis. Next, the results are restricted to preterm infants in the absence of a term born control group. The cohort in the present study represented a relatively healthy preterm population, with no infants born below 25 weeks of gestation and without severe brain pathology. Finally, there are no Dutch norm values for the BSITD-III available yet. Therefore we do not know if Dutch children perform differently on the subtests compared to children from the United States of America.

To conclude, ventricular volumes were negatively associated with cognition, fine motor and gross motor skills after correction for neonatal and maternal parameters. Brain tissue volumes corrected for brain size and PMA at TEA may serve as biomarkers for neurodevelopmental outcome at two years in preterm infants.

**Acknowledgments:**

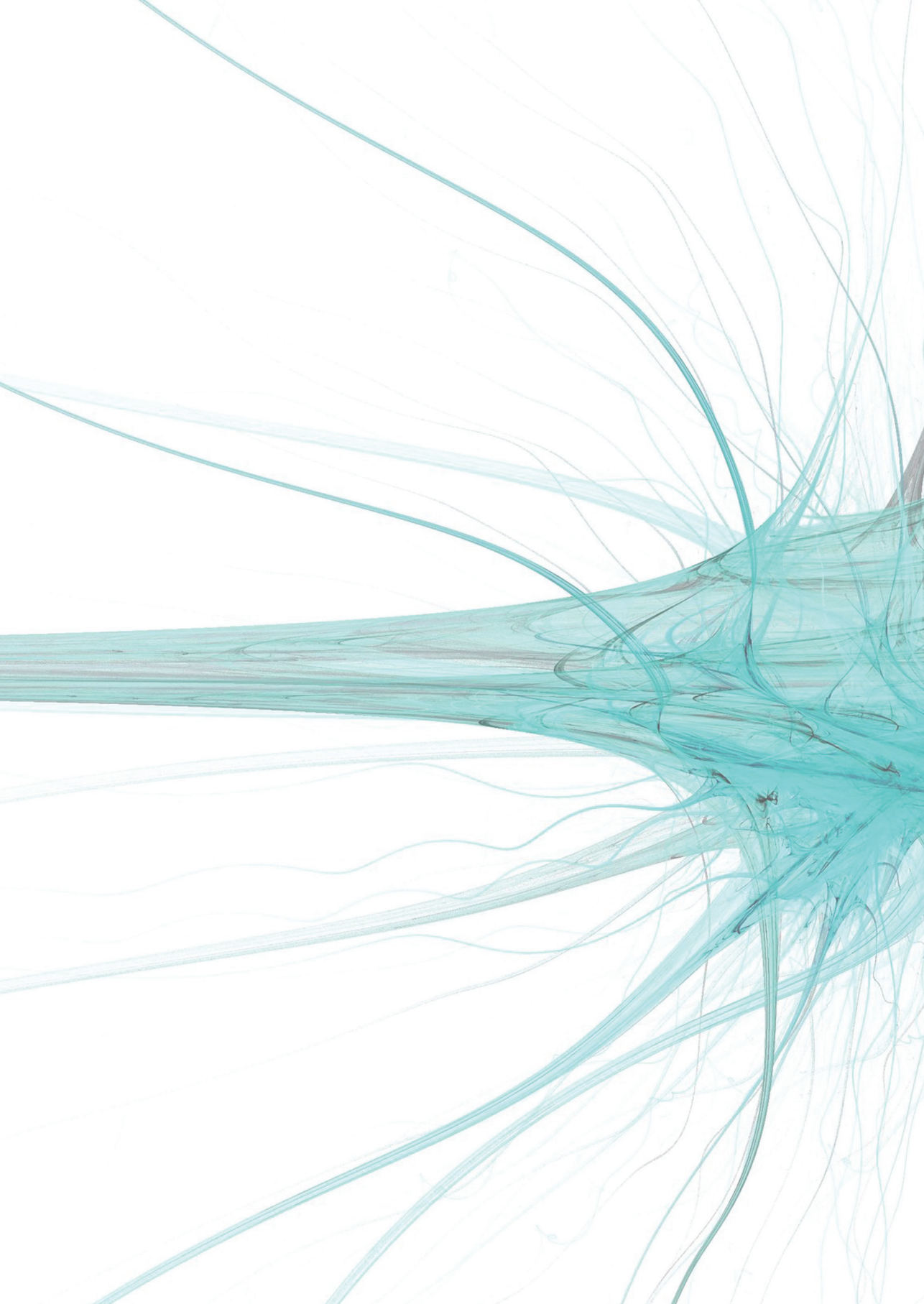
The authors thank Karina Kersbergen and Marian Tas for their contribution in the segmentation process, the families who took part in the study, Niels Blanken and the other MR technicians of the Imaging Division for their expert and enthusiastic support and our colleagues of the Neonatal Intensive Care Unit and Medium Care of the Wilhelmina Children's Hospital in Utrecht, The Netherlands.

## Reference List

- (1) Saigal S, Doyle LW. An overview of mortality and sequelae of preterm birth from infancy to adulthood. *Lancet* 2008; 371(9608):261-269.
- (2) Marlow N. Neurocognitive outcome after very preterm birth. *Arch Dis Child Fetal Neonatal Ed* 2004; 89(3):F224-F228.
- (3) Brown NC, Inder TE, Bear MJ, Hunt RW, Anderson PJ, Doyle LW. Neurobehavior at term and white and gray matter abnormalities in very preterm infants. *J Pediatr* 2009; 155(1):32-8, 38.
- (4) Miller SP, Ferriero DM, Leonard C, Piecuch R, Glidden DV, Partridge JC et al. Early brain injury in premature newborns detected with magnetic resonance imaging is associated with adverse early neurodevelopmental outcome. *J Pediatr* 2005; 147(5):609-616.
- (5) Dyet LE, Kennea N, Counsell SJ, Maalouf EF, Ajayi-Obe M, Duggan PJ et al. Natural history of brain lesions in extremely preterm infants studied with serial magnetic resonance imaging from birth and neurodevelopmental assessment. *Pediatrics* 2006; 118(2):536-548.
- (6) Anbeek P, Vincken KL, Groenendaal F, Koeman A, van Osch MJ, van der Grond J. Probabilistic brain tissue segmentation in neonatal magnetic resonance imaging. *Pediatr Res* 2008; 63(2):158-163.
- (7) Prastawa M, Gilmore JH, Lin W, Gerig G. Automatic segmentation of MR images of the developing newborn brain. *Med Image Anal* 2005; 9(5):457-466.
- (8) Warfield SK, Kaus M, Jolesz FA, Kikinis R. Adaptive, template moderated, spatially varying statistical classification. *Med Image Anal* 2000; 4(1):43-55.
- (9) Mewes AU, Huppi PS, Als H, Rybicki FJ, Inder TE, McNulty GB et al. Regional brain development in serial magnetic resonance imaging of low-risk preterm infants. *Pediatrics* 2006; 118(1):23-33.
- (10) Ment LR, Kesler S, Vohr B, Katz KH, Baumgartner H, Schneider KC et al. Longitudinal brain volume changes in preterm and term control subjects during late childhood and adolescence. *Pediatrics* 2009; 123(2):503-511.
- (11) Nosarti C, Giouroukou E, Healy E, Rifkin L, Walshe M, Reichenberg A et al. Grey and white matter distribution in very preterm adolescents mediates neurodevelopmental outcome. *Brain* 2008; 131(Pt 1):205-217.
- (12) Martinussen M, Flanders DW, Fischl B, Busa E, Lohaugen GC, Skranes J et al. Segmental brain volumes and cognitive and perceptual correlates in 15-year-old adolescents with low birth weight. *J Pediatr* 2009; 155(6):848-853.
- (13) Inder TE, Warfield SK, Wang H, Huppi PS, Volpe JJ. Abnormal cerebral structure is present at term in premature infants. *Pediatrics* 2005; 115(2):286-294.
- (14) Beauchamp MH, Thompson DK, Howard K, Doyle LW, Egan GF, Inder TE et al. Preterm infant hippocampal volumes correlate with later working memory deficits. *Brain* 2008; 131(Pt 11):2986-2994.

- (15) Shah DK, Guinane C, August P, Austin NC, Woodward LJ, Thompson DK et al. Reduced occipital regional volumes at term predict impaired visual function in early childhood in very low birth weight infants. *Invest Ophthalmol Vis Sci* 2006; 47(8):3366-3373.
- (16) Woodward LJ, Anderson PJ, Austin NC, Howard K, Inder TE. Neonatal MRI to predict neurodevelopmental outcomes in preterm infants. *N Engl J Med* 2006; 355(7):685-694.
- (17) Bayley N. Bayley Scales of Infant and Toddler Development, Third edition. San Antonio, USA: Harcourt Assessment; 2006.
- (18) Maunu J, Lehtonen L, Lapinleimu H, Matomaki J, Munck P, Rikalainen H et al. Ventricular dilatation in relation to outcome at 2 years of age in very preterm infants: a prospective Finnish cohort study. *Dev Med Child Neurol* 2011; 53(1):48-54.
- (19) Lind A, Parkkola R, Lehtonen L, Munck P, Maunu J, Lapinleimu H et al. Associations between regional brain volumes at term-equivalent age and development at 2 years of age in preterm children. *Pediatr Radiol* 2011.
- (20) Zacharia A, Zimine S, Lovblad KO, Warfield S, Thoeny H, Ozdoba C et al. Early assessment of brain maturation by MR imaging segmentation in neonates and premature infants. *AJNR Am J Neuroradiol* 2006; 27(5):972-977.
- (21) Huppi PS, Warfield S, Kikinis R, Barnes PD, Zientara GP, Jolesz FA et al. Quantitative magnetic resonance imaging of brain development in premature and mature newborns. *Ann Neurol* 1998; 43(2):224-235.
- (22) Tolsa CB, Zimine S, Warfield SK, Freschi M, Sancho RA, Lazeyras F et al. Early alteration of structural and functional brain development in premature infants born with intrauterine growth restriction. *Pediatr Res* 2004; 56(1):132-138.
- (23) Allin M, Matsumoto H, Santhouse AM, Nosarti C, AlAsady MH, Stewart AL et al. Cognitive and motor function and the size of the cerebellum in adolescents born very pre-term. *Brain* 2001; 124(Pt 1):60-66.
- (24) Messerschmidt A, Fuiko R, Prayer D, Brugger PC, Boltshauser E, Zoder G et al. Disrupted cerebellar development in preterm infants is associated with impaired neurodevelopmental outcome. *Eur J Pediatr* 2008; 167(10):1141-1147.
- (25) Shah DK, Anderson PJ, Carlin JB, Pavlovic M, Howard K, Thompson DK et al. Reduction in cerebellar volumes in preterm infants: relationship to white matter injury and neurodevelopment at two years of age. *Pediatr Res* 2006; 60(1):97-102.
- (26) Tzarouchi LC, Astrakas LG, Zikou A, Xydis V, Kosta P, Andronikou S et al. Periventricular leukomalacia in preterm children: assessment of grey and white matter and cerebrospinal fluid changes by MRI. *Pediatr Radiol* 2009;1327-1332.
- (27) Andiman SE, Haynes RL, Trachtenberg FL, Billiards SS, Folkerth RD, Volpe JJ et al. The cerebral cortex overlying periventricular leukomalacia: analysis of pyramidal neurons. *Brain Pathol* 2010; 20(4):803-814.

- (28) Kesler SR, Ment LR, Vohr B, Pajot SK, Schneider KC, Katz KH et al. Volumetric analysis of regional cerebral development in preterm children. *Pediatr Neurol* 2004; 31(5):318-325.
- (29) Kanold PO, Luhmann HJ. The subplate and early cortical circuits. *Annu Rev Neurosci* 2010; 33:23-48.
- (30) Kostovic I, Judas M. Transient patterns of cortical lamination during prenatal life: do they have implications for treatment? *Neurosci Biobehav Rev* 2007; 31(8):1157-1168.
- (31) Prayer D, Kasprian G, Krampfl E, Ulm B, Witzani L, Prayer L et al. MRI of normal fetal brain development. *Eur J Radiol* 2006; 57(2):199-216.
- (32) McQuillen PS, Ferriero DM. Perinatal subplate neuron injury: implications for cortical development and plasticity. *Brain Pathol* 2005; 15(3):250-260.





## CHAPTER FIVE

# Cerebellar volume and proton MR spectroscopy at term and neurodevelopment at two years of age in preterm infants

Britt J.M. van Kooij, Manon J.N.L. Benders, Petronella Anbeek, Ingrid C. van Haastert,  
Linda S. de Vries, Floris Groenendaal

*Submitted*

**ABSTRACT**

**Aim** - To assess the relation between cerebellar volume (CV) and spectroscopy at term equivalent age (TEA) and neurodevelopment at 24 months corrected age in preterm infants.

**Methods** - Magnetic resonance imaging of the brain was performed around TEA in 112 preterm infants born with a mean gestation age of 28 weeks and 3 days  $\pm$  1 week and 5 days. CV and in a subgroup cerebellar proton MR spectroscopy ( $^1\text{H}$ -MRS) were assessed in relation to cognitive, fine motor and gross motor scores on the Bayley Scales of Infant and Toddler Development-III. Different neonatal variables and maternal education were considered to be possible confounders.

**Results** - CV was significantly associated with postmenstrual age (PMA) a time of scanning. CV corrected for PMA was significantly associated with cognition. Cognitive scores related significantly with N-acetylaspartate/choline (NAA/Cho) ratio obtained from cerebellar  $^1\text{H}$ -MRS in 53 infants. Correction for neonatal and maternal variables did not change these results. Cerebellar variables were not related to motor performance.

**Interpretation** - In preterm infants, CV and cerebellar NAA/Cho ratio at TEA were associated with cognition; however no relation was found with motor outcome at two years of age. These findings support the importance of the cerebellum in cognitive development in preterm infants.

## INTRODUCTION

Preterm infants are known to be at risk for an impaired neurodevelopment.<sup>1</sup> Many studies have focused on cerebral injury and altered development in relation to neurological outcome.<sup>2-4</sup> New insights have recognized that the cerebellum plays a role in higher functioning, such as motor learning, memory and cognition and in behavior.<sup>5,6</sup>

Disrupted cerebellar development in the first twelve weeks after birth has been reported following extreme prematurity.<sup>7</sup> The exponential growth of the cerebellum between 28-42 weeks of gestation may explain an increased vulnerability of the cerebellum during late gestation.<sup>8,9</sup> While extensive cerebellar injury can be visualized with dedicated cranial ultrasound through the mastoid window, smaller punctate lesions are best detected with magnetic resonance imaging (MRI). Cerebellar haemorrhagic lesions are related to long-term neurodevelopmental disabilities and the underrecognized role for the cerebellum regarding cognition, learning and behavior has been revealed.<sup>10</sup> Several studies have now demonstrated a relation between cerebellar volume (CV) and neurodevelopment assessed from early childhood into adolescence.<sup>11-13</sup> Reduced CVs are usually seen in the context of associated supratentorial lesions.<sup>11,14</sup>

Proton magnetic resonance spectroscopy (<sup>1</sup>H-MRS) can be used to assess brain integrity and maturation with age.<sup>15</sup> A decreased cerebral N-acetylaspartate/choline (NAA/Cho) ratio has been shown to predict abnormal neuromotor development in full-term infants with perinatal asphyxia.<sup>16</sup> In addition, a two-fold increase of cerebellar NAA/Cho is seen between the brain of the preterm and term infants and between term age and adulthood.<sup>17</sup> To the best of our knowledge, no studies have been performed in preterm infants relating changes in cerebellar <sup>1</sup>H-MRS with neurodevelopmental outcome.

We hypothesized that CV and cerebellar NAA/Cho ratio at term equivalent age (TEA) are associated with neurodevelopment at 24 months corrected age in preterm infants after correction for neonatal variables and maternal education. Cerebellar <sup>1</sup>H-MRS was performed in a subgroup of the cohort.

## METHODS

### Patients

Neonates born below 31 weeks' gestation who reached TEA between January 2007 and June 2008 were recruited for a prospective preterm cohort study performed in the Wilhelmina Children's Hospital in Utrecht, the Netherlands. Nine neonates who were either born outside our referral district, had dysmorphic features or had a congenital infection were excluded. Of the 167 consecutively admitted neonates, 19 died in the neonatal period, parents of 15 neonates refused to cooperate, 15 neonates were

**Table 1: Characteristics of the infants**

	Total (n=112)
<b>Gestational age, mean ± SD (weeks+days)</b>	28+4 ± 1+5
<b>Birth weight, mean ± SD (gram)</b>	1129 ± 324
<b>Male, no (%)</b>	60 (53.6)
<b>Birthset: Singleton / Twins, no (%)</b>	83 (74.1) / 29 (25.9)
<b>PPROM, no (%)</b>	24 (21.4)
<b>Sufficient antenatal steroids, no (%)</b>	86 (76.8)
<b>Race, no (%)</b>	
Caucasian	88 (78.6)
Other	18 (16.1)
Mixed	6 (5.4)
<b>Apgar score at 5 min, median (range)</b>	9 (1-10)
<b>Sepsis with positive blood culture, no (%)</b>	51 (45.5)
<b>Days of ventilation, median (range)</b>	5 (0-40)
<b>Intraventricular hemorrhage (IVH), no (%)</b>	
No IVH	74 (66.1)
IVH I	8 (7.1)
IVH II	19 (17.0)
IVH III	8 (7.2)
IVH IV	3 (2.7)
<b>Maternal education, no (%)*</b>	
Low	28 (25.0)
Middle	47 (42.0)
High	35 (31.3)
<b>Postmenstrual age at MRI, mean ± SD (weeks+days)</b>	41+5 ± 1+1
<b>Cerebellar variables†</b>	
Volume, median (IQR)	24.3 (3.7) ml
<sup>1</sup> H-MRS TE 35 NAA/Cho, median (IQR)	0.663 (0.181)
<sup>1</sup> H-MRS TE 144 NAA/Cho, median (IQR)	0.333 (0.092)
<sup>1</sup> H-MRS TE 144 Lac/NAA, median (IQR)	-0.160 (0.174)
<sup>1</sup> H-MRS TE 144 Lac/Cho, median (IQR)	-0.050 (0.057)

Abbreviations: wks, weeks; d, days; no, number; PPROM, preterm prolonged rupture of membranes; sufficient antenatal steroids, two doses of steroids administered 24 hours before labour; IQR, interquartile range; <sup>1</sup>H-MRS TE 35, proton magnetic resonance spectroscopy with echo time of 35 ms (short echo

time); <sup>1</sup>H-MRS TE 144, proton magnetic resonance spectroscopy with echo time of 144 ms (long echo time); NAA/Cho, N-acetylaspartate/choline ratio; Lac/NAA, Lactate/ N-acetylaspartate ratio; Lac/Cho, lactate/choline ratio

\*Maternal education of two mothers is missing

‡Cerebellar volume: results presented of 112 infants; cerebellar <sup>1</sup>H-MRS TE 35: results presented of 47 infants; cerebellar <sup>1</sup>H-MRS TE144: results presented of 53 infants

examined on a 1.5 Tesla system and six were lost to follow-up. The study cohort therefore consisted of 112 infants. Neonatal details are represented in Table 1. MRI of the brain was acquired around TEA, with a mean age of 41wks and 5days (range 39-45 weeks). Written informed parental consent was obtained for all infants. This study was approved by the Medical Ethics Committee of the University Medical Center Utrecht.

## MRI

MR investigations were performed on a 3.0 Tesla MR system (Achieva, Philips Medical Systems, Best, The Netherlands) using a Sense head coil. The infants were sedated with 50-60 mg/kg oral chloralhydrate. Heart rate, transcutaneous oxygen saturation and respiratory rate were monitored during scanning. For hearing protection Minimuffs® (Natus Medical Incorporated, San Carlos, CA) were used. A neonatologist was present throughout the examination.

The protocol contained conventional sagittal T1-weighted (repetition time (TR)=886 ms; echo time (TE)=15 ms; scan time=3.03 min; slice thickness=3.0 mm), axial 3D T1-weighted (TR=9.4 ms; TE=4.6 ms; scan time=3.44 min; slice thickness=2.0 mm) and axial T2-weighted imaging (TR=6293 ms; TE=120 ms; scan time=5.40 min; slice thickness=2.0 mm). From May 2007 <sup>1</sup>H-MRS was added to the scanning protocol. In 58 infants cerebellar <sup>1</sup>H-MRS was acquired with short and/or long echo time (TR=2000 ms; TE=35 ms (short TE)/144 ms (long TE); PRESS; NSA=96; automatic water suppression).

MRI was evaluated independently by two experienced neonatologists and blinded to the results of the neurodevelopmental assessment. In case of disagreement, a third reader was consulted. The white matter (WM) signal intensity, size of the subarachnoid space, presence of WM cysts, size of the ventricles and thickness of the corpus callosum were scored as (1) normal, (2) mildly abnormal and (3) moderately/severely abnormal (adjusted from Woodward et al.4; Table 2). The WM score is the sum of these subscores (range 5-15) and was applied as an indicator for WMI.

## Cerebellar variables

The number of cerebellar lesions was recorded on the conventional MRI (Figure 1). These lesions had a decreased signal intensity on the T2-weighted and an increased intensity on the T1-weighted sequence, suggestive of haemorrhage.

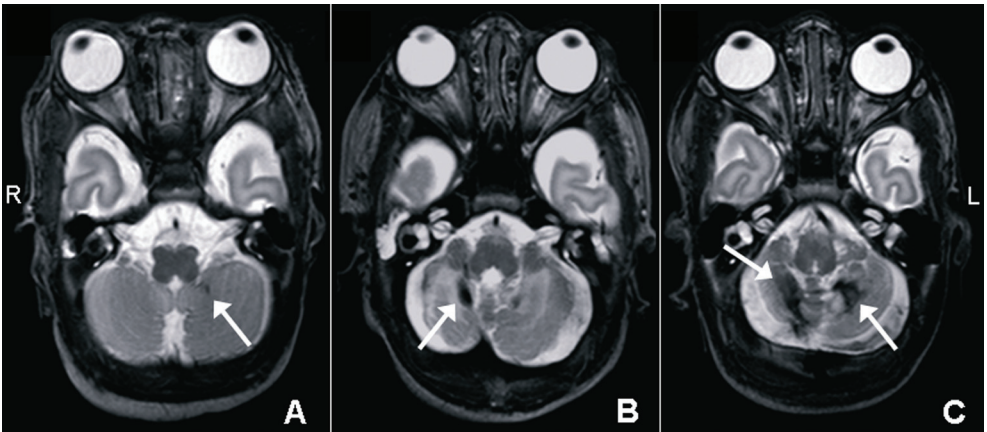
Cerebellar <sup>1</sup>H-MRS was acquired with a short and/or long TE. Forty-four infants had spectra of good quality with both echo times, three only with short TE and nine only with long TE. Two infants were excluded due to poor quality of both spectra and in 54

**Table 2: White matter scoring system, adjusted from Woodward *et al.*<sup>4</sup>**

	Normal = 1	Mildly abnormal = 2	Moderate/severe = 3
<b>White matter signal intensity</b>	Normal	Areas of increased signal intensity on T2-weighted images in the centrum semiovale	Diffuse increased signal intensity on T2-weighted images in centrum semiovale and subcortical, low intensity in these areas on the T1-weighted images
<b>Subarachnoid space</b>	Normal size	Anterior > 4 mm	Parieto-occipital > 4 mm
<b>Presence of cysts</b>	No cysts	Cysts following parenchymal hemorrhage, solitary subcortical cysts	Cystic periventricular leukomalacia
<b>Size of Ventricles</b>	Largest diameter < 8 mm	Largest diameter between 8-10 mm	Largest diameter > 10 mm
<b>Thickness of the corpus callosum*</b>	Both measurements ≥ 2.4 mm	At least one measurement between 1.8-2.3 mm	Both measurements ≤ 1.7 mm

*\*Measured by one independent researcher at the location of 0.5 cm from the natural incurvation near the level of the genu and the splenium and perpendicular to the contour and to the middle of the corpus callosum*

**Figure 1: Examples of cerebellar lesions**



*In most cases of cerebellar lesions (n=17), punctate lesions were found (Figure A), except in one child who showed signs of a larger hemorrhage in one hemisphere as well as a punctate lesion in the contralateral hemisphere (Figure B) and one child with a large bilateral cerebellar hemorrhages. (Figure C). The lesions are indicated by white arrows (R, right side; L, left side).*

infants no spectroscopy was performed because of changes in the protocol and/or time constraints. A region of interest was positioned to be as large as possible (minimum size: 1.0 cm<sup>3</sup>). (Figure 2) NAA (2.02 ppm), Cho (3.25 ppm), Creatine (Cr, 3.02 ppm) and if present the lactate peak (Lac; 1.33 ppm) were fitted by software of the Philips MR system. The peak area ratios were calculated of NAA/Cho (both TE), Lac/NAA and Lac/Cho (TE 144 ms).

The CV was measured with an in-home developed, fully automatic, probabilistic brain segmentation method.<sup>18</sup> Voxels were classified by K-Nearest Neighbour classification. Voxel features were the signal intensities and the x-, y- and z-coordinates on the axial T1- and T2-weighted images. To eliminate overclassified gray matter tissue, an atlas, composed from coregistered manual cerebellum segmentations of a set of training patients, was used. (Figure 3) Validation of the method was performed on seven representative infants. Manual segmentation of the cerebellum was used as gold standard. The Dice similarity index for the cerebellum was 0.93. The accurateness of all segmentations was visually confirmed independently by two researchers (BJMvK and MJNLB). Because of large haemorrhages in the cerebellum of two infants, the automatic segmentation was inadequate and manual editing was needed.

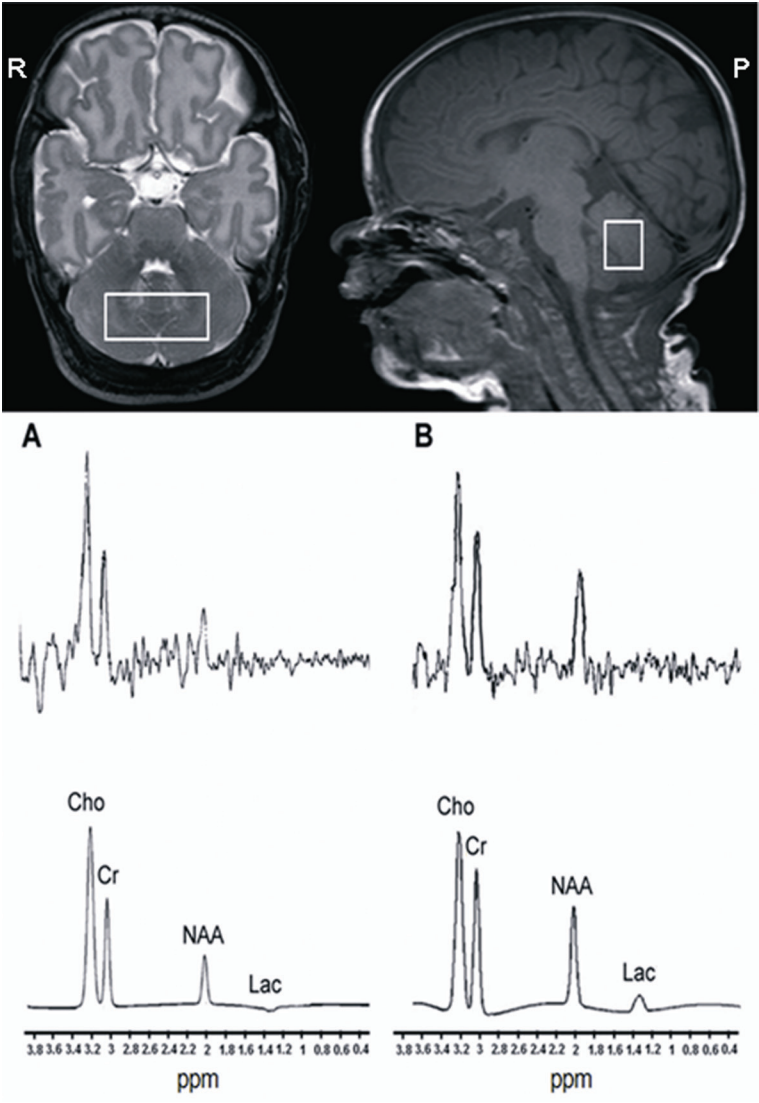
### Neurodevelopmental outcome

At two years corrected age (mean 24.2±0.6 months), the children were assessed with the BSITD-III by a single developmental specialist who was blinded to the MRI findings.<sup>19</sup> Only the cognitive and fine and gross motor subtests were used. The language subtest was not performed due to the limited time a child can concentrate on the different tasks during one session. Both scaled scores of these subtests as well as the cognitive and total motor composite scores were calculated corrected for prematurity (mean in a normative population: 10±3 and 100±15, respectively).

### Other factors included in the analysis

An intraventricular haemorrhage (IVH) and maternal education were included as possible confounders. An IVH was graded as normal/mild (no IVH or IVH I-II) or moderate/severe (IVH III-IV).<sup>20</sup> Education was classified as low, middle and high, according to the CBS (Statistics Netherlands, The Hague; <http://www.cbs.nl/en-GB/menu/home/default.htm>).

**Figure 2: Cerebellar proton MR spectroscopy**



*Planning of the region of interest in the cerebellum in the axial and sagittal plane to perform MR spectroscopy. Examples of spectra acquired at long echo time (144 ms), showing in (A) a low NAA/Cho ratio and (B) indicates a normal NAA/Cho ratio. (top: crude spectra; bottom: fitted spectra; R, right side; P, posterior).*

## Data analyses and statistics

SPSS version 15.0 was utilized for all analyses. The distribution of the different variables were analysed for normality. Linear regression was used to assess the relation between CV or cerebellar NAA/Cho ratio and neurodevelopmental outcome. The neonatal variables GA, BW Z-score, gender, WM score and IVH and maternal education were included in the analysis as possible confounders. As the absolute CV showed a significant relation with postmenstrual age (PMA), the CV/PMA ratio was used in the analyses. Only the cerebellar NAA/Cho ratio ( $n=53$ ) was used in the multivariable regression analyses as the quality of this spectra was better than the spectra acquired with TE 35 ms and in the univariable analyses the relation between the NAA/Cho ratio at TE 35 ms and BSITD-III was not significant. A  $p<0.05$  was considered statistically significant.

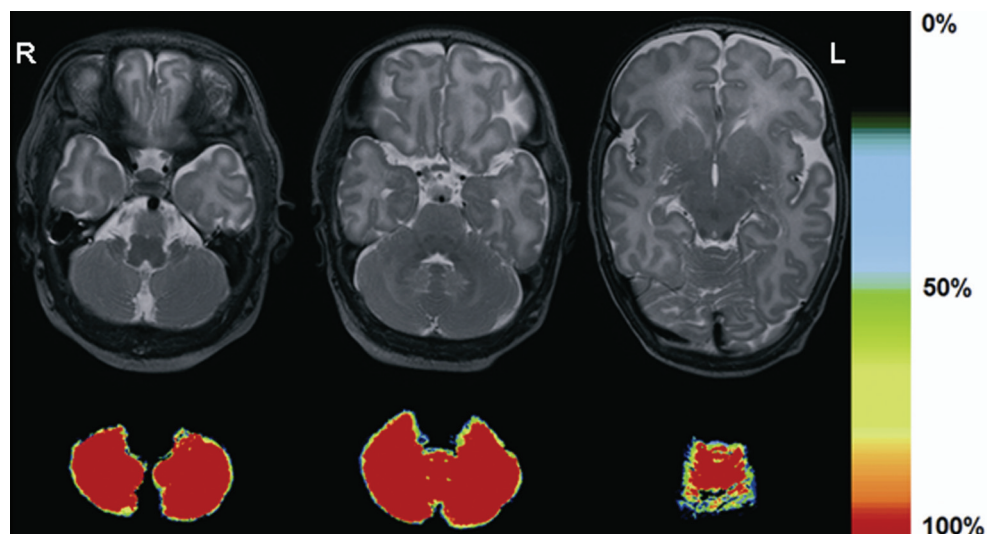
## RESULTS

### MRI findings

In this cohort, 11 infants (9.8%) showed a normal MRI scan, 87 (77.7%) mildly abnormal WM and 14 (12.5%) moderately abnormal WM. No infants showed severe WMI. During the neonatal period, 38 infants were diagnosed with an IVH on cranial ultrasound examinations (Table 1). Eight neonates developed post-haemorrhagic ventricular dilatation (PHVD) requiring intervention. Fifteen infants had small ( $<1$  cm) punctate haemorrhages in the cerebellum. Two infants had a larger haemorrhage (one bilateral, one unilateral) associated with volume loss in the affected cerebellar hemisphere (Figure 1). Infants with a moderate/severe IVH showed significantly more often cerebellar lesions than infants with no/mild IVH (4/17 versus 7/95, respectively;  $p=0.039$ ). The infant with a larger unilateral cerebellar haemorrhage had an IVH grade III and the infant with bilateral haemorrhages also had an IVH with an ipsilateral small venous infarction. No association was found between cerebellar lesions and WMI.

### Cerebellar $^1\text{H}$ -MRS

In this study, 56 infants were included with quantifiable spectra performed with TE 35 and/or 144 ms (Figure 2). In the two infants with larger cerebellar haemorrhages no cerebellar  $^1\text{H}$ -MRS was performed. There was a significant relation between GA and NAA/Cho, Lac/Cho and Lac/NAA (TE 144 ms;  $p$ -value=0.010;  $p$ -value $<0.001$ , and  $p$ -value $<0.001$ , respectively). No other statistically significant relations were found between the metabolite ratios and GA, PMA and neither with WMI or cerebellar lesions.

**Figure 3: Example of cerebellar segmentation at different levels**

The color bar indicates the probability (0-100%) that a voxel is cerebellar tissue. For example, the red voxels are 100% cerebellar tissue, whereas 25% of the volume of light blue voxels contribute to the cerebellar volume (R, right side; L, left side).

### Cerebellar volume

The CV was normally distributed. The median (interquartile range) of the CV in the total study cohort was 24.3 (3.7) ml. GA showed a relation with CV, however this was biased by the two infants with a larger unilateral or bilateral cerebellar haemorrhage and this association disappeared after exclusion of these two infants (GA 26wks 2days: CV=14.1 ml and GA 25wks: CV=7.0 ml, respectively). No volume differences were found between the other fifteen infants with cerebellar lesions and those without cerebellar lesions ( $n=15$ : 24.2 (6.1) ml,  $n=95$ : 24.5 (3.6) ml, respectively). CV was related with PMA at the time of the scan ( $p<0.001$ ). No relation was demonstrated between CV and the different metabolite ratios at TE 35 and 144 ms, WMI or IVH grade. These associations did not change after exclusion of the two infants with larger cerebellar haemorrhages.

### Neurodevelopmental outcome and relationship to MRI findings

The median (range) cognitive scaled score and composite score were 11 (4-19; 8.9% of infants scored  $\leq -1$ SD) and 105 (70-145; 8.9% of infants scored  $\leq -1$ SD), respectively. The median (range) fine motor scaled score was 13 (5-19; 2.7% of infants scored  $\leq -1$ SD) and gross motor scaled score 9 (6-15; 8.0% of infants scored  $\leq -1$ SD) resulting in a total motor composite score of 107 (73-142; 2.7% of infants scored  $\leq -1$ SD). Mann-Whitney U analysis showed no differences in the BSITD-III scores between infants with ( $n=17$ ) and without ( $n=95$ ) cerebellar lesions. Kruskal-Wallis analysis showed that cognitive scores were significantly different between children of a mother with a low, middle or high educational level ( $p=0.001$ ; median 9, 10 and 12, respectively).

CV/PMA and the cerebellar NAA/Cho ratio acquired with TE 144 ms showed a significant relation with cognition ( $p=0.019$  and  $p=0.007$ , respectively). A trend was seen between CV/PMA and fine motor performance and between the cerebellar NAA/Cho ratio acquired at TE 144 ms and gross motor skills ( $p=0.076$  and  $p=0.095$ , respectively). After correction for the neonatal variables and maternal education, the relation between cognitive scores and both cerebellar volume and NAA/Cho ratio remained statistical significant ( $p=0.009$  and  $p=0.036$ , respectively; Table 3). In addition to the neonatal parameters and maternal education, no association could be demonstrated between cerebellar variables and motor function.

Exclusion of the two infants with large cerebellar haemorrhages did not alter the results of the multivariable linear regression analyses.

**Table 3: Cerebellar variables in relation to neurodevelopmental outcome**

	Univariable			Multivariable		
	$\beta$	95% CI	p	$\beta$	95% CI	p
<b>Cognition</b>						
- CV/PMA*	7.46	1.33 – 13.59	0.018	8.62	2.16 – 15.09	0.009
- NAA/Cho‡	13.28	3.88 – 22.69	0.007	11.70	0.78 – 22.61	0.036
<b>Fine motor</b>						
- CV/PMA	5.78	-0.62 – 12.17	0.076	3.49	-3.24 – 10.22	0.306
- NAA/Cho	7.09	-5.45 – 19.63	0.261	-0.29	-13.30 – 12.72	0.964
<b>Gross motor</b>						
- CV/PMA	-0.19	-4.63 – 4.24	0.931	-4.11	-8.50 – 0.27	0.066
- NAA/Cho	6.65	-1.21 – 14.50	0.095	3.74	-4.05 – 11.53	0.338

Abbreviations:  $\beta$ , regression coefficient; 95% CI, 95% confidence interval; p, p-value; Cognition, relations for cerebellar variables and cognitive score on the Bayley Scores of Infant and Toddler Development, third edition (BSITD-III); CV, cerebellar volume; PMA, postmenstrual age at time of scanning; Fine motor, relations for cerebellar variables and fine motor score on the BSITD-III; NAA/Cho, N-acetylaspartate/Choline ratio acquired with proton MR spectroscopy with a echo time of 144 ms; gross motor, relations for cerebellar variables and gross motor scores on the BSITD-III. In the multivariable regression analyses, potential confounders i.e. gestational age, birth weight Z-score, gender, white matter score, intraventricular hemorrhage and maternal education were included in the model. \* Sample size to fit the model regarding cerebellar volume:  $n=110$  (educational level of two mothers was missing) ‡ Sample size to fit the model regarding NAA/Cho ratio:  $n=51$  (educational level of two mothers was missing).

## DISCUSSION

This study assessed the relation between CV and cerebellar spectroscopy at TEA of preterm infants and neurodevelopment at 24 months corrected age. An association could be demonstrated between cognitive scores on the BSITD-III and both CV/PMA and cerebellar NAA/Cho ratio at TE 144 ms after correction for neonatal and maternal confounders. CV showed a positive relation with PMA. The cerebellar variables did not reveal an association with motor scores.

Prediction of developmental abilities in preterm infants is challenging. This study implies that CV and NAA/Cho ratio at TEA are associated with developmental outcome at two years corrected age. This highlights their potential role as biomarkers for prognostic purposes. The CV obtained in this cohort was in the range of data reported previously<sup>21</sup>, although the volumes were larger compared to data reported by Shah *et al.*<sup>11</sup> It was hypothesized this could be due to differences in segmentation techniques and the infants in our cohort were older at birth. Others have shown that CV in preterm infants assessed at TEA is reduced compared to full-term controls and this reduction is more common in the presence of supratentorial lesions.<sup>8;11;14</sup> We were however unable to show an association with an IVH or WMI. This could be due to the smaller number of infants with a severe IVH or severe WMI, a higher mean GA in our cohort and earlier intervention of PHVD.<sup>22</sup> Our findings are in agreement with Limperopoulos *et al.*, who also found reduced CVs in preterm infants with normal MRI findings.<sup>8</sup> This does suggest that only visual analysis of the MRI is not sufficient to detect subtle cerebellar changes. Both direct destructive injury and indirect events like ischemia, infection or deficits in trans-synaptic communication between cerebellum and cerebrum could cause cerebellar disease.<sup>9</sup> This hypothesis is supported by one study showing reduced grey and WM volumes on the contralateral cerebral hemisphere in infants with unilateral cerebellar injury.<sup>23</sup>

We were able to demonstrate a significant relation between CV at TEA and developmental outcome at two years corrected age in preterm infants after correction for WMI. Shah *et al.* found no relation with IVH and a weak association between CV and outcome that disappeared after correction for WMI.<sup>11</sup> We employed a different version of the Bayley Scales (BSITD-III versus BSID-II by Shah *et al.*). Additionally, they used a semi-automatic segmentation method with manually outlining of the cerebellum and we used a fully automatic segmentation method, which may have led to more objective measurements. Other studies reporting CVs assessed at an age range from 24 months into adolescence did reveal an association between CV and cognition.<sup>12;13</sup> Parker *et al.* reported a decline in CV between adolescence and young adulthood in adolescents who were born prematurely and they hypothesized that altered cerebellar development in children born prematurely persists until adolescence.<sup>24</sup>

In our study, a reduced CV was significantly associated with cognition, however the association with motor performance did not reach statistical significance. Limperopoulos *et al.* assessed in both preterm infants and full-term infants the relation between cerebellar lesions and neurodevelopment.<sup>10;25</sup> An impaired motor function was reported in infants with large cerebellar haemorrhages resulting in cerebellar hemispheric and/or vermis atrophy compared to preterm controls without cerebellar lesions or to term infants with

small punctate cerebellar lesions, respectively. In our study, fifteen infants displayed small punctate cerebellar lesions only recognized with MRI, one further infant had a large unilateral and another a large bilateral haemorrhage, both recognized with cranial ultrasound. The cognitive and total motor outcome of the first child was well within the normal range, the second child had composite scores of 70 and 88, respectively.

Using  $^1\text{H}$ -MRS cerebellar metabolism can be demonstrated *in vivo*. The NAA/Cho ratio increases in cerebrum and cerebellum of healthy preterm infants between 30 and 44 weeks' gestation.<sup>17</sup> NAA is considered to increase with neuronal development and to be synthesized by proliferating oligodendrocyte progenitor cells in the developing WM.<sup>26</sup> A positive relation was found between cerebellar NAA/Cho ratio and both GA and cognition, indicating differences in neuronal density and function that could be linked to maturation and neurodevelopment. A positive trend was found between cerebellar NAA/Cho ratio and PMA, however the increase in NAA/Cho in this timeframe was not significant. It was considered that we were unable to demonstrate this association due to the narrow timeframe the infants were scanned. The increase in CV in this short period was more extensive and therefore we were able to show a positive relation between PMA and CV. In this study, CV and cerebellar NAA/Cho ratios at TEA were used as 'readout' for the events in the neonatal period and it was assessed whether these features could be used as biomarkers for neurodevelopment. Further studies will be needed to determine the role of different potential risk factors for changes in cerebellar development.

In this population, there was no association between GA or BW and cognition. The mean GA of this cohort was almost 29 weeks (25-31 weeks) and only five infants had a BW <10<sup>th</sup> percentile. Only seven children scored  $\leq -1\text{SD}$  on the cognitive scale. Apparently, the population in our region is relatively affluent and benefits from adequate (prenatal) health care. This could contribute to the small number of infants with a poor score on the BSITD-III compared to studies performed in other countries. It has recently been suggested that developmental delay is underestimated on the BSITD-III.<sup>27</sup> However, the mean of the Griffiths' Developmental Assessment scale at 15 months corrected age in this study cohort was 102 with only three infants scoring below 85 (data not shown). None of the infants was diagnosed with cerebral palsy (CP) at the corrected age of two years, however one child was diagnosed to have mild CP at the age of 3,5 years. This is in agreement with the decreasing incidence of CP in infants admitted to our unit as recently presented by Van Haastert *et al.*<sup>28</sup>

This study has several limitations that need to be addressed. The language scale was not assessed due to time constraints. Comparison with the Mental Developmental Index of the BSID-II is therefore not possible. However, the cognitive outcome of the BSITD-III is possibly a better reflection of the cognition in non-Caucasian infants, as language difficulties do not affect this score. Next, findings of this study are restricted to preterm infants, without comparison to healthy full-term controls. Finally, CV was assessed at one time point. We hypothesize that sequential imaging soon after birth and at TEA will provide additional information regarding cerebellar growth allowing a more accurate prediction of adverse developmental outcome.

In conclusion, CV and NAA/Cho ratio assessed in preterm infants at TEA were associated with cognition at two years corrected age, but no relation was found with motor function. Our results suggest that the cerebellum should be taken into account, when trying to understand subsequent neurodevelopmental outcome of preterm infants.

### **Acknowledgements**

The authors thank Dr. Cuno S.P.M. Uiterwaal for his support in the statistical analysis. The authors are grateful to the families who took part in the study, Niels Blanken and the other MR technicians of the MR institute for their expertise and enthusiastic help and we thank our colleagues in the Neonatal Intensive Care Unit of the Wilhelmina's Children's Hospital in Utrecht, The Netherlands.

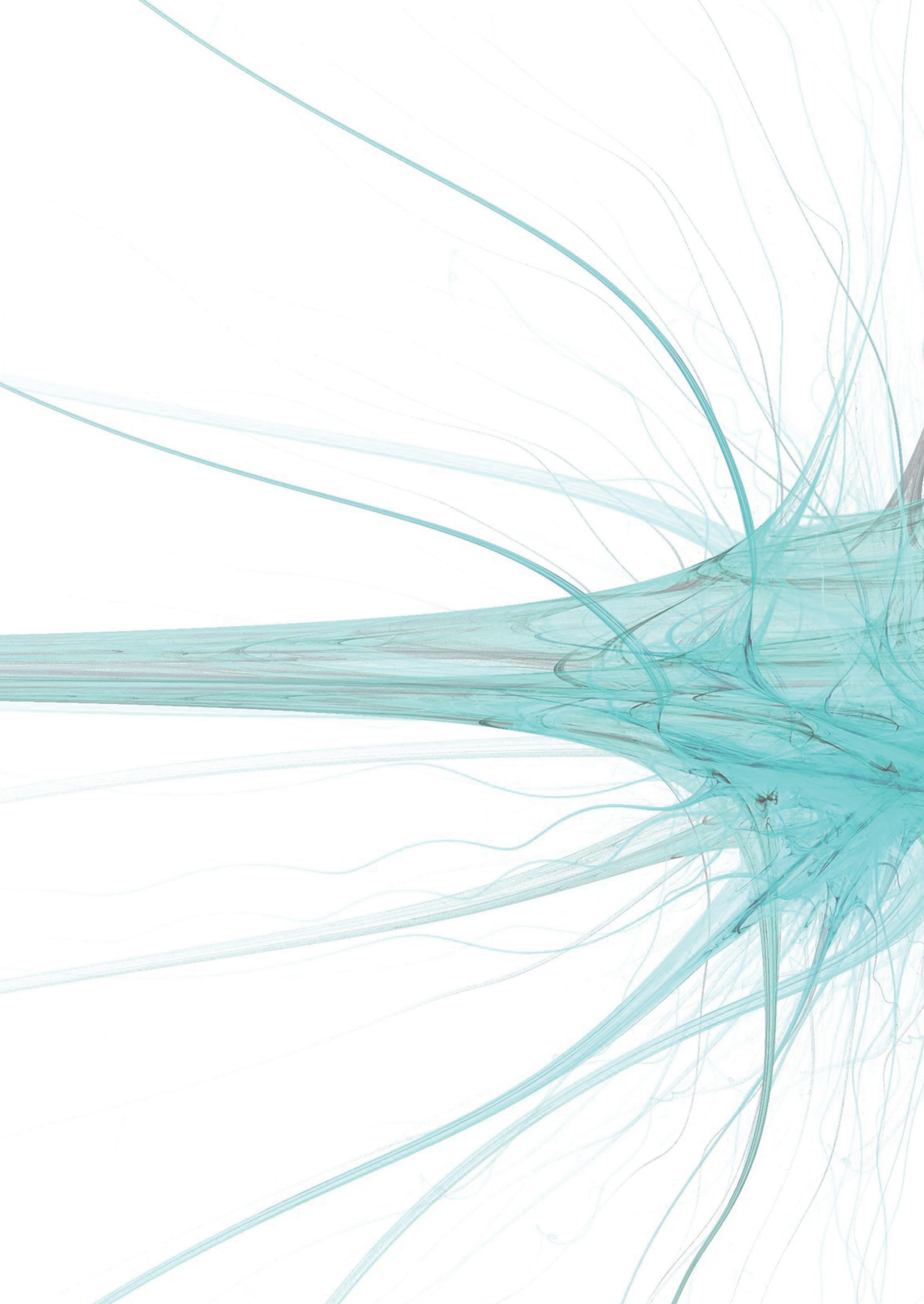
This research was funded by The Netherlands Organization for Health Research and Development, project 94527022. There was no involvement of the funder in study design, data collection, data analysis, manuscript preparation and / or publication decisions.

## Reference List

- (1) Larroque B, Ancel PY, Marret S, Marchand L, Andre M, Arnaud C et al. Neurodevelopmental disabilities and special care of 5-year-old children born before 33 weeks of gestation (the EPIPAGE study): a longitudinal cohort study. *Lancet* 2008; 371(9615):813-820.
- (2) Dyet LE, Kennea N, Counsell SJ, Maalouf EF, Ajayi-Obe M, Duggan PJ et al. Natural history of brain lesions in extremely preterm infants studied with serial magnetic resonance imaging from birth and neurodevelopmental assessment. *Pediatrics* 2006; 118(2):536-548.
- (3) Miller SP, Ferriero DM, Leonard C, Piecuch R, Glidden DV, Partridge JC et al. Early brain injury in premature newborns detected with magnetic resonance imaging is associated with adverse early neurodevelopmental outcome. *J Pediatr* 2005; 147(5):609-616.
- (4) Woodward LJ, Anderson PJ, Austin NC, Howard K, Inder TE. Neonatal MRI to predict neurodevelopmental outcomes in preterm infants. *N Engl J Med* 2006; 355(7):685-694.
- (5) Baillieux H, De Smet HJ, Paquier PF, De Deyn PP, Marien P. Cerebellar neurocognition: insights into the bottom of the brain. *Clin Neurol Neurosurg* 2008; 110(8):763-773.
- (6) Tavano A, Grasso R, Gagliardi C, Triulzi F, Bresolin N, Fabbro F et al. Disorders of cognitive and affective development in cerebellar malformations. *Brain* 2007; 130(Pt 10):2646-2660.
- (7) Messerschmidt A, Brugger PC, Boltshauser E, Zoder G, Sterniste W, Birnbacher R et al. Disruption of cerebellar development: potential complication of extreme prematurity. *AJNR Am J Neuroradiol* 2005; 26(7):1659-1667.
- (8) Limperopoulos C, Soul JS, Gauvreau K, Huppi PS, Warfield SK, Bassan H et al. Late gestation cerebellar growth is rapid and impeded by premature birth. *Pediatrics* 2005; 115(3):688-695.
- (9) Volpe JJ. Cerebellum of the premature infant: rapidly developing, vulnerable, clinically important. *J Child Neurol* 2009; 24(9):1085-1104.
- (10) Limperopoulos C, Bassan H, Gauvreau K, Robertson RL, Jr., Sullivan NR, Benson CB et al. Does cerebellar injury in premature infants contribute to the high prevalence of long-term cognitive, learning, and behavioral disability in survivors? *Pediatrics* 2007; 120(3):584-593.
- (11) Shah DK, Anderson PJ, Carlin JB, Pavlovic M, Howard K, Thompson DK et al. Reduction in cerebellar volumes in preterm infants: relationship to white matter injury and neurodevelopment at two years of age. *Pediatr Res* 2006; 60(1):97-102.
- (12) Allin M, Matsumoto H, Santhouse AM, Nosarti C, AlAsady MH, Stewart AL et al. Cognitive and motor function and the size of the cerebellum in adolescents born very pre-term. *Brain* 2001; 124(Pt 1):60-66.

- (13) Messerschmidt A, Fuiko R, Prayer D, Brugger PC, Boltshauser E, Zoder G et al. Disrupted cerebellar development in preterm infants is associated with impaired neurodevelopmental outcome. *Eur J Pediatr* 2008; 167(10):1141-1147.
- (14) Srinivasan L, Allsop J, Counsell SJ, Boardman JP, Edwards AD, Rutherford M. Smaller cerebellar volumes in very preterm infants at term-equivalent age are associated with the presence of supratentorial lesions. *AJNR Am J Neuroradiol* 2006; 27(3):573-579.
- (15) Dezortova M, Hajek M. (1)H MR spectroscopy in pediatrics. *Eur J Radiol* 2008; 67(2):240-249.
- (16) Roelants-van Rijn AM, van der GJ, de Vries LS, Groenendaal F. Value of (1)H-MRS using different echo times in neonates with cerebral hypoxia-ischemia. *Pediatr Res* 2001; 49(3):356-362.
- (17) Huppi PS, Posse S, Lazeyras F, Burri R, Bossi E, Herschkowitz N. Magnetic resonance in preterm and term newborns: 1H-spectroscopy in developing human brain. *Pediatr Res* 1991; 30(6):574-578.
- (18) Anbeek P, Vincken KL, Groenendaal F, Koeman A, van Osch MJ, van der Grond J. Probabilistic brain tissue segmentation in neonatal magnetic resonance imaging. *Pediatr Res* 2008; 63(2):158-163.
- (19) Bayley N. Bayley Scales of Infant and Toddler Development, Third edition. San Antonio, USA: Harcourt Assessment; 2006.
- (20) Papile LA, Burstein J, Burstein R, Koffler H. Incidence and evolution of subependymal and intraventricular hemorrhage: a study of infants with birth weights less than 1,500 gm. *J Pediatr* 1978; 92(4):529-534.
- (21) Benders MJ, Groenendaal F, van Bel F, Ha VR, Dubois J, Lazeyras F et al. Brain development of the preterm neonate after neonatal hydrocortisone treatment for chronic lung disease. *Pediatr Res* 2009; 66(5):555-559.
- (22) Brouwer A, Groenendaal F, van Haastert IL, Rademaker K, Hanlo P, de Vries L. Neurodevelopmental outcome of preterm infants with severe intraventricular hemorrhage and therapy for post-hemorrhagic ventricular dilatation. *J Pediatr* 2008; 152(5):648-654.
- (23) Limperopoulos C, Chilingaryan G, Guizard N, Robertson RL, du Plessis AJ. Cerebellar injury in the premature infant is associated with impaired growth of specific cerebral regions. *Pediatr Res* 2010; 68(2):145-150.
- (24) Parker J, Mitchell A, Kalpakidou A, Walshe M, Jung HY, Nosarti C et al. Cerebellar growth and behavioural & neuropsychological outcome in preterm adolescents. *Brain* 2008; 131(Pt 5):1344-1351.
- (25) Limperopoulos C, Robertson RL, Sullivan NR, Bassan H, du Plessis AJ. Cerebellar injury in term infants: clinical characteristics, magnetic resonance imaging findings, and outcome. *Pediatr Neurol* 2009; 41(1):1-8.
- (26) Bjartmar C, Battistuta J, Terada N, Dupree E, Trapp BD. N-acetylaspartate is an axon-specific marker of mature white matter in vivo: a biochemical and immunohistochemical study on the rat optic nerve. *Ann Neurol* 2002; 51(1):51-58.

- (27) Anderson PJ, De Luca CR, Hutchinson E, Roberts G, Doyle LW. Underestimation of developmental delay by the new Bayley-III Scale. *Arch Pediatr Adolesc Med* 2010; 164(4):352-356.
- (28) van Haastert IC, Groenendaal F, Uiterwaal CS, Termote JU, Heide-Jalving M, Eijssermans MJ et al. Decreasing Incidence and Severity of Cerebral Palsy in Prematurely Born Children. *J Pediatr* 2011.





# CHAPTER SIX

## Neonatal tract-based spatial statistics findings and outcome in preterm infants

Britt J.M. van Kooij, Linda S. de Vries, Gareth Ball, Ingrid C. van Haastert,  
Manon J.N.L. Benders, Floris Groenendaal, Serena J. Counsel

*American Journal of Neuroradiology, January 2011*

**ABSTRACT**

**Background** - White matter injury is associated with different disabilities that children born prematurely may experience during their life. The aim of this study was to use tract-based spatial statistics (TBSS) to test the hypothesis that white matter microstructure at term equivalent age in preterm infants is correlated with cognitive and motor outcome at two years corrected age.

**Methods** - 63 preterm infants, born at a mean gestational age of 28.7 weeks, underwent magnetic resonance imaging and diffusion tensor imaging (DTI) at term equivalent age. Neurodevelopmental performance was assessed using the Bayley Scales of Infant and Toddler Development-III. Voxelwise analysis of the DTI data was performed using TBSS to assess the relationship between fractional anisotropy (FA), axial and radial diffusivity at term equivalent age and cognitive, fine motor and gross motor scores at two years corrected age.

**Results** - Cognitive scores were correlated with FA values in the corpus callosum. Fine motor scores were correlated with FA and radial diffusivity throughout the white matter. Gross motor scores were associated with radial diffusivity in the corpus callosum, fornix and internal and external capsule.

**Conclusion** - White matter microstructure in preterm infants at term equivalent age was associated with cognitive, fine motor and gross motor performance at two years corrected age. This study suggests that TBSS of DTI data at term equivalent age has the potential to be used as a biomarker for subsequent neurodevelopment.

## INTRODUCTION

With improvements in neonatal care, the mortality rate of preterm infants is decreasing. However, they remain at risk for neurodevelopmental impairments in later childhood.<sup>1;2</sup> Magnetic resonance imaging (MRI) is increasingly performed to assess brain damage in preterm infants. With the reduction in major focal lesions such as cystic periventricular leukomalacia, diffuse white matter (WM) injury is now the most common abnormality observed on MRI.<sup>3</sup>

Diffusion tensor imaging (DTI) is an MRI technique that may be used to assess WM development and injury.<sup>4</sup> Image contrast in DTI is based on the Brownian motion of water molecules. In WM, water molecular motion is influenced by various factors e.g. axonal density and degree of myelination.<sup>5</sup> Water diffuses preferentially along WM fibers and is restricted across fiber bundles. Thus, the location and direction of cerebral WM tracts can be determined by assessing the preferential direction of water diffusion.<sup>6</sup> Objective measures, e.g. fractional anisotropy (FA), axial diffusion (AD, diffusion parallel to WM tracts,  $\lambda_1$ ) and radial diffusion (RD, diffusion perpendicular to WM tracts,  $(\lambda_2 + \lambda_3)/2$ ) can be derived from DTI and provide information regarding WM microstructure. DTI studies of the preterm brain have shown that FA increases with increasing age 7-10 which is mainly driven by a decrease in RD<sup>11;12</sup> and that FA is reduced and apparent diffusion coefficient values increased in WM injury.<sup>13;14</sup>

Tract-based spatial statistics (TBSS) is a recently developed, observer independent tool for analyzing DTI data.<sup>15</sup> Using TBSS, WM microstructural abnormalities have been identified in the absence of focal injury in the preterm brain at term equivalent age (TEA).<sup>16</sup> Additionally, Counsell et al. demonstrated a relationship between FA in specific WM tracts and neurodevelopment, assessed using the Griffiths Mental Developmental Scales, in children who were born preterm and studied at two years of age.<sup>17</sup>

The aim of the present study was to test the hypothesis that WM microstructure, assessed by TBSS, in preterm infants at TEA is associated with neurodevelopmental performance at two years corrected age.

## METHODS

### Patients

Neonates who were born below 31 weeks' gestation and reached TEA between January 2007 and July 2008 were recruited for a prospective preterm cohort study. Neonates with dysmorphic features or an infection of the central nervous system were excluded. Of the 174 consecutively admitted neonates, 22 died in the neonatal period, informed parental consent was not obtained for 14 neonates and 15 neonates were not examined in our 3.0 Tesla system. MRI of the brain was performed around TEA. Written informed parental consent was obtained for all neonates and this prospective study was approved by the Medical Ethical Committee of our institute.

## MRI

MR investigations were performed on a 3.0 Tesla MR system using an eight-channel phased array head coil. The infants were sedated with 50-60 mg/kg chloral hydrate orally, fifteen minutes prior to the MRI. Heart rate, transcutaneous oxygen saturation and respiratory rate were monitored during scanning. For hearing protection Minimuffs® were used. A neonatologist was present throughout the MRI examination.

The MRI protocol included sagittal T1-weighted (repetition time (TR)=886 ms; echo time (TE)=15 ms; slice thickness=3.0 mm; number of slices=31), axial 3D T1-weighted (TR=9.4 ms; TE=4.6 ms; slice thickness=2.0 mm; number of slices=50) and axial T2-weighted imaging (TR=6293 ms; TE=120 ms; slice thickness=2.0 mm; number of slices=50). WM injury was scored as reported previously.<sup>18</sup>

In 117/123 neonates, DTI was performed using a single-shot-EPI sequence with diffusion gradients in 32 non-collinear directions (TR=7745 ms; TE=48 ms; voxel size=1.41x1.41x2 mm; number of slices=50; field of view=180 mm; scan matrix=128; fold-over direction=AP; b-value=800 s/mm<sup>2</sup>). In six infants DTI was not performed due to time constraints. The quality of the DTI data and the derived FA maps were evaluated by two researchers. Data with artifacts arising from patient motion or technical errors in reconstruction was discarded, resulting in 66/117 (56.4%) neonates with DTI images that were considered to be eligible for further analysis.

## Neurodevelopmental assessment

At two years corrected age (mean  $24.1 \pm 0.3$  months), the children were assessed with the Bayley Scales of Infant and Toddler Development-III (BSITD-III) by a single developmental specialist who was blinded to the MRI findings.<sup>19</sup> Cognition and both fine and gross motor function were assessed. The language subtest was not assessed, due to the limited time children are able to concentrate during one session. Scaled scores of the three subtests and cognitive and total motor composite scores (i.e. an overall score for fine and gross motor function) were calculated corrected for prematurity (mean in a normative population:  $10 \pm 3$  and  $100 \pm 15$ , respectively). Three of the 66 children were lost to follow-up, consequently 63 neonates included in this study.

## Data analysis

DTI data were analyzed with the FMRIB's software library (FSL) version 4.1.4.<sup>20</sup> The diffusion-tensor images were registered to the b0 image to minimize image artifacts due to eddy current distortions. The skull was removed from the images with the brain extraction tool.<sup>21</sup> FA, AD and RD maps were calculated using the FMRIB's Diffusion Toolbox. All subjects' FA images were aligned to a target in a common space using an optimized TBSS protocol for neonates.<sup>22</sup> Two linear registration steps were performed prior to non-linear registration (6 degrees of freedom (DOF) and 12 DOF), in order to register every subject's FA map to each other. We selected the target with the minimum mean warp displacement score as our chosen target and then each infant's FA map was aligned in target space. Following alignment to the target an average FA map was created, that is the mean FA

map. A second set of registrations was then performed to register every individual FA map to the mean FA map. The aligned images were then used to create another mean FA map and a mean FA skeleton, which represented the centers of all tracts common to the group. This FA skeleton was thresholded at  $FA \geq 0.15$  to exclude peripheral tracts with high inter-subject variability and/or partial volumes effects with grey matter. Each subject's aligned FA, AD and RD data were projected onto this mean FA skeleton. Voxelwise cross subject statistics was performed in order to assess the relationship between FA, AD and RD and performance scores of the BSITD-III, corrected for GA and postmenstrual age at the time of the scan. The results were corrected for multiple comparisons by controlling family-wise error rate following threshold-free cluster enhancement (TFCE).<sup>23</sup>

In order to visualize the relationship between local tissue abnormalities and neurodevelopmental performance scores, regions of interest were generated from areas that demonstrated a significant correlation with FA. Scores for cognitive, fine motor and gross motor performance were plotted against FA, AD and RD values in these regions. (Figures 1-3) In all analyses a  $p$ -value  $< 0.05$  was considered to be statistically significant.

## RESULTS

Neonatal details are presented in Table 1. There were no differences in neonatal parameters between the infants included in this study and infants excluded due to the absence of DTI images (of adequate quality), although included infants tended to be older at birth (GA 28.7 and 28.1 weeks, respectively;  $p=0.054$ ).

### MRI findings

During the neonatal period, 17 infants were diagnosed to have an IVH on cranial ultrasound examination and 3/17 developed post-hemorrhagic ventricular dilatation requiring treatment. Based on the WM scoring system by Woodward *et al.*, 54 (85.7%) infants displayed normal or mildly abnormal WM and only 9 (14.3%) had moderately abnormal WM.<sup>18</sup> No infants had severe WM injury or cystic periventricular leukomalacia, although one neonate showed a small subcortical cyst frontally and one child had a cyst due to a hemorrhage in the temporal lobe.

### Neurodevelopmental outcome

Table 2 shows the results for the BSITD-III scores. Fine motor scores were significantly higher than gross motor scores ( $p < 0.001$ ). No infant developed cerebral palsy or had other major motor deficits. Girls tended to have better cognitive scores than boys ( $p=0.063$ , median score 11 and 10, respectively). TBSS did not reveal significant differences in FA between females and males.

**Table 1: Neonatal characteristics of the neonates included in this study**

	Total (n=63)
<b>Gestational age, mean ± SD in weeks (range)</b>	28.7 ± 1.7 (25.1-30.9)
<b>Birth weight, mean ± SD in grams (range)</b>	1146 ± 335 (650-1910)
<b>Male, no (%)</b>	36 (57.1)
<b>Birthset: Singleton / Twins, no (%)</b>	51 (81.0) / 12 (19.0)
<b>PPROM, no (%)</b>	13 (20.6)
<b>Antenatal steroids, no (%)</b>	47 (74.6)
<b>Race, no (%)</b>	
Caucasian	50 (79.4)
Other	12 (9.0)
Mixed	1 (1.6)
<b>Apgar at 5 min, median (range)</b>	9 (5-10)
<b>Late onset sepsis positive blood culture, no (%)</b>	23 (36.5)
<b>Days of ventilation, median (range)</b>	5 (0-23)
<b>IVH, no (%)</b>	
No IVH	46 (73.0)
IVH I	5 (7.9)
IVH II	7 (11.1)
IVH III	4 (6.3)
IVH IV	1 (1.6)
<b>Educational level mother, no (%)*</b>	
Low	14 (22.2)
Middle	21 (33.3)
High	26 (41.3)
<b>Postmenstrual age, mean ± SD in weeks (range)</b>	41.6 ± 1.0 (39.6-44.7)

*Abbreviations: SD, standard deviation; no, number; PPROM, preterm prolonged rupture of membranes; antenatal steroids, two doses of steroids administered 24 hours before labour; postmenstrual age, postmenstrual age at the time of the scan*

**Table 2: Cognitive and motor outcome on the BSITD-III at two years corrected age**

	Median	Range	Infants with score $\leq -1SD$
<b>Cognition:</b>			
- Scaled score corrected age	11	6-19	n = 5
- Composite score corrected age	105	80 - 145	n = 5
- Composite score chronological age	95	75 - 130	n= 13
<b>Fine motor:</b> Scaled score corrected age			
	13	7-19	n = 1
<b>Gross motor:</b> Scaled score corrected age			
	9	6-15	n = 6
<b>Total motor:</b>			
- Composite score corrected age	107	88 - 133	n = 0
- Composite score chronological age	97	82 - 121	n = 4

*Abbreviations: Scaled score: mean in a normative population 10 with standard deviation (SD) 3; Composite score: mean in a normative population 100 with SD 15*

*Corrected age, score corrected for prematurity; Chronological age, score uncorrected for prematurity*

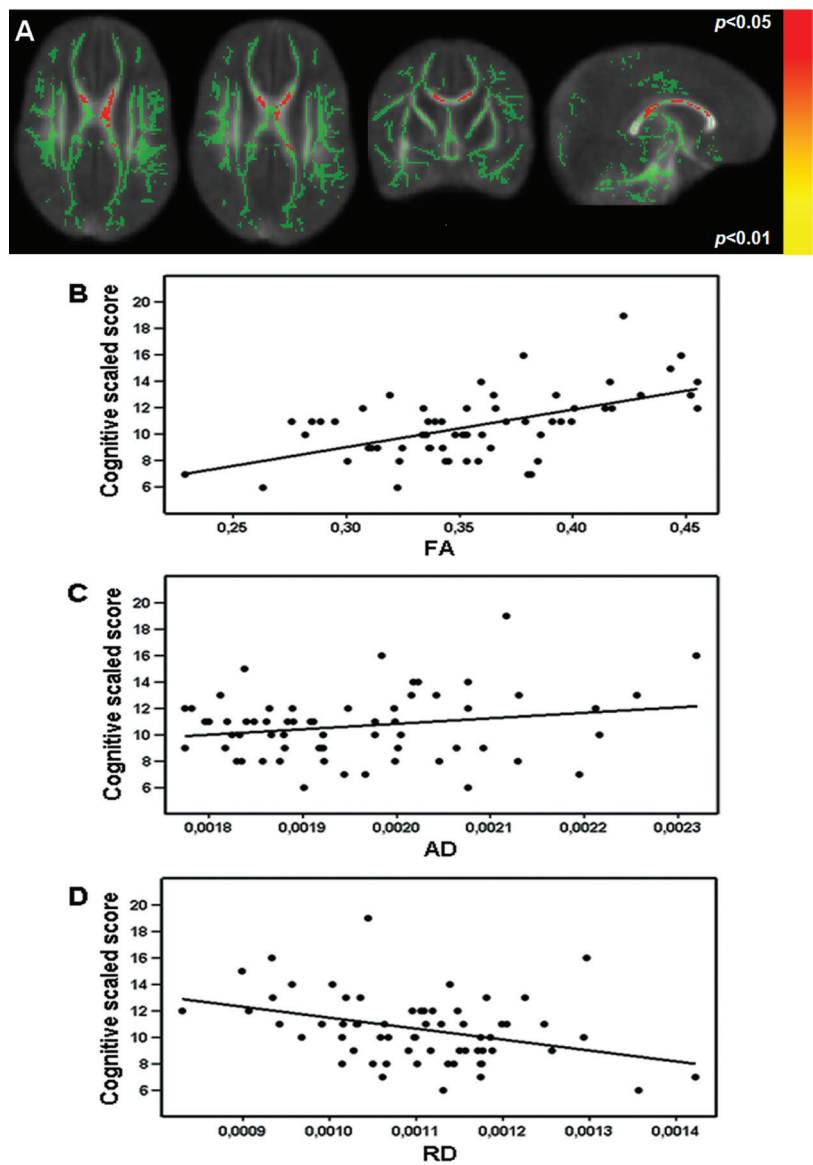
## White matter diffusion parameters and neurodevelopment

### Cognitive outcome

Following TFCE correction for multiple comparisons, TBSS showed a positive relationship between FA values in the body and splenium of the corpus callosum (CC) and the cognitive scores of the BSITD-III. (Figure 1A) The relationship between FA values in the fornix and cognitive outcome just failed to reach significance ( $p=0.051$ ). No voxels showed a negative correlation between FA and cognitive score. There was no relation between cognition and AD or RD.

Mean FA, AD and RD data were extracted from voxels in the CC showing a significant relationship between FA and cognitive scores. The data were plotted in a graph to visualize the relationship between cognitive scores and FA (Figure 1B:  $R^2=0.31$ ), AD (Figure 1C:  $R^2=0.04$ ) and RD (Figure 1D:  $R^2=0.13$ ).

**Figure 1: Diffusion parameters in relation to cognitive outcome**



Mean fractional anisotropy (FA) skeleton (green) overlaid on the mean FA map in axial, coronal and sagittal plane. Regions of the mean FA skeleton in green represent voxels where there was no correlation between FA and cognitive score. Voxels showing a significant correlation between FA and cognitive scores are shown in red-yellow (Figure 1A). The graphs demonstrate the relationship between FA ( $R^2 = 0.31$ , Figure 1B), axial diffusivity (AD;  $R^2 = 0.04$ , Figure 1C) and radial diffusivity (RD;  $R^2 = 0.13$ , Figure 1D) and cognitive scaled scores from voxels in the corpus callosum (170 voxels) which showed a significant correlation between FA and cognitive score.

### *Fine motor outcome*

FA was significantly correlated with fine motor scores throughout the WM with many regions significant at a threshold of  $p < 0.01$ . The significant regions included the whole CC, fornix, corona radiata, the external capsule, the corticospinal tract from the level of the posterior limb of the internal capsule (PLIC) to the cerebral peduncle, the superior longitudinal fasciculus, the inferior longitudinal and fronto-occipital fasciculus, cingulum and the uncinate fasciculus (all bilaterally, except for the uncinate fasciculus and the cingulum which were only significant right sided). (Figure 2A) No voxels showed a negative correlation between FA and fine motor score. There was a significant negative relationship between RD in the PLIC on the right and the corticospinal tract from the level of the PLIC to the cerebral peduncle on the left. There was no relationship between fine motor score and AD.

Mean FA, AD and RD data were extracted from voxels in the left PLIC that showed a significant relationship between FA and fine motor outcome. The data were plotted in a graph to visualize the relation between FA (Figure 2B:  $R^2 = 0.26$ ), AD (Figure 2C:  $R^2 = 0.04$ ) and RD (Figure 2D:  $R^2 = 0.28$ ) and fine motor score.

### *Gross motor outcome*

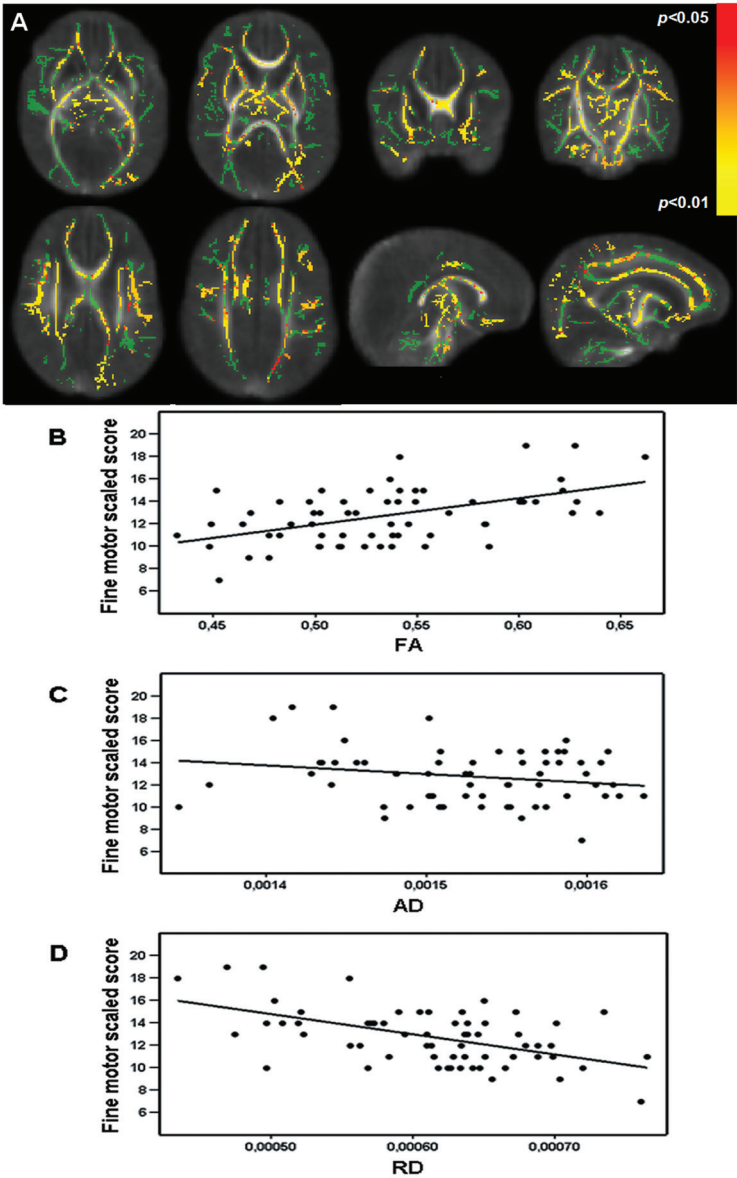
Gross motor function was significantly correlated with FA values in the fornix, the left PLIC and in the thalamus. No voxels showed a negative correlation between FA and gross motor score. RD displayed a significant negative relationship with gross motor scores more extensively throughout the WM, including the fornix, the CC (mainly left sided), the PLIC and the posterior part of the cingulum bilaterally. (Figure 3A) There was no relation between gross motor outcome and AD.

Mean FA, AD and RD data were extracted from voxels in the left PLIC showing a significant relationship between FA and gross motor scores. The data were plotted in a graph to visualize the relation between FA (Figure 3B:  $R^2 = 0.26$ ), AD (Figure 3C:  $R^2 = 0.02$ ) and RD (Figure 3D:  $R^2 = 0.22$ ) and gross motor score.

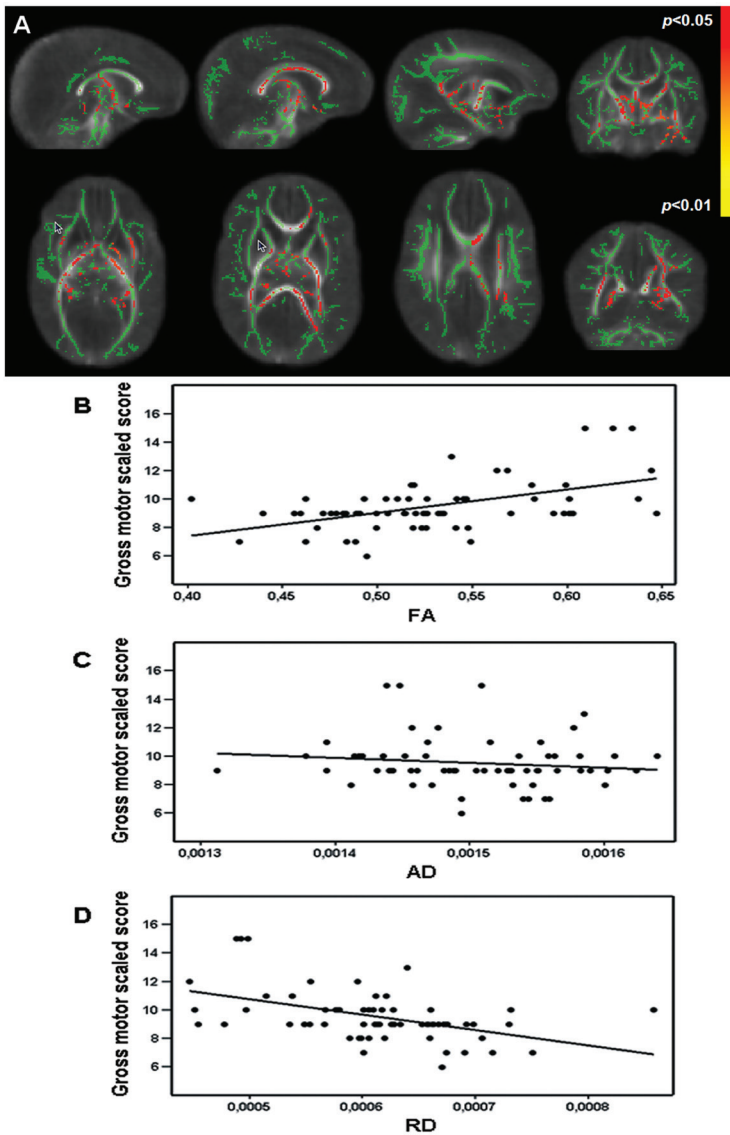
### *Total motor scores*

There was a significant correlation between total motor score and FA values throughout the WM and many WM regions were significant at a threshold of  $p < 0.01$ . The regions included the CC, fornix, corona radiata, the external capsule, the corticospinal tract from the level of the PLIC to the cerebral peduncle, the superior longitudinal fasciculus, the inferior longitudinal and fronto-occipital fasciculus, cingulum and the uncinate fasciculus bilaterally. No voxels showed a negative correlation between FA and total motor score. There was a significant negative relationship between total motor score and RD in the CC, fornix, left external capsule, left inferior longitudinal and fronto-occipital fasciculus, corticospinal tracts bilaterally and the left uncinate fasciculus. There was no relationship between total motor outcome and AD.

**Figure 2: Diffusion parameters in relation to fine motor scores**



Mean fractional anisotropy (FA) skeleton (green) overlaid on the mean FA map in axial, coronal and sagittal plane. Regions of the mean FA skeleton in green represent voxels where there was no correlation between FA and fine motor score. Voxels showing a significant correlation between FA and fine motor scores are shown in red-yellow. (Figure 2A) The graphs demonstrate the relationship between FA ( $R^2 = 0.26$ , Figure 2B), axial diffusivity (AD;  $R^2 = 0.04$ , Figure 2C) and radial diffusivity (RD;  $R^2 = 0.28$ , Figure 2D) and fine motor scaled scores from voxels in the left posterior limb of the internal capsule (45 voxels) which showed a significant correlation between FA and fine motor score.

**Figure 3: Diffusion parameters in relation to gross motor score**

Mean fractional anisotropy (FA) skeleton (green) overlaid on the mean FA map in axial, coronal and sagittal plane. Voxels showing a significant correlation between radial diffusivity (RD) and gross motor scores are shown in red-yellow (Figure 3A). The graphs demonstrate the relationship between FA ( $R^2 = 0.26$ , Figure 3B), axial diffusivity (AD;  $R^2 = 0.02$ , Figure 3C) and RD ( $R^2 = 0.22$ , Figure 3D) and gross motor scaled scores from voxels in the left posterior limb of the internal capsule (52 voxels) which showed a significant correlation between FA and gross motor score.

## DISCUSSION

In this study TBSS, optimized for the neonatal brain<sup>22</sup>, was used for the first time at TEA in preterm infants born below 31 weeks' gestation to assess the relationship between diffusion parameters and neurodevelopmental performance at two years of age. TBSS provides an objective and reproducible voxelwise survey of cerebral WM which reveals features that are consistent across a group of subjects and avoids subjective selection of locations of interest or hypothesis based selections of WM regions.<sup>15</sup> Using this approach, we have shown that higher FA in the CC at TEA was associated with better cognitive performance. In addition, a widespread association was demonstrated between FA in the major WM tracts and fine motor performance whilst gross motor scores were associated with FA values in the PLIC, fornix and thalamus. The findings for total motor scores were similar to those for fine motor scores suggesting that our results for the total motor scores were largely influenced by fine motor performance and not by gross motor abilities.

The increase in FA with respect to better BSITD-III scores observed here was mainly driven by a decrease in RD. The relationship between diffusion measures, e.g. FA and RD, and underlying WM microstructure is complex. The increase in FA observed with increasing maturation is largely due to a decrease in RD.<sup>11;12</sup> FA is largely dependent on axonal thickness, axonal density and myelination.<sup>24;25</sup> The development of oligodendroglia precursors induce anisotropy in WM in a process primarily driven by changes in RD.<sup>26</sup> At TEA only the PLIC and the brain stem are myelinated<sup>27</sup> and so the reduction in FA in association with subsequent poor neurodevelopment demonstrated here probably represents deficits or delays in pre-myelination events such as increasing axonal thickness, alterations in axonal permeability and pre-myelination wrapping of the oligodendrocyte around the axon.<sup>28</sup>

We recognize that cognitive deficits are difficult to diagnose in early childhood and usually first become evident during school age.<sup>2</sup> Nevertheless, our findings of FA in the anterior limb of the internal capsule, the PLIC, and the genu and splenium of the CC. They observed a relationship between FA in the PLIC at TEA and psychomotor score of the BSID-II at 18 months corrected age.<sup>32</sup> Using TBSS to survey whole brain WM, we have shown this relationship exists more extensively throughout the WM. It is of interest that the regions where we observed a positive correlation between fine motor score and FA values were more extensive than those for gross motor score. In addition to the PLIC and the corticospinal tracts, a correlation with FA was found in the association tracts including the cingulum, fornix, uncinate fasciculus and in the frontal WM. The frontal lobes are involved in working memory, planning, monitoring and organizing retrieval processes.<sup>33</sup> The uncinate fasciculus provides a corticocortical link between the frontal and temporal lobes and is thought to be important in episodic memory.<sup>34</sup> The cingulum is involved with high order motor control and organization of motor control processes.<sup>35</sup> Lesions in this region are associated with deficits in working memory performance<sup>36</sup> and reduced FA in the cingulum in schizophrenia is associated with attention and working memory deficits.<sup>37</sup> The fornix connects the hippocampus to the hypothalamus, and lesions in this structure are associated with memory and learning dysfunction.<sup>38;39</sup> These regions, therefore,

are associated with working memory and manipulating information, processes that are assessed in the fine motor component of the BSITD-III. In this study we observed that better gross motor function was related to a region of higher FA in the left PLIC, while decreased RD was correlated with gross motor outcome in many regions throughout the brain. On examination of those voxels in the left PLIC showing a significant relationship between FA and gross motor scores, we observed a strong positive correlation between AD and RD. These findings may explain the lack of association between FA and gross motor scores, as an increase in both AD and RD could leave FA relatively unchanged.

Previous studies have used voxel based approaches to assess the relationship between WM microstructure and performance in children who were born preterm. Skranes *et al.* assessed adolescents born prematurely and age-matched term born controls. They revealed lower FA in the internal and external capsule, CC and the inferior and superior longitudinal fasciculus in the preterm group. Importantly, lower FA in these areas was related to worse performance on the visual motor integration and the Grooved Pegboard test.<sup>40</sup> At two years of age, sub-scores of the Griffiths Mental Developmental Scales were related to FA in the CC, cingulum, fornix, anterior commissure and the right uncinate fasciculus.<sup>17</sup> Our results suggest that the relationship between WM integrity and neurodevelopment, demonstrated by others in children born prematurely, are already evident at TEA.

We were able to analyze only 56% of the DTI data. DTI data are inherently sensitive to artifacts due to patient motion. Although the infants were sedated and noise reduction was administered, some infants woke up during the DTI sequence. In addition, some data were acquired with a SENSE factor of 3, which resulted in lower signal to noise ratio and a visible artifact across the brain and so these data sets were rejected. Nevertheless, our study group was relatively large, consisting of 63 infants with data amenable to analysis using TBSS. This study used DTI data acquired at 3 Tesla, which offers higher signal-to-noise ratio and allows improved spatial resolution than could be achieved at lower field strengths. However, at the resolution achievable in vivo, the imaging voxels will inevitably contain fibre populations with different orientations, resulting in a reduction in the measured FA. A further limitation of this approach is that TBSS is not always able to assess WM where there is an abrupt change in direction of the fiber pathway, for example at the junction of tracts.<sup>15</sup> Finally, these findings were restricted to preterm infants, without the possibility to compare the results with healthy full-term controls. We accept that the lack of healthy term born controls is a limitation of this study. However, previous studies have already shown differences between preterm infants at term and healthy term born controls.<sup>9;16</sup> Our aim here was to explore the relationship between WM injury and early neurodevelopmental performance in the preterm population.

To conclude, an increase in FA and a decrease in RD in specific WM regions in preterm infants at TEA were related to cognitive, fine motor and gross motor outcome at two years corrected age. These findings support the potential of diffusion parameters, obtained in preterm infants at TEA, as biomarkers for subsequent neurodevelopmental performance.

**Acknowledgements**

The authors are grateful to the families who took part in the study and to our colleagues of the Neonatal intensive care unit and the MR technicians for their expertise and enthusiastic help.

**Funding**

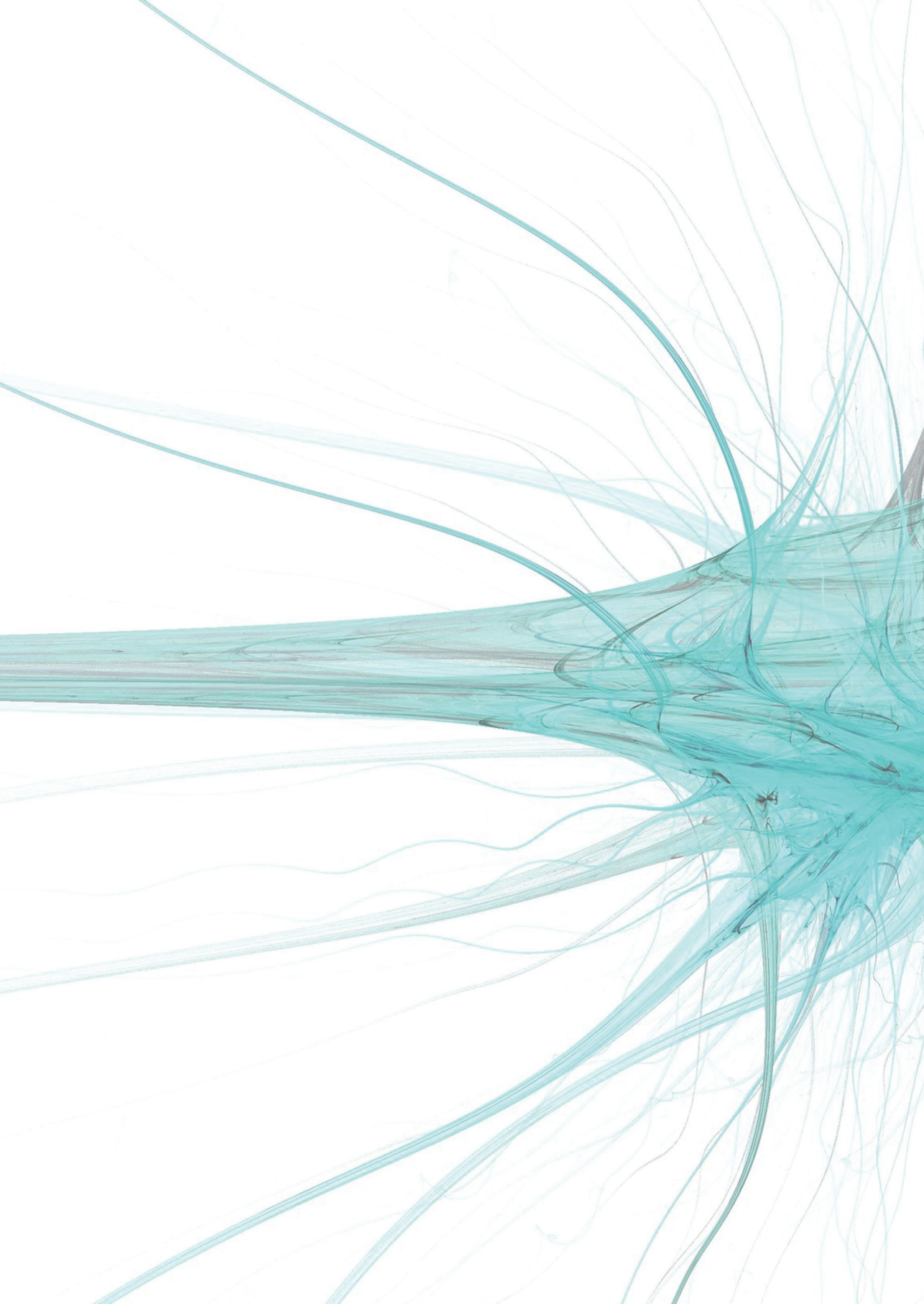
This work was supported by the Young Investigator Exchange Program Fellowship of the International Pediatric Research Foundation and The Netherlands Organisation for Health Research and Development [project 94527022].

## Reference List

- (1) Saigal S, Doyle LW. An overview of mortality and sequelae of preterm birth from infancy to adulthood. *Lancet* 2008; 371(9608):261-269.
- (2) Latal B. Prediction of neurodevelopmental outcome after preterm birth. *Pediatr Neurol* 2009; 40(6):413-419.
- (3) Volpe JJ. Cerebral white matter injury of the premature infant-more common than you think. *Pediatrics* 2003; 112(1 Pt 1):176-180.
- (4) Huppi PS, Dubois J. Diffusion tensor imaging of brain development. *Semin Fetal Neonatal Med* 2006; 11(6):489-497.
- (5) Le Bihan D, Breton E, Lallemand D, Grenier P, Cabanis E, Laval-Jeantet M. MR imaging of intravoxel incoherent motions: application to diffusion and perfusion in neurologic disorders. *Radiology* 1986; 161(2):401-407.
- (6) Moseley ME, Cohen Y, Kucharczyk J, Mintorovitch J, Asgari HS, Wendland MF et al. Diffusion-weighted MR imaging of anisotropic water diffusion in cat central nervous system. *Radiology* 1990; 176(2):439-445.
- (7) Dubois J, Dehaene-Lambertz G, Perrin M, Mangin JF, Cointepas Y, Duchesnay E et al. Asynchrony of the early maturation of white matter bundles in healthy infants: quantitative landmarks revealed noninvasively by diffusion tensor imaging. *Hum Brain Mapp* 2008; 29(1):14-27.
- (8) Miller SP, Vigneron DB, Henry RG, Bohland MA, Ceppi-Cozzio C, Hoffman C et al. Serial quantitative diffusion tensor MRI of the premature brain: development in newborns with and without injury. *J Magn Reson Imaging* 2002; 16(6):621-632.
- (9) Huppi PS, Maier SE, Peled S, Zientara GP, Barnes PD, Jolesz FA et al. Microstructural development of human newborn cerebral white matter assessed in vivo by diffusion tensor magnetic resonance imaging. *Pediatr Res* 1998; 44(4):584-590.
- (10) Neil JJ, Shiran SI, McKinstry RC, Schefft GL, Snyder AZ, Almlil CR et al. Normal brain in human newborns: apparent diffusion coefficient and diffusion anisotropy measured by using diffusion tensor MR imaging. *Radiology* 1998; 209(1):57-66.
- (11) Partridge SC, Mukherjee P, Henry RG, Miller SP, Berman JL, Jin H et al. Diffusion tensor imaging: serial quantitation of white matter tract maturity in premature newborns. *Neuroimage* 2004; 22(3):1302-1314.
- (12) Suzuki Y, Matsuzawa H, Kwee IL, Nakada T. Absolute eigenvalue diffusion tensor analysis for human brain maturation. *NMR Biomed* 2003; 16(5):257-260.
- (13) Cheong JL, Thompson DK, Wang HX, Hunt RW, Anderson PJ, Inder TE et al. Abnormal White Matter Signal on MR Imaging Is Related to Abnormal Tissue Microstructure. *AJNR Am J Neuroradiol* 2009.
- (14) Counsell SJ, Shen Y, Boardman JP, Larkman DJ, Kapellou O, Ward P et al. Axial and radial diffusivity in preterm infants who have diffuse white matter changes on magnetic resonance imaging at term-equivalent age. *Pediatrics* 2006; 117(2):376-386.

- (15) Smith SM, Jenkinson M, Johansen-Berg H, Rueckert D, Nichols TE, Mackay CE et al. Tract-based spatial statistics: voxelwise analysis of multi-subject diffusion data. *Neuroimage* 2006; 31(4):1487-1505.
- (16) Anjari M, Srinivasan L, Allsop JM, Hajnal JV, Rutherford MA, Edwards AD et al. Diffusion tensor imaging with tract-based spatial statistics reveals local white matter abnormalities in preterm infants. *Neuroimage* 2007; 35(3):1021-1027.
- (17) Counsell SJ, Edwards AD, Chew AT, Anjari M, Dyet LE, Srinivasan L et al. Specific relations between neurodevelopmental abilities and white matter microstructure in children born preterm. *Brain* 2008; 131(Pt 12):3201-3208.
- (18) Woodward LJ, Anderson PJ, Austin NC, Howard K, Inder TE. Neonatal MRI to predict neurodevelopmental outcomes in preterm infants. *N Engl J Med* 2006; 355(7):685-694.
- (19) Bayley N. Bayley Scales of Infant and Toddler Development, Third edition. San Antonio, USA: Harcourt Assessment; 2006.
- (20) Smith SM, Jenkinson M, Woolrich MW, Beckmann CF, Behrens TE, Johansen-Berg H et al. Advances in functional and structural MR image analysis and implementation as FSL. *Neuroimage* 2004; 23 Suppl 1:S208-S219.
- (21) Smith SM. Fast robust automated brain extraction. *Hum Brain Mapp* 2002; 17(3):143-155.
- (22) Ball G, Counsell SJ, Anjari M, Merchant N, Arichi T, Doria V et al. An optimised tract-based spatial statistics protocol for neonates: Applications to prematurity and chronic lung disease. *Neuroimage* 2010.
- (23) Smith SM, Nichols TE. Threshold-free cluster enhancement: addressing problems of smoothing, threshold dependence and localisation in cluster inference. *Neuroimage* 2009; 44(1):83-98.
- (24) Sakuma H, Nomura Y, Takeda K, Tagami T, Nakagawa T, Tamagawa Y et al. Adult and neonatal human brain: diffusional anisotropy and myelination with diffusion-weighted MR imaging. *Radiology* 1991; 180(1):229-233.
- (25) Takagi T, Nakamura M, Yamada M, Hikishima K, Momoshima S, Fujiyoshi K et al. Visualization of peripheral nerve degeneration and regeneration: monitoring with diffusion tensor tractography. *Neuroimage* 2009; 44(3):884-892.
- (26) Drobyshevsky A, Song SK, Gamkrelidze G, Wyrwicz AM, Derrick M, Meng F et al. Developmental changes in diffusion anisotropy coincide with immature oligodendrocyte progression and maturation of compound action potential. *J Neurosci* 2005; 25(25):5988-5997.
- (27) Yakovlev PI, Lecours AR. The myelogenic cycles of regional maturation of the brain. In: Minkowski A, editor. *Regional Development of the Brain in Early Life*. Oxford: Blackwell Scientific Publications; 1967. 3-70.
- (28) Wimberger DM, Roberts TP, Barkovich AJ, Prayer LM, Moseley ME, Kucharczyk J. Identification of "premyelination" by diffusion-weighted MRI. *J Comput Assist Tomogr* 1995; 19(1):28-33.

- (29) Caldu X, Narberhaus A, Junque C, Gimenez M, Vendrell P, Bargallo N et al. Corpus callosum size and neuropsychologic impairment in adolescents who were born preterm. *J Child Neurol* 2006; 21(5):406-410.
- (30) Peterson BS, Vohr B, Staib LH, Cannistraci CJ, Dolberg A, Schneider KC et al. Regional brain volume abnormalities and long-term cognitive outcome in preterm infants. *JAMA* 2000; 284(15):1939-1947.
- (31) Schmithorst VJ, Wilke M, Dardzinski BJ, Holland SK. Cognitive functions correlate with white matter architecture in a normal pediatric population: a diffusion tensor MRI study. *Hum Brain Mapp* 2005; 26(2):139-147.
- (32) Rose J, Butler EE, Lamont LE, Barnes PD, Atlas SW, Stevenson DK. Neonatal brain structure on MRI and diffusion tensor imaging, sex, and neurodevelopment in very-low-birthweight preterm children. *Dev Med Child Neurol* 2009; 51(7):526-535.
- (33) Kopelman MD. Disorders of memory. *Brain* 2002; 125(Pt 10):2152-2190.
- (34) Klinger J, Gloor P. The connections of the amygdala and of the anterior temporal cortex in the human brain. *J Comp Neurol* 1960; 115:333-369.
- (35) Aralasmak A, Ulmer JL, Kocak M, Salvan CV, Hillis AE, Yousem DM. Association, commissural, and projection pathways and their functional deficit reported in literature. *J Comput Assist Tomogr* 2006; 30(5):695-715.
- (36) Petrides M, Milner B. Deficits on subject-ordered tasks after frontal- and temporal-lobe lesions in man. *Neuropsychologia* 1982; 20(3):249-262.
- (37) Kubicki M, Westin CF, Nestor PG, Wible CG, Frumin M, Maier SE et al. Cingulate fasciculus integrity disruption in schizophrenia: a magnetic resonance diffusion tensor imaging study. *Biol Psychiatry* 2003; 54(11):1171-1180.
- (38) Park SA, Hahn JH, Kim JI, Na DL, Huh K. Memory deficits after bilateral anterior fornix infarction. *Neurology* 2000; 54(6):1379-1382.
- (39) Aggleton JP, McMackin D, Carpenter K, Hornak J, Kapur N, Halpin S et al. Differential cognitive effects of colloid cysts in the third ventricle that spare or compromise the fornix. *Brain* 2000; 123 ( Pt 4):800-815.
- (40) Skranes J, Vangberg TR, Kulseng S, Indredavik MS, Evensen KA, Martinussen M et al. Clinical findings and white matter abnormalities seen on diffusion tensor imaging in adolescents with very low birth weight. *Brain* 2007; 130(Pt 3):654-666.





## CHAPTER SEVEN

### Fiber tracking at term displays gender differences regarding cognitive and motor outcome at two years of age in preterm infants

Britt J.M. van Kooij, Carola van Pul, Manon J.N.L. Benders, Ingrid C. van Haastert,  
Linda S. de Vries, Floris Groenendaal

*Pediatric Research. 2011 Aug 18.*

**ABSTRACT**

**Background** - White matter microstructural changes can be detected with Diffusion Tensor Imaging. It was hypothesized that diffusion parameters in the posterior limb of the internal capsule (PLIC) and corpus callosum (CC) bundles in preterm infants at term equivalent age (TEA) were associated with neurodevelopment at two years corrected age.

**Methods** - In 67 preterm infants, fiber tracking was performed at TEA for the CC and both PLIC bundles. Volume, length, fractional anisotropy (FA), mean diffusivity, axial diffusivity and radial diffusivity were determined for the three bundles. These parameters were assessed in relation to outcome on the Bayley Scales of Infant and Toddler Development-III.

**Results** - In girls, volume and length of the CC bundle and right PLIC bundle volume were associated with cognition. In boys, volume, FA, mean and radial diffusivity and length of the left PLIC were associated with fine motor scores. Correction for gestational age, birth weight, intraventricular haemorrhage, white matter injury and maternal education did not change the results.

**Conclusion** - Fiber tracking parameters in the PLIC and CC bundles in preterm infants at TEA revealed different associations with neurodevelopment between boys and girls. This study suggested that fiber tracking is a useful method to predict neurodevelopment in preterm infants.

## INTRODUCTION

Preterm infants are susceptible to brain injury, mainly intraventricular haemorrhages (IVH) and white matter (WM) injury.<sup>1</sup> Abnormal magnetic resonance imaging (MRI) findings have been shown to be related to impaired neurodevelopment in preterm infants.<sup>2;3</sup> Conventional MRI is commonly performed to assess WM injury. However, outcome has been noted to be abnormal in the absence of abnormalities on conventional MRI.<sup>4</sup> Therefore, more objective analysis of (subtle) brain injury may be needed with more advanced methods to understand the underlying pathology and subsequent neurodevelopment in children born prematurely.

Diffusion tensor imaging (DTI) can be used to assess brain connectivity.<sup>5</sup> DTI describes the diffusion of water molecules in tissues and is assumed to reflect the direction of the underlying microstructure.<sup>6;7</sup> With fiber tracking it is possible to reconstruct and visualize the underlying linear structure defined by the diffusion tensor.<sup>7</sup> WM maturation is accompanied by an increase in fractional anisotropy (FA) and a decrease in apparent diffusion coefficient (ADC).<sup>8</sup> In preterm infants, lower FA and higher ADC values in WM have been described before abnormalities were seen on conventional MRI.<sup>9</sup> In addition, the expected increase in FA and decrease in ADC values failed to appear in infants with WM injury.<sup>10</sup>

It has been hypothesized that boys and girls show variations in brain development and men should have more numerous, smaller neuronal units, however they display less neuronal processes compared to females.<sup>11</sup> Additionally, gender differences in diffusion parameters have been described previously.<sup>12;13</sup> Information regarding the relation between diffusion parameters around term equivalent age (TEA) in preterm infants and neurodevelopment is scarce. Lower FA values in the posterior limb of the internal capsule (PLIC) assessed between birth and TEA in preterm infants were related to an impaired neuromotor development at 18 to 24 months.<sup>14-16</sup> ADC values in the WM illustrated a negative relation with the Griffiths' developmental quotient at two years.<sup>17</sup> In most studies diffusion parameters were assessed in manually drawn regions of interest (ROIs) and only few studies examined entire WM bundles.<sup>18-20</sup>

It was investigated whether fiber tracking parameters, i.e. diffusion parameters and volume and length of WM bundles passing through the PLIC and the corpus callosum (CC), in preterm infants at TEA were causally associated with neurodevelopment at two years corrected age, which was assessed with the Bayley Scales of Infant and Toddler Development, Third Edition (BSITD-III).

## METHODS

Newborns admitted to our level three NICU, with a gestation below 31 weeks' and who reached TEA between January 2007 and July 2008 were recruited for a prospective preterm cohort study performed in the Wilhelmina Children's Hospital in Utrecht, the Netherlands. Neonates with either dysmorphic features or an infection of their central nervous system were excluded. Of the 175 consecutively admitted neonates, 22 died in the neonatal period, no parental consent was obtained for 14 neonates and 15 neonates

were examined on a 1.5 Tesla system. MRI of the brain was acquired around TEA. Written informed parental consent was obtained for all included infants. This study was approved by the Medical Ethics Committee of the University Medical Center Utrecht.

### **Cranial ultrasound and MRI**

Cerebral ultrasound was performed daily in the first week after birth and then once a week until discharged. They were evaluated by two independent researchers, who were unaware of the MRI findings and neurodevelopment. Periventricular leukomalacia (PVL) and the presence of an IVH were scored according to De Vries *et al.*<sup>21</sup>

MRIs were performed on a 3.0 Tesla MR system (Achieva, Philips Medical Systems, Best, The Netherlands) using a eight-channel Sense head coil. The infants were sedated with 50-60 mg/kg oral chloralhydrate. Heart rate, transcutaneous oxygen saturation and respiratory rate were monitored during scanning. For hearing protection Minimuffs® (Natus Medical Incorporated, San Carlos, CA) were used. A neonatologist was present throughout the examination.

The protocol contained conventional sagittal T1-weighted imaging (repetition time (TR)=886 ms; echo time (TE)=15 ms; slice thickness=3.0 mm), axial 3D T1-weighted imaging (TR=9.4 ms; TE=4.6 ms; slice thickness=2.0 mm) and axial T2-weighted imaging (TR=6293 ms; TE=120 ms; slice thickness=2.0 mm). DTI was performed using a single-shot-EPI sequence with diffusion gradients in 32 directions (TR=7745 ms; TE=48 ms; voxel size=1.41x1.41x2 mm; number of slices=50; FOV=180 mm RL; scan matrix=128; fold-over direction=AP; b-value=0 and 800 s/mm<sup>2</sup>).

MRIs were evaluated independently by two neonatologists with a special interest in neuro-imaging, blinded to the results of the neurodevelopmental assessment. In case of disagreement, a third reader was consulted to achieve consensus. WM injury was scored as published previously (adjusted from Woodward *et al.*<sup>22</sup>). The WM score varies between 5 (normal) and 15 (severely abnormal) and was applied in the analysis as an indicator for WM injury.

### **DTI**

In 118/124 (95.2%) neonates DTI was performed at TEA. In the other six infants DTI could not be performed due to time constraints. The quality of the DTI and the result of the tractography were assessed independently by two researchers and when needed, consensus was reached using the opinion of a third researcher. DTI data were analysed using an in-home developed fiber tracking program.<sup>23</sup> Twenty-one datasets were excluded because of large artefacts in the FA colourmaps, suggestive of motion, and three datasets because of sense artefacts. In the remaining 94 neonates, tractography was performed. The tracts through the left and right PLIC (denoted as 'PLIC bundle') and the CC (denoted as 'CC bundle') were identified primarily by the colour-coded FA map. The PLIC and the CC bundles were chosen a priori since those structures are two of the most developed regions in the newborn brain and known to be affected by premature birth.<sup>24;25</sup> For both PLIC bundles, one ROI was placed on an axial slice at the level of the foramen of Monro

and the second on the adjacent slice above this landmark. For the CC bundle, two ROIs were placed on sagittal slices around the midplane of the CC. All fibers passing through both ROIs were traced. Fiber tracking was based on a line propagation technique, starting in every voxel in the brain and stopping for the 'case linear' anisotropy index ( $CI < 0.12$  ( $CI = (\lambda_1 - \lambda_2) / (\lambda_1 + \lambda_2 + \lambda_3)$ ) and maximum angle  $\alpha > 10^\circ$ ). Tracts were excluded from the analysis when it was visually estimated that more than 10% of the volume was artificially traced, e.g. due to corrupted data caused by motion. In 69/94 (73.4%) neonates both PLIC and CC bundles were traced correctly and eligible for assessment. For these traced bundles, different fiber tracking parameters were extracted, i.e. mean FA, mean diffusivity (MD, in  $10^{-3} \text{ mm}^2/\text{s}$ ), axial diffusivity (AD,  $\lambda_1$ ; in  $10^{-3} \text{ mm}^2/\text{s}$ ), radial diffusivity (RD,  $(\lambda_2 + \lambda_3)/2$ ; in  $10^{-3} \text{ mm}^2/\text{s}$ ) and volume (in  $\text{mm}^3$ ) and length (in mm) of the fiber bundles.<sup>25</sup> The volume of the bundle was defined as the volume of all voxels through which one or more fibers passed and the average length of the bundle as the average length of all fibers included in the bundle.

### Neurodevelopmental outcome

At two years' corrected age (mean  $24.2 \pm 0.6$  months), all children were assessed with the BSITD-III by a single developmental specialist who was blinded to the MRI findings.<sup>26</sup> Only the cognitive and fine and gross motor subtests were used, and not the language subtest due to the limited time the child was able to concentrate during one session. Both scaled scores of the three subtests as well as the cognitive and total motor composite scores were calculated corrected for prematurity (mean in a normative population:  $10 \pm 3$  and  $100 \pm 15$ , respectively).

### Data analysis and statistics

SPSS version 15 was used for the analysis. Linear regression was used to assess the relation between the fiber tracking parameters and neurodevelopmental outcome. Gestational age (GA), birth weight (BW) Z-score, WM score, IVH and maternal education were considered to be possible confounders. In the multivariable linear regression analyses, it was assessed whether the associations between the fiber tracking parameters and neurodevelopment remained statistical significant after correction for the neonatal and maternal confounders. Analyses were performed for the total study population and additionally for boys and girls separately. In the analysis, DTI parameters were corrected for postmenstrual age at time of the scan. A  $p$ -value  $< 0.05$  was considered statistically significant.

**Table 1: neonatal characteristics of the neonates included in this study**

	Total (n=67)	Boys (n=38)	Girls (n=29)
<b>Gestational age, mean ± SD (weeks)</b>	28.6 ± 1.8	28.6 ± 1.9	28.5 ± 1.7
<b>Birth weight, mean ± SD (gram)</b>	1130 ± 349	1180 ± 368	1066 ± 316
<b>Birthset: Singleton / Twins, no (%)</b>	51 (76.1) / 16 (23.9)	32 (84.2) / 6 (15.8)	19 (65.5) / 10 (34.5)
<b>PPROM, no (%)</b>	15 (22.4)	6 (15.8)	9 (32.1)
<b>Antenatal steroids, no (%)</b>	54 (80.6)	28 (73.7)	26 (89.7)
<b>Race, no (%)</b>			
Caucasian	50 (74.6)	31 (81.6)	19 (65.5)
Other	13 (19.4)	6 (15.8)	7 (24.1)
Mixed	4 (6.0)	1 (2.6)	3 (10.3)
<b>Apgar 5 min, median (range)</b>	9 (5-10)	8 (6-10)	9 (5-10)‡
<b>Sepsis, no (%)</b>	27 (40.3)	12 (31.6)	16 (51.7)
<b>Ventilation, median (range)</b>	4.5 (0-40)	5.5 (0-40)	1.5 (0-23)‡
<b>IVH, no (%)</b>			
No IVH	49 (73.1)	28 (73.7)	21 (72.4)
IVH I	6 (9.0)	3 (7.9)	3 (10.3)
IVH II	7 (10.4)	4 (10.5)	3 (10.3)
IVH III	3 (4.5)	1 (2.6)	2 (6.9)
IVH IV	2 (3.0)	2 (5.2)	0 (0)
<b>Maternal education, no (%)*</b>			
Low	16 (23.9)	11 (28.9)	5 (17.2)
Middle	22 (32.8)	12 (31.5)	(34.5)
High	27 (40.3)	13 (34.2)	14 (48.3)
<b>PMA, mean ± SD (weeks)</b>	41.5 ± 1.1	41.7 ± 1.1	41.3 ± 1.1

Abbreviations: no, number; PPROM, preterm prolonged rupture of membranes; antenatal steroids, two doses of steroids administered 24 hours before labour; sepsis, late onset sepsis positive blood culture; Ventilation, Days of ventilation; PMA, postmenstrual age at the time of the scan; \*Maternal education of two infants are missing; ‡ significant difference between boys and girls ( $p<0.05$ )

## RESULTS

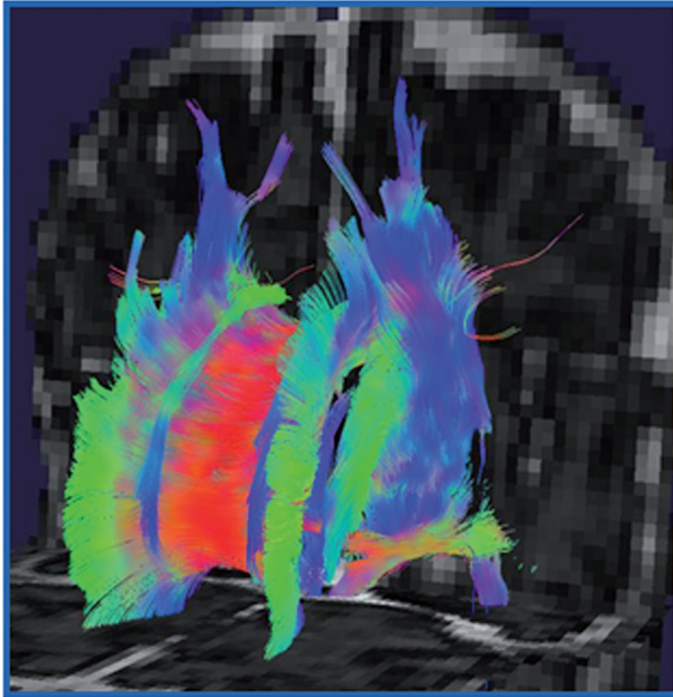
Of the 69 infants with evaluable fiber tracts in both PLIC and CC bundles, two infants were lost to follow-up at the corrected age of two years. Consequently, 67/69 infants were evaluated in this study (Table 1). There were no differences in neonatal parameters between boys and girls and between the children included in this study and children who were excluded because 3.0 Tesla DTI data was not eligible for evaluation. However, the excluded children were scanned at a slightly older age than the children in this study (41.9 weeks and 41.5 weeks, respectively).

**Table 2: DTI parameters in total population and differences between boys and girls**

	Total	Boys	Girls	p-value
<b>Number of infants</b>	67	38	29	
<b>CC volume, cm<sup>3</sup></b>	7349.69 ± 2247.49	7747.17 ± 2426.52	6828.87 ± 1905.38	0.098
<b>CC FA</b>	0.375 ± 0.017	0.377 ± 0.015	0.374 ± 0.020	0.518
<b>CC MD, 10<sup>-3</sup> mm<sup>2</sup>/s</b>	1.487 ± 0.081	1.471 ± 0.076	1.509 ± 0.083	0.054
<b>CC AD, 10<sup>-3</sup> mm<sup>2</sup>/s</b>	2.115 ± 0.102	2.094 ± 0.098	2.143 ± 0.103	0.051
<b>CC RD, 10<sup>-3</sup> mm<sup>2</sup>/s</b>	1.174 ± 0.073	1.159 ± 0.068	1.192 ± 0.077	0.069
<b>CC length, mm</b>	29.71 ± 5.59	31.15 ± 5.78	27.81 ± 4.79	0.014
<b>PLIC L volume, cm<sup>3</sup></b>	4484.58 ± 855.19	4680.52 ± 866.92	4227.83 ± 781.28	0.031
<b>PLIC L FA</b>	0.414 ± 0.025	0.417 ± 0.023	0.410 ± 0.029	0.292
<b>PLIC L MD, 10<sup>-3</sup> mm<sup>2</sup>/s</b>	1.087 ± 0.064	1.080 ± 0.056	1.095 ± 0.074	0.333
<b>PLIC L AD, 10<sup>-3</sup> mm<sup>2</sup>/s</b>	1.600 ± 0.073	1.594 ± 0.063	1.609 ± 0.086	0.482
<b>PLIC L RD, 10<sup>-3</sup> mm<sup>2</sup>/s</b>	0.830 ± 0.061	0.823 ± 0.054	0.840 ± 0.070	0.272
<b>PLIC L length, mm</b>	34.09 ± 4.10	34.94 ± 4.00	32.98 ± 4.04	0.052
<b>PLIC R volume, cm<sup>3</sup></b>	4680.42 ± 948.63	4802.40 ± 932.57	4520.58 ± 961.94	0.231
<b>PLIC R FA</b>	0.408 ± 0.023	0.409 ± 0.020	0.406 ± 0.027	0.701
<b>PLIC R MD, 10<sup>-3</sup> mm<sup>2</sup>/s</b>	1.087 ± 0.066	1.078 ± 0.055	1.100 ± 0.077	0.162
<b>PLIC R AD, 10<sup>-3</sup> mm<sup>2</sup>/s</b>	1.591 ± 0.077	1.579 ± 0.064	1.607 ± 0.090	0.135
<b>PLIC R RD, 10<sup>-3</sup> mm<sup>2</sup>/s</b>	0.836 ± 0.062	0.827 ± 0.052	0.847 ± 0.072	0.189
<b>PLIC R length, mm</b>	33.24 ± 4.15	33.88 ± 4.23	32.40 ± 3.96	0.151

Values presented are the mean ± SD

Abbreviations: PLIC L, left posterior limb of the internal capsule; PLIC R, right posterior limb of the internal capsule; p-value, represents the significance for the difference in fiber tracking parameters between boys and girls

**Figure 1: Example of fiber tracking in the neonatal brain at TEA**

View from front left. Fiber tracking was performed using stopping criteria  $CI < 0.12$  and  $\alpha > 10^\circ$ , starting in every voxel in the brain, displaying only fibers longer than 20mm. The 3D fiber tracking image is superimposed on a 2D ADC map.

Color coding: red are fibers from left to right (e.g. cc), blue from cranial to caudal (corticospinal tract) and green from anterior to posterior.

### **Cranial ultrasound and conventional MRI findings**

During the neonatal period, 35/67 (52.2%) neonates had PVL grade I on sequential cranial ultrasound examinations; however cystic evolution was not seen in any of the infants. Eighteen infants were diagnosed to have a germinal matrix haemorrhage-IVH (Table 1). Three neonates developed post-hemorrhagic ventricular dilatation requiring intervention. The median WM score based on the MRI was 8 (range: 5 (normal) to 12 (moderately abnormal)).

### **Fiber tracking parameters**

Figure 1 shows a representative example of fiber tracking in the whole neonatal brain. The results of the fiber tracking parameters are illustrated in Table 2.

In boys, the average length was longer and the volume was larger for the CC bundle and left PLIC bundle compared to girls. However, only the differences in CC bundle length and PLIC bundle volume were statistically significant ( $p=0.014$  and  $p=0.031$ , respectively).

**Table 3: Cognitive and motor outcome on the BSITD-III at two years corrected age**

		Median (range)		Infants with score $\leq -1SD$	
		Boys	Girls	Boys	Girls
<b>Cognition:</b>					
-	SS CA	10 (4-15)	11(6 – 19)	n = 5	n = 1
-	CS CA	100 (70-125)	105 (80 – 145)	n = 5	n = 1
-	CS ChronA	95 (70-115)	95 (75 – 130)	n= 11	n= 5
<b>Fine motor:</b> SS CA					
		12 (7-19)	13 (7 – 18)	n = 1	n = 1
<b>Gross motor:</b> SS CA					
		9 (6-15)	9 (7 – 13)	n = 3	n = 1
<b>Total motor:</b>					
-	CS CA	103 (88-133)	107 (85 – 133)	n = 0	n = 1
-	CS ChronA	95.5 (79-121)	100 (76 – 121)	n = 4	n = 2

Abbreviations: SS, scaled score: mean in a normative population 10 with standard deviation (SD) 3; CS, composite score: mean in a normative population 100 with SD 15; CA, corrected age, score corrected for prematurity; ChronA, chronological age, score uncorrected for prematurity

### Neurodevelopmental outcome

Table 3 shows the results for the cognitive, fine motor, gross motor and total motor scores on the BSITD-III. The infants scored significantly better on the fine motor subtests than on the gross motor subtests ( $p < 0.001$ ). There were no children who developed cerebral palsy or had other major motor deficits at two years corrected age. ANOVA showed a main effect of maternal education on cognitive scores. Subsequent post-hoc analyses showed that both infants of a mother with a low education or with middle education scored significantly poorer than infants of a mother who attended high education ( $p = 0.019$  and  $p = 0.023$ , respectively). Girls demonstrated better cognitive scores than boys ( $p = 0.045$ ).

### Fiber tracking parameters and neurodevelopment

Assessing the total study cohort, no relations could be demonstrated between the fiber tracking parameters at term and neurodevelopment after correction for GA, BW Z-score, WM score, IVH and maternal education. However, boys and girls showed different associations between the diffusion parameters and neurodevelopment after correction for the neonatal variables and maternal education, as detailed below (Table 4 and Figure 2).

#### Corpus callosum bundle

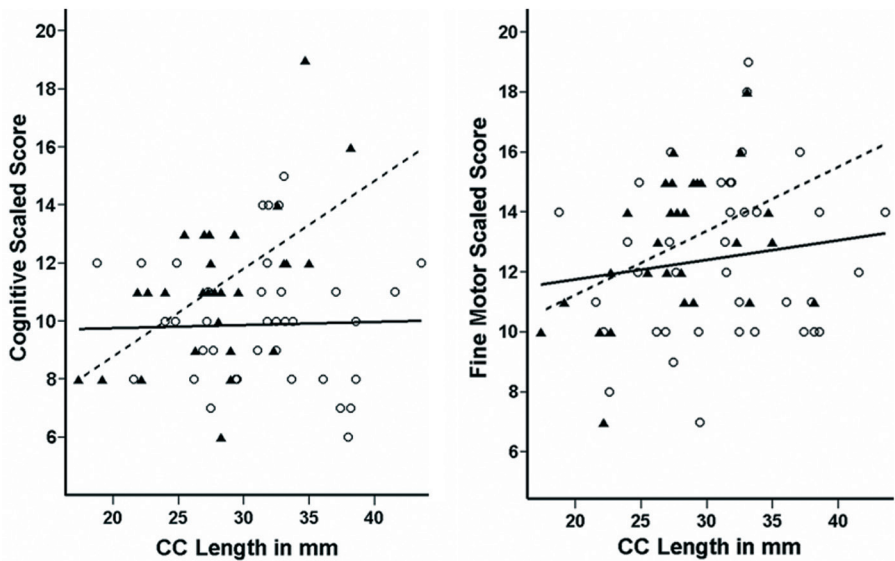
Better cognitive and fine motor scores were seen in girls with larger CC bundle volume or bundle length at TEA (cognition:  $p < 0.01$ ; fine motor score:  $p < 0.05$ ). In boys, an association was found between the MD, AD and RD of the CC bundle and gross motor

Table 4: DTI parameters in relation to BSITD-III scores

DTI parameter	Univariate			Multivariate*		
	$\beta$	95% CI	P	$\beta$	95% CI	p
Girls: cognition**						
CC volume/PMA	0.03	0.01 – 0.05	0.006	0.03	-0.00 – 0.05	0.056
CC length/PMA	12.62	4.33 – 20.90	0.004	14.13	4.70 – 23.56	0.005
PLIC R volume/PMA	0.05	0.00 – 0.09	0.052	0.10	0.05 – 0.15	<0.001
Boys: fine motor†						
PLIC L volume/PMA	0.06	0.02 – 0.10	0.007	0.05	-0.00 – 0.10	0.055
PLIC L FA/PMA*100	26.38	8.55 – 44.21	0.005	21.11	-0.31 – 42.52	0.053
PLIC L length/PMA	15.81	6.71 – 24.90	0.001	13.13	3.08 – 23.17	0.012

Abbreviations:  $\beta$ , regression coefficient; PMA, postmenstrual age; PLIC R, right PLIC  
\*Adjusted for GA, BW Z-score, WM injury score, maternal education and the presence of an IVH  
\*\* DTI parameters in girls in relation to cognitive scores  
† DTI parameters in boys in relation to fine motor scores

Figure 2: Corpus callosum length in relation to cognition and fine motor scores



Relation between length of the CC in mm and BSITD-III cognitive or fine motor scaled scores in both boys (displayed by 'O', uninterrupted regression line '—') and girls (displayed by '▲', interrupted regression line '- - -') at the corrected age of 24 months.  
Mean scaled score (standard deviation) in normative population: 10 (3)

performance ( $p \leq 0.05$ ). After correction for GA, BW Z-score, WM score, IVH and maternal education, only the associations in girls between cognition and CC bundle volume and length remained statistically significant (Table 4). No other relations could be demonstrated between fiber tracking parameters in the CC bundle and cognition, fine motor and gross motor scores.

#### *Left PLIC bundle*

Fiber tracking parameters in the left PLIC bundle were related to neurodevelopmental outcome only in boys. Better fine motor outcome was demonstrated in boys with a larger bundle volume, FA and bundle length and lower MD, AD and RD of the left PLIC bundle ( $p < 0.01$ ). Gross motor performance was associated with MD, AD, RD and length of the left PLIC bundle ( $p \leq 0.05$ ). After correction for GA, BW Z-score, WM score, IVH and maternal education, only associations between fine motor scores and fiber tracking parameters in the left PLIC bundle were demonstrated, showing a more significant relation with volume, FA and bundle length than with diffusivity (volume, FA and length:  $p \leq 0.055$ ; MD, AD and RD  $p = 0.07-0.14$ ) (Table 4). No other relations could be demonstrated between fiber tracking parameters in the left PLIC bundle and cognition, fine motor and gross motor scores.

#### *Right PLIC bundle*

In girls, a positive association was found between right PLIC bundle volume and cognition ( $p = 0.052$ ) and a negative relation between the length of the right PLIC bundle and gross motor outcome ( $p = 0.019$ ). In boys a negative association was seen between the MD and RD of the right PLIC and fine motor outcome ( $p \leq 0.05$ ). However, only the association between right PLIC bundle volume and cognition in girls remained statistical significant after correction for GA, BW Z-score, WM score, IVH and maternal education ( $p < 0.001$ ) (Table 4). No other relations could be demonstrated between fiber tracking parameters in the right PLIC bundle and cognition, fine motor and gross motor scores.

## **DISCUSSION**

In this study, fiber tracking parameters in the CC bundle and both PLIC bundles at TEA were assessed in relation to neurodevelopment at two years' corrected age in preterm infants born before 31 weeks' gestation. It appeared that both size of the bundles (i.e. length and volume) and their microstructural differences were related with outcome at two years' corrected age. In girls, DTI parameters in the CC bundle demonstrated more associations with both cognition and motor outcome compared to parameters in both PLIC bundles. Nevertheless in boys, most relations were seen between DTI parameters in the left PLIC bundle and motor outcome.

To the best of our knowledge, this was the first study assessing fiber tracking parameters in the CC and PLIC bundles in preterm infants at TEA in relation to neurodevelopmental outcome. Fiber tracking in newborns is a major challenge because the signal to noise ratio is relatively small due to the smaller voxel size needed as a consequence of the smaller anatomic structures. Moreover, the higher water content

and the lower degree of myelination result in lower FA values compared to adults.<sup>1;27</sup> Nevertheless, we were able to implement this technique in a large sample of preterm infants at TEA. For girls, we observed higher CC bundle volume and bundle length at TEA in relation to better cognitive outcome at two years' corrected age, which is in agreement with the literature. Only in female adults born prematurely, larger callosal size was demonstrated to be associated with better cognitive performance.<sup>28</sup> Additionally, Kontis *et al.* displayed that only in females higher MD in the genu of the CC was associated with lower performance IQ in prematurely born young adults.<sup>29</sup> It has been hypothesized that the greater interhemispheric connectivity in females facilitates cognitive performance while the processing is more bilateral. In contrast, males show a greater lateralisation of cognitive functioning and therefore the interhemispheric connectivity may not affect their cognitive capacities.<sup>28</sup>

In the present study, fiber tracking parameters in the PLIC bundles were associated with motor outcome. These findings are in agreement with previous studies using DTI. Reduced FA values in the PLIC have been displayed in preterm infants at TEA compared to term born controls and lower FA values assessed between childhood and (pre)adolescence were related to abnormal neuromotor outcome.<sup>14-16;30;31</sup> In general, it is expected that a more mature brain, resulting in higher FA and CI values due to more advanced myelination, is related to a better performance. With this fiber tracking method, higher CI gives rise to longer length of the fiber bundles, since the anisotropy index  $CI < 0.12$  was a stopping criteria.

Boys demonstrated a larger volume and length of the CC and left PLIC bundle compared to girls, although only the differences in CC bundle length and left PLIC bundle volume were statistically significant. In preterm infants, larger gray and WM volumes at TEA were exhibited in preterm males compared to preterm females.<sup>32;33</sup> Larger brain volumes seen in men could (partly) explain that we found larger volumes and length of the CC and PLIC in boys in the present study.

In this study, boys and girls displayed different associations between DTI parameters in the CC and PLIC bundles and neurodevelopment. It has been hypothesized that boys and girls demonstrate variations in brain development. Vasileiadis *et al.* revealed that girls had a larger cortical folding area compared to boys with similar brain volumes. They declared that the more 'compact' female brain provided evidence for an early sexually dimorphic brain development.<sup>32</sup> The gender differences in brain morphogenesis considering the tension-based theory,<sup>34</sup> could follow underlying microstructural variations, detected e.g. as tissue anisotropy. Variations in diffusion parameters reflect WM maturation, which depends on fiber organisation, density, diameter and myelination.<sup>5</sup> Schmithorst *et al.* presented developmental differences in WM microstructure in healthy term born boys and girls at a mean age of 12 years. They hypothesized that a more constrained brain volume in females could be related to a lower fiber density. Therefore girls may have a greater dependence on brain connectivity with more crossing fibers, resulting in lower FA and higher ADC values.<sup>12</sup>

Several studies support the hypothesis that sexual dimorphism in brain development could be related to differences in neurodevelopment. In healthy adults, women demonstrated a relation between intelligence and both WM and callosal volume, whereas cognition in males was more related to gray matter volume.<sup>28;35</sup> In preterm infants, sex differences in cerebral gray and WM were displayed at eight years of age, however only prematurely born girls demonstrated a positive correlation between gray matter/total brain volume ratio and cognitive measurements.<sup>36</sup> Male gender has been shown to be a relevant risk factor for an adverse neurodevelopmental outcome.<sup>37</sup> This may be aggravated by a more serious neonatal course. Also in the present study, boys appeared to be more ill than girls, showing significantly lower Apgar scores and a longer ventilation period. The male-female differences in the associations between neuroanatomical variables, i.e. fiber tracking parameters, and neurodevelopmental outcome found in the present study may be related to differences in brain development and subsequent outcome between prematurely born boys and girls. Our results may indicate that the sexual dimorphism in WM maturation is already detectable in newborns, which supports the suggestion it is important to take gender into account in DTI developmental studies.<sup>12</sup>

This study is subject to several limitations. Fiber tracking in the neonatal brain is difficult due to the low degree of myelination and the high water content compared to the adult brain. Using fiber tracking, we were only able to assess the most mature WM structures. A remark has to be made regarding the limited DTI data amenable for this study. We were able to analyze only the DTI data of 59% of the infants in our study cohort. DTI is inherently sensitive to artefacts due to small patient movements. Although the infants were sedated and noise reduction was administered, it could not be prevented that some infants woke up during the DTI sequence, which was at the end of our 30-minute scanning protocol. Nevertheless, in our relatively large study cohort, consisting of 67 preterm infants, we were able to display different associations for boys and girls between fiber tracking parameters at TEA and neurodevelopmental outcome at two years corrected age. In this study, we used fiber tracking parameters as 'readout' for the neonatal period. Further research will be needed to determine the role of different potential risk factors for changes in the WM microstructure. Next, the BSITD-III reveals information concerning general cognitive, fine and gross motor skills. More specific evaluation of tasks which are processed by the CC and PLIC bundles, could have shown additional details to predict neurodevelopment in preterm infants. Finally, our results are limited to preterm infants due to the lack of a term born control group.

In conclusion, fiber tracking parameters at TEA in the CC and PLIC bundles were associated with neurodevelopmental outcome at two years' corrected age. In female preterm infants, the CC bundle was the most important WM structure showing an association with cognitive, fine motor and gross motor performance. In boys, fiber tracking parameters in the left PLIC bundle were related to fine and gross motor function.

**Acknowledgments**

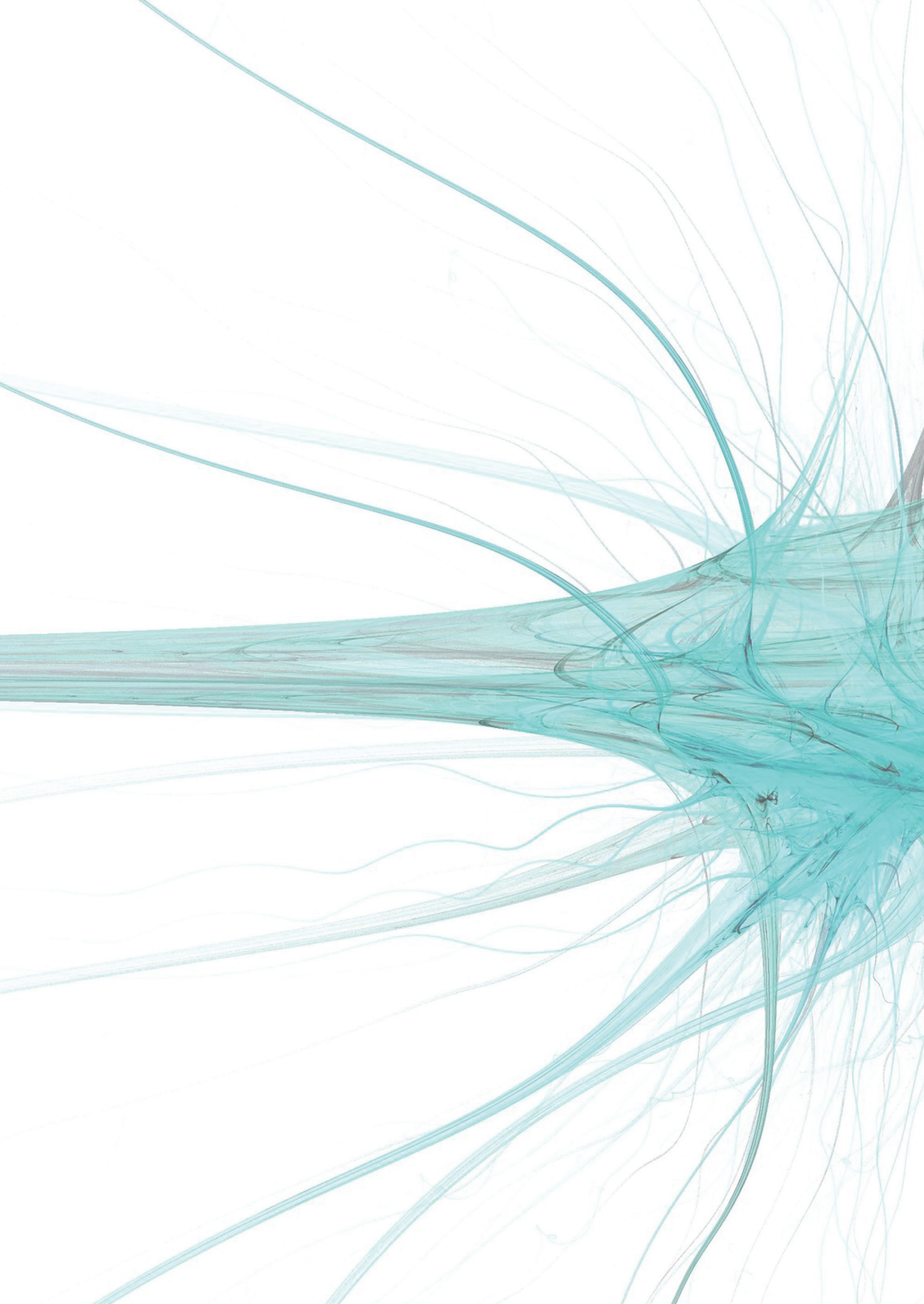
The authors thank Dr. Cuno S.P.M. Uiterwaal for his support in the statistical analysis, the families who took part in the study, Niels Blanken and the other MR technicians of the MR institute for their expert and enthusiastic help and our colleagues of the NICU and Medium care of the Wilhelmina Children's Hospital in Utrecht, The Netherlands.

## Reference List

- (1) Volpe JJ. Neurology of the newborn. 5th ed. Philadelphia: Saunders; 2008.
- (2) Dyet LE, Kennea N, Counsell SJ, Maalouf EF, Ajayi-Obe M, Duggan PJ et al. Natural history of brain lesions in extremely preterm infants studied with serial magnetic resonance imaging from birth and neurodevelopmental assessment. *Pediatrics* 2006; 118(2):536-548.
- (3) Spittle AJ, Boyd RN, Inder TE, Doyle LW. Predicting motor development in very preterm infants at 12 months' corrected age: the role of qualitative magnetic resonance imaging and general movements assessments. *Pediatrics* 2009; 123(2):512-517.
- (4) Mirmiran M, Barnes PD, Keller K, Constantinou JC, Fleisher BE, Hintz SR et al. Neonatal brain magnetic resonance imaging before discharge is better than serial cranial ultrasound in predicting cerebral palsy in very low birth weight preterm infants. *Pediatrics* 2004; 114(4):992-998.
- (5) Huppi PS, Dubois J. Diffusion tensor imaging of brain development. *Semin Fetal Neonatal Med* 2006; 11(6):489-497.
- (6) Basser PJ, Mattiello J, LeBihan D. MR diffusion tensor spectroscopy and imaging. *Biophys J* 1994; 66(1):259-267.
- (7) Mori S, van Zijl PC. Fiber tracking: principles and strategies - a technical review. *NMR Biomed* 2002; 15(7-8):468-480.
- (8) Ment LR, Hirtz D, Huppi PS. Imaging biomarkers of outcome in the developing preterm brain. *Lancet Neurol* 2009; 8(11):1042-1055.
- (9) Mathur AM, Neil JJ, Inder TE. Understanding brain injury and neurodevelopmental disabilities in the preterm infant: the evolving role of advanced magnetic resonance imaging. *Semin Perinatol* 2010; 34(1):57-66.
- (10) Miller SP, Vigneron DB, Henry RG, Bohland MA, Ceppi-Cozzio C, Hoffman C et al. Serial quantitative diffusion tensor MRI of the premature brain: development in newborns with and without injury. *J Magn Reson Imaging* 2002; 16(6):621-632.
- (11) Rabinowicz T, Petetot JM, Gartside PS, Sheyn D, Sheyn T, de CM. Structure of the cerebral cortex in men and women. *J Neuropathol Exp Neurol* 2002; 61(1):46-57.
- (12) Schmithorst VJ, Holland SK, Dardzinski BJ. Developmental differences in white matter architecture between boys and girls. *Hum Brain Mapp* 2008; 29(6):696-710.
- (13) Wilde EA, McCauley SR, Chu Z, Hunter JV, Bigler ED, Yallampalli R et al. Diffusion tensor imaging of hemispheric asymmetries in the developing brain. *J Clin Exp Neuropsychol* 2009; 31(2):205-218.
- (14) Arzoumanian Y, Mirmiran M, Barnes PD, Woolley K, Ariagno RL, Moseley ME et al. Diffusion tensor brain imaging findings at term-equivalent age may predict neurologic abnormalities in low birth weight preterm infants. *AJNR Am J Neuroradiol* 2003; 24(8):1646-1653.

- (15) Drobyshevsky A, Bregman J, Storey P, Meyer J, Prasad PV, Derrick M et al. Serial diffusion tensor imaging detects white matter changes that correlate with motor outcome in premature infants. *Dev Neurosci* 2007; 29(4-5):289-301.
- (16) Rose J, Butler EE, Lamont LE, Barnes PD, Atlas SW, Stevenson DK. Neonatal brain structure on MRI and diffusion tensor imaging, sex, and neurodevelopment in very-low-birthweight preterm children. *Dev Med Child Neurol* 2009; 51(7):526-535.
- (17) Krishnan ML, Dyet LE, Boardman JP, Kapellou O, Allsop JM, Cowan F et al. Relationship between white matter apparent diffusion coefficients in preterm infants at term-equivalent age and developmental outcome at 2 years. *Pediatrics* 2007; 120(3):e604-e609.
- (18) Yoo SS, Park HJ, Soul JS, Mamata H, Park H, Westin CF et al. In vivo visualization of white matter fiber tracts of preterm- and term-infant brains with diffusion tensor magnetic resonance imaging. *Invest Radiol* 2005; 40(2):110-115.
- (19) Zhai G, Lin W, Wilber KP, Gerig G, Gilmore JH. Comparisons of regional white matter diffusion in healthy neonates and adults performed with a 3.0-T head-only MR imaging unit. *Radiology* 2003; 229(3):673-681.
- (20) Berman JI, Mukherjee P, Partridge SC, Miller SP, Ferriero DM, Barkovich AJ et al. Quantitative diffusion tensor MRI fiber tractography of sensorimotor white matter development in premature infants. *Neuroimage* 2005; 27(4):862-871.
- (21) de Vries LS, van Haastert IC, Rademaker KJ, Koopman C, Groenendaal F. Ultrasound abnormalities preceding cerebral palsy in high-risk preterm infants. *J Pediatr* 2004; 144(6):815-820.
- (22) Woodward LJ, Anderson PJ, Austin NC, Howard K, Inder TE. Neonatal MRI to predict neurodevelopmental outcomes in preterm infants. *N Engl J Med* 2006; 355(7):685-694.
- (23) Vilanova A, Berenschot G, van Pul C. Visualization with streamsurfaces and evenly-spaced volume seeding. *Eurographics/IEEE TCVG VisSym* 2004;173-182.
- (24) Gilmore JH, Lin W, Corouge I, Vetsa YS, Smith JK, Kang C et al. Early postnatal development of corpus callosum and corticospinal white matter assessed with quantitative tractography. *AJNR Am J Neuroradiol* 2007; 28(9):1789-1795.
- (25) van Pul C, Buijs J, Vilanova A, Roos FG, Wijn PF. Infants with perinatal hypoxic ischemia: feasibility of fiber tracking at birth and 3 months. *Radiology* 2006; 240(1):203-214.
- (26) Bayley N. Bayley Scales of Infant and Toddler Development, Third edition. San Antonio, USA: Harcourt Assessment; 2006.
- (27) Huppi PS, Warfield S, Kikinis R, Barnes PD, Zientara GP, Jolesz FA et al. Quantitative magnetic resonance imaging of brain development in premature and mature newborns. *Ann Neurol* 1998; 43(2):224-235.
- (28) Davatzikos C, Resnick SM. Sex differences in anatomic measures of interhemispheric connectivity: correlations with cognition in women but not men. *Cereb Cortex* 1998; 8(7):635-640.

- (29) Kontis D, Catani M, Cuddy M, Walshe M, Nosarti C, Jones D et al. Diffusion tensor MRI of the corpus callosum and cognitive function in adults born preterm. *Neuroreport* 2009; 20(4):424-428.
- (30) Nagy Z, Westerberg H, Skare S, Andersson JL, Lilja A, Flodmark O et al. Preterm children have disturbances of white matter at 11 years of age as shown by diffusion tensor imaging. *Pediatr Res* 2003; 54(5):672-679.
- (31) Skranes J, Vangberg TR, Kulseng S, Indredavik MS, Evensen KA, Martinussen M et al. Clinical findings and white matter abnormalities seen on diffusion tensor imaging in adolescents with very low birth weight. *Brain* 2007; 130(Pt 3):654-666.
- (32) Vasileiadis GT, Thompson RT, Han VK, Gelman N. Females follow a more "compact" early human brain development model than males. A case-control study of preterm neonates. *Pediatr Res* 2009; 66(5):551-555.
- (33) Gilmore JH, Lin W, Prastawa MW, Looney CB, Vetsa YS, Knickmeyer RC et al. Regional gray matter growth, sexual dimorphism, and cerebral asymmetry in the neonatal brain. *J Neurosci* 2007; 27(6):1255-1260.
- (34) Van Essen DC. A tension-based theory of morphogenesis and compact wiring in the central nervous system. *Nature* 1997; 385(6614):313-318.
- (35) Haier RJ, Jung RE, Yeo RA, Head K, Alkire MT. The neuroanatomy of general intelligence: sex matters. *Neuroimage* 2005; 25(1):320-327.
- (36) Reiss AL, Kesler SR, Vohr B, Duncan CC, Katz KH, Pajot S et al. Sex differences in cerebral volumes of 8-year-olds born preterm. *J Pediatr* 2004; 145(2):242-249.
- (37) Wood NS, Costeloe K, Gibson AT, Hennessy EM, Marlow N, Wilkinson AR. The EPICure study: associations and antecedents of neurological and developmental disability at 30 months of age following extremely preterm birth. *Arch Dis Child Fetal Neonatal Ed* 2005; 90(2):F134-F140.





## CHAPTER EIGHT

### Anatomy of the circle of Willis and blood flow in the brain-feeding vasculature in prematurely born Infants

B.J.M. van Kooij, J. Hendrikse, M.J.N.L. Benders, L.S. de Vries, F. Groenendaal

*Neonatology. 2010;97:235-41*

**ABSTRACT**

**Background** - Previous studies have shown a disrupted development of cerebral blood vessels at term-equivalent age in prematurely born infants.

**Objective** - To assess the anatomy of the circle of Willis in preterm neonates (gestational age 25–31 weeks) at term-equivalent age and to evaluate the relation between anatomic variations and blood flow through the internal carotid arteries (ICAs) and basilar artery (BA).

**Methods** - In 72 preterm neonates, flow measurements (ml/min) were obtained with 2-D phase-contrast magnetic resonance angiography (MRA) at term-equivalent age. Time-of-flight MRA was used to assess the circle of Willis for a dominant A1 segment of the anterior cerebral artery or a fetaltype posterior cerebral artery. Differences in flow were assessed with ANOVA.

**Results** - In our cohort, 53/72 (74%) neonates showed a variant type of the circle of Willis. The flow in the ICA at the side of a dominant A1 segment (43.3ml/min) was significantly increased compared to the flow in the contralateral ICA (33.0 ml/min;  $p = 0.009$ ) and tended to be higher than in the ICA in children with a normal anterior anatomy (38.4 ml/min;  $p = 0.1$ ). The flow in the BA was highest in neonates with a normal configuration of the posterior part of the circle of Willis (32.6 ml/min) compared to children with a unilateral (25.3 ml/min;  $p = 0.002$ ) or bilateral fetaltype posterior cerebral artery (18.6 ml/min;  $p < 0.001$ ).

**Conclusion** - Preterm neonates show a high prevalence of variant types of the circle of Willis at term-equivalent age. A relation could be demonstrated between variations in the circle of Willis and the flow in the ICA and BA.

## INTRODUCTION

Recently, it has been reported that prematurely born neonates show a decreased tortuosity in all proximal segments of the cerebral vasculature at term-equivalent age compared to full-term infants, indicating that preterm delivery alters the development of the cerebral blood vessels.<sup>1</sup> For normal brain function and development, an adequate blood flow to the brain is required and alterations in cerebral blood flow (CBF) play an important role in the pathogenesis of brain injury in neonates.<sup>2,3</sup> The blood flow from the vasculature in the neck, through the circle of Willis towards the major intracranial brain feeding arteries is crucial to perfuse the brain tissue. Hendrikse *et al.*<sup>4</sup> showed in adults that the anatomical configuration of the circle of Willis was closely related to blood flow in the brain-feeding arteries. In embryos, the internal carotid arteries (ICAs) are formed between 28–30 days, and the basilar artery (BA) is formed between 31–36 days, when the longitudinal neural arteries combine.<sup>5–7</sup> A completely formed circle of Willis appears in the 52-day embryo and all segments are slender and have an identical caliber.<sup>8,9</sup> In the remaining fetal period, important changes occur in the basic anatomy of the cerebral vasculature. One of the most obvious ones is the change from a dominant fetal-type feeding of the posterior cerebral arteries (PCAs) from the ICA via the posterior communicating artery (PCoA) towards a normal adult configuration with feeding of the PCAs from the vertebrobasilar system via the precommunicating part of the PCA (P1). The PCoAs normally regress in caliber as the vertebrobasilar system develops.<sup>6</sup> As pointed out by Van Overbeeke *et al.*<sup>10</sup>, this process will be either complete, resulting in a normal adult-type circle of Willis, or incomplete with a persisting fetal-type feeding of the PCA. Also on the anterior aspect of the circle of Willis, the anatomical development will result in several variations.<sup>11</sup> In an anatomically normal circle of Willis, the ICA provides blood to the ipsilateral anterior cerebral artery (ACA) and to the middle cerebral artery (MCA), and the BA to both PCAs.

In the study by Van Overbeeke *et al.*<sup>10</sup>, the anatomy of the circle of Willis in neonates was evaluated postmortem. He concluded that the prevalence of the anatomical variations in the posterior part of the circle of Willis alters in relation to the development of the brain: 12–20 weeks after conception 73% of the fetuses show a transitional configuration (PCoA and P1 have the same diameter), but after 21 weeks the difference in diameter between the PCoA and P1 increases, resulting in the appearance of a normal or fetal configuration. Thus far, no prevalence of the various major variations of the circle of Willis has been reported in neonates with noninvasive imaging techniques. Noninvasive imaging techniques may allow a combined anatomical evaluation of the circle of Willis with a functional evaluation of the blood flow in the brain-feeding arteries.<sup>12</sup>

The aim of this study was to assess the anatomy of the circle of Willis in prematurely born infants at term-equivalent age and to evaluate if these anatomic variations have an effect on blood flow through the ICAs and the BA.

## SUBJECTS AND METHODS

### Subjects

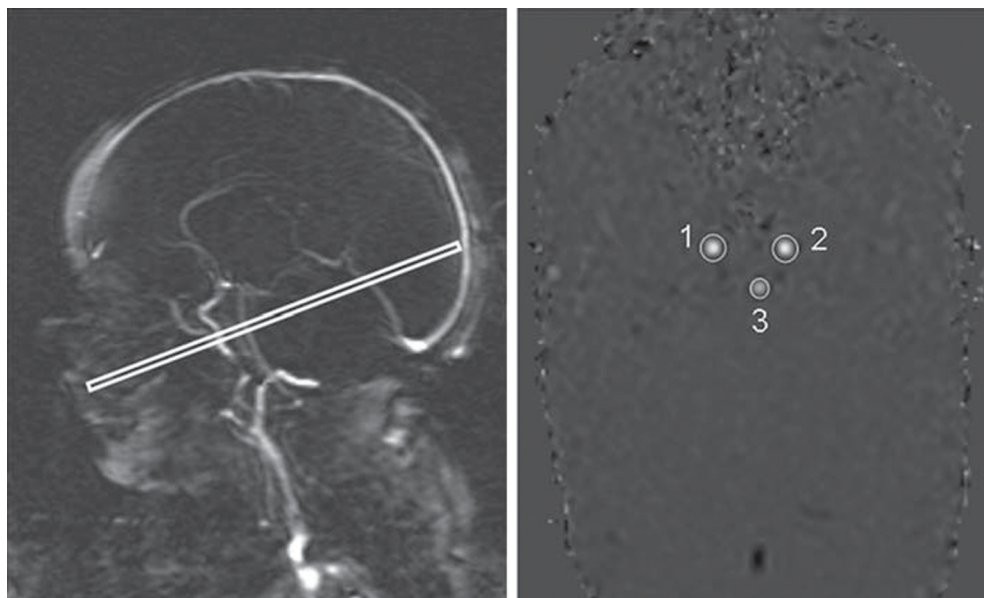
In a large preterm cohort study, 112 neonates were included. They were enrolled when they were born at a gestational age (GA) between 25–31 weeks and were admitted to the Neonatal Intensive Care Unit of the Wilhelmina Children's Hospital in the Netherlands. An MRI of their brain was acquired at term-equivalent age which they all reached in 2007. For the 72 children included in this study, a 3-D time-of-flight (TOF) magnetic resonance angiography (MRA) and a phase-contrast MRA (PC-MRA) was acquired. In the other 40 neonates, the TOF-MRA was not performed due to time restraints. The mean GA of the included infants was 28.9 weeks (range 25.0–30.9 weeks) and their mean birthweight was 1,147 g (range 630–1,860 g). The GA and birthweight did not differ between neonates from whom a TOF-MRA was acquired and the neonates without a TOF-MRA. There were 33 (45.8%) girls and 39 (54.2%) boys in the study group. The neonates were examined at a mean postmenstrual age of 41.6 weeks (range 39.6–45.7 weeks). During MR examination, the neonates were placed in a vacuum fixation pillow (Med Vac Infant Immobilizer Bag, Radstadt, Austria). Monitoring was performed using pulse oximetry (Nonin, Minneapolis, Minn., USA) and respiration rate was observed using the standard Philips equipment (Philips Medical Systems, Best, The Netherlands). For hearing protection, Minimuffs® (Natus Medical Incorporated, San Carlos, Calif., USA) were used. The children were sedated with 50–60 mg/kg chloralhydrate by gastric tube 15 min before the examination. A neonatologist was present during the whole examination.

Informed parental consent was obtained, and this prospective study was approved by the Medical Ethical Committee of the University Medical Centre Utrecht.

### Magnetic Resonance Angiography

The MR investigations were performed on a 3.0-tesla wholebody system (Achieva platform, Philips Medical Systems) using a sense head coil. On the basis of a localizer MRA slab in the sagittal plane, a 2-D PC section was positioned perpendicular to the BA, just below the carotid siphon (Figure 1), to measure the volume flow in the ICAs and the BA (shortest repetition time, TR, 13–16 ms; shortest echo time, TE, 8–10 ms; flip angle, 10°; section thickness, 5 mm; field of view, 150 x 103 mm; matrix, 256 x 256; 8 averages; velocity sensitivity, 30 cm/s; scan time, 20 s).<sup>13</sup> With Philips software on the 3.0-tesla MR system, quantitative flow values (ml/min) were calculated in each vessel by integrating across manually drawn regions of interests that enclosed the vessel lumen closely. Previously, we (J.H. and F.G.) have reported this method to be accurate to calculate the flow values, with an intraobserver variability of 5.6% and an interobserver variability of 5.5%.<sup>12</sup>

To assess the anatomy of the circle of Willis, a TOF-MRA was acquired (TR, 23 ms; TE, 3.5 ms; flip angle, 18°; field of view, 160 x 128 mm; matrix size, 512 x 512; 2 averages, section thickness, 1.0 mm with 0.5 mm overlap; number of sections, 60; scan time, 1.52 min) with a subsequent maximum-intensity projection reconstruction.

**Figure 1**

Sagittal localizer MRA slab. Position of the 2-D PC section perpendicular to the BA, just below the carotid siphon to measure the flow in the ICAs (1, right-sided; 2, left-sided) and the BA (3).

The TOF MRAs were scored independently by two examiners (J.H and B.J.M.K) and afterwards consensus was acquired. The fetal and normal adult anatomy of the circle of Willis are illustrated in Figure 2. The anatomy of the circle of Willis was classified as described by Krabbe-Hartkamp *et al.*<sup>11</sup> The anterior part of the circle of Willis was categorized as normal (Figure 3A) when the ICA distributed flow into the ipsilateral ACA and the pre-communicating segments of the ACA (A1 segments) were symmetrical on the source images of the 3-D TOF MRA data set. A dominant A1 segment was present when a single ICA fed both ACAs with an absent or hypoplastic A1 segment on the contralateral side (Figure 3B). The posterior part of the circle of Willis was normal when the BA provided blood to both PCAs, and it was scored as having a fetal-type PCA (Figure 3C) when the diameter of the PCoAs visually exceeded that of the corresponding P1 segments of the posterior cerebral arteries. A fetal-type PCA could be present on one or both sides.

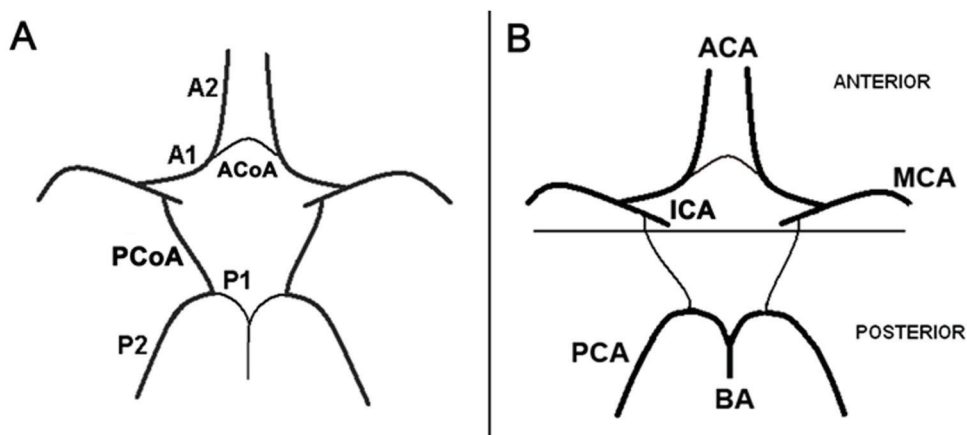
**Figure 2**

Figure A: The circle of Willis in a 52-day embryo, in which all segments are slender and have an identical caliber and the ICA provides blood to all ipsilateral cerebral arteries.

Figure B: A normal adult configuration of the circle of Willis with the ICA providing blood to the ipsilateral ACA and MCA and the BA to both PCAs. Adjusted from Krabbe-Hartkamp et al.<sup>11</sup>.

The MR examination contained T1-weighted (TR, 9.4 ms; TE, 4.6 ms; field of view, 180 × 143 mm; matrix size, 512 × 512; slice thickness, 2.0 mm; number of slices, 50; scan time, 3.44 min) and T2-weighted imaging (TR, 6,293 ms; TE, 120 ms; field of view, 180 × 143 mm; matrix size, 512 × 512; slice thickness, 2.0 mm; number of slices, 50; scan time, 5.40 min) as well to assess the maturation of the brain and to detect anatomical lesions. All children showed a normal MRI for their age or had minor lesions only, such as residual blood in the ventricles after a small intraventricular hemorrhage or mild changes of signal intensity in the white matter (DEHSI).<sup>14</sup> None of the preterm neonates in the present study had a stroke.

### Data Analyses

SPSS version 15.0 was used for all analyses. The mean flow in the three main cerebral arteries, the total CBF and the standard deviation were measured in ml/min. With ANOVA, differences in flow in the ICAs were assessed between a normal anterior part of the circle of Willis, a dominant or hypoplastic A1 segment and differences in flow in the ICAs and the BA were analyzed between a normal posterior part of the circle of Willis, a unilateral, or a bilateral fetal-type PCA. A  $p < 0.05$  was considered statistically significant.

**Table 1: Anatomy of the circle of Willis in preterm infants at term equivalent age**

Anterior part of circle of Willis	Posterior part of circle of Willis				Total (%)
	Normal	Fetal-type PCA R	Fetal-type PCA L	Bil. fetal-type PCA	
Normal	19	14	5	9	47 (65.3)
Dominant A1 R	4	1	2	2	9 (12.5)
Dominant A1 L	7	3	4	2	16 (22.2)
Total (%)	30 (41.7)	18 (25.0)	11 (15.3)	13 (18.1)	72 (100)

Numbers represent infants with a normal or variant of the circle of Willis  
Abbreviations: PCA, posterior cerebral artery; R, right; L, left; Bil, bilateral.

RESULTS

Table 1 illustrates the different variations in the circle of Willis in our cohort. Of the 72 children, 19 (26.4%) showed an entirely normal anatomy of the circle of Willis. twenty-five children (34.7%) had a dominant A1 segment of the ACA. In 30 (41.7%) children, the BA distributed flow into both posterior arteries in contrast to 42 (58.3%) children who showed a fetal-type PCA, of whom 13 (18.1%) showed a bilateral fetal-type PCA.

The flow in the right and left ICA did not differ significantly in the 19 children with a totally normal configuration of the circle of Willis. The flows in the ICAs and the BA were analyzed separately for having a variation in the anterior part of the circle of Willis or in the posterior part. In table 2, the mean flows in the ICAs are compared between a normal anterior part of the circle of Willis and a dominant A1 segment, and the contralateral side with a hypoplastic or absent A1 segment. The flows in the left and right ICA in neonates with a normal configuration of the anterior part of the circle of Willis were pooled, so these children provided two normal ICA flows. The flow in the ICA at the side of a dominant A1 segment was significantly increased compared to the flow in the contralateral ICA ( $43.3 \pm 16.3$  ml/min vs.  $33.0 \pm 9.0$  ml/min,  $p = 0.009$ ), and tended to be higher than the flow in the ICA in children with a normal anterior anatomy of the circle of Willis ( $38.4 \pm 14.0$  ml/min,  $p = 0.1$ ). The flow in the ICA was decreased in the contralateral ICA in the case of the presence of a dominant A1 segment compared to a normal anterior circle of Willis ( $p = 0.025$ ). The total CBF was very similar between the neonates with a normal anterior anatomy of the circle of Willis and the children with a dominant A1 segment ( $103.4 \pm 31.8$  ml/min vs.  $104.1 \pm 28.1$  ml/min;  $p = 0.9$ ).

**Table 2: Flow in relation to the anatomy of the anterior circle of Willis**

Flow (ml/min)	Normal anterior circle of Willis (n=47)	Dominant A1 segment (n=25)	
		Ipsilateral	Contralateral
ICA (SD)	38.4 (14.0)	43.3 (16.3)*	33.0 (9.0)†
BA (SD)	26.6 (9.2)	28.0 (9.4)	
Total (SD)	103.4 (31.8)	104.1 (28.1)	

Mean internal carotid artery (ICA), basilar artery (BA) and total volume flow (ICAs and BA) in ml/min ( $\pm$  SD). The flows in the ICA of children with an anatomically normal anterior part were pooled. The side with the dominant A1 segment was considered the ipsilateral side and the side with the hypoplastic or absent A1 segment was considered the contralateral side.

\*  $p=0.009$ , ICA with a dominant A1 segment versus contralateral ICA; †  $p=0.025$ , ICA with hypoplastic or absent A1 segment versus normal anatomy.

Table 3 shows the results of the analyses of the flow in the ICAs and BA in relation to a variation in the posterior part of the circle of Willis. The flow in the left and right ICA was pooled in neonates with an anatomically normal posterior circle of Willis and left and right ICA flow was also pooled in neonates with a bilateral fetal-type PCA. The flow in the BA decreased proportionately to the presence of a unilateral or bilateral fetal-type PCA ( $R^2 = 0.35$ ). The flow in the BA in the case of a normal posterior configuration was 32.6 ml/min, with a unilateral fetal-type PCA 25.3 ml/min ( $p < 0.001$ ), and in the case of a bilateral fetal-type PCA 18.6 ml/min ( $p < 0.001$ ). There was a trend towards an increased flow volume in the ICA with a fetal-type PCA (40.6 ml/min) compared to the flow in the ICA with a normal posterior anatomy (36.9 ml/min  $p = 0.13$ ). The total CBF was once more very similar between the children with a normal posterior anatomy of the circle of Willis or a unilateral or bilateral fetal-type PCA ( $106.9 \pm 32.8$  vs.  $102.1 \pm 29.2$  vs.  $100.2 \pm 29.4$ ;  $p = 0.8$ , respectively).

Several studies mentioned the relationship between a variant circle of Willis and the presence of an aneurysm.<sup>15;16</sup> In our present study, findings in neonates with or without an intraventricular hemorrhage were similar. In addition, the GA did not influence the prevalence of variations in the circle of Willis.

**DISCUSSION**

In the present MRA study, we have shown a high prevalence of variant types of the circle of Willis in preterm infants with a gestation age between 25 and 31 weeks examined at term-equivalent age. A normal adult-type circle of Willis was present in only 26% of the neonates. Furthermore, we assessed the blood flow through the brainfeeding arteries in these neonates and demonstrated the relation between variations in the anterior and posterior circle of Willis and the volume flow measurements in the ICAs and BA.

**Table 3: Flow in relation to the anatomy of the posterior circle of Willis**

Flow (ml/min)	No fetal-type PCA	Fetal-type PCA	
		(unilateral n=29; bilateral n=13)	
		Unilateral	Bilateral
<b>ICA (SD)</b>	36.9 (13.5)	40.4 (17.7)	40.8 (13.5)
<b>BA (SD)</b>	32.6 (8.8)*	25.3 (6.0)†	18.6 (6.0)
<b>Total (SD)</b>	106.9 (32.8)	102.1 (29.2)	100.2 (29.4)

Mean internal carotid artery (ICA), basilar artery (BA) and total volume flow (ICAs and BA) in ml/min ( $\pm$  SD). The flows in the ICA were pooled for the children with an anatomically normal posterior part and for the children with a bilateral fetal-type PCA.

\*  $p < 0.001$ , BA with normal anatomy versus unilateral fetal-type PCA and versus bilateral fetal-type PCA; †  $p = 0.002$ , BA with unilateral fetal-type PCA versus bilateral fetal-type PCA.

The ICAs and the BA are the major feeding arteries of the brain. In an anatomically normal circle of Willis, the ICA distributes flow into the ipsilateral ACA and MCA and the BA feeds both PCAs. In neonates, the circle of Willis modifies from a predominantly fetal configuration in fetuses 12–20 weeks after conception to a mainly normal configuration around term-equivalent age. The rapid growth of the occipital lobes could be responsible for this transformation.<sup>10</sup> In this study, we found a higher prevalence of variations in the circle of Willis in prematurely born infants at term-equivalent age compared to the reported prevalence in adults. To the best of our knowledge, no studies have been done regarding the anatomy of the circle of Willis in (healthy) full-term infants. In adults, the anterior part of the circle of Willis is normal in 68–86% of the subjects. A unilateral fetal-type PCA is reported in 25% and a bilateral fetal-type PCA in 7% of angiograms of adults. Forty-two percent of adults show a completely normal circle of Willis.<sup>11</sup> Lazorthes *et al.*<sup>5</sup> showed that the calibers of the segments of the circle of Willis differentiate as a result of differences in blood flow. Great amplitude of neck movement causes a more evenly distributed pressure on the arteries in the neck and results in a balanced blood flow in the segments of the circle of Willis. Reduced amplitude of neck movement evolves towards an unbalanced blood flow in the brain-feeding arteries and the caliber of the segments in the circle of Willis differentiates, resulting in the loss of (the entire) function of some segments. Milenkovic *et al.*<sup>8</sup> suggested that reduced movements of a preterm neonate compared to the movement of the fetus could influence the development of (the variations in) the circle of Willis. Further research should be performed to address this hypothesis. In our study, the children were prematurely born infants examined at term-equivalent age, so it is possible that the anatomy of the circle of Willis differs in these children from infants born at term.

Several techniques have been used to study the CBF in neonates. Some studies performed measurements at the brain tissue level and others performed measurements of the total CBF in the brain-feeding vasculature.<sup>12;17;18</sup> The <sup>133</sup>Xenon inhalation is considered the gold standard method for CBF measurement.<sup>19;20</sup> The total CBF in neonates at term

measured using  $^{133}\text{Xe}$  method is in the range of 20–55 ml/100 g/min.<sup>19;21;22</sup> We found an overall mean total CBF of 104 ml/min, which is consistent with reported data assuming an average brain weight of 300 g.<sup>23</sup> The PC-MRA method is able to provide quantitative flow values in ml/min at the level of the skull base for the ICAs and the BA in addition to the MRA information of the brain vasculature and anatomical details. An advantage of these flow measurements is their complete noninvasiveness.

Furthermore, the PC-MRA scan has a short scan time and can easily be combined with MRA imaging of the brain vasculature and anatomical MR scans. Another technique for noninvasive assessment of the flow in the brain feeding vasculature is Doppler flow measurements.<sup>24;25</sup> Recently, we showed a good correlation between the Doppler flow measurements and the flow measurements acquired with PC-MRA.<sup>26</sup> However, we consider the PC-MRA to be the superior technique to measure the CBF, because the diameter of the arteries can be assessed more reliably. In neonatology, MRI is increasingly performed to detect neonatal brain injury and to predict long-term outcome in preterm neonates. MR-PC flow measurement is a simple noninvasive technique to provide hemodynamic information in combination with anatomical information and MRA images of the brain vasculature.<sup>27</sup> The scanning time is only 2.12 min, and these methods could be of scientific interest to assess the relationship between brain structure and CBF.

Evidence that prematurely born infants may differ in vascular anatomy compared to infants born at term was previously provided in a study which showed a decreased tortuosity in all proximal segments of the cerebral vasculature in prematurely born infants compared to full-term infants.<sup>1</sup> To the best of our knowledge, no other studies have been performed in preterm neonates to analyze the anatomy of the circle of Willis at term-equivalent age. A limitation of this study is the lack of a full-term control group. However, compared to a postmortem study published by Overbeeke *et al.*<sup>10</sup> who showed a fetal-type PCA in 20% of full-term neonates and young infants (postmenstrual age 38–60 weeks), we found a higher percentage (58.3%) of this variation in the posterior part of the circle of Willis, suggesting there is a difference in the maturation of the cerebral arteries in preterm infants compared to full terms. Although we found a high prevalence of variations in the anatomy of the circle of Willis, differences in prevalence between the present study and other studies may to some extent be explained by different techniques used to study the anatomy of the circle of Willis. Nevertheless, the total CBF, the sum of the flow in both ICAs and BA, was equal in all neonates, irrespective of the anatomy of the circle of Willis. That means that though there are differences in the flow in the three main cerebral arteries, adequate perfusion of the brain issue appears to be guaranteed. It is unknown if the variations in the anatomy of the circle of Willis will persist into adult life and, for example, become a risk factor for stroke.

Finally, stroke in preterm infants is increasingly recognized.<sup>28</sup> Neonatal stroke could be related to differences in blood flow in the cerebral arteries. The children in this study showed an anatomically normal MRI or only minor lesions without parenchymal involvement, indicating that our population represents relatively healthy preterm neonates born between a GA of 25–31 weeks. Further research is necessary to assess the relation

between differences in flow in the ICAs and BA, the circle of Willis and the prevalence of neonatal stroke. In the present study, we focused on the relation between the anatomy of the circle of Willis and the blood flow in premature neonates who were in a good clinical condition at term-equivalent age. We did not examine neonates in the acute phase of illness. The relationship observed in the present study may be a starting point for future investigations.

In conclusion, 74% of the prematurely born infants with a GA between 25 and 31 weeks in this study showed a variant type of the anatomy of the circle of Willis in its anterior or posterior part or both at term-equivalent age. The flow in the ICA at the side of a dominant A1 segment was higher compared to the contralateral side and to the ICA with a normal configuration of the anterior part of the circle of Willis.

Furthermore, the flow in the BA was highest in neonates with a normal configuration of the posterior part of the circle of Willis compared to children with a unilateral or bilateral fetal-type PCA. The flow in the BA in children with a bilateral fetal-type PCA was the lowest of all. Total CBF was similar in all groups and independent of variations in the anatomy of the circle of Willis.

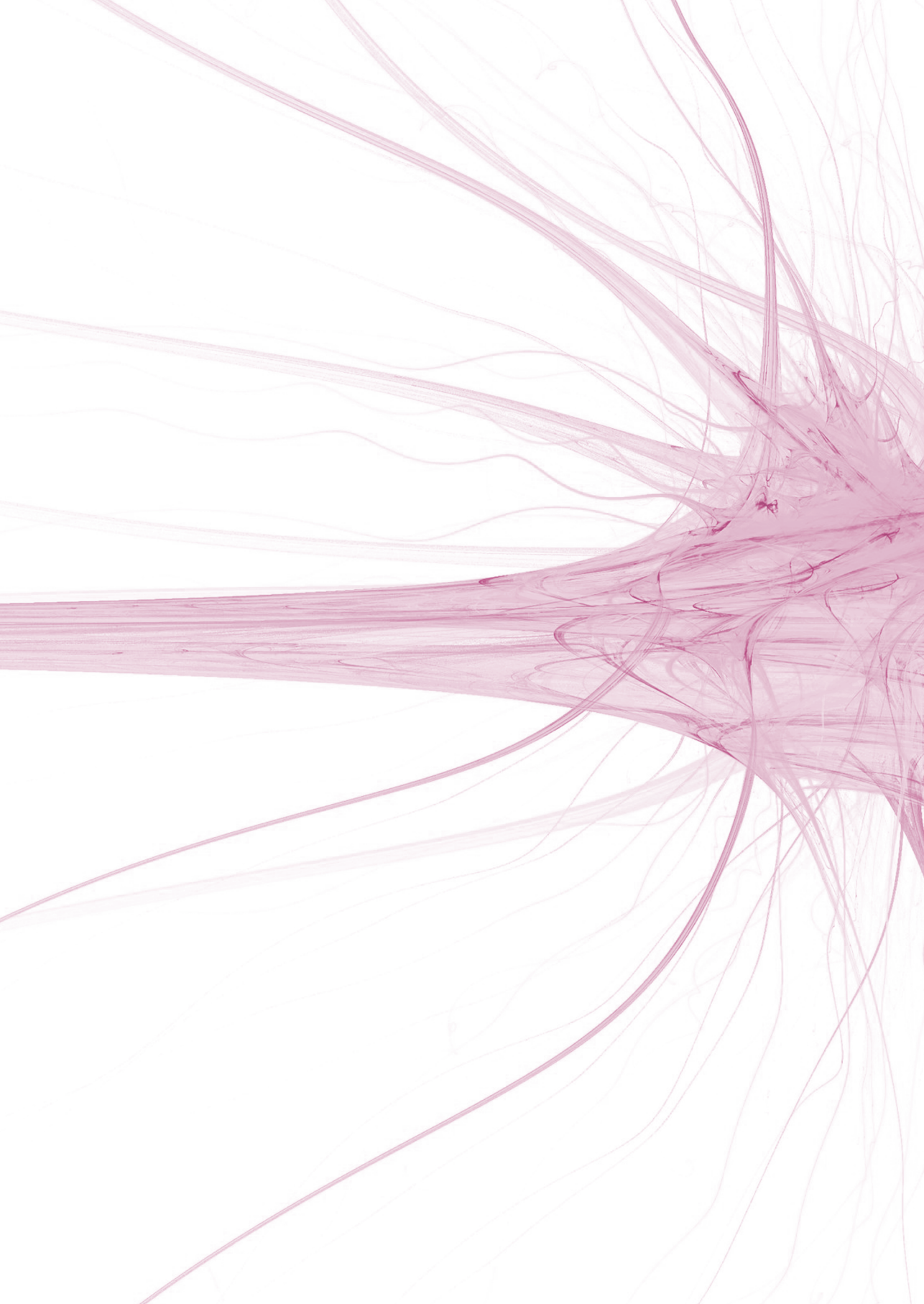
### **Acknowledgments**

The authors thank Niels Blanken and the other MR technicians of the MR institute for their expert and enthusiastic help. This study was funded by The Netherlands Organisation for Health Research and Development, project 94527022.

## Reference List

- (1) Malamateniou C, Counsell SJ, Allsop JM, Fitzpatrick JA, Srinivasan L, Cowan FM et al. The effect of preterm birth on neonatal cerebral vasculature studied with magnetic resonance angiography at 3 Tesla. *Neuroimage* 2006; 32(3):1050-1059.
- (2) Back SA, Riddle A, McClure MM. Maturation-dependent vulnerability of perinatal white matter in premature birth. *Stroke* 2007; 38(2 Suppl):724-730.
- (3) Volpe JJ. Brain injury in the premature infant--from pathogenesis to prevention. *Brain Dev* 1997; 19(8):519-534.
- (4) Hendrikse J, van Raamt AF, van der GY, Mali WP, van der GJ. Distribution of cerebral blood flow in the circle of Willis. *Radiology* 2005; 235(1):184-189.
- (5) Lazorthes G, Gouaze A, Santini JJ, Salomon G. The arterial circle of the brain (circulus arteriosus cerebri). *Anat Clin* 1979; 1:241-257.
- (6) Okahara M, Kiyosue H, Mori H, Tanoue S, Sainou M, Nagatomi H. Anatomic variations of the cerebral arteries and their embryology: a pictorial review. *Eur Radiol* 2002; 12(10):2548-2561.
- (7) van Raamt AF, Mali WP, van Laar PJ, van der Graaf Y. The fetal variant of the circle of Willis and its influence on the cerebral collateral circulation. *Cerebrovasc Dis* 2006; 22(4):217-224.
- (8) Milenkovic Z, Vucetic R, Puzic M. Asymmetry and anomalies of the circle of Willis in fetal brain. Microsurgical study and functional remarks. *Surg Neurol* 1985; 24(5):563-570.
- (9) Padget DH. The development of the cranial arteries in the human embryo. *Contrib Embryol* 1948; 32:206-261.
- (10) Van Overbeeke JJ, Hillen B, Tulleken CA. A comparative study of the circle of Willis in fetal and adult life. The configuration of the posterior bifurcation of the posterior communicating artery. *J Anat* 1991; 176:45-54.
- (11) Krabbe-Hartkamp MJ, van der Grond J, de Leeuw FE, de Groot JC, Algra A, Hillen B et al. Circle of Willis: morphologic variation on three-dimensional time-of-flight MR angiograms. *Radiology* 1998; 207(1):103-111.
- (12) Hendrikse J, de Vries LS, Groenendaal F. Magnetic resonance angiography of cerebral arteries after neonatal venoarterial and venovenous extracorporeal membrane oxygenation. *Stroke* 2006; 37(2):e15-e17.
- (13) Bakker CJ, Hartkamp MJ, Mali WP. Measuring blood flow by nontriggered 2D phase-contrast MR angiography. *Magn Reson Imaging* 1996; 14(6):609-614.
- (14) Maalouf EF, Duggan PJ, Counsell SJ, Rutherford MA, Cowan F, Azzopardi D et al. Comparison of findings on cranial ultrasound and magnetic resonance imaging in preterm infants. *Pediatrics* 2001; 107(4):719-727.
- (15) Alnaes MS, Isaksen J, Mardal KA, Romner B, Morgan MK, Ingebrigtsen T. Computation of hemodynamics in the circle of Willis. *Stroke* 2007; 38(9):2500-2505.

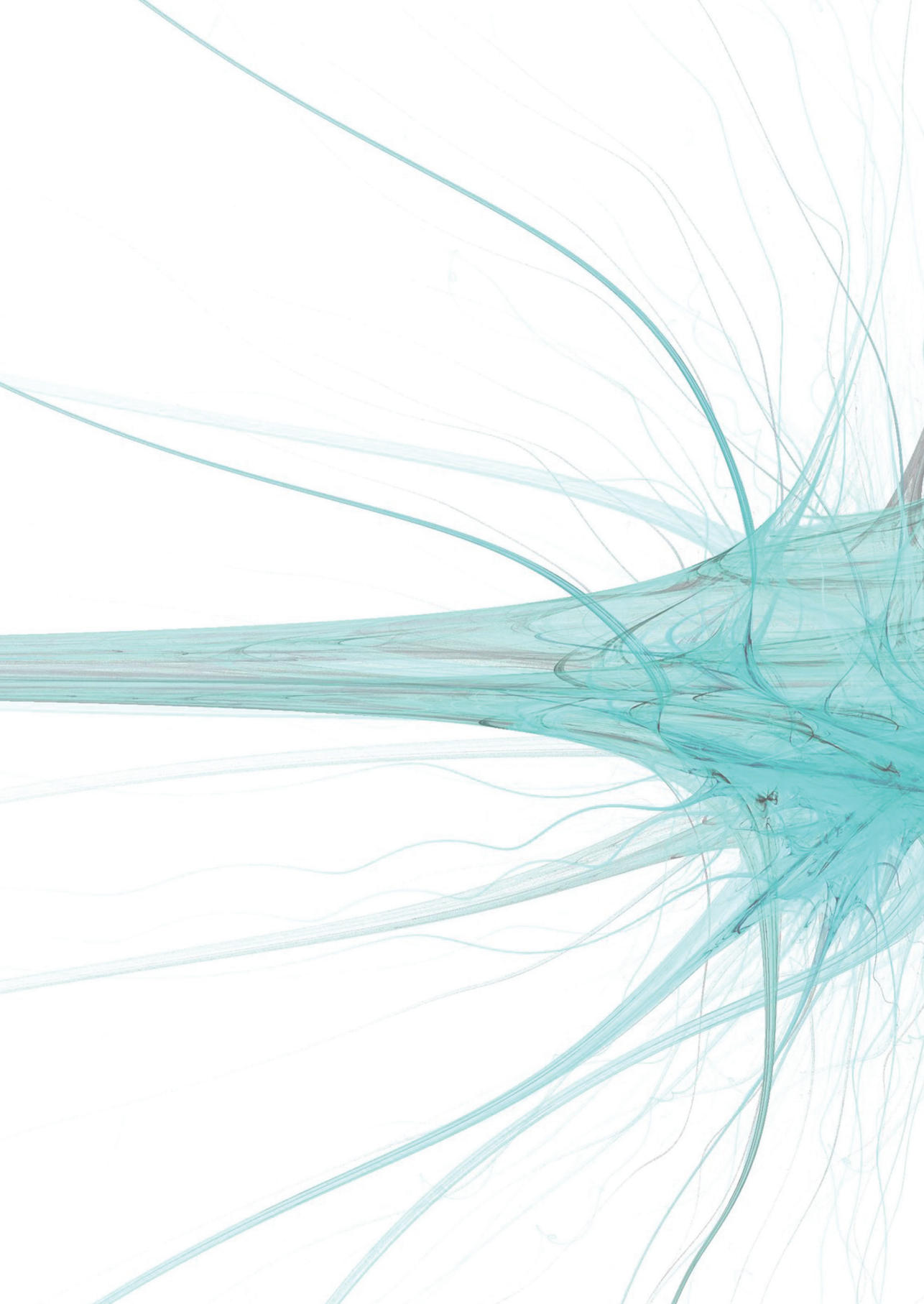
- (16) Kayembe KN, Sasahara M, Hazama F. Cerebral aneurysms and variations in the circle of Willis. *Stroke* 1984; 15(5):846-850.
- (17) Ehehalt S, Kehrer M, Goelz R, Poets C, Schoning M. Cerebral blood flow volume measurements with ultrasound: Interobserver reproducibility in preterm and term neonates. *Ultrasound Med Biol* 2005; 31(2):191-196.
- (18) Miranda MJ, Olofsson K, Sidaros K. Noninvasive measurements of regional cerebral perfusion in preterm and term neonates by magnetic resonance arterial spin labeling. *Pediatr Res* 2006; 60(3):359-363.
- (19) Chiron C, Raynaud C, Maziere B, Zilbovicius M, Laflamme L, Masure MC et al. Changes in regional cerebral blood flow during brain maturation in children and adolescents. *J Nucl Med* 1992; 33(5):696-703.
- (20) Risberg J, Ali Z, Wilson EM, Wills EL, Halsey JH. Regional cerebral blood flow by 133xenon inhalation. *Stroke* 1975; 6(2):142-148.
- (21) Baenziger O, Moenkhoff M, Morales CG, Waldvogel K, Wolf M, Bucher H et al. Impaired chemical coupling of cerebral blood flow is compatible with intact neurological outcome in neonates with perinatal risk factors. *Biol Neonate* 1999; 75(1):9-17.
- (22) Lou HC, Lassen NA, Friis-Hansen B. Impaired autoregulation of cerebral blood flow in the distressed newborn infant. *J Pediatr* 1979; 94(1):118-121.
- (23) Stocker JT. Organ Weights. In: Stocker JT, Dehner LP, editors. *Pediatric Pathology*. 2 ed. Philadelphia: Lippincott; 2001. 1431-1475.
- (24) Archer LN, Levene MI, Evans DH. Cerebral artery Doppler ultrasonography for prediction of outcome after perinatal asphyxia. *Lancet* 1986; 2(8516):1116-1118.
- (25) Van BF, Schipper J, Guit GL, Visser MO. The contribution of colour Doppler flow imaging to the study of cerebral haemodynamics in the neonate. *Neuroradiology* 1993; 35(4):300-306.
- (26) Phase contrast MRA measurements of total cerebral blood flow compared to doppler measurements in newborns. *Ped Res / Proceedngs of the annual meeting of the Pediatric Academic Societies. Annual Meeting of the Pediatric Academic Societies*; 2007.
- (27) de Vries LS, Groenendaal F. Neuroimaging in the preterm infant. *Ment Retard Dev Disabil Res Rev* 2002; 8(4):273-280.
- (28) Benders MJ, Groenendaal F, Uiterwaal CS, Nikkels PG, Bruinse HW, Nievelstein RA et al. Maternal and infant characteristics associated with perinatal arterial stroke in the preterm infant. *Stroke* 2007; 38(6):1759-1765.





## **PART THREE**

**Summary, discussion and  
future directions of research**



The background of the page is an abstract composition of flowing, translucent teal and grey lines. These lines originate from the left side and sweep across the page, creating a sense of movement and depth. The lines vary in opacity, with some appearing as solid, dark strokes and others as lighter, wispy trails. The overall effect is a modern, artistic backdrop for the chapter title.

# CHAPTER NINE

## Summary and future directions of research

Britt van Kooij

## Summary and discussion

In the Neonatal Intensive Care Unit of the Wilhelmina Children's Hospital in Utrecht, The Netherlands, around 180 infants with a gestational age (GA) below 30 weeks are admitted each year. Preterm infants are at increased risk for neurological disabilities later in life.<sup>1</sup> With the increasing numbers of preterm infants who survive the neonatal period, it is of great importance to be able to predict outcome to improve parental counselling and to identify neonates susceptible for neurological disabilities who could benefit from 'developmental support' programs.<sup>2</sup> The aim of this thesis was to quantify magnetic resonance imaging (MRI) findings at term-equivalent age (TEA) in a cohort of preterm infants. Additionally, it was assessed whether MR techniques could be used in the prediction of neurodevelopmental outcome at two years corrected age.

In **Chapter 1** a brief overview was given of the most common patterns of white matter (WM) injury in preterm infants and the role of MRI in detecting these abnormalities. The most common forms of brain injury in the preterm infant are a germinal matrix haemorrhage-intraventricular haemorrhage (GMH-IVH), periventricular white matter injury (PWWI), 'diffuse excessive high signal intensity' (DEHSI) seen on T2-weighted images and punctate WM lesions. Analysis of brain tissue volumes, changes in WM microstructure, metabolites or cerebral vasculature could yield more insight into brain development.

The **first part** of this thesis contained the implementation of two advanced MR techniques to assess more subtle brain abnormalities in our preterm cohort. In

**Chapter 2** an in-house developed automatic neonatal brain segmentation method was presented. In formerly presented segmentation methods, the volumes of cortical (CoGM) and central gray matter (ceGM), myelinated (MWM) and unmyelinated white matter (UWM) and cerebrospinal fluid were measured.<sup>3,4</sup> With our method, which expands on the method of Anbeek *et al.*<sup>5</sup>, it is possible to automatically segment eight different brain structures, i.e. CoGM, CeGM, UWM, MWM, cerebrospinal fluid in the ventricles (VENT), cerebrospinal fluid in the extra-cerebral space (CSF), brain stem (BS) and cerebellum (CB). Voxels were classified by k-Nearest Neighbor classification. The voxel features used for classification were their signal intensities on the T1- and T2- weighted images and their x-, y- and z-coordinates. For each voxel the probability was calculated that the voxel belonged to one of the eight tissue types. We calculated the volume of the different brain structures by the sum of the probabilities times the voxel volume.

WM maturation may best be followed with diffusion tensor imaging (DTI), since this technique is sensitive to changes in the WM microstructure, such as fiber organization and myelination. In **Chapter 3** diffusion parameters were assessed in the left and right posterior limbs of the internal capsule (PLIC) and in the corpus callosum (CC). The bundles passing through these structures were traced using an deterministic fiber tracking technique. Both size (volume and length) and microstructural parameters of these three bundles, i.e. fractional anisotropy (FA), 'case linear anisotropy' ( $CI = (\lambda_1 - \lambda_2) / (\lambda_1 + \lambda_2 + \lambda_3)$ ), apparent diffusion coefficient ( $ADC = (\lambda_1 + \lambda_2 + \lambda_3) / 3$ ) and axial ( $AD = \lambda_1$ ) and radial diffusivity ( $RD = (\lambda_2 + \lambda_3) / 2$ ) were calculated. In our cohort, the CC bundle volume and length were smaller for infants with WM injury and in addition, in this group lower FA and CI were

observed in combination with an increased ADC, which suggests less restricted diffusion. The decrease in FA was mainly driven by an increased RD in infants with focal thinning of the CC, whereas both AD and RD were increased in the group with generalized thinning of their CC. AD and RD, the latter only left-sided, in the PLIC were positively related with WM injury. The infants in our cohort were scanned at a mean postmenstrual age (PMA) of  $41.7 \pm 1.7$  weeks. In this relatively short timeframe, a decrease in RD and an increase in FA and CI were seen with increasing PMA. This may not only reflect myelination, but also the development of various axonal components and maturation of the oligodendroglia.<sup>6</sup> GA was positively associated with the volume and length of the CC bundle and negatively associated with ADC in the left PLIC, which indicates an effect of GA on brain maturation.

As part of our follow-up protocol, the preterm infants were tested with the Bayley Scales of Infant and Toddler Development-Third edition (BSITD-III) at two years corrected age. In the **second part** of this thesis, (advanced) MRI techniques and analysis methods were applied and the relation with neurodevelopmental outcome was assessed. In **Chapter 4** brain volumes were calculated with the method described in *Chapter 2*. In 108 preterm infants (mean GA  $28.5 \pm 1.7$  weeks), brain tissue volumes at TEA were assessed in relation to neurodevelopmental outcome at two years corrected age. These infants were scanned at a PMA between 39-43 weeks. Brain tissue volumes were related to gender, PMA and body weight at time of scanning, however the confounding effect was removed after correction for brain size. Linear regression was performed to assess whether the absolute tissue volumes and/or tissue volumes corrected for both PMA at time of scanning and for total brain size were associated with neurodevelopmental outcome. The relative CoGM volume in reference to brain size increased and the relative UWM volume decreased in the time period the scans were performed. Only the ventricular volume at TEA adjusted for brain size and PMA was negatively associated with both cognition and fine motor and gross motor function at two years corrected age.

Since several studies have highlighted the role of the cerebellum regarding neurodevelopment in preterm infants<sup>7-9</sup>, we separately analysed cerebellar volume and <sup>1</sup>H-MRS at TEA in relation to outcome. In the study presented in **Chapter 5**, 112 preterm infants with a mean GA of  $28.5 \pm 1.7$  weeks were scanned at a mean PMA of  $41.7 \pm 1.1$  weeks. In all infants cerebellar volume was calculated using the method described in *Chapter 2*. In addition, in a subcohort of infants (n=53) cerebellar <sup>1</sup>H-MRS was acquired. In the total cohort, 15 infants had small (<1 cm) punctate haemorrhages in the cerebellum, whereas one infant showed a larger unilateral haemorrhage and one displayed a large bilateral cerebellar haemorrhage. The mean cerebellar volume in the total cohort was  $24.4 \pm 3.6$  ml, however the cerebellum was smaller in the infants with larger unilateral or bilateral haemorrhages (14.1 ml and 7.0 ml, respectively). PMA was positively related to cerebellar volume and therefore correction for PMA was performed in the analysis concerning cerebellar volume and neurodevelopment. Both cerebellar volume corrected for PMA and the N-acetylaspartate/Choline (NAA/Cho) ratio at TEA were significantly associated with cognitive outcome. The cerebellar parameters were not associated with motor function at two years corrected age. Exclusion of the two infants with large cerebellar haemorrhages

did not alter the results. These findings support the importance of the cerebellum in cognitive development in preterm infants.

In **Chapter 6** abnormalities in the WM microstructure at TEA were related to cognitive and motor outcome. In 63 preterm infants the DTI data was without motion and/or sense artefacts and neurodevelopmental assessment was carried out at two years' corrected age. The mean GA of this study population was  $28.7 \pm 1.7$  weeks and they were scanned at a mean PMA of  $41.5 \pm 1.1$  weeks. Tract-based spatial statistics (TBSS) was used to analyse FA, AD and RD in relation to cognition, fine motor and gross motor performance. FA values in the CC were significantly associated with cognitive outcome, whereas there was a tendency towards a significant relation between FA in the fornix and cognition. Fine motor score was extensively related to FA values and RD throughout the WM. The increase in FA was primarily driven by a reduction in RD. A decrease in RD in the CC, fornix and internal and external capsule was associated with better gross motor function. This study showed that in preterm infants, microstructural abnormalities in specific regions of cerebral WM TEA age were associated with cognitive, fine motor and gross motor outcome at two years' corrected age.

In *Chapter 3* diffusion parameters were derived using deterministic fiber tracking and both size (volume and length) and microstructural parameters of the CC and left and right PLIC were calculated. In **Chapter 7** these results were analyzed in relation to outcome. In 67 preterm infants, all three fiber bundles were traced and neurodevelopmental assessment was performed at two years' corrected age. The mean GA of the infants included in this study was  $28.6 \pm 1.8$  weeks and their mean PMA at time of scanning  $41.5 \pm 1.1$  weeks. Boys showed a longer average length and larger volume of the CC and the left PLIC than girls. Boys and girls displayed different associations between the diffusion parameters and neurodevelopment after correction for neonatal factors, i.e. GA, birth weight Z-score, WM injury and IVH, and maternal education. Taking these confounders into account, the volume and the length of the CC bundle were associated with cognition and fine motor scores, whereas a positive relation was found between right PLIC bundle volume and cognitive outcome in girls. In boys, fiber tracking parameters in the left PLIC were related with fine motor scores after correction for the neonatal parameters and maternal education. The studies presented in *Chapters 6* and *7* suggest that both TBSS and deterministic fiber tracking can be used to analyse diffusion parameters at TEA, which have potential to serve as biomarker for subsequent neurodevelopment in preterm infants.

Previous studies have shown a disrupted development of cerebral blood vessels at TEA in prematurely born infants.<sup>10</sup> In **Chapter 8** the anatomy of the circle of Willis in preterm infants at TEA was assessed and additionally, it was evaluated whether there was a relation between anatomic variations in the circle of Willis and blood flow through the internal carotid arteries (ICAs) and basilar artery (BA). In 72 preterm neonates with a mean GA of  $28.9 \pm 1.5$  weeks, flow measurements (ml/min) were obtained with 2D phase-contrast magnetic resonance angiography (MRA). Time-of-flight MRA was used to assess the anatomy of the circle of Willis for a dominant A1 segment of the anterior cerebral artery or a fetal-type posterior cerebral artery (PCA). In our cohort, 53/72 neonates showed a

variant type of the circle of Willis. The flow in the ICA at the side of a dominant A1 segment (43.3 ml/min) was significantly increased compared to the flow in the contralateral ICA (33.0 ml/min;  $p=0.009$ ) and tended to be higher than the flow in the ICA in children with a normal anterior anatomy (38.4 ml/min,  $p=0.1$ ). The flow in the BA was higher in neonates with a normal configuration of the posterior part of the circle of Willis (32.6 ml/min) than in children with a unilateral (25.3 ml/min,  $p=0.002$ ) or bilateral fetal-type PCA (18.6 ml/min,  $p<0.001$ ). In this cohort, 74% demonstrated a variation of the circle of Willis at TEA, which was associated with alteration in the flow through the ICAs and BA. Further research is necessary to assess whether deviations in flow in the ICAs and BA and the anatomy of the circle of Willis are clinically relevant, e.g. indicative of an increase in the prevalence of neonatal stroke.

### The main findings of this thesis are:

- It is possible to segment the neonatal brain at TEA using an automatic probabilistic segmentation method which is based on k-Nearest Neighbor. This is the first method that can segment CoGM, CeGM, UWM, MWM, cerebrospinal fluid in the ventricles and in the extra-cerebral space, BS and CB separately. All structures can be segmented fast and in one run (*Chapter 2*).
- Fiber tracking of the CC and PLIC bundles can be performed in preterm infants at TEA. Bundle volumes and lengths and diffusion parameters in these bundles are associated with WM injury. Therefore quantitative fiber tracking can provide insight into the underlying changes in WM microstructure in addition to information from conventional T1- and T2-weighted images (*Chapter 3*).
- Relative volume changes of cerebral structures normalised to the ICV occur in preterm infants around TEA. Ventricular volumes corrected for both ICV and PMA are negatively associated with cognition, fine motor and gross motor skills at two years' corrected age in addition to neonatal parameters and maternal education (*Chapter 4*).
- Both cerebellar volume corrected for PMA and cerebellar NAA/Cho ratio were related to cognitive skills after correction for neonatal and maternal confounders. Cerebellar volume and NAA/Cho ratio at TEA were not significantly associated with motor performance at two years' corrected age (*Chapter 5*).
- The results presented in *Chapters 4* and *5* reveal the possibility to use brain volumes at TEA as biomarkers for neurodevelopmental outcome in preterm infants.
- TBSS, optimized for the neonatal brain, can be used to assess the relationship between diffusion parameters at TEA and neurodevelopmental outcome at two years' corrected age. An increase in FA and a decrease in RD in specific WM regions are related to cognition, fine motor and gross motor outcome (*Chapter 6*).
- Fiber tracking parameters in the CC in girls and in the left PLIC for boys were associated with cognitive scores, fine motor and gross motor performance (*Chapter 7*).

- The results presented in *Chapters 6 and 7* exhibit the potential use of diffusion parameters at TEA as biomarkers for neurodevelopment in preterm infants.
- Preterm infants demonstrate a high prevalence of variant types of the circle of Willis at TEA. Variations in the anatomy of the circle of Willis are related to alterations in the flow through the ICAs and the BA (*Chapter 8*).

## **FUTURE DIRECTIONS OF RESEARCH**

### **Volumetric measurements of brain structures**

With the development of a fully automatic neonatal brain segmentation method, progress has been made in analyzing brain development in preterm infants. The possibility to quantify these brain structure volumes is of value since it provides additional information to predict the neurodevelopment of preterm infants at an early stage. Although, the association between brain structure volumes at term-equivalent age (TEA) and neurodevelopmental outcome at two years corrected age in this cohort is rather limited, the volumes of especially the cerebellum and the lateral ventricles at TEA can help to improve parental counseling and to select preterm infants who may profit from special developmental programs to improve their neurological outcome.

However, further studies are needed to assess regional brain development. These regional volume changes that could lead to subsequent neurological impairments could be missed when only total brain structure volumes per tissue class are assessed. Voxel-based morphometry is a potential tool to detect locations of decreased or increased volumes and the implementation of this technique is an ongoing goal of our research. Additionally, it would be of great benefit to be able to calculate brain structure volumes in the left and right hemisphere and to calculate volumes of different lobes (frontal, parietal, temporal and occipital) separately, for example in infants with unilateral lesions such as a unilateral stroke or a parenchymal haemorrhage.

We only analyzed tissue volumes at TEA. Nowadays, we also try to perform an MRI scan in our preterm infants soon after birth as standard clinical care. A learning set will be composed for the segmentation of the preterm brain. A recently started longitudinal research project in which preterm infants are scanned soon after birth and around TEA will not only provide information regarding brain growth, but also about cortical folding between 30 weeks' and 40 weeks' gestation. Both growth and cortical folding may be able to give more insight in the variations of brain development and subsequent neurodevelopmental outcome.

In our preterm cohort, an indefinite border was seen between the unmyelinated white matter (UWM) and cortical gray matter in preterm infants with white matter (WM) injury. It was hypothesized that dysfunctioning of the subplate neurons could result in incomplete migration of neuroblasts into the cortex and an incomplete apoptotic process of subplate neurons, especially in infants with WM injury. The outlining for an animal study with both MRI and histopathological analyses has already started to enable us to evaluate this hypothesis.

## Changes in the white matter microstructure

The analysis of diffusion parameters in preterm infants is a major challenge because the signal to noise ratio is relatively small due to the smaller voxel size needed as a consequence of the smaller anatomical structures. Moreover, the higher water content and the lower degree of myelination result in lower FA values compared to adults. Fractional anisotropy and axial and radial diffusivity are often assessed in manually drawn regions of interest. An anatomical atlas of the WM tracts of preterm infants of different gestational ages could be helpful to analyse the diffusion parameters automatically. An atlas of healthy preterm infants could provide information regarding brain development of an individual infant. To construct such an atlas, longitudinal research needs to be performed in which preterm infants are scanned weekly after birth. Furthermore, infants without brain injury are essential to obtain for this atlas and their neurodevelopmental outcome should be normal.

## Additional role of MRI

At the moment of birth and in the first few weeks after birth, several concerns that influence neurodevelopment are already present and easy to identify, such as gestation age, birth weight, perinatal infection, respiratory problems, an intraventricular haemorrhage and maternal education. We used the MRI at TEA as a 'read-out' for the pre- and perinatal period. Further studies are necessary to assess pre- and perinatal risk factors for brain injury with subsequent volume changes and alterations in the WM microstructure, which are shown to be associated with neurodevelopmental impairments. More insight into these risk factors makes interventions and treatment directed towards the prevention of those features possible. The main question that needs to be addressed is which advanced MRI tools add to the prior knowledge based on these neonatal and maternal parameters regarding neurodevelopment. We have demonstrated a role for brain volumes and changes in the WM microstructure in our preterm cohort. Larger etiological and predictive studies are necessary to analyse the predictive value of these new developed MRI applications in preterm infants in general.

Cranial ultrasound of the brain is routinely performed in our unit to detect brain injury. However, an MRI is more sensitive to identify more subtle lesions, like punctate WM lesions and (small) cerebellar haemorrhages. An MRI performed soon after birth could specify abnormalities seen on cranial ultrasound in more detail. (Subtle) WM injury with subsequent sequelae, like ventriculomegaly, can be missed on cranial ultrasound and can even have resolved at TEA. Further studies need to be performed to assess the additional role of an early MRI besides cranial ultrasound in preterm infants, though one could suggest to perform an MRI in all infants born before 28 weeks' gestation to detect (subtle) brain injury, since these infants are known to be susceptible to WM injury.

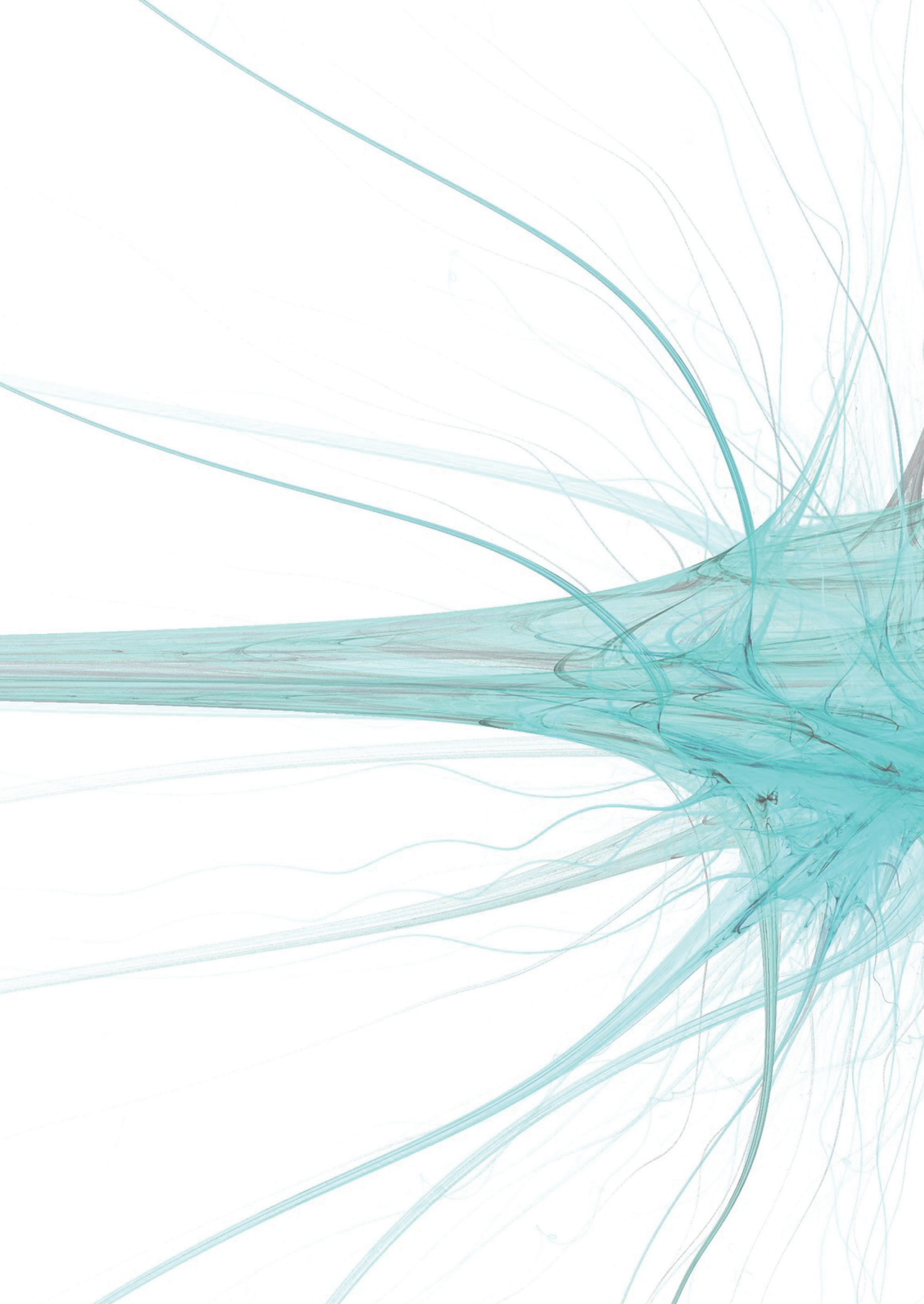
## Long term neurodevelopment

In this study, the neurological assessment was acquired at two years corrected age. It would be really interesting to relate MRI findings at TEA, i.e. the visual scoring of the injury seen on conventional MRI, brain tissue volumes and

changes in the WM microstructure, with MRI findings acquired between childhood and adolescence. It would be desirable to evaluate brain growth over a longer period of time, for example to see whether there is a catch-up growth which could indicate there is only a delay in development, or on the contrary a decline in growth what could point to irreversible brain injury causing an abnormal structure or innervation of brain tissue. Additionally, it has been hypothesized that infants grow into their deficits, so it could be that brain structure volumes are not related to cognition or motor function at two years of age, but are still associated with impairments at an older age. Therefore we would like to re-evaluate this cohort at the age of 8 to 10 years with both neuro-imaging (conventional MRI and fMRI) and with neuropsychological tests to assess, besides an intelligence quotient and motor function, skills such as executive functions, memory and behavior. It is important to estimate neurodevelopmental outcome of an individual preterm infant at an early stage to determine the proper approach to support both the preterm infants as their parents.

## Reference List

- (1) Saigal S, Doyle LW. An overview of mortality and sequelae of preterm birth from infancy to adulthood. *Lancet* 2008; 371(9608):261-269.
- (2) Spittle AJ, Orton J, Doyle LW, Boyd R. Early developmental intervention programs post hospital discharge to prevent motor and cognitive impairments in preterm infants. *Cochrane Database Syst Rev* 2007;(2):CD005495.
- (3) Prastawa M, Gilmore JH, Lin W, Gerig G. Automatic segmentation of MR images of the developing newborn brain. *Med Image Anal* 2005; 9(5):457-466.
- (4) Warfield SK, Kaus M, Jolesz FA, Kikinis R. Adaptive, template moderated, spatially varying statistical classification. *Med Image Anal* 2000; 4(1):43-55.
- (5) Anbeek P, Vincken KL, Groenendaal F, Koeman A, van Osch MJ, van der Grond J. Probabilistic brain tissue segmentation in neonatal magnetic resonance imaging. *Pediatr Res* 2008; 63(2):158-163.
- (6) Adams E, Chau V, Poskitt KJ, Grunau RE, Synnes A, Miller SP. Tractography-based quantitation of corticospinal tract development in premature newborns. *J Pediatr* 2010; 156(6):882-8, 888.
- (7) Allin M, Matsumoto H, Santhouse AM, Nosarti C, AlAsady MH, Stewart AL et al. Cognitive and motor function and the size of the cerebellum in adolescents born very pre-term. *Brain* 2001; 124(Pt 1):60-66.
- (8) Messerschmidt A, Fuiko R, Prayer D, Brugger PC, Boltshauser E, Zoder G et al. Disrupted cerebellar development in preterm infants is associated with impaired neurodevelopmental outcome. *Eur J Pediatr* 2008; 167(10):1141-1147.
- (9) Shah DK, Anderson PJ, Carlin JB, Pavlovic M, Howard K, Thompson DK et al. Reduction in cerebellar volumes in preterm infants: relationship to white matter injury and neurodevelopment at two years of age. *Pediatr Res* 2006; 60(1):97-102.
- (10) Malamateniou C, Counsell SJ, Allsop JM, Fitzpatrick JA, Srinivasan L, Cowan FM et al. The effect of preterm birth on neonatal cerebral vasculature studied with magnetic resonance angiography at 3 Tesla. *Neuroimage* 2006; 32(3):1050-1059.



The background of the page is an abstract composition of flowing, translucent teal and grey lines. These lines originate from the left side and sweep across the page, creating a sense of movement and depth. The lines vary in opacity, with some appearing as solid, dark strokes and others as lighter, wispy trails. The overall effect is a modern, artistic backdrop for the text.

# CHAPTER TEN

## Nederlandse samenvatting

Britt van Kooij

## SAMENVATTING EN DISCUSSIE

Elk jaar worden op de NICU afdeling van het Wilhelmina Kinderziekenhuis in Utrecht ongeveer 180 kinderen opgenomen die geboren zijn na een zwangerschap van minder dan 31 weken. Te vroeg geboren kinderen hebben een verhoogd risico op problemen in hun ontwikkeling. Voor een goede counseling van de ouders is het van belang om in een vroeg stadium de ontwikkeling van deze kinderen te voorspellen. Te vroeg geboren kinderen kunnen baat hebben bij speciale programma's die hun ontwikkeling stimuleren. In deze studie is onderzocht of een MRI van de hersenen op de uitgerekende datum kan bijdragen aan het voorspellen van de ontwikkeling van te vroeg geboren kinderen.

In **Hoofdstuk 1** is een overzicht gegeven van de meest voorkomende cerebrale afwijkingen bij te vroeg geboren kinderen. In de praktijk wordt naast schedelechografie MRI gebruikt om deze schade op te sporen. Een germinale matrix bloeding / intraventriculaire bloeding, periventriculaire witte stof afwijkingen, een diffuus verhoogd signaal in de witte stof op de T2-gewogen opnames (genaamd 'DEHSI') en puntbloedingen in de witte stof behoren tot de meest voorkomende afwijkingen in de hersenen. Volumes van verschillende hersenstructuren, veranderingen in de microstructuur van de witte stof, metabolieten in het cerebellum of de cerebrale vasculatuur kunnen meer inzicht geven in de ontwikkeling van de hersenen.

In **Deel 1** van dit proefschrift zijn twee geavanceerde MRI methodes beschreven om subtiele veranderingen in de neonatale hersenen te detecteren in een cohort te vroeg geboren kinderen die onderzocht werd rond de uitgerekende datum. In **Hoofdstuk 2** is een nieuwe segmentatiemethode beschreven om de hersenen van een neonaat te segmenteren. Deze methode is een uitbreiding van de segmentatiemethode die eerder beschreven is. Voorheen was het alleen mogelijk om automatisch de volumes te berekenen van de corticale (CoGS) en centrale grijze stof (CeGS), van de ongemyeliniseerde witte stof (OnMWS) en van de totale hoeveelheid liquor in de hersenen. Door deze nieuwe methode was het mogelijk om naast het volume van de OnMWS ook het volume te berekenen van de gemyeliniseerde witte stof (MWS), van de liquor in de ventrikels en in de subarachnoidale ruimte (SAR) apart en tevens konden het cerebellum (CB) en de hersenstam (HS) als aparte structuren gesegmenteerd worden. Met deze nieuwe methode konden dus in totaal acht verschillende hersenstructuren gesegmenteerd worden. De k-Nearest Neighbor classificatie methode werd gebruikt om voxels te classificeren op basis van hun signaalintensiteit op de T1- en de T2- gewogen MR opnames en hun x-, y- en coördinaten. Voor elke voxel werd berekend wat de kans was dat het voxel tot een specifieke hersenstructuur behoorde. De volumes van de acht verschillende hersenstructuren werden berekend door de som van het voxelvolume vermenigvuldigd met de kans dat het voxel tot de specifieke hersenstructuur behoorde.

Rijping van de witte stof kan goed worden bepaald door Diffion Tensor Imaging (DTI), een MRI sequentie die gevoelig is voor veranderingen in de microstructuur van de witte stof, zoals vezelorganisatie en myelinisatie. In **Hoofdstuk 3** zijn diffusieparameters bepaald in het achterste been van de linker en rechter capsula interna (afgekort als 'PLIC' = posterior limb of the internal capsule) en in het corpus callosum (CC). Zowel parameters

voor grootte, namelijk volume en lengte, als parameters op microstructureel niveau, te weten fractionele anisotropie (FA), 'case linear' anisotropie ( $CI=(\lambda_1-\lambda_2)/(\lambda_1+\lambda_2+\lambda_3)$ ), apparent diffusion coefficient ( $ADC=(\lambda_1+\lambda_2+\lambda_3)/3$ ) en axiale ( $AD=\lambda_1$ ) en radiale diffusie ( $RD=(\lambda_2+\lambda_3)/2$ ) werden geanalyseerd in deze drie vezelbundels. Bij kinderen met witte stof schade waren het volume en de lengte van het CC kleiner en werden lagere FA en CI waardes gevonden in combinatie met hogere ADC waardes. Deze combinatie suggereerde dat witte stof schade gepaard ging met een toegenomen diffusie. De afname in FA werd voornamelijk veroorzaakt door een toename in de RD bij kinderen met een focaal dun CC, terwijl bij kinderen met een gegeneraliseerd dun CC zowel de AD als de RD toegenomen waren. AD en RD in de PLIC waren positief gerelateerd aan de mate van witte stof schade. De kinderen in dit cohort werden onderzocht op een postmenstruele leeftijd (PMA = postmenstrual age) van  $41,7 \pm 1,7$  weken. In dit relatieve korte tijdsbestek (range 39-44 weken) werd er een afname in RD en een toename in FA en CI waardes gezien met een stijgende PMA. Dit werd niet alleen veroorzaakt door myelinisatie, maar ook door de ontwikkeling van verschillende axonale componenten en de maturatie van oligodendroglia cellen. De zwangerschapsduur had een effect op de rijping van de hersenen, wat werd verklaard door een positieve associatie met lengte en volume van het CC en negatieve relatie met de ADC waarde in de linker PLIC.

De te vroeg geboren kinderen in dit studiecohort werden in de tijd gevolgd en op de gecorrigeerde leeftijd van twee jaar getest met behulp van de Bayley Scales of Infant and Toddler Development, Third edition (BSITD-III). In **Deel 2** van dit proefschrift zijn verschillende (geavanceerde) MRI technieken en analysemethodes toegepast en de relatie met de BSITD-III scores geanalyseerd. In **Hoofdstuk 4** zijn de volumes van de verschillende hersenstructuren berekend met de segmentatiemethode die we de afgelopen jaren ontwikkeld hebben (zie *Hoofdstuk 2*). Onderzocht werd of de hersenvolumes van 108 te vroeg geboren kinderen rond de uitgerekende datum (gemiddelde zwangerschapsduur  $28,5 \pm 1,7$  weken) gerelateerd waren aan de neurologische ontwikkeling op de gecorrigeerde leeftijd van twee jaar. De kinderen waren onderzocht op een PMA tussen de 39 en 43 weken. De hersenvolumes werden gerelateerd aan geslacht, scanleeftijd en lichaamsgewicht ten tijde van de scan. Deze drie variabelen bleken allemaal significant gerelateerd aan de totale hersengrootte. Zowel het absolute volume van de verschillende hersenstructuren als de volumes gecorrigeerd voor zowel scanleeftijd als totale hersengrootte werden gerelateerd aan de BSITD-III scores. Ten opzichte van het totale hersenvolume steeg het relatieve CoGS volume en daalde het relatieve OnMWS volume. Alleen het volume van de ventrikels rond de uitgerekende datum bleek negatief geassocieerd te zijn met cognitie, fijne motoriek en grove motoriek op de gecorrigeerde leeftijd van twee jaar.

Steeds meer studies hebben aangetoond dat het cerebellum niet alleen belangrijk is voor de motorische ontwikkeling, maar dat het ook een rol speelt bij de verstandelijke ontwikkeling. In **Hoofdstuk 5** zijn het cerebellaire volume, berekend met de methode uit *Hoofdstuk 2*, en de resultaten van proton MR spectroscopie ( $^1H$ -MRS) in het cerebellum rond de uitgerekende datum gerelateerd aan de neurologische ontwikkeling op de gecorrigeerde leeftijd van twee jaar. In deze studie werden 112 kinderen geïncludeerd die

geboren zijn bij een zwangerschapsduur van  $28,5 \pm 1,7$  weken en ze werden gescand op een PMA van  $41,7 \pm 1,1$  weken. Er waren 15 kinderen met een kleine cerebellaire bloeding ( $<1$  cm), één kind had een grote unilaterale cerebellaire bloeding en één kind had een grote bilaterale cerebellaire bloeding. Het gemiddelde volume van het cerebellum bedroeg  $24,4 \pm 3,6$  ml, het cerebellaire volume van het kind met een unilaterale bloeding was echter 14,1 ml en van het kind met de bilaterale bloeding 7,0 ml. Aangezien er een positieve relatie bestond tussen cerebellair volume en scanleeftijd, werd het volume in de verdere analyses gecorrigeerd voor PMA. Zowel het cerebellaire volume gecorrigeerd voor PMA als de N-acetylaspartate/Choline (NAA/Cho) ratio waren significant gerelateerd aan cognitie. Exclusie van de twee kinderen met een grotere cerebellaire bloeding had geen invloed op de gevonden resultaten. Deze studie ondersteunt de hypothese dat het cerebellum een rol speelt bij de verstandelijke ontwikkeling van te vroeg geboren kinderen.

In **Hoofdstuk 6** zijn 63 kinderen geïnccludeerd (gemiddelde zwangerschapsduur:  $28,7 \pm 1,7$  weken, gemiddelde scanleeftijd:  $41,5 \pm 1,1$  weken) met kwalitatief goede DTI data. Onderzocht werd of er een relatie bestond tussen de afwijkingen in de microstructuur van de witte stof rond de uitgerekende datum en de scores voor cognitie en motoriek op de gecorrigeerde leeftijd van twee jaar. *Tract-based spatial statistics* (TBSS) werden toegepast om de FA, AD en RD waardes te analyseren in relatie tot cognitie en fijne en grove motoriek. FA waardes in het CC waren significant geassocieerd met de cognitieve ontwikkeling en er werd een trend gezien met FA waardes in de fornix. Fijne motoriek was gerelateerd aan de FA en RD waardes diffuus in de witte stof. De toename in FA werd voornamelijk veroorzaakt door een afname in RD. Er bestond een negatieve relatie tussen RD waardes in het CC, fornix, PLIC en de capsula externa en grove motoriek. Deze studie toonde aan dat er bij te vroeg geboren kinderen een relatie bestaat tussen diffusieparameters in de witte stof rond de uitgerekende datum en neurologische ontwikkeling op de gecorrigeerde leeftijd van twee jaar.

In **Hoofdstuk 7** zijn de diffusieparameters die berekend waren in *Hoofdstuk 3* gerelateerd aan de BSITD-III scores. In totaal werden 67 kinderen in deze studie geïnccludeerd met een gemiddelde zwangerschapsduur van  $28,6 \pm 1,8$  weken en gemiddelde scanleeftijd van  $41,5 \pm 1,1$  weken. Het volume en de lengte van het CC en de linker PLIC van jongens waren groter en langer dan die van meisjes. Er werden verschillende associaties gevonden voor jongens en voor meisjes tussen de diffusieparameters en de BSITD-III scores na correctie voor de zwangerschapsduur, Z-score van het geboortegewicht, witte stof schade op de conventionele MRI, een intraventriculaire bloeding en educatie van de moeder. Het volume en de lengte van het CC waren geassocieerd met cognitie en fijne motoriek bij meisjes. Tevens bestond er bij meisjes een positieve relatie tussen het volume van de rechter PLIC en cognitie. Voor jongens waren de diffusieparameters in de linker PLIC van belang voor de fijne motoriek. De studies gepresenteerd in *Hoofdstuk 6* en *7* laten zien dat TBSS en fiber tracking bruikbare methodes zijn om diffusieparameters rond de uitgerekende datum bij te vroeg geboren kinderen te analyseren en dat deze parameters gebruikt kunnen worden als biomarker voor neurologische ontwikkeling op de gecorrigeerde leeftijd van twee jaar.

In **Hoofdstuk 8** is de anatomie van de Cirkel van Willis onderzocht in het cohort te vroeg geboren kinderen. Geanalyseerd werd of er een relatie bestond tussen de anatomie en de bloedstroomsnelheid in de linker en rechter carotis interna arterie (ACI) en de basilaris arterie (AB). Bij 72 neonaten (gemiddelde zwangerschapsduur  $28,9 \pm 1,5$  weken) werd de bloedstroomsnelheid gemeten in de 3 arteriën met behulp van een 2D fase-contrast MR angiografie (MRA). Een time-of-flight MRA werd gemaakt om de anatomie van de Cirkel van Willis te beoordelen op de aanwezigheid van een dominant A1 segment van de arterie cerebri anterior (ACA) of een foetaal-type arterie cerebri posterior (ACP). Bij 53 van de 72 kinderen werd er een variatie in de anatomie van de Cirkel van Willis gevonden. De bloedstroomsnelheid in de ACI aan de kant van het dominante A1 segment was zowel hoger dan in de ACI aan de contralaterale zijde als in beide ACI's in het geval van een normale anatomie van het voorste deel van de Cirkel van Willis (respectievelijk 43,3 ml/min; 33,0 ml/min,  $p=0,009$ ; en 38,4 ml/min,  $p=0,1$ ). De bloedstroomsnelheid in de AB was hoger bij neonaten met een normale anatomie van het achterste deel van de Cirkel van Willis (32,6 ml/min) dan bij kinderen met een unilateraal foetaal-type ACP (25,3 ml/min,  $p=0,002$ ) of een bilateraal foetaal-type ACP (18,6 ml/min,  $p<0,001$ ). Een variatie in de Cirkel van Willis rond de uitgerekenende datum werd gezien bij 74% van de te vroeg geboren kinderen. Nader onderzoek zal moeten aantonen of uitsluiten of veranderingen in de bloedstroomsnelheid door de ACI en de AB, die samenhangen met deze variaties in de anatomie, een klinische betekenis hebben, zoals een toename in de incidentie van een neonata(a)l(e) herseninfarct of -bloeding.

#### **De belangrijkste bevindingen van dit onderzoek zijn:**

- Het is mogelijk om de hersenen van een neonaat volledig automatisch te segmenteren in acht verschillende structuren: CoGS, CeGS, OnMWS, MWS, ventrikels, liquor in de SAR, HS en CB (*Hoofdstuk 2*).
- *Fiber tracking* van de zenuwvezels door het CC en de PLIC is mogelijk bij te vroeg geboren kinderen rond de uitgerekenende datum. Het volume en de lengte van de bundels evenals de diffusieparameters in deze bundels zijn geassocieerd met schade in de witte stof. Naast informatie van conventionele T1- en T2-gewogen MR opnames, kan kwantitatieve fiber tracking meer inzicht geven in veranderingen in de microstructuur van de witte stof (*Hoofdstuk 3*).
- De groeisnelheid van de acht gemeten hersenstructuren is ten opzichte van elkaar verschillend in de weken rondom de uitgerekenende datum. Na correctie voor zwangerschapsduur, Z-score van het geboortegewicht, witte stof schade op de conventionele MRI, een intraventriculaire bloeding en educatie van de moeder is het volume van de ventrikels rond de uitgerekenende datum, gecorrigeerd voor de scanleeftijd en de totale hersengrootte, bij te vroeg geboren kinderen gerelateerd aan cognitie en fijne en grove motoriek op de gecorrigeerde leeftijd van 2 jaar (*Hoofdstuk 4*).

- Zowel het cerebellaire volume als de NAA/Cho ratio rond de uitgerekende datum zijn gerelateerd aan cognitie op de gecorrigeerde leeftijd van twee jaar na correctie voor zwangerschapsduur, Z-score van het geboortegewicht, witte stof schade op de conventionele MRI, een intraventriculaire bloeding en educatie van de moeder. Het cerebellaire volume en de NAA/Cho ratio hadden geen relatie met de motoriek (*Hoofdstuk 5*).
- Het is mogelijk om de volumes van hersenstructuren rond de uitgerekende datum van te vroeg geboren kinderen te gebruiken als biomarker voor neurologische ontwikkeling op de gecorrigeerde leeftijd van twee jaar (*Hoofdstuk 4 en 5*).
- TBSS geoptimaliseerd voor de hersenen van een neonaat kan gebruikt worden om de relatie te onderzoeken tussen diffusieparameters rond de uitgerekende datum en de neurologische ontwikkeling op de gecorrigeerde leeftijd van twee jaar. Een toename in FA waardes en een afname in RD in specifieke gebieden in de witte stof waren gerelateerd aan cognitie en aan fijne en grove motoriek (*Hoofdstuk 6*).
- Bij te vroeg geboren kinderen waren diffusieparameters in het CC bij meisjes en in de PLIC bij jongens rond de uitgerekende datum gerelateerd aan scores op de B BSITD-III op de gecorrigeerde leeftijd van twee jaar. Deze parameters werden verkregen door *fiber tracking* van de witte stof bundels (*Hoofdstuk 7*).
- De resultaten beschreven in *Hoofdstuk 6 en 7* laten zien dat diffusieparameters rond de uitgerekende datum bij te vroeg geboren kinderen gebruikt kunnen worden als biomarker voor de neurologische ontwikkeling op de gecorrigeerde leeftijd van twee jaar.
- Te vroeg geboren kinderen vertonen een hoge prevalentie van variaties in de Cirkel van Willis. Variaties in de anatomie zijn gerelateerd aan veranderingen in de bloedstroomsnelheid in de ACI en de AB (*Hoofdstuk 8*).

## TOEKOMST

### Volume metingen van hersenstructuren

Door de ontwikkeling van een volledig automatische segmentatiemethode waarmee de hersenen van een neonaat gesegmenteerd kunnen worden, kan de ontwikkeling van de hersenen bij neonaten nog beter bestudeerd worden. Het kwantificeren van hersenvolumes is van belang, omdat het in een vroeg stadium additionele informatie verschaft over de neurologische ontwikkeling van het kind. Deze volumes kunnen bijdragen aan het counsellen van ouders van te vroeg geboren kinderen en daarnaast kunnen kinderen worden geselecteerd die baat kunnen hebben van speciale ontwikkelingsprogramma's. In dit cohort waren alleen het volume van het cerebellum en de ventrikels rond de uitgerekende datum gerelateerd aan de ontwikkeling op de gecorrigeerde leeftijd van twee jaar.

Vervolgonderzoek is echter noodzakelijk om veranderingen in regionale hersenvolumes te analyseren. Regionale veranderingen kunnen samenhangen met problemen in de neurologische ontwikkeling en kunnen worden gemist wanneer alleen de totale volumes van hersenstructuren worden berekend. *Voxel-based morphometry* is een

methode die gebruikt zou kunnen worden om locale toe- en/of afname in hersenvolume te detecteren en deze techniek zal in de toekomst geïmplementeerd worden. Daarnaast zou het van toegevoegde waarde zijn om volumes te kunnen berekenen van de linker en rechter hemisfeer apart of om volumes te berekenen van de frontale, parietale, temporale en occipitale hersenkwabben apart. Dit is bijvoorbeeld een voordeel bij neonaten met een unilaterale laesie, zoals een unilateraal neonataal infarct.

We hebben hersenvolumes van te vroeg geboren kinderen alleen onderzocht rond de uitgerekende datum. Tegenwoordig wordt er ook al een MRI van de hersenen gemaakt vlak na de geboorte rond een PMA van 30 weken. Er wordt gewerkt aan een leerset om ook deze MRI scans automatisch te kunnen segmenteren. Recent is er een longitudinale studie gestart waarbij te vroeg geboren kinderen vlak na geboorte en rond de uitgerekende datum worden gescand. Dit stelt ons in staat te kijken naar de groei van de hersenen, maar tevens kunnen we ook de *cortical folding* kwantificeren. Zowel groei als mate van *cortical folding* van de hersenen geven informatie over de variaties in hersenontwikkeling en de daarmee samenhangende neurologische ontwikkeling.

Bij kinderen in ons cohort met witte stof afwijkingen werd er een onduidelijke grens gezien op de conventionele T1- en T2-gewogen opnames tussen OnMWS en CoGS. Er werd gedacht aan een dysfunctie van de subplaatneuronen, waardoor de migratie van neuroblasten in de cortex incompleet zou kunnen zijn en daarnaast een insufficiënt apoptotische proces van de subplaatneuronen. Dit fenomeen zal verder onderzocht worden in een dierproefmodel waarin zowel een MRI als histopathologische analyses verricht zullen worden in ratten met en zonder witte stof schade.

### **Veranderingen in de microstructuur van de witte stof**

Het analyseren van diffusieparameters bij neonaten is een uitdaging. Er is een relatief lage signaal-ruisverhouding als gevolg van een kleine voxelgrootte door de kleine anatomische structuren. Daarnaast zijn een hoger watergehalte en een lagere graad van myelinisatie verantwoordelijk voor lagere FA waardes vergeleken met volwassenen. FA, AD en RD worden vaak geanalyseerd in manueel gedefinieerde gebieden. Een anatomische atlas van de witte stof banen van te vroeg geboren kinderen op verschillende leeftijden kan helpen om deze analyses te automatiseren. Een atlas van gezonde, te vroeg geboren kinderen kan informatie verschaffen over de hersenontwikkeling van het individuele kind. Om zo'n atlas te maken moet er een longitudinale studie opgezet worden waarin te vroeg geboren kinderen na de geboorte wekelijks worden gescand. Het is essentieel dat deze kinderen geen cerebrale afwijkingen hebben en hun neurologische ontwikkeling moet binnen de normale range vallen.

### **Additionele rol voor de MRI**

In de eerste weken na de geboorte zijn er al veel parameters bekend die de neurologische ontwikkeling beïnvloeden, zoals zwangerschapsduur, geboortegewicht, perinatale infectie, respiratoire problemen, intraventriculaire bloedingen, maar ook educatie van de moeder. In deze studie werd de MRI rond de uitgerekende datum als anatomische

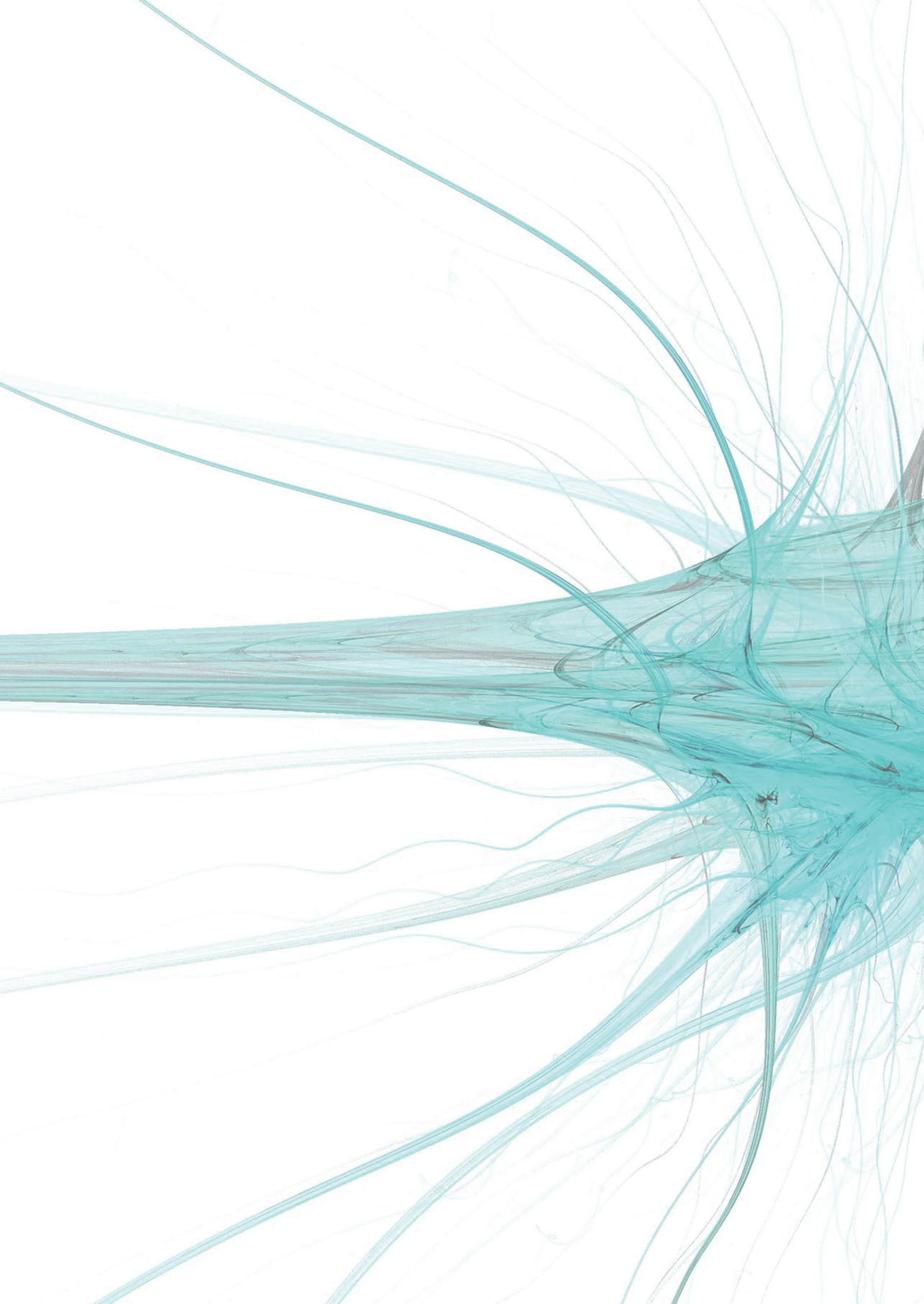
weerslag gebruikt van de pre-, peri- en postnatale problematiek. Aanvullend onderzoek is noodzakelijk om te achterhalen welke risicofactoren in deze periode een rol spelen bij het ontstaan van hersenschade, veranderingen in hersenvolume en afwijkingen in de microstructuur van de witte stof, allemaal variabelen waarvan in deze studie is aangetoond dat ze samenhangen met problemen in de neurologische ontwikkeling. Kennis van deze risicofactoren maakt interventie en behandeling gericht op preventie van deze factoren mogelijk. Er zijn verschillende neonatale en maternale factoren, waarvan bekend is dat ze van invloed zijn op cognitie en motoriek. De toegevoegde waarde van een MRI cerebrum in de voorspelling van de neurologische ontwikkeling is beperkt onderzocht. In ons cohort te vroeg geboren kinderen hebben we een rol gevonden voor hersenvolumes en diffusieparameters. Grotere etiologische en predictieve studies zijn nodig om te analyseren of deze recent ontwikkelde MR applicaties ook toepasbaar zijn in andere groepen te vroeg geboren kinderen.

Echografie van het hersenen wordt routinematig uitgevoerd op onze unit om hersenlaesies te ontdekken. Een MRI is echter sensitiever om meer subtiele cerebrale afwijkingen, zoals puntbloedingen in de witte stof en (kleine) cerebellaire bloedingen, te detecteren. Een MRI vlak na geboorte kan afwijkingen specificeren die gezien zijn bij echografie. (Subtiele) witte stof afwijkingen kunnen gemist worden bij een echografie of kunnen zijn opgelost wanneer het kind de uitgerekende datum bereikt heeft. Vervolgonderzoek is noodzakelijk om vast te stellen of een vroege MRI vlak na geboorte naast seriële echografie kan bijdragen aan het detecteren van witte stof afwijkingen. Men zou kunnen overwegen om een MRI te maken van de hersenen van alle kinderen die geboren zijn na een zwangerschap van minder dan 28 weken, aangezien deze kinderen at risk zijn voor witte stof schade.

### **Lange termijn ontwikkeling**

Voor deze studie zijn de te vroeg geboren kinderen onderzocht op de gecorrigeerde leeftijd van twee jaar. Het zou interessant zijn om de MRI bevindingen rond de uitgerekende datum, dus zowel de visuele beoordeling als de hersenvolumes en de diffusieparameters in de witte stof, te relateren aan bevindingen op een MRI die gemaakt is tussen schoolleeftijd en adolescentie. Het is wenselijk om hersengroei over een langere periode te volgen om te analyseren of er sprake is van een zogenaamde *catch-up* groei, wat kan betekenen dat de hersenontwikkeling rond de uitgerekende datum alleen vertraagd was, of dat hersenvolumes kleiner blijven ten opzichte van controlekinderen wat kan samenhangen met onherstelbare hersenschade en daardoor een abnormale innervatie van zenuwweefsel. Daarnaast wordt er gespeculeerd dat de problemen bij te vroeg geboren kinderen zich pas later openbaren. Dat zou kunnen verklaren dat de hersenvolumes rond de uitgerekende datum niet gerelateerd zijn aan de ontwikkeling op de gecorrigeerde leeftijd van twee jaar, maar wel een associatie kunnen laten zien met problemen op latere leeftijd. We zouden deze groep kinderen graag weer terug willen zien op de leeftijd van 8-10 jaar voor zowel neurologische beeldvorming (zowel conventionele als functionele MRI) als uitgebreide psychologische testen om behalve het IQ en motorische functies ook executieve functies, geheugen en gedrag te onderzoeken. Om zowel ouders als kind zo goed mogelijk te begeleiden is het van belang de neurologische ontwikkeling van een te vroeg geboren kind in een zo vroeg mogelijk stadium te voorspellen.





The background of the page is an abstract composition of flowing, organic lines. A dark grey horizontal band spans the top third of the image. Below this, the background is white, with a dense network of teal and dark blue lines that originate from the left side and flow towards the right. These lines vary in thickness and opacity, creating a sense of depth and movement. The lines appear to be layered, with some being more prominent than others.

**List of co-authors**  
**List of publications**

## LIST OF CO-AUTHORS

**Anbeek, Petronella**, Department of Neonatology, University Medical Center Utrecht, Lundlaan 6, Utrecht, The Netherlands

**Ball, Gareth**, Imaging Sciences Department, MRC Clinical Sciences Centre, Imperial College London, DuCane Road, London, W12 0HS, UK

**Benders, Manon J.N.L.**, Department of Neonatology, University Medical Center Utrecht, Lundlaan 6, Utrecht, The Netherlands

**Counsell, Serena J.**, Imaging Sciences Department, MRC Clinical Sciences Centre, Imperial College London, DuCane Road, London, W12 0HS, UK / Hammersmith/St Mary's Comprehensive Biomedical Research Centre, Du Cane Road, London, W12 0HS, UK

**Groenendaal, Floris**, Department of Neonatology, University Medical Center Utrecht, Lundlaan 6, Utrecht, The Netherlands

**Haastert, Ingrid C. van**, Department of Neonatology, University Medical Center Utrecht, Lundlaan 6, Utrecht, The Netherlands

**Hendrikse, Jeroen**, Department of Radiology, University Medical Center Utrecht, Lundlaan 6, Utrecht, The Netherlands

**Işgum, Ivana**, Image Sciences Institute, University Medical Center Utrecht, Heidelberglaan 100, Utrecht, The Netherlands

**Kersbergen, Karina J.**, Department of Neonatology, University Medical Center Utrecht, Lundlaan 6, Utrecht, The Netherlands

**Nievelstein, Rutger A.J.**, Department of Radiology, University Medical Center Utrecht, Lundlaan 6, Utrecht, The Netherlands

**Pul, Carola van**, Department of Neonatology, University Medical Center Utrecht, Lundlaan 6, Utrecht, The Netherlands / Department of Clinical Physics, Máxima Medical Center Veldhoven, De Run 4600, PO Box 7777, 5500 MB Veldhoven, The Netherlands.

**Viergever, Max A.**, Image Sciences Institute, University Medical Center Utrecht, Heidelberglaan 100, Utrecht, The Netherlands

**Vilanova, Anna**, Biomedical Engineering, Eindhoven University of Technology, Den Dolech 2, 5600 MB, Eindhoven, The Netherlands

**Vries, Linda S. de**, Department of Neonatology, University Medical Center Utrecht, Lundlaan 6, Utrecht, The Netherlands

## LIST OF PUBLICATIONS

van Kooij B.J.M., van Handel M, Uiterwaal C.S., Groenendaal F, Nievelstein R.A.J., Rademaker K.J., Jongmans M.J., de Vries L.S. Corpus callosum size in relation to motor performance in 9- to 10-year-old children with neonatal encephalopathy. *Pediatr Res.* 2008;63:103-8.

van Kooij B.J.M., Hendrikse J, Benders M.J.N.L., de Vries L.S., Groenendaal F. Anatomy of the circle of Willis and blood flow in the brain feeding vasculature in prematurely born infants. *Neonatology* 2009;97:235-241

van Kooij B.J.M., van Handel M, Nievelstein R.A.J., Groenendaal F, Jongmans M.J., de Vries L.S. Serial MRI and Neurodevelopmental Outcome in 9-10 Year Old Children with Neonatal Encephalopathy. *J Pediatr.* 2010;157:221-227.e2.

van Kooij Britt J.M., de Vries Linda S , Ball Gareth, van Haastert Ingrid C, Benders Manon J.N.L., Groenendaal Floris, Counsell Serena J. Neonatal tract-based spatial statistics findings and outcome in preterm infants. Accepted for publication in *AJNR*

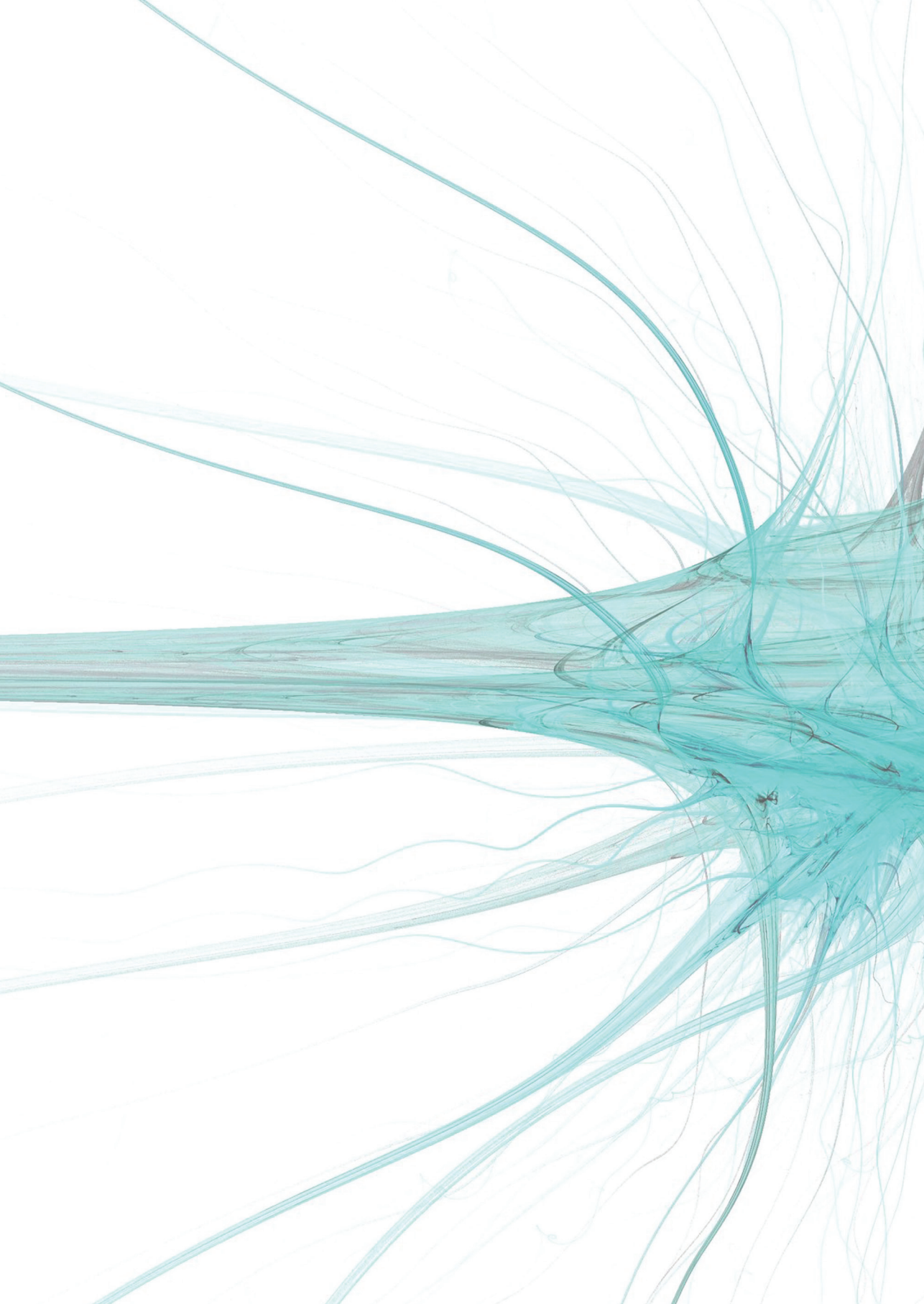
van Kooij Britt J.M, van Pul Carola, Benders Manon J.N.L., van Haastert Ingrid C, de Vries Linda S., Groenendaal Floris Fiber tracking at term displays gender differences regarding cognitive and motor outcome at two years in preterm infants. Accepted for publication in *Pediatr. Res* 2011 Aug 18

van Pul Carola, van Kooij Britt J.M., de Vries Linda S., Benders Manon J.N.L., Vilanova Anna, Groenendaal Floris. Quantitative fiber tracking in corpus callosum and internal capsule reveals microstructural abnormalities in preterm infants at term equivalent age. Accepted for publication in *AJNR*

van Kooij Britt J.M., Benders Manon J.N.L., Anbeek Petronella, van Haastert Ingrid C, de Vries Linda S. Cerebellar volume and <sup>1</sup>H-MRS at term and neurodevelopmental outcome at two years in preterm infants. Groenendaal Floris Submitted for publication

van Kooij Britt J.M, Anbeek Petronella, van haastert Ingrid C., Nievelstein Rutger A.J., Groenendaal Floris, de Vries Linda S., Viergever Max A., Benders Manon J.N.L. Brain tissue volume at term equivalent age: biomarker for neurodevelopmental outcome in preterm infants Submitted for publication

Hemels Marieke A, Nijman Joppe, Leemans Alexander, van kooij Britt J.M., van den Hoogen Agnes, Benders Manon J.N.L., Koopman Corine, van Haastert Ingrid C., de Vries Linda S., Krediet Tannette G., Groenendaal Floris. White matter apparent diffusion coefficients and neurodevelopmental outcome after coagulase-negative staphylococcal sepsis in preterm infants *Submitted* for publication



The background of the page is an abstract composition. The top half is a solid dark grey rectangle. The bottom half is white, featuring a complex network of thin, flowing, teal-colored lines that originate from the left edge and spread out towards the right. These lines vary in thickness and opacity, creating a sense of movement and depth. The overall effect is modern and artistic.

Dankwoord

## DANKWOORD

Promoveren was voor mij echt meer dan alleen maar leren hoe je onderzoek moet doen. Gelukkig stond ik er niet alleen voor en waren er veel mensen die ieder op zijn eigen manier deze leerschool wat makkelijker voor me maakte. Met onderzoek ben je 24/7 bezig en je bent ook nooit klaar. Met de hulp van de volgende mensen kan ik met trots zeggen dat het boekje af is.

Prof. Dr. L.S. de Vries, beste Linda, een bron van inspiratie. Als de dag van gisteren weet ik nog dat ik het kantoor binnenstapte van 'Prof. Dr. L.S. de Vries' om te praten over een onderzoeksstage op de afdeling neonatologie. Een van de eerste woorden die je tegen me zei: 'Het is gewoon Linda' en daarmee was de toon voor een prettige samenwerking gezet. Toen ik mijn artsensbul kreeg, zei je tegen me: 'je hoeft nu nog niet alles te weten' maar ik vraag me af of ik ooit wel zo veel zal weten als jij. Ik ben blij dat je door 'Wervelwind Britt' heen hebt kunnen kijken en me het vertrouwen hebt gegeven om deze sprong te wagen. Ook tijdens dit traject was je steun voor zowel de wetenschappelijke als de persoonlijke zaken groot. Het gouden ei is nu gelegd. Ik heb de afgelopen jaren veel van je mogen leren en ik hoop dat onze wegen in de toekomst nog vaker zullen kruisen.

Prof. M.A. Viergever, beste Max. Mijn vader wilde altijd dat ik de techniek inging, maar ik koos voor de Geneeskunde. Tijdens dit onderzoek heb ik een soort brug proberen te zijn tussen de medische wereld en de wereld van de beeldvormende techniek. Dank je wel dat jij me in die laatste wereld een beetje wegwijs hebt gemaakt. Jouw 'technische' kijk op zaken hebben voor mij weer nieuwe deuren geopend. Ik hoop dat de samenwerking tussen het Image Sciences Institute en de neonatologie nog lang zal blijven bestaan.

Dr. F. Groenendaal, beste Floris. Allereerst dank je wel voor de kans die je me gaf om dit onderzoek te doen. Je zei ooit tegen ouders toen we door de lange tunnel naar het AZU liepen voor een MRI: 'Ik heb haar aangenomen omdat ze met haar lange benen tenminste snel kan lopen'. Die ritjes waren zeker goed voor mijn conditie, maar ik hoop dat je nu aan het einde van de rit ook kunt terugkijken op een geslaagd eindresultaat van het onderzoek. Meerdere keren heb je me weer op het rechte pad gezet als de chaos in mijn hoofd me alle kanten op bracht. Soms is beter inderdaad de vijand van goed, een les die je me hebt geleerd en die ik niet snel zal vergeten.

Dr. M.J.N.L. Benders, beste Manon. Samen hebben we een nieuwe 'hobby' ontwikkeld: pixelpoetsen, ofwel 'kleuren voor gevorderden'. Ik waardeer je inzet, je (nachtelijk) uren en kennis die je hebt bijgedragen om de segmentatiemethode tot een succes te maken. Ik ben blij dat je met mij de hoge bergen, maar ook de diepe dalen hebt getrotseerd. Ik wil je bedanken voor alle steun die je me hebt gegeven tijdens deze leerschool, ook wat betreft zaken die niets te maken hadden met het onderzoek. Ik zal de dingen die je tegen me gezegd hebt goed onthouden!

Beste Inge-Lot, Linda, Karen, Niek, Karina, Margaretha en Johanneke, lieve (oud-)kamerengenootjes, wat heb ik een wervelende tijd met jullie beleefd! Inge-Lot, ik heb een bewondering voor je manier van werken. Je kunt een bom naast je hoofd laten ontploffen, maar jij blijft stug doorgaan en alles blijft even geordend en netjes. Dank je wel voor het testen van al 'mijn' kindjes. Je hebt er soms een zware kluif aan gehad, maar ik weet zeker dat je uit ze hebt gehaald wat erin zat. Linda, dank je wel voor de gezellige theemomenten, voor de momenten waarop we frustraties konden delen en de tips die je me gegeven hebt voor de leuke en minder leuke promotiezaken. Karen, als fellow was je niet vaak op de kamer, maar toch hebben we menig goede gesprekken gehad. Ik hoop dat je het in Harderwijk naar je zin hebt. Niek, naast dat het gewoon erg handig was om een eigen IT'er op de kamer te hebben, zal ik vooral onze gesprekken buiten kantooruren onder het genot van een Leffe Blond herinneren. Ook al werk ik niet meer in het WKZ, die gezellige uren hou ik er graag in. Karina, als student was je al een zeer goede 'pixelpoetser' en ik ben blij dat je nu, voor mijn gevoel, als arts-onderzoeker verder bent gegaan waar ik gebleven ben. Dank je wel voor een leuke samenwerking en voor al je inzet. Ik ben heel benieuwd naar de resultaten van jouw onderzoek. Margaretha, ik dacht dat ik het zwaar had met het afronden van mijn promotie en een nieuwe baan tegelijk, maar jij bent tijdens het afronden van je promotie je bruiloft aan het regelen en je nieuw gekochte huis aan het inrichten waar je na je bruiloft in gaat wonen, zodat je bed wat dichterbij is voor het geval je wilt slapen na je nachtdiensten die horen bij je nieuwe baan! Heel veel succes en vooral veel liefde en plezier in je 'nieuwe' leven. Johanneke, wij doen haast aan stuivertje wisselen, jij naar mijn oude kamer in het WKZ en ik naar jouw oude werkplek in Nieuwegein. Je hebt geweldige kamerengenoten, ik hoop dat je er net zo'n leuke tijd beleeft als ik! Lieve (oud) kamerengenootjes, heel veel dank voor alles wat we samen hebben mogen beleven, het luisterende oor wat jullie voor me wilde zijn en allemaal heel veel succes met het behalen van de finish op jullie, mogelijk wat bobbelige, weg van de wetenschap. Ik kijk uit naar jullie promoties!

Zonder de collega's in het WKZ was het onderzoek niet mogelijk. Verpleging van de neonatologie, deze studie bracht extra werkbelasting voor jullie met zich mee. Dank jullie wel voor jullie inzet en de gezelligheid als ik op de afdeling was. Neonatologen uit het WKZ, bedankt voor alle steun en interesse de afgelopen jaren en voor de inzet om de kinderen voor deze studie te includeren. Barbara Peels, onze 'personal assistent', dank je wel dat je soms voor vliegende keep speelde en daar wilde inspringen waar we je nodig hadden. Het was vooral erg gezellig om met je samen te werken. Secretariaresses van de NICU en het stafsecretariaat, beste Hanneke, Karin, Annemiek, Fiona, Marian, Ellen, Ineke, Danielle, Lot en Bertina, jullie zijn van alle markten thuis. Dank jullie wel voor de dingen die jullie voor me geregeld en gedaan hebben, voor het luisterende oor en de gezelligheid. En dan niet te vergeten de laboranten van de MR. De donderdagen waren altijd weer een belevenis en sorry dat ik me af en toe met de instellingen bemoeide, maar ik wilde niet dat de kinderen een kleiner breinvolume kregen omdat we een half hoofd vergaten te scannen. Dank jullie wel voor alle inzet en flexibiliteit. Zonder jullie hadden we nooit in totaal 139 kinderen voor de studie kunnen scannen.

Dear Serena, I would like to thank you for the wonderful time I have had in London. You learnt me a lot. Never thought that I could windsurf! Dear Mary Rutherford and Frances Cowan, thank you that I could be part of your team for half a year. The MRI reading sessions and the ultrasound teaching were very educational. Dear Phumza, Miriam, Amy, Gareth, Ida, Isotta and Jasenka, thank you for the fun, the laughs, the tears, the support, the good suggestions and the wonderful time I could spend in your presence.

Dr. P Anbeek, beste Nelly. De perikelen van de segmentatiemethode hebben we overleefd. Het eindresultaat is een mooie automatische methode om acht verschillende structuren van de hersenen van een neonat te segmenteren en dat kan nog niemand anders in de wereld. Dank je wel voor al je inzet. Ik hoop dat je in je nieuwe baan je ei kwijt kan. Beste Sabina, dank je wel voor je inzet en hulp in het segmentatie-project. Het was een gezelligheid om met je samen te werken. Succes met jouw eigen project.

Dr. J. Hendriks, beste Jeroen. We hebben samen mijn eerste artikel voor dit proefschrift geschreven. Dank je wel voor al je input, het was een plezier om met je te werken en een goed begin is het halve werk!

Beste Maartje, Anja, Greetje, Daniël, Kajo, Jan Willem en Joris, beste mensen van de promovendiraad, dank jullie wel voor het me wegwijzen maken in de wereld van de beeldverwerking, het meedenken en natuurlijk de leuke uren voor en na de promovendidagen.

Beste collega arts-assistenten en kinderartsen uit Nieuwegein, ik wil jullie bedanken voor het warme welkom dat ik gevoeld heb toen ik bij jullie aan de slag ging. Ik vind het echt heel fijn dat ik van jullie de ruimte heb gekregen om de laatste zaken van mijn proefschrift af te ronden en nu dit allemaal klaar is zal ik me voor de volle 100% inzetten in de kliniek.

Naast heel veel steun en inzet van mensen op de werkvloer, heb ik ook veel lieve familie en vrienden die er altijd voor me waren.

Lieve Vera, de afgelopen jaren hebben we veel met elkaar gedeeld en zijn we gegroeid tot de mensen die we nu zijn. Wat heb ik genoten van de reizen die we samen hebben gemaakt en ik ben trots dat je vandaag naast me staat als paranimf. Lieve Sanne, we hebben een bijzondere vriendschap en samen verschillende ups and downs meegemaakt. Ik had in Suriname niet kunnen denken dat de jaren erna zo zouden lopen. Dank je wel voor de meerdere keren dat je voor me gekookt hebt, vanaf nu kunnen we hopelijk wat langer genieten van de avond met een glaasje wijn. Lieve Monique, ineens was je vertrokken naar Nijmegen toen ik in Londen zat en werden de spontane eet-acties een beetje lastiger. Maar ook ik heb inmiddels een auto! Eindelijk mag jij gaan beginnen aan het grote promotieavontuur. Ik wens je heel veel succes met jouw leerschool. Lieve

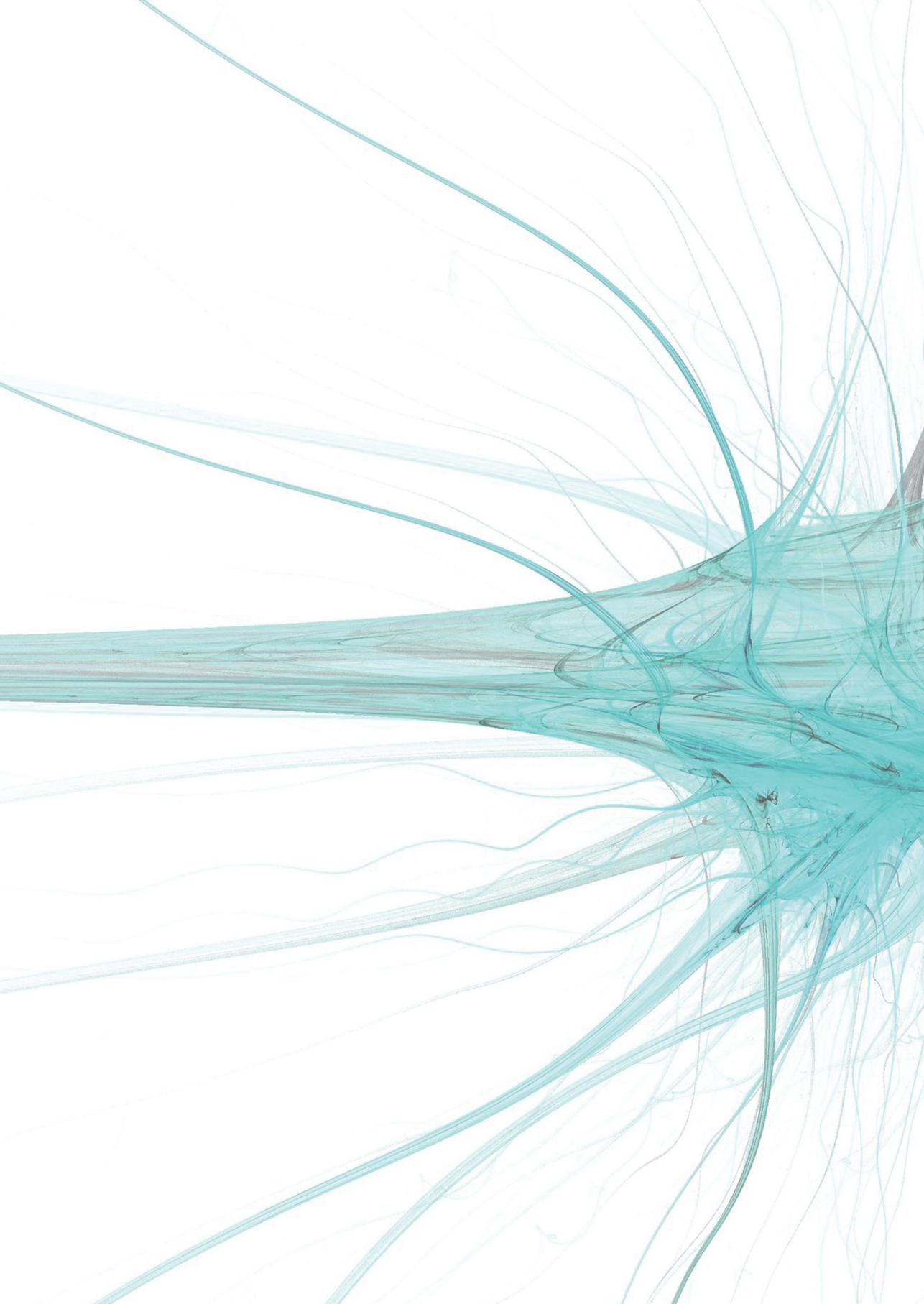
Elske, ik ben zo trots op je dat je in opleiding bent tot kinderarts, zo zie je maar, jij hebt helemaal geen promotieonderzoek nodig! Hard werken hoort erbij, maar zullen we vanaf nu gaan proberen om dat ene verwenweekendje per jaar erin te houden? Lieve Kate, ik heb er zo'n bewondering voor dat je ervoor gekozen hebt om alsnog je droom achterna te gaan, het roer om te gooien en Geneeskunde weer op te pakken. Nederland is straks weer een goede dokter rijker. Lieve Jessica & Bart, we zien elkaar niet veel, maar ik wist dat de Brabantse deur altijd open stond. Nu dit afgelopen is zal ik wat vaker daadwerkelijk door die deur stappen. Lieve Nienke, ook al zijn we elkaar een aantal jaar uit het oog verloren, toen we elkaar weer gevonden hadden was het alsof je altijd in mijn omgeving bent geweest. Fijn! Heel veel succes met jouw promotietraject. Lieve Erik, in mijn hoofd heb ik je al meerdere keren verslagen met snookeren, maar misschien wordt het eens tijd dat we in het echte leven een potje snooker gaan spelen?! Lieve Els en Cees, ik heb mijn agenda bij me en er is nu echt weer ruimte. Die beloofde eetdate moeten we nu echt snel plannen. Lieve vrienden, ik wil jullie allemaal bedanken voor jullie vriendschap, de gezelligheid en de support, ik kon altijd op jullie terugvallen. Nu mijn gouden ei dan toch echt gelegd is, is er weer tijd voor borrelen, dagjes weg, saunabezoekjes en wat frequentere eetafspraken. Ik kijk ernaar uit!

Lieve Hanneke & Peter, Maartje & Martin, Lars en Jesse, lieve schoonfamilie, dank jullie wel voor de interesse, de handige tips, en de gezellige avondjes. Ik zal er vanaf nu weer vaker bij zijn.

Lieve Kim & Richard en Liz, wat ben ik blij met zo'n zus, 'broer' en nichtje. Lieve Kim, we hebben niet veel woorden nodig om te begrijpen wat de ander bedoelt. Ik ben zo blij dat je op deze dag naast me staat. Lieve Richard, dank je wel voor de vormgeving van mijn ei. Ik heb het met een gerust hart aan je overgelaten. Lieve Lizzie, wat ben je toch een bijzonder mensje. Je ontwikkelt je zo snel en ik hoop daar nu ook meer van mee te kunnen maken. Ik hou van jullie.

Lieve papa & mama, jullie zijn mijn stabiele, veilige thuisbasis en daar ben ik zo dankbaar voor. Of het nou ging om een luisterend oor, praktische tips, een arm om me heen, hulp bij de Nederlandse teksten of een bord warm eten, ik kon altijd bij jullie terecht. Dank jullie wel voor jullie onvoorwaardelijke liefde, ik hou van jullie.

Lieve Jurrian, wat ben ik blij dat jij die bewuste 28e van november, al weer bijna drie jaar geleden, naar de verjaardag van Richard bent gegaan. *En het is eigenlijk heel simpel, het is gewoon zo.* Meer hoeft ik volgens mij niet te zeggen, dank je wel voor alles. Het is nu echt klaar! Ik hou van je!



The background of the page is an abstract composition. The top half is a solid dark grey rectangle. The bottom half is white, featuring a complex network of overlapping, flowing lines in various shades of teal and light blue. These lines originate from the left side and sweep across the page, creating a sense of movement and depth. The lines vary in thickness and opacity, with some appearing as sharp, dark strokes and others as thin, ethereal wisps.

# Curriculum vitae



## **CURRICULUM VITAE**

Britt van Kooij werd op 20 mei 1983 geboren in Oosterhout. Ze groeide op in Vlijmen, een dorpje naast 's-Hertogenbosch, waar ze op zeventienjarige leeftijd haar diploma behaalde aan het Stedelijk Gymnasium. Vanaf 2000 studeerde ze Geneeskunde aan de Universiteit Utrecht. Van 2003 t/m 2006 deed ze haar co-assistentschappen, waaronder haar co-assistentschap Gynaecologie in het 's Lands Hospitaal in Paramaribo, Suriname. Tevens volgde ze een extra stage Kinderneurologie in BC Children's Hospital in Vancouver, Canada. Tijdens haar studie verrichtte ze onderzoek naar de ontwikkeling van kinderen met perinatale asfyxie op de afdeling neonatologie van het Wilhelmina Kinderziekenhuis (Prof. Dr. L.S. de Vries). In 2006 behaalde ze haar artsexamen. Hierna is ze op dezelfde afdeling begonnen aan het onderzoek wat geresulteerd heeft tot dit proefschrift onder leiding van Dr. F. Groenendaal en Prof. Dr. L.S. de Vries. Mede door het behalen van het 'Young Investigator Exchange Program Fellowship' van de 'International Pediatric Research Foundation (IPRF)' kon een deel van het onderzoek worden uitgevoerd in het Hammersmith Hospital in Londen, Engeland, waardoor ze haar huis in de prachtwijk Overvecht voor een half jaar verruilde voor een kamer in West Kensington in Londen. Vanaf 1 juni is ze werkzaam als ANIOS in het Sint Antonius Ziekenhuis te Nieuwegein.